

**Mechanisms of Embryonic and Adult Neurogenesis in the Development of
Epilepsy**

by

Xi Du Plummer

A dissertation submitted in partial fulfillment
of the requirement for the degree of
Doctor of Philosophy
(Neuroscience)
in the University of Michigan
2017

Doctoral Committee:

Professor Jack M. Parent, Chair
Professor Roman J. Giger
Professor Lori L. Isom
Associate Professor David L. Turner
Professor Michael D. Uhler

© Xi Du Plummer

xidu@umich.edu

ORCID iD: 0000-0003-1581-5053

2017

To Mom, I owe everything that I am to you

&

To my husband, Bradley, you are my best half

Acknowledgements

First and foremost, I would like to thank Jack for his patience, guidance and constant support. Jack has inspired, challenged and motivated me in ways that have brought out the best in me. I have grown tremendously under his mentorship and will always be grateful for everything that I have learned.

I have been blessed with an incredible first mentor and friend who encouraged me to pursue all my dreams. Isabelle, thank you.

My colleagues both past and present have contributed so much of their time, effort and snacks towards the work presented in this dissertation. Especially Helen, Ali, Gustavo and Louis, who not only taught me scientific rigor but were also constant sources of friendship and laughter. I especially would like to thank Dani, Aaron, Kasia, Preethi, Matt, Wei, Kanagu, Anhdao and Elyse, who have all made my time in lab a joy.

I would also like to thank my thesis committee. Roman, Lori, Dave and Mike, thank you for your technical help, valuable insight and for keeping my progress on track.

Finally, I owe a deep and heartfelt thank you to my friends and family. To my husband, Bradley, you are the kindest and most courageous person I know and none of this would have been possible without you. To Mom and Dad, your unconditional love kept me grounded. To my in-laws, Donald and Renee, thank you for always believing in me.

Table of Contents

Dedications	ii
Acknowledgements	iii
List of Figures	vi
List of Tables	viii
List of Appendices	ix
List of Abbreviations and Acronyms	x
Abstract	xii
Chapter 1: Introduction	1
Adult neurogenesis	2
Mesial temporal lobe epilepsy	5
Animal models of TLE	6
Dentate gyrus reorganization in TLE	7
Consequences of seizure-induced hippocampal reorganization	12
Embryonic cortical development.....	14
The iPSC method	16
iPSC modeling of genetic epilepsies	19
Protocadherin-19 female limited epilepsy.....	23
The role of PCDH19 in development.....	26
Questions addressed in this dissertation.....	28
References	30
Figures.....	48
Chapter 2: Monosynaptic Tracing of Hippocampal Circuit Remodeling in Experimental Temporal Lobe Epilepsy	53

Summary	53
Introduction	54
Materials and methods	56
Results	62
Discussion	69
References	77
Figures	83
Chapter 3: Potential Mechanisms of Protocadherin-19 in Early Infantile Epileptic Encephalopathy type 9.....	92
Summary	92
Introduction	93
Materials and methods	97
Results	104
Discussion	116
References	123
Figures	129
Tables	140
Chapter 4: Dissertation Summary and Future Directions	142
Summary of results	142
Adult-born and early-born DGCs are hyperconnected in the hippocampal circuitry in experimental TLE.....	143
Disruptions in PCDH19 alter cell-cell homophilic interactions and contribute to altered excitability	149
A look ahead.....	156
Conclusions	159
References	161
Appendices	169

List of Figures

Chapter 1

1.1 - Adult neurogenesis in the hippocampal dentate gyrus.....	48
1.2 - Schematic of the dual-viral tracing strategy	49
1.3 - The utility of iPSCs for modeling neural development.....	50
1.4 - Structure of the PCDH19 protein and its postulated role in PCDH19 FLE ..	51

Chapter 2

2.1 - RV-RbV dual-viral tracing of presynaptic inputs onto early- and adult-born DGCs	83
2.2 - RbV-mCh retrograde spread in epileptic and control rats is dependent on the presence of Rgp	84
2.3 - Prox1+ DGC inputs onto early- and adult-born DGCs differ in the sham versus epileptic brain	85
2.4 - RbV tracing of hilar somatostatin-expressing interneuron inputs onto birthdated DGCs.....	86
2.5 - RbV tracing of dentate gyrus parvalbumin-expressing interneuron inputs onto birthdated DGCs.....	87
2.6 - Hippocampal CA3 and CA1 pyramidal cells innervate DGCs in the epileptic brain.....	88
2.7 - Quantification of entorhinal cortex and subicular inputs	90
2.8 - Hippocampal circuitry remodeling in the epileptic brain	91

Chapter 3

3.1 - Generation and validation of PCDH19 FLE patient iPSC lines	129
3.2 - Generation of <i>PCDH19</i> -null male lines using CRISPR/Cas9.....	130
3.3 - Neural rosettes derived from PCDH19 FLE patient iPSCs have defects in apical polarity and adherens junctions	131
3.4 - Cortical-like excitatory neurons differentiated from PCDH19 FLE patient iPSCs demonstrate abnormal migration and morphology	133

3.5 - Mixed cultures of male control and <i>PCDH19</i> -mutant neurons demonstrate morphologic defects and abnormal segregation of cell populations	134
3.6 - MEA recordings suggest that <i>PCDH19</i> FLE cortical-like excitatory neurons have increased excitability as compared with female control neurons	135
3.7 - MEA analysis of male mixed cultures of control and <i>PCDH19</i> -null cortical-like excitatory neurons	136
3.8 - <i>PCDH19</i> FLE GABAergic interneurons show morphological abnormalities and possible increased MEA activity as compared with controls	137
3.9 - Mixed control and <i>PCDH19</i> -null GABAergic interneurons have normal morphology but demonstrate increased excitability on MEA recordings	138

Appendix A

A.1 - Hippocampal PV-expressing interneuron inputs onto birthdated DGCs in the intact and epileptic brain	181
A.2 - Hippocampal SST-expressing interneuron inputs onto age-defined populations of DGCs in the intact and epileptic brain	182

Appendix B

B.1 - Cerebral organoids generated with the intrinsic protocol have sparse cortical-like regions and are electrophysiologically active	197
B.2 - Forebrain organoids generated with Spin Ω mimic the developing human cortex with ventricular zone-like areas surrounded by cortical-like neurons	198

List of Tables

Chapter 3

Table 1 - Primer sequences for Sanger sequencing	140
Table 2 - Primer sequences for qRT-PCR.....	141

List of Appendices

A: Inhibitory Inputs to the Dentate Gyrus from Extra-dentate Hippocampal Regions	169
.....	169
Summary	169
Introduction	170
Materials and methods	171
Results	174
Discussion	175
References	179
Figures.....	181
B: Forebrain Organoids as a Model for Neural Development	183
.....	183
Summary	183
Introduction	184
Materials and methods	185
Results	190
Discussion	191
References	195
Figures.....	197

List of Abbreviations and Acronyms

AED: Anti-epileptic drug
ASD: Autism spectrum disorder
Cas9: CRISPR associated protein 9
CNS: Central nervous system
CRISPR: Clustered regularly interspaced short palindromic repeats
DCX: Doublecortin
DGC: Dentate granule cell
EIEE9: Early infantile epileptic encephalopathy type 9
EnvA: Avian envelope subgroup A
FLE: Female limited epilepsy
GABA: Gamma-aminobutyric acid
GFAP: Glial fibrillary acidic protein
GFP: Green fluorescent protein
HBD: Hilar basal dendrite
hESC: Human embryonic stem cell
ICC: Immunocytochemistry
IHC: Immunohistochemistry
iPSC: Induced pluripotent stem cell
mCh: mCherry
oRG: Outer radial glia
oSVZ: Outer subventricular zone
MFS: Mossy fiber sprouting
MGE: Medial ganglionic eminence
PCDH19: Protocadherin-19
PV: Parvalbumin

RGL: Radial-glia like cell
Rgp: Rabies glycoprotein
RbV: Rabies virus
RMS: Rostral migratory stream
RV: Retrovirus
SE: Status epilepticus
SGZ: Subgranular zone
SST: Somatostatin
SVZ: Subventricular zone
TLE: Temporal lobe epilepsy
TVA: Avian sarcoma leukosis virus receptor
VZ: Ventricular zone
XIST: X-inactive specific transcript

Abstract

The epilepsies encompass a constellation of syndromes that possess the cardinal feature of spontaneous recurrent seizures. Epilepsy etiologies are classified in part based on two broad categories: acquired and genetic. Acquired epilepsies often arise as a result of a previous neurological insult while genetic epilepsies arise from gene mutations that affect the brain. While the two are causally distinct, both acquired and genetic epilepsies often involve abnormal neural development, whether during adulthood or embryonically, as an underlying component of epileptogenesis.

This dissertation aims to explore how alterations in embryonic and adult neurogenesis lead to morphological and functional changes that may underlie the development of seizures. We utilize a rat pilocarpine-induced status epilepticus (SE) model of temporal lobe epilepsy (TLE), an acquired epilepsy, to ask how adult-born dentate granule cells (DGCs) differentially integrate into the chronically epileptic brain. By employing a dual-virus tracing strategy combining retroviral-birthdating with rabies virus-mediated retrograde trans-synaptic spread, we explore how first-order presynaptic inputs onto adult-born DGCs in the epileptic brain differ from those in the intact brain. Furthermore, we compare the presynaptic inputs onto adult-born DGCs with those onto early-born DGCs that were mature at the time of SE.

Our results demonstrate that both adult- and early-born DGCs in the epileptic brain receive recurrent excitatory inputs from normotopic DGCs while adult-born DGCs are

preferentially targeted by hilar ectopic DGCs. We also show that other regions of the hippocampus that normally do not project to the dentate gyrus, such as CA3 and CA1, sprout axon collaterals after SE that preferentially synapse onto adult- and early-born DGCs, respectively. Finally, we describe changes in the hippocampal inhibitory interneuron network with differential sprouting by both parvalbumin and somatostatin interneurons onto different age-defined DGC populations.

In addition to modeling an acquired epilepsy, we also employ an induced pluripotent stem cell (iPSC) model of protocadherin-19 (*PCDH19*) female-limited epilepsy (FLE), a genetic epilepsy. Female patients with heterozygous mutations in the X-linked *PCDH19* gene develop the disease while mutation carrying males are asymptomatic. Interestingly, there are several cases of affected males who have somatic mosaicism for the *PCDH19* gene. We generate iPSCs from female FLE patients with pathogenic mutations in *PCDH19* and address the hypothesis that FLE arises from cellular interference during development between wildtype and mutant *PCDH19*-expressing neurons. We find that cortical-like excitatory and inhibitory neurons derived from FLE patient-derived iPSCs have aberrant morphologies and increased excitability. We also use the clustered regularly interspaced short palindromic repeats (CRISPR)/CRISPR associated protein 9 (Cas9) gene editing technology to generate *PCDH19*-null male iPSCs. We mix the *PCDH19*-null iPSCs with their isogenic control iPSCs to mimic disease phenotype in affected mosaic males. This approach recapitulates some of the morphological and functional changes found in female FLE patient-iPSC derived neurons, further lending support to the idea that altered cell-cell interactions contribute to the disease pathogenesis.

The work presented in this dissertation gives new insights into how the adult neural circuitry remodels after epileptic seizures, as well as how deviations in embryonic development can mediate hyperexcitability. However, these two processes are not mutually exclusive and understanding both should better inform our knowledge of the mechanisms of epileptogenesis and uncover future therapeutic strategies.

Chapter 1

Introduction

The epilepsies encompass a diverse set of disorders that affect an estimated 50 million people worldwide (Banerjee et al., 2009). Despite their high prevalence, we understand very little of the basic cellular and molecular mechanisms that underlie the development of seizures. The hallmark of all epilepsies is spontaneous recurrent seizures yet their underlying pathophysiology can be diverse and complex. We can classify their etiology in part based on two broad categories: acquired and genetic. Acquired epilepsies often arise as a result of a previous neurological injury including but not limited to brain trauma, stroke, central nervous system (CNS) tumors and infections. However, not every person that experiences a brain insult will go on to develop epilepsy. On the other hand, genetic epilepsies arise from gene mutations that affect the brain and often occur in the pediatric population. These disorders generally include seizures as a component of a syndrome that often presents with other neurodevelopmental changes such as intellectual disability and autism as well as behavioral and psychiatric symptoms. The distinction between acquired and genetic epilepsy can often be blurred as underlying genetics can predispose a person to the development of epilepsy after brain insults.

Epileptogenesis is the process by which a gene mutation, brain malformation or acquired brain insult leads to the development of spontaneous recurrent seizures (i.e., epilepsy). To understand epileptogenesis, the epilepsy research field relies on model systems to recapitulate the fundamental features of disease. Unfortunately, no model system can perfectly reproduce the full spectrum of abnormalities that occur in human disease, hence the need to rely on several systems. As pathogenic insults can be difficult to replicate in cell culture systems, we frequently turn to animal studies to understand acquired neurological disorders. Genetic neurological disorders are also frequently modeled with transgenic animals, predominantly mice. However, using mouse models often has its own drawbacks particularly when there is no overt phenotype or the phenotype does not correlate with human disease. In these instances, human cell culture models are now available using state-of-the-art technologies such as induced pluripotent stem cells (iPSCs) and genome editing with clustered regularly interspaced short palindromic repeats (CRISPR)/CRISPR associated protein 9 (Cas9). While they are causally distinct, both acquired and genetic epilepsies often involve abnormal neurodevelopment, whether during adulthood in regions where neurogenesis persists or during early development, as an underlying component of epileptogenesis.

Adult neurogenesis

In mammals, neurogenesis progressing beyond the early developmental period was first demonstrated in rodents (Altman and Das, 1965) and subsequently in humans (Eriksson et al., 1998). The vast majority of adult neurogenesis occurs in two distinct areas in the brain: the subventricular zone (SVZ) of the lateral ventricle and the subgranular zone (SGZ) of the hippocampal dentate gyrus. New neurons departing the

SVZ migrate through the rostral migratory stream to the olfactory bulb and become interneurons while those in the SGZ become dentate granule cells (DGCs). The general consensus is that postnatal neurogenesis in other brain regions is rare or only occurs in the presence of injury (reviewed in Gould, 2007).

Adult hippocampal neurogenesis

Under basal conditions, approximately 9,000 new neurons are generated in the rat hippocampal dentate gyrus each day (Cameron and McKay, 2001) (**Figure 1.1**). The stem cells of the dentate gyrus are the radial glia-like cells (RGLs) that reside in the SGZ between the hilus and the granule cell layer. RGLs express nestin, glial fibrillary acidic protein (GFAP) as well as SRY-box 2 (SOX2) and are generally quiescent but can become activated under various physiological and environmental conditions. When activated, RGLs can divide symmetrically to self-renew or asymmetrically to self-renew and give rise to daughter cells, the transit amplifying progenitors. Transit amplifying progenitors are highly proliferative but only a small proportion of precursors survive and subsequently exit the cell cycle (Kempermann et al., 2003). These immature neurons ultimately mature into DGCs that send dendrites into the molecular layer and extend axons into the hilus towards CA3. While it is generally accepted that a fully mature adult-born DGC is functionally and anatomically indistinguishable from its neonatally-born counterpart in the intact brain (van Praag et al., 2002; Laplagne et al., 2006; Ge et al., 2007), the work presented in this dissertation and other recent evidence (Vivar et al., 2016) suggest specific intrinsic differences between these two populations.

Function and regulation of adult-born neurons

The exact role and function of newborn neurons in the intact or pathologic adult brain is still not well understood. The dentate gyrus has been implicated in learning and memory and there is evidence to suggest that adult-born neurons play a role in both functions (reviewed in Deng et al., 2010). Enhancing dentate gyrus neurogenesis in mice improves performance in the water maze (Kempermann et al., 1997; van Praag et al., 1999b) while reducing neurogenesis disrupts performance (Lemaire et al., 2000; Koo et al., 2003). Although a causal relationship between neurogenesis and learning remains uncertain, mounting evidence suggests that immature adult-born DGCs have unique intrinsic and synaptic properties that are distinct from their mature counterparts. For instance, young adult-born DGCs are hyperexcitable (Couillard-Despres et al., 2006) and have enhanced synaptic plasticity (Snyder et al., 2001; Schmidt-Hieber et al., 2004). In nestin-thymidine kinase (tk) transgenic mice, the temporary reduction of adult DGC neurogenesis using ganciclovir leads to deficiencies in long-term spatial memory (Deng et al., 2009).

Many environmental and physiological stimuli can influence adult neurogenesis. For instance, aging leads to a decline in both the progenitor population as well as the proliferative capacity of the neurogenic niche (Kuhn et al., 1996; Drapeau et al., 2003; Driscoll et al., 2006). On the other hand, running has been demonstrated to potentiate SGZ progenitor proliferation (van Praag et al., 1999a; Kronenberg et al., 2003) and environmental enrichment promotes neuronal survival (Kempermann et al., 1997; Kempermann et al., 2002).

Pathological influences on adult neurogenesis

Various pathological states have differential effects on adult neurogenesis. For example, cell proliferation in the dentate gyrus SGZ decreases in several stress models in multiple species (Gould et al., 1997; Malberg and Duman, 2003; Pham et al., 2003; Heine et al., 2004). On the other hand, experimental models of stroke have been shown to increase proliferation and neurogenesis in both the SVZ and SGZ (Jin et al., 2001; Arvidsson et al., 2002; Parent et al., 2002). Another well-characterized and potent stimulator of adult neurogenesis is seizures (Bengzon et al., 1997; Parent et al., 1997; Gray and Sundstrom, 1998). Seizures have also been shown to increase survival of newborn DGCs and accelerate their development (Mohapel et al., 2004; Overstreet-Wadiche et al., 2006). In addition to developmental changes, DGCs in human and experimental models of epilepsy display characteristic structural abnormalities (described in detail below) such as mossy fiber sprouting, persistent hilar basal dendrites, ectopic soma placement, and granule cell layer dispersion (Houser, 1990; Houser et al., 1990; Parent et al., 1997; Kron et al., 2010).

Mesial temporal lobe epilepsy

One of the most common acquired epilepsies is mesial temporal lobe epilepsy (TLE), a disorder that has been estimated to comprise 25 percent of adult epilepsies (Asadi-Pooya et al., 2016). As the name suggests, seizures arise from the temporal lobe and despite its prevalence, many patients with TLE have medically intractable seizures that fail to respond to anti-epileptic drugs (AEDs) (Engel et al., 2012). Furthermore, a diagnosis of TLE often is accompanied by cognitive and psychiatric co-morbidities that

may be a result of the underlying brain insult or abnormality, the seizures themselves or from AED therapy (Carreno et al., 2008).

The pathogenesis of TLE is not well understood and likely varies amongst patients. For many, there is an initial precipitating injury followed by a latent period before the onset of spontaneous recurrent seizures. The duration of the latent period is highly variable. Most people who experience a brain injury do not go on to develop TLE and it remains unclear what additional factors contribute to epileptogenesis. As a last resort for patients who have poorly-controlled seizures, surgical resection of the temporal lobe is an option but not every patient is eligible and brain surgery presents its own set of risks and challenges. In resected tissue from TLE patients, the hippocampus often displays the pathological hallmark of this syndrome, hippocampal sclerosis presenting with characteristic neuronal cell loss, gliosis and structural reorganization of the dentate gyrus.

Animal models of TLE

As humans with TLE often present with an initial precipitating injury, this paradigm is generally utilized when devising experimental models of TLE. Several established animal models of TLE utilize a range of neurological insults and faithfully recapitulate the most important aspects of disease. The less severe insults, such as tetanus toxin injection and electrical kindling, evoke acute seizures but rarely lead to the development of epilepsy (spontaneous recurrent seizures). The more severe injuries, such as electrical and chemical induction of status epilepticus (SE), lead to spontaneous recurrent seizures and hippocampal sclerosis.

The rodent work presented in Chapter 2 of this dissertation was based upon the pilocarpine-induced SE model of TLE, a widely-used and well-established TLE model.

Pilocarpine is a muscarinic acetylcholine receptor agonist and acts as a chemoconvulsant in the brain to increase neuronal excitability and induce SE. After receiving a high dose of pilocarpine, animals are maintained in SE for 90 minutes and then the seizures are terminated with diazepam. After a latent period of days to approximately 2-4 weeks, over 90% of rats display spontaneous recurrent seizures that continue throughout their lifetime (Buckmaster, 2004). Accompanying the seizures, the hippocampus develops overt pathologies including characteristic sclerosis and dentate gyrus reorganization that recapitulate those seen in human disease. For these reasons, this model was chosen for our studies. However, there are several limitations to the SE experimental paradigm worth mentioning. First, the hippocampal cell loss is much more bilateral and symmetric than in humans where these changes are unilateral and generally affect one temporal lobe. Additionally, neuronal damage in the rodent pilocarpine model is not limited to the hippocampus and often involves other brain regions such as the olfactory cortex and the thalamus (Turski et al., 1983; Clifford et al., 1987).

Dentate gyrus reorganization in TLE

In both human TLE and rodent experimental models, the dentate gyrus develops several abnormalities including massive hilar cell loss, mossy fiber sprouting, DGCs with persistent hilar basal dendrites, ectopic migration of DGCs, and granule cell layer dispersion. While the pathological consequences of these features are still largely debated, each display unique properties that will be described in the following sections.

Mossy fiber sprouting

The axons of DGCs, collectively known as the mossy fibers, extend basally into the dentate hilus and then into stratum lucidum of area CA3 of the hippocampus proper. In the hilus, the mossy fibers synapse onto inhibitory interneurons and excitatory mossy cells, and in CA3 they primarily innervate pyramidal cells. Mossy fiber boutons contain a high concentration of zinc and can be easily visualized with Timm's sulfide silver staining. Under normal conditions, Timm staining is densest in the hilus and extending into stratum lucidum of CA3 but also demonstrates very minor staining in the granule cell layer, suggesting the presence of rare mossy fiber to DGC connections (Haug, 1974). These minor projections have been shown to increase with physiological aging (Cassell and Brown, 1984; Wolfer and Lipp, 1995) but are most robustly increased with seizures in a well-characterized phenomenon termed mossy fiber sprouting (MFS).

In human TLE and experimental models, MFS results in extensive axonal projections into the dentate granule cell layer and the supragranular inner molecular layer where they synapse onto DGC dendrites (Sutula et al., 1989; Houser et al., 1990; Babb et al., 1991; Buckmaster et al., 2002). This results in a recurrent, excitatory DGC-to-DGC feedback loop that has been postulated to underlie the development of seizures. Indeed, functional data indicate that, in hippocampal slice recordings from epileptic animals with MFS, stimulating DGCs generates excitatory potentials in other DGCs (Scharfman et al., 2003). It was a long-held belief that only DGCs that were being born or still developing at the time of SE were capable of MFS (Parent et al., 1997; Jessberger et al., 2007) and older DGCs that were mature at the time of SE did not sprout (Kron et al., 2010). However, other work demonstrated that inhibiting DGC neurogenesis after SE did not eliminate MFS (Parent et al., 1999) and recent evidence suggests that DGCs that were mature at

the time of SE are also capable of sprouting (Althaus et al., 2016). More recent data using retrograde trans-synaptic tracing, discussed in Chapter 2 of this dissertation, extend these findings to show that neonatally-born and adult-born DGCs after SE are both capable of receiving recurrent excitatory innervation from other DGCs. Thus, the role of MFS in the pathogenesis of TLE remains controversial.

Persistent hilar basal dendrites

In a normal rodent hippocampus, hilar basal dendrites (HBDs) are transient structures on newly-generated DGCs that do not receive synaptic inputs (Shapiro and Ribak, 2006) and disappear with maturation (Seress and Pokorny, 1981). After SE, however, HBDs develop rapidly and synaptic contacts onto HBDs appear within 4 days (Shapiro et al., 2007). These synapses persist and the HBDs have a high density of spines that receive mainly excitatory inputs from their neighboring DGCs (Ribak et al., 2000; Thind et al., 2008). Several groups have shown that only DGCs still developing at the time of SE or generated shortly after exhibit persistent HBDs suggesting that the adult-born population is involved (Jessberger et al., 2007; Walter et al., 2007; Kron et al., 2010). This idea is supported by the finding that most DGCs with HBDs after SE are found near the SGZ, the neurogenic niche of the dentate gyrus (Spigelman et al., 1998). It is possible that persistent HBDs represent an expansion of the normal developmental process of DGCs. That is to say, DGCs that are developing or being born in a pathological environment may be unable to retract their HBDs because they receive immediate, excessive synapses from mossy fibers.

Hilar ectopic granule cells

Most DGCs that are born in the SGZ, even after SE, migrate normally into the granule cell layer. A fraction of them, however, migrate aberrantly into the dentate hilus in both human and experimental models of TLE (Houser, 1990; Parent et al., 1997; Dashtipour et al., 2001; Parent et al., 2006). While the mechanism for ectopic migration is not well understood, altered reelin signaling has been implicated. Reelin signaling is important for proper migration of newly-born DGCs (Gong et al., 2007; Teixeira et al., 2012) and loss of reelin is enough to induce ectopic migration (Teixeira et al., 2012) and reduce seizure threshold (Korn et al., 2016) in an otherwise normal mouse.

Hilar ectopic DGCs have been suggested to be the population most susceptible to hyperexcitability in the epileptic environment (Scharfman et al., 2000; Zhan et al., 2010; Althaus et al., 2015) with their major innervation arising from mossy fibers (Pierce et al., 2005; Jessberger et al., 2007) and their occurrence positively correlating with seizure frequency (Hester and Danzer, 2013). However, electrophysiological evidence demonstrates that hilar ectopic DGCs in human TLE actually contribute to a decrease in overall excitability, contradicting the findings in rodents (Althaus et al., 2015). One explanation for these results could be that the rodent data were generated during the early chronic phase while the human data were collected from patients who had experienced recurrent seizures for many years, even decades.

Innervation of adult-born DGCs after SE

Thus far, I have described structural abnormalities of adult-born and, to a lesser extent, pre-existing DGCs in experimental TLE, including changes in their axonal projections. However, little is known about how the *inputs* onto birthdated DGCs are

altered during epileptogenesis. Previous studies indicate that DGCs with HBDs receive higher amounts of excitatory inputs than inhibitory inputs (Thind et al., 2008) and also more mossy fiber inputs onto their apical dendrites (Murphy et al., 2011). Others have shown that normotopic and hilar ectopic DGCs in the epileptic brain receive increased excitatory inputs (Scharfman et al., 2000; Zhan et al., 2010; Zhang et al., 2012) as compared with those in the intact brain. Despite these findings, less is known about exactly what cell types are contributing to increased excitatory inputs and the age of the DGCs that are receiving these inputs.

Rabies virus retrograde trans-synaptic tracing represents an ideal strategy to understand and quantify the changes in presynaptic inputs onto age-defined cohorts of DGCs in the intact brain. First introduced by Wickersham et al., the technique takes advantage of the unique properties of the rabies virus to travel retrogradely across synapses (Wickersham et al., 2007). To apply this approach for mapping inputs onto specific DGC cohorts, we first birthdate DGCs either neonatally or during adulthood by injecting a retrovirus that expresses green fluorescent protein (GFP), the avian sarcoma leukosis virus receptor (TVA) and the rabies glycoprotein (Rgp) (**Figure 1.2**). We later inject an avian envelope subgroup A (EnvA) pseudotyped rabies virus that expresses mCherry (mCh) in place of Rgp. With the recognition of EnvA with its cognate receptor, TVA, the rabies virus only enters cells that have previously been infected by the retrovirus marking them GFP+/mCh+. As the rabies virus requires Rgp to travel retrogradely across synapses, the virus will complement with Rgp within these dual-infected 'starter' cells and travel a single synapse back to the starter cell's first-order presynaptic inputs and label them mCh+ only. In these presynaptic cells, the rabies virus no longer has access to Rgp

and thus it cannot travel across any more synapses. This method allows us to selectively identify and compare presynaptic inputs onto birthdated populations of DGCs.

The rabies virus approach has been previously used to study the monosynaptic inputs onto adult-born DGCs in the intact mouse brain under various physiologic stimuli and environmental conditions. Several studies utilized the approach to understand how inputs onto adult-born DGCs evolved as they progressed through development (Vivar et al., 2012; Deshpande et al., 2013). Others have shown that exercise increased the total number of afferent inputs onto adult-born DGCs (Vivar et al., 2016) while environmental enrichment in the early phases of their maturation promoted increased afferent inputs as well as the recruitment of new neuronal connections (Bergami et al., 2015). In Chapter 2 and Appendix A, I describe how we applied this approach to examine the differences in first-order presynaptic inputs onto adult- and early-born DGCs in a rat SE model of TLE. We compare differences in presynaptic inputs from the dentate gyrus itself as well as extra-dentate areas to determine whether adult- and early-born DGCs integrate differently after SE as compared with those in the intact brain.

Consequences of seizure-induced hippocampal reorganization

The increase in hippocampal neurogenesis after SE also leads to accelerated maturation and integration of DGCs (Overstreet-Wadiche et al., 2006). There is debate on the overall effect of this faster differentiation on the hippocampal network, but some recent studies may shed light on this important question. Eliminating adult-born DGCs shortly before SE (Cho et al., 2015; Hosford et al., 2016) and immediately after (Jung et al., 2004) reduces seizure frequency, suggesting that the adult-born population plays an integral role in the development of the pro-seizure network. However, others have found

that adult-born DGCs may mitigate excitability (Jakubs et al., 2006) and that hilar ectopic DGCs have increased tonic gamma-aminobutyric acid (GABA) inhibition (Zhan and Nadler, 2009). These differing findings suggest that there are subpopulations of adult-born DGCs of which some are pro-excitatory and others pro-inhibitory.

Several recent studies have demonstrated that relatively small populations of highly-innervated cells are capable of exerting powerful influences on the hippocampal network. These cells were first termed 'hub cells' by Morgan and Soltesz who demonstrated with computational modeling that as few as 5 percent of highly interconnected DGCs were enough to induce seizure activity (Morgan and Soltesz, 2008). Hilar ectopic DGCs in particular have a high capacity for sprouting and receiving synapses (Cameron et al., 2011; Scharfman and Pierce, 2012), potentially giving them the ability to orchestrate large-scale changes in network excitability.

In addition to DGCs, other cell types in the dentate gyrus are also capable of sprouting after SE. An important population is the somatostatin-positive hilar perforant path-associated interneurons that have been shown to sprout axons in human TLE (Mathern et al., 1995) and in rodent experimental models where they synapse onto DGCs (Zhang et al., 2009; Thind et al., 2010). The mechanism of this sprouting remains unclear. One possibility is that, because somatostatin interneurons are especially vulnerable to SE-induced death in both TLE patients and experimental models (de Lanerolle et al., 1989; Buckmaster and Dudek, 1997), the surviving population sprouts to compensate for the loss of GABAergic cells and synapses. Another hypothesis is that inhibitory sprouting occurs to target the increased numbers of excitatory DGCs arising from seizure-induced neurogenesis. The teleological conclusion is that inhibitory sprouting may serve to

mitigate the pro-excitatory environment in the dentate gyrus after SE, but recent evidence demonstrates that it might not be sufficient to overcome the hyperexcitability (Hofmann et al., 2016).

Beyond DGC-to-DGC connections, other areas of the hippocampus have been shown to participate in sprouting, particularly towards the dentate gyrus. Under basal conditions, CA3 neurons send backprojections to the dentate gyrus, mostly arising from inhibitory interneurons (Li et al., 1994; Bergami et al., 2015; Vivar et al., 2016). However, after SE, functional evidence suggests that axonal projections to the dentate gyrus from CA3 pyramidal cells increase dramatically (Scharfman et al., 2000; Zhang et al., 2012) which may enhance recurrent excitation. Similar to the results in CA3, CA1 pyramidal cells axons also sprout in various epilepsy models (Perez et al., 1996; Esclapez et al., 1999; Bausch and McNamara, 2000, 2004). Remarkably, Peng et al. recently showed that CA1 somatostatin interneurons are capable of sprouting axon collaterals across the hippocampal fissure into the dentate gyrus where they inhibit DGCs (Peng et al., 2013). These findings suggest that several areas of the hippocampus demonstrate extensive remodeling after SE to create a multiplicity of coordinated, recurrent excitatory and inhibitory loops, some of which may contribute to seizure activity.

Embryonic cortical development

Abnormalities in adult neurogenesis appear to play a critical role in the development of experimental TLE. In contrast, genetic epilepsies usually present in the pediatric population and their pathophysiological processes often involve changes during embryonic or early postnatal development. During development of the mammalian neocortex, the neuroepithelium adjacent to the lateral ventricle expands and becomes the

ventricular zone (VZ). As neurogenesis continues, a secondary layer, the SVZ, grows above the VZ. The VZ-SVZ contain the neural progenitor population, radial glia cells, that are responsible for generating a significant proportion of the post-mitotic neurons in the neocortex (Noctor et al., 2004). The cortex develops in an inside-out manner where the deep layer VI neurons are born first and subsequent layers migrate past them with layer I being the last to develop (Angevine and Sidman, 1961). While both contain a proliferative VZ (Hockfield and McKay, 1985), the developing primate and rodent neocortex differ in that primates also demonstrate the presence of an outer SVZ (oSVZ) (Smart et al., 2002; Zecevic et al., 2005), a neurogenic zone that is largely absent in rodents. Recent evidence suggests that outer radial glia cells (oRGs), the progenitor population in the oSVZ, contribute significantly to human cortical expansion and may be responsible for the increased brain surface area and gyrification (Fietz et al., 2010; Hansen et al., 2010; Reillo et al., 2011).

Understanding neurodevelopmental disease mechanisms has traditionally involved the use of animal models or studies of postmortem human tissue. For neurogenetic disorders in particular, genetically modified mice have been useful. For genetic disorders that impact neurodevelopment, however, these mouse models often fail to recapitulate critical aspects of the human development, such as expansion of the oSVZ that may influence disease phenotypes. Postmortem human tissues may be difficult to acquire and generally represent late stages of disease that offer limited mechanistic information in many instances. The advent of the iPSC method by Yamanaka and colleagues in 2006 (Takahashi and Yamanaka, 2006) redefined the field of translational research by providing access to patient-derived cells for clinical disease studies

(Takahashi et al., 2007; Yu et al., 2007). The iPSC approach not only enables the study of neural development and function in neurogenetic disorders using patient-specific neurons (Dolmetsch and Geschwind, 2011; Marchetto et al., 2011; Pasca et al., 2014; Parent and Anderson, 2015), but the neurons also harbor both the mutant gene of interest as well as other potential modifier genes within the patient's specific genomic background.

The iPSC method

Generating iPSCs from somatic cells involves introducing specific transcription factors — the most common being Oct3/4, Klf4, Sox2, and c-Myc — into the cells to reprogram them into a pluripotent state. Initially, Yamanaka and colleagues introduced the transcription factors using retroviral vectors (Takahashi et al., 2007); however, concerns regarding the genomic integration of these vectors, particularly if iPSCs would ultimately be used in a clinical setting, quickly drove the field towards non-integrating approaches such as episomal vectors (Yu et al., 2009) or Sendai viral vectors (Fusaki et al., 2009). The somatic cell source used most often is dermal fibroblasts, although recent studies have demonstrated the feasibility of using less invasive sources such as hematopoietic cells or kidney epithelial cells derived from urine (Zhou et al., 2011; Wang et al., 2013). After introduction of the reprogramming factors, fibroblasts are maintained in a reprogramming media that is similar to pluripotent stem cell maintenance media. Within a period of 2-4 weeks, granular colonies begin to appear within the fibroblasts. These colonies are manually isolated and maintained in pluripotent stem cell media for expansion. After reprogramming, iPSCs share remarkable similarities to human embryonic stem cells (hESCs). They have similar morphologies to hESCs and express pluripotency markers such as OCT3/4, NANOG and SSEA4 (**Figure 1.3A-A''**). They also

can be differentiated *in vitro* to generate all three germ cell layers and are capable of forming teratomas after injection into immunocompromised mice (Takahashi et al., 2007).

Directed neuronal differentiation

Based upon increasing knowledge of the molecular cues that underlie embryonic brain development, various protocols have been developed to direct pluripotent stem cells towards specific neuronal cell fates such as cortical-like excitatory neurons (**Figure 1.3B, C**) (Chambers et al., 2009; Shi et al., 2012), cortical-like medial ganglionic eminence (MGE)-derived inhibitory interneurons (Liu et al., 2013a; Maroof et al., 2013), astrocytes (Krencik and Zhang, 2011; Juopperi et al., 2012) and many other cell types. To date, iPSCs have been generated for over 20 different CNS disorders, ranging from neurodevelopmental to neurodegenerative diseases (Reviewed in Marchetto et al., 2011; Srikanth and Young-Pearse, 2014), and this number is growing rapidly. Additionally, new gene editing technologies such as CRISPR/Cas9 now allow for the generation of 'virtual patients' using control iPSCs and for correcting disease-causing mutations in patient cells to produce isogenic controls (Cong et al., 2013).

Organoid technology

Adherent cultures offer important insight into cellular and molecular mechanisms of disease but are incapable of mimicking the expansive three-dimensional (3D) architecture of normal neuronal circuitry *in vivo*. The first 3D neuronal culturing techniques took advantage of the self-aggregating properties of pluripotent stem cells to generate polarized neural tissue (Eiraku et al., 2008; Gaspard et al., 2008; Danjo et al., 2011). However, these cultures lacked the organization and complexity of the human neocortex.

The advent of cerebral organoid technology (Lancaster et al., 2013) offered the ability to probe disease mechanisms and understand human neural development by allowing for studies in a system that is more anatomically relevant in its spatial organization. By relying on fluid dynamic principles, these cerebral organoids were constantly spun in a bioreactor and share many features of the human brain including progenitor zones that variably recapitulate the dorsal cortical VZs, laminar cortical structures, primitive regional specifications, as well as an enlarged SVZ with oRGs. Since then, the technology has been honed by several groups to create brain region-specific organoids, particularly cortical organoids (Mariani et al., 2012; Kadoshima et al., 2013; Pasca et al., 2015; Qian et al., 2016).

Paşca et al. developed laminar cortical spheroids that were electrophysiologically active (Pasca et al., 2015), while Mariani et al. reported an alternative cortical organoid strategy that generates neurons of both dorsal and ventral telencephalic origins (Mariani et al., 2012). However, the feasibility of using these organoids in biological applications, particularly disease modeling and drug discovery, is limited by factors such as the inability to generate all six cortical layers, disorganization of structures, and concerns regarding reproducibility and heterogeneity. Qian et al. recently pioneered a miniature bioreactor (Spin Ω) (**Figure 1.3D**) accompanied by an innovative protocol utilizing Wnt agonists and SMAD inhibitors to generate highly organized cortical tissue (**Figure 1.3E-G**) that assembles into six cortical layers with a distinct oRG layer — both critical components in the developing human neocortex (Qian et al., 2016). The brain organoid approach holds great promise for studying human brain developmental changes underlying epileptogenesis and as a drug-screening platform for personalized therapies.

Disadvantages of iPSCs

It is important to note that despite certain advantages over rodents, human iPSC disease models have their own disadvantages. For one, patient iPSCs have a limited, if any, role for the investigation of acquired epilepsies. Another critical issue is the difficulty of generating fully mature cell types, including neurons, from iPSCs. Functional studies of iPSC-derived neurons demonstrate an immature electrophysiological profile that more closely mimics neurons within the developing embryonic brain rather than those of the adult brain. This hurdle is significant particularly for studies of late-onset neurological disorders such as Parkinson's and Alzheimer's diseases. However, many groups are working to overcome this obstacle by creative measures such as prematurely aging cells (Miller et al., 2013) as well as deriving new culture conditions to promote neuronal maturation and the acquisition of mature electrophysiological properties (Bardy et al., 2015). Lastly, as a result of erosion of X-inactivation, concerns exist regarding variability when using female iPSCs. Studies have demonstrated that derivation conditions, passage number, and feeder cells all heavily impact the X-inactivation status of female iPSCs (Tchieu et al., 2010; Tomoda et al., 2012). Work in the field has shown that the inactive X-chromosome can reactivate in female iPSCs and remain active despite neuronal differentiation, leading cells to aberrantly express some genes through active transcription from both X-chromosomes (Mekhoubad et al., 2012). These findings point to a need to carefully monitor the X-inactivation status in female iPSCs and their terminally differentiated progeny, particularly in X-linked disorders.

iPSC modeling of genetic epilepsies

In the 25 years since the first gene linked to a clinical seizure phenotype was

discovered (Shoffner et al., 1990), there has been an explosion in the number of genetic loci that are reported to be important in epilepsy. To date, over 500 genes are listed and this number is rising rapidly (Noebels, 2015; Ran et al., 2015). Using iPSCs to model genetic epilepsies with early childhood or infantile onset is currently favored by many groups owing to the ease of modeling early development with iPSCs. Disorders with complete or near complete epilepsy penetrance that have been modeled to date include Dravet syndrome (Higurashi et al., 2013; Jiao et al., 2013; Liu et al., 2013b), Angelman syndrome (Chamberlain et al., 2010), and a Rett syndrome variant caused by cyclin-dependent kinase-like 5 (*CDKL5*) mutations (Ricciardi et al., 2012; Livide et al., 2015).

Modeling epileptic syndromes

Beyond “pure” genetic epilepsy syndromes, several other neurodevelopmental disorders with seizures as a manifestation have been studied using iPSCs. These include Rett syndrome, fragile X syndrome (Urbach et al., 2010; Sheridan et al., 2011; Bar-Nur et al., 2012; Liu et al., 2012; Teliás et al., 2013), Timothy Syndrome (Pasca et al., 2011; Yazawa et al., 2011; Krey et al., 2013), 15q11.2 deletion syndrome (Yoon et al., 2014) and Phelan-McDermid syndrome (Shcheglovitov et al., 2013). Several studies have utilized iPSCs to explore the mechanisms of Rett syndrome, an autism spectrum disorder (ASD) caused by mutations in the X-linked methyl-CpG-binding protein 2 (MeCP2) gene. Various groups reported that Rett syndrome patient iPSC-derived cortical-like excitatory neurons have decreased synapses, smaller somas and altered electrophysiological properties (Marchetto et al., 2010; Ananiev et al., 2011; Cheung et al., 2011). Another study using Rett syndrome iPSCs found that patient iPSCs have similar neural progenitor formation as compared with controls but have alterations in neuronal maturation (Kim et

al., 2011a). This defect may be a result of a downstream target of MeCP2 that is critical for the proper maturation of neurons. Indeed, Tang et al. recently found that a neuron-specific K^+ - Cl^- cotransporter 2 (KCC2) is decreased in Rett syndrome iPSC-derived neurons, leading to a defect in GABA functional switching (Tang et al., 2016). Overexpression of KCC2 was able to rescue the impairment in Rett syndrome neurons. The functional switch of GABA from excitation to inhibition is a crucial part of excitatory neuron development and may partially explain the synaptic transmission and maturation defects found by other groups.

Using organoids to model neurological disorders

Modeling neurological diseases in 3D culture is a relatively new field and thus studies using it to model neurodevelopmental disorders are few. The ability to more faithfully recapture the progress of human neurodevelopment, however, makes organoid technology an attractive system for future studies that aim to understand disease mechanisms in a more spatially relevant system. A landmark paper from Lancaster et al. demonstrated that human pluripotent stem cells can organize into cerebral organoid structures (Lancaster et al., 2013). In the same report, they also described the generation of organoids from iPSCs derived from a patient with autosomal recessive primary microcephaly due to a truncation mutation of cyclin-dependent kinase 6 regulatory subunit-associated protein 2 (*CDK5RAP2*). They found that patient-derived organoids have premature neuronal maturation, smaller progenitor zones and fewer neurons as compared with control organoids, phenotypes that could be partially rescued by restoring the missing protein. Others have used cerebral organoids to model ASD, demonstrating that organoids derived from ASD-patient iPSCs have an overproduction of GABAergic

interneurons (Mariani et al., 2015). Lastly, Bershteyn et al. harnessed organoid technology to model Miller-Dieker syndrome (MDS), a severe form of lissencephaly that presents with intractable seizures. They report that MDS patient iPSC-derived organoids had defects in neural stem cell migration, oRG mitotic defects and premature apoptosis of neuroepithelial cells (Bershteyn et al., 2017).

An important area of organoid research is understanding how external perturbations may affect the development of the early human embryonic brain. Much work has been done to understand how the Zika virus (ZKV) causes one of the most devastating consequences of its infection, microcephaly. Several groups have utilized the organoid technology to probe this question and the unifying theme has emerged that organoids infected with ZKV show depletion, apoptosis and premature differentiation of neural progenitor cells (Cugola et al., 2016; Garcez et al., 2016; Qian et al., 2016; Wells et al., 2016; Gabriel et al., 2017), potentially as the underlying cause of infantile microcephaly. Of note, Li et al. highlighted the unique capability of organoids when they generated organoids from hESCs with a phosphatase and tensin homolog (PTEN) knockout. The group found that PTEN mutant human organoids, but not PTEN mutant mouse organoids, demonstrated surface expansion and folding, giving an important clue into gyrification of the human brain. In the same study, surface folding could be impaired with the introduction of ZKV, providing further evidence that ZKV impairs expansion of neural stem cells (Li et al., 2016). These studies point to the utility of organoid technology for disease modeling, particularly when there are aspects of the disease, such as oRG defects or SVZ organizational changes, that are subtle and more difficult to capture in adherent cultures.

Protocadherin-19 female limited epilepsy

Protocadherin-19 (PCDH19) female limited epilepsy (FLE), also known as early infantile epileptic encephalopathy type 9 (EIEE9), is a condition first described by Juberg and Hellman in 1971 (Juberg and Hellman, 1971). The clinical presentation is highly variable but the hallmark findings are early onset seizures, cognitive impairment and psychiatric features (Ryan et al., 1997; Scheffer et al., 2008; Depienne et al., 2009). The range of cognitive impairment varies from normal intellect to mental retardation within families. Upon imaging, magnetic resonance images (MRIs) of FLE patient brains showed no structural abnormalities or morphological differences as compared with normal, healthy controls (Scheffer et al., 2008). There has been a single report, however, of a patient whose postmortem surgical frontal lobe specimen demonstrated cortical dysplasia, abnormal neurons in the white matter and abnormal morphology of individual cortical neurons (Ryan et al., 1997).

Inheritance pattern of PCDH19 FLE

A cardinal feature of PCDH19 FLE is its remarkable inheritance pattern. The condition is X-linked with the phenotype only affecting females (Juberg and Hellman, 1971; Ryan et al., 1997). Males carrying disease mutations are spared with normal cognitive development and no evidence of seizures. Recently, sequencing analysis uncovered that the disorder is attributable to mutations in the X-linked *PCDH19* gene encoding the PCDH19 protein (Dibbens et al., 2008). Most of the reported pathogenic mutations in *PCDH19* to date are inherited (typically from the father) or *de novo* loss-of-function mutations in exon 1 of the gene (Dibbens et al., 2008; Depienne et al., 2009; van Harsseel et al., 2013) with sporadic reports of other exons also being affected. In addition,

some patients carry large gene deletions that encompass the entire *PCDH19* gene (Depienne et al., 2011). This inheritance pattern differs from the classical X-linked modes of inheritance in which males are generally affected more severely than females. While many FLE patients carry *de novo* mutations, within a family, most female offspring of carrier males are affected while male-to-male inheritance does not occur (Scheffer et al., 2008). Disease-causing mutations are highly (>90%) penetrant (Dibbens et al., 2008). Currently, mutations in *PCDH19* are recognized as the second leading cause of monogenic epilepsies (Depienne and LeGuern, 2012).

Postulated mechanisms of disease

Perhaps the most widely accepted theory of how FLE develops is the cellular interference hypothesis (Johnson, 1980; Wieland et al., 2004). In heterozygously affected females, the cellular interference model posits that random X-inactivation creates a state of tissue mosaicism. The coexistence of both wildtype and mutant *PCDH19*-expressing cells causes abnormal neural development through aberrant interactions between these two cell populations (**Figure 1.4B**). Normal males and females have one and two copies of wildtype *PCDH19*, respectively, and thus have a homogeneous cell population without disease. Similarly, males who are affected hemizygotously by a mutant copy of *PCDH19* would also have a homogeneous cell population and thus would not develop the disease. In addition to males with germline *PCDH19* mutations being unaffected carriers, the cellular interference theory is supported by several reported cases of EIEE9 in males with somatic mosaicism who express wildtype *PCDH19* in some cells and mutant *PCDH19* in others (Depienne et al., 2009; Terracciano et al., 2016; Thiffault et al., 2016). Further support is found in a different disorder with a similar inheritance pattern, craniofrontonasal

syndrome (CFNS). CFNS is also an X-linked developmental disorder that results in multiple skeletal abnormalities in females with no or very mild abnormalities in males (Saavedra et al., 1996). The disease has been mapped to mutations in Ephrin-B1 (EFNB1) (Wieland et al., 2004), a ligand for the Eph class of receptor tyrosine kinases, postulated to be important in skeletal development and patterning. Studies of an *Efnb1*^{+/-} mouse model show that ephrin-B1-positive and ephrin-B1-negative cells segregate into separate compartments after random X-inactivation, leading to various skeletal abnormalities (Compagni et al., 2003). Importantly, polydactyly was exclusively found in the heterozygous female mice, suggesting that ectopic interactions between ephrin-B1-positive and negative cells mediate boundary formation. Taken together, these data support the cellular interference hypothesis for the inheritance of PCDH19 FLE, yet its exact mechanism remains elusive.

Several other hypotheses have been proposed for the mechanism of PCDH19 FLE with less evidence than the cellular interference theory. One thought is that *PCDH19* is dispensable for the development of the male brain and that the male brain could be protected from the adverse effects of *PCDH19* mutations by fetal androgens (Ryan et al., 1997). A second theory is that there is a functional homologue of the *PCDH19* gene on the Y-chromosome that is protective in males. Indeed, a protocadherin gene is found on the Y-chromosome, *PCDH11Y*. It is plausible that in the absence of a functional copy of *PCDH19*, *PCDH11Y* compensates. This hypothesis is supported by evidence of a functional paralogue of *PCDH11Y* on the X-chromosome, *PCDH11X*. These two genes have strong sequences similarities but different brain expression patterns (Dibbens et al., 2008). The differences in expression may explain the different abilities of the two sexes

to compensate for a *PCDH19* mutation. However, this theory does not explain the presence of affected males with mosaic mutations. A final theory is that there is regional interference of *PCDH19* mutations with the X-inactivation process downstream of the X-inactive specific transcript (*XIST*). Escape from X-inactivation requires region-specific signaling and mutations interfering with this process could result in gene-specific failure of X-inactivation. It is possible that the mutant *PCDH19* gene in FLE fails to inactivate and causes the disease through functional disomy. There have, in fact, been several reports of patients with functional disomy of the Xq28 chromosome region that present clinically with epilepsy and cognitive impairment (Sanlaville et al., 2005; Sanlaville et al., 2009).

The role of PCDH19 in development

PCDH19 belongs to the $\delta 2$ non-clustered protocadherin subclass of the cadherin superfamily of cell-cell adhesion molecules (Wolverton and Lalande, 2001) and is widely expressed throughout the embryonic and adult CNS in mammals (Gaitan and Bouchard, 2006; Dibbens et al., 2008; Kim et al., 2010; Kim et al., 2011b). The *PCDH19* protein has six extracellular domains that are responsible for its adhesive function (**Figure 1.4A**). While its biological role is still debated, previous studies indicate that *PCDH19* interacts with N-cadherin and the WAVE complex (**Figure 1.4A**) and that these interactions are important for cellular migration as well as formation and maintenance of cell-cell junctions, respectively, during brain development (Biswas et al., 2010; Emond et al., 2011). How *PCDH19* mediates neural development remains largely unknown, but evidence in the zebrafish may shed some light on its function. Morpholino knockdown of *pcdh19* in the zebrafish embryo results in a disruption of brain morphogenesis and anterior neurulation (Emond et al., 2009; Biswas et al., 2010). In another study, deletion of *pcdh19* in zebrafish

using transcription activator-like effector nucleases (TALENs) disrupts the axonal arborization and columnar organization of the zebrafish optic tectum (Cooper et al., 2015). In the *Pcdh19* knockout mouse, Pederick et al. observed no gross morphological, structural or functional abnormalities in the brains of *Pcdh19*^{+/-} females. However, they did notice subtle regional differences and clonal cortical columns that were either *Pcdh19*-expressing or null, but not both (Pederick et al., 2016). The lack of an overt phenotype in the *Pcdh19*-mutant mouse is not surprising as human and murine X-inactivation are very different (Goto et al., 1998) and protocadherins have redundant functions in the mouse brain (Lefebvre et al., 2012). These features highlight the importance of selecting specific models for diseases that may not manifest in all experimental systems.

Other protocadherins have been shown to play important roles in early neural development such as cellular migration, axon outgrowth, dendritic patterning and synaptogenesis. For instance, in the zebrafish, overexpression of protocadherin-18a results in splitting of the neural tube, diminished cell migration and increased cell aggregation (Aamar and Dawid, 2008). In mice, protocadherin-17 is important for determining the quantity and docking of synaptic vesicles in the basal ganglia (Hoshina et al., 2013) while protocadherin-10 functions in synaptic pruning by aiding in postsynaptic degradation and elimination (Tsai et al., 2012). Lefebvre et al. knocked out all 22 genes of the mouse γ -subcluster protocadherins (*Pcdhg*) and found that it disrupted dendritic tiling and self-avoidance in starburst amacrine cells and cerebellar Purkinje cells. In the same study, simply restoring one isoform of the 22 deleted *Pcdhg* genes was able to reverse the dendritic phenotype suggesting that redundancies exist in the mouse protocadherins (Lefebvre et al., 2012). Nonetheless, others have found that several of the

individual protocadherins are required for axonal outgrowth and fiber tract formation in both mammals and zebrafish (Uemura et al., 2007; Piper et al., 2008; Biswas et al., 2014; Hayashi et al., 2014).

Questions addressed in this dissertation

This dissertation aims to explore how alterations in neurodevelopment, both during adulthood and embryonically, can lead to morphological and functional changes that may underlie epileptogenesis. In Chapter 2, the question of how adult-born DGCs differentially integrate into the chronically epileptic brain is addressed. The first-order presynaptic inputs onto adult-born DGCs in the epileptic brain are compared to those in the intact brain as well as presynaptic inputs onto early-born DGCs that were mature at the time of SE. The results indicate that both adult- and early-born DGCs receive excessive recurrent, excitatory inputs from various areas of the hippocampus in distinct patterns, highlighting that both populations of DGCs may play a role in the changes that lead to chronic seizures.

Chapter 3 describes an investigation into how mutations in the *PCDH19* gene leads to PCDH19 FLE using an iPSC model. We use patient-derived iPSCs to generate both cortical-like excitatory and inhibitory neurons in adherent cultures and show that the neurons have morphological and functional changes as compared with controls. Finally, we also utilize 3D culturing techniques to generate cortical organoids to explore defects in corticogenesis and lamination.

Notes to Chapter 1

Parts of this chapter were published in modified form as:

Du X, Parent JM (2015) Using Patient-Derived Induced Pluripotent Stem Cells to Model and Treat Epilepsies. *Curr Neurol Neurosci Rep* 15:71.

References

- Aamar E, Dawid IB (2008) Protocadherin-18a has a role in cell adhesion, behavior and migration in zebrafish development. *Developmental biology* 318:335-346.
- Althaus AL, Zhang H, Parent JM (2016) Axonal plasticity of age-defined dentate granule cells in a rat model of mesial temporal lobe epilepsy. *Neurobiology of disease* 86:187-196.
- Althaus AL, Sagher O, Parent JM, Murphy GG (2015) Intrinsic neurophysiological properties of hilar ectopic and normotopic dentate granule cells in human temporal lobe epilepsy and a rat model. *Journal of neurophysiology* 113:1184-1194.
- Altman J, Das GD (1965) Autoradiographic and histological evidence of postnatal hippocampal neurogenesis in rats. *J Comp Neurol* 124:319-335.
- Ananiev G, Williams EC, Li H, Chang Q (2011) Isogenic pairs of wild type and mutant induced pluripotent stem cell (iPSC) lines from Rett syndrome patients as in vitro disease model. *PLoS one* 6:e25255.
- Angevine JB, Jr., Sidman RL (1961) Autoradiographic study of cell migration during histogenesis of cerebral cortex in the mouse. *Nature* 192:766-768.
- Arvidsson A, Collin T, Kirik D, Kokaia Z, Lindvall O (2002) Neuronal replacement from endogenous precursors in the adult brain after stroke. *Nature medicine* 8:963-970.
- Asadi-Pooya AA, Stewart GR, Abrams DJ, Sharan A (2016) Prevalence and incidence of drug-resistant mesial temporal lobe epilepsy in the United States. *World Neurosurg*.
- Babb TL, Kupfer WR, Pretorius JK, Crandall PH, Levesque MF (1991) Synaptic reorganization by mossy fibers in human epileptic fascia dentata. *Neuroscience* 42:351-363.
- Banerjee PN, Filippi D, Allen Hauser W (2009) The descriptive epidemiology of epilepsy—a review. *Epilepsy Res* 85:31-45.
- Bar-Nur O, Caspi I, Benvenisty N (2012) Molecular analysis of FMR1 reactivation in fragile-X induced pluripotent stem cells and their neuronal derivatives. *Journal of molecular cell biology* 4:180-183.
- Bardy C, van den Hurk M, Eames T, Marchand C, Hernandez RV, Kellogg M, Gorris M, Galet B, Palomares V, Brown J, Bang AG, Mertens J, Bohnke L, Boyer L, Simon S, Gage FH (2015) Neuronal medium that supports basic synaptic functions and activity of human neurons in vitro. *Proceedings of the National Academy of Sciences of the United States of America*.

- Bausch SB, McNamara JO (2000) Synaptic connections from multiple subfields contribute to granule cell hyperexcitability in hippocampal slice cultures. *Journal of neurophysiology* 84:2918-2932.
- Bausch SB, McNamara JO (2004) Contributions of mossy fiber and CA1 pyramidal cell sprouting to dentate granule cell hyperexcitability in kainic acid-treated hippocampal slice cultures. *Journal of neurophysiology* 92:3582-3595.
- Bengzon J, Kokaia Z, Elmer E, Nanobashvili A, Kokaia M, Lindvall O (1997) Apoptosis and proliferation of dentate gyrus neurons after single and intermittent limbic seizures. *Proceedings of the National Academy of Sciences of the United States of America* 94:10432-10437.
- Bergami M, Masserdotti G, Temprana SG, Motori E, Eriksson TM, Gobel J, Yang SM, Conzelmann KK, Schinder AF, Gotz M, Berninger B (2015) A critical period for experience-dependent remodeling of adult-born neuron connectivity. *Neuron* 85:710-717.
- Bershteyn M, Nowakowski TJ, Pollen AA, Di Lullo E, Nene A, Wynshaw-Boris A, Kriegstein AR (2017) Human iPSC-Derived Cerebral Organoids Model Cellular Features of Lissencephaly and Reveal Prolonged Mitosis of Outer Radial Glia. *Cell stem cell*.
- Biswas S, Emond MR, Jontes JD (2010) Protocadherin-19 and N-cadherin interact to control cell movements during anterior neurulation. *The Journal of cell biology* 191:1029-1041.
- Biswas S, Emond MR, Duy PQ, Hao le T, Beattie CE, Jontes JD (2014) Protocadherin-18b interacts with Nap1 to control motor axon growth and arborization in zebrafish. *Mol Biol Cell* 25:633-642.
- Buckmaster PS (2004) Laboratory animal models of temporal lobe epilepsy. *Comp Med* 54:473-485.
- Buckmaster PS, Dudek FE (1997) Neuron loss, granule cell axon reorganization, and functional changes in the dentate gyrus of epileptic kainate-treated rats. *J Comp Neurol* 385:385-404.
- Buckmaster PS, Zhang GF, Yamawaki R (2002) Axon sprouting in a model of temporal lobe epilepsy creates a predominantly excitatory feedback circuit. *The Journal of neuroscience : the official journal of the Society for Neuroscience* 22:6650-6658.
- Cameron HA, McKay RD (2001) Adult neurogenesis produces a large pool of new granule cells in the dentate gyrus. *J Comp Neurol* 435:406-417.
- Cameron MC, Zhan RZ, Nadler JV (2011) Morphologic integration of hilar ectopic granule cells into dentate gyrus circuitry in the pilocarpine model of temporal lobe epilepsy. *J Comp Neurol* 519:2175-2192.

- Carreno M, Donaire A, Sanchez-Carpintero R (2008) Cognitive disorders associated with epilepsy: diagnosis and treatment. *Neurologist* 14:S26-34.
- Cassell MD, Brown MW (1984) The distribution of Timm's stain in the nonsulphide-perfused human hippocampal formation. *J Comp Neurol* 222:461-471.
- Chamberlain SJ, Chen PF, Ng KY, Bourgois-Rocha F, Lemtiri-Chlieh F, Levine ES, Lalande M (2010) Induced pluripotent stem cell models of the genomic imprinting disorders Angelman and Prader-Willi syndromes. *Proceedings of the National Academy of Sciences of the United States of America* 107:17668-17673.
- Chambers SM, Fasano CA, Papapetrou EP, Tomishima M, Sadelain M, Studer L (2009) Highly efficient neural conversion of human ES and iPS cells by dual inhibition of SMAD signaling. *Nature biotechnology* 27:275-280.
- Cheung AY, Horvath LM, Grafodatskaya D, Pasceri P, Weksberg R, Hotta A, Carrel L, Ellis J (2011) Isolation of MECP2-null Rett Syndrome patient hiPS cells and isogenic controls through X-chromosome inactivation. *Human molecular genetics* 20:2103-2115.
- Cho KO, Lybrand ZR, Ito N, Brulet R, Tafacory F, Zhang L, Good L, Ure K, Kernie SG, Birnbaum SG, Scharfman HE, Eisch AJ, Hsieh J (2015) Aberrant hippocampal neurogenesis contributes to epilepsy and associated cognitive decline. *Nature communications* 6:6606.
- Clifford DB, Olney JW, Maniotis A, Collins RC, Zorumski CF (1987) The functional anatomy and pathology of lithium-pilocarpine and high-dose pilocarpine seizures. *Neuroscience* 23:953-968.
- Compagni A, Logan M, Klein R, Adams RH (2003) Control of skeletal patterning by ephrinB1-EphB interactions. *Developmental cell* 5:217-230.
- Cong L, Ran FA, Cox D, Lin S, Barretto R, Habib N, Hsu PD, Wu X, Jiang W, Marraffini LA, Zhang F (2013) Multiplex genome engineering using CRISPR/Cas systems. *Science* 339:819-823.
- Cooper SR, Emond MR, Duy PQ, Liebau BG, Wolman MA, Jontes JD (2015) Protocadherins control the modular assembly of neuronal columns in the zebrafish optic tectum. *The Journal of cell biology* 211:807-814.
- Couillard-Despres S, Winner B, Karl C, Lindemann G, Schmid P, Aigner R, Laemke J, Bogdahn U, Winkler J, Bischofberger J, Aigner L (2006) Targeted transgene expression in neuronal precursors: watching young neurons in the old brain. *Eur J Neurosci* 24:1535-1545.
- Cugola FR et al. (2016) The Brazilian Zika virus strain causes birth defects in experimental models. *Nature* 534:267-271.

- Danjo T, Eiraku M, Muguruma K, Watanabe K, Kawada M, Yanagawa Y, Rubenstein JL, Sasai Y (2011) Subregional specification of embryonic stem cell-derived ventral telencephalic tissues by timed and combinatory treatment with extrinsic signals. *The Journal of neuroscience : the official journal of the Society for Neuroscience* 31:1919-1933.
- Dashtipour K, Tran PH, Okazaki MM, Nadler JV, Ribak CE (2001) Ultrastructural features and synaptic connections of hilar ectopic granule cells in the rat dentate gyrus are different from those of granule cells in the granule cell layer. *Brain Res* 890:261-271.
- de Lanerolle NC, Kim JH, Robbins RJ, Spencer DD (1989) Hippocampal interneuron loss and plasticity in human temporal lobe epilepsy. *Brain Res* 495:387-395.
- Deng W, Aimone JB, Gage FH (2010) New neurons and new memories: how does adult hippocampal neurogenesis affect learning and memory? *Nat Rev Neurosci* 11:339-350.
- Deng W, Saxe MD, Gallina IS, Gage FH (2009) Adult-born hippocampal dentate granule cells undergoing maturation modulate learning and memory in the brain. *The Journal of neuroscience : the official journal of the Society for Neuroscience* 29:13532-13542.
- Depienne C, LeGuern E (2012) PCDH19-related infantile epileptic encephalopathy: an unusual X-linked inheritance disorder. *Human mutation* 33:627-634.
- Depienne C et al. (2009) Sporadic infantile epileptic encephalopathy caused by mutations in PCDH19 resembles Dravet syndrome but mainly affects females. *PLoS genetics* 5:e1000381.
- Depienne C et al. (2011) Mutations and deletions in PCDH19 account for various familial or isolated epilepsies in females. *Human mutation* 32:E1959-1975.
- Deshpande A, Bergami M, Ghanem A, Conzelmann KK, Lepier A, Gotz M, Berninger B (2013) Retrograde monosynaptic tracing reveals the temporal evolution of inputs onto new neurons in the adult dentate gyrus and olfactory bulb. *Proceedings of the National Academy of Sciences of the United States of America* 110:E1152-1161.
- Dibbens LM et al. (2008) X-linked protocadherin 19 mutations cause female-limited epilepsy and cognitive impairment. *Nature genetics* 40:776-781.
- Dolmetsch R, Geschwind DH (2011) The human brain in a dish: the promise of iPSC-derived neurons. *Cell* 145:831-834.
- Drapeau E, Mayo W, Aurousseau C, Le Moal M, Piazza PV, Abrous DN (2003) Spatial memory performances of aged rats in the water maze predict levels of hippocampal neurogenesis. *Proceedings of the National Academy of Sciences of the United States of America* 100:14385-14390.

- Driscoll I, Howard SR, Stone JC, Monfils MH, Tomanek B, Brooks WM, Sutherland RJ (2006) The aging hippocampus: a multi-level analysis in the rat. *Neuroscience* 139:1173-1185.
- Eiraku M, Watanabe K, Matsuo-Takasaki M, Kawada M, Yonemura S, Matsumura M, Wataya T, Nishiyama A, Muguruma K, Sasai Y (2008) Self-organized formation of polarized cortical tissues from ESCs and its active manipulation by extrinsic signals. *Cell stem cell* 3:519-532.
- Emond MR, Biswas S, Jontes JD (2009) Protocadherin-19 is essential for early steps in brain morphogenesis. *Developmental biology* 334:72-83.
- Emond MR, Biswas S, Blevins CJ, Jontes JD (2011) A complex of Protocadherin-19 and N-cadherin mediates a novel mechanism of cell adhesion. *The Journal of cell biology* 195:1115-1121.
- Engel J, Jr., McDermott MP, Wiebe S, Langfitt JT, Stern JM, Dewar S, Sperling MR, Gardiner I, Erba G, Fried I, Jacobs M, Vinters HV, Mintzer S, Kieburtz K, Early Randomized Surgical Epilepsy Trial Study G (2012) Early surgical therapy for drug-resistant temporal lobe epilepsy: a randomized trial. *JAMA* 307:922-930.
- Eriksson PS, Perfilieva E, Bjork-Eriksson T, Alborn AM, Nordborg C, Peterson DA, Gage FH (1998) Neurogenesis in the adult human hippocampus. *Nature medicine* 4:1313-1317.
- Esclapez M, Hirsch JC, Ben-Ari Y, Bernard C (1999) Newly formed excitatory pathways provide a substrate for hyperexcitability in experimental temporal lobe epilepsy. *J Comp Neurol* 408:449-460.
- Fietz SA, Kelava I, Vogt J, Wilsch-Brauninger M, Stenzel D, Fish JL, Corbeil D, Riehn A, Distler W, Nitsch R, Huttner WB (2010) OSVZ progenitors of human and ferret neocortex are epithelial-like and expand by integrin signaling. *Nature neuroscience* 13:690-699.
- Fusaki N, Ban H, Nishiyama A, Saeki K, Hasegawa M (2009) Efficient induction of transgene-free human pluripotent stem cells using a vector based on Sendai virus, an RNA virus that does not integrate into the host genome. *Proceedings of the Japan Academy Series B, Physical and biological sciences* 85:348-362.
- Gabriel E et al. (2017) Recent Zika Virus Isolates Induce Premature Differentiation of Neural Progenitors in Human Brain Organoids. *Cell stem cell*.
- Gaitan Y, Bouchard M (2006) Expression of the delta-protocadherin gene *Pcdh19* in the developing mouse embryo. *Gene expression patterns : GEP* 6:893-899.
- Garcez PP, Loiola EC, Madeiro da Costa R, Higa LM, Trindade P, Delvecchio R, Nascimento JM, Brindeiro R, Tanuri A, Rehen SK (2016) Zika virus impairs growth in human neurospheres and brain organoids. *Science* 352:816-818.

- Gaspard N, Bouschet T, Hourez R, Dimidschstein J, Naeije G, van den Aemele J, Espuny-Camacho I, Herpoel A, Passante L, Schiffmann SN, Gaillard A, Vanderhaeghen P (2008) An intrinsic mechanism of corticogenesis from embryonic stem cells. *Nature* 455:351-357.
- Ge S, Yang CH, Hsu KS, Ming GL, Song H (2007) A critical period for enhanced synaptic plasticity in newly generated neurons of the adult brain. *Neuron* 54:559-566.
- Gong C, Wang TW, Huang HS, Parent JM (2007) Reelin regulates neuronal progenitor migration in intact and epileptic hippocampus. *The Journal of neuroscience : the official journal of the Society for Neuroscience* 27:1803-1811.
- Goto S, Yamamoto H, Hamasaki T, Miyamoto E (1998) [Calcineurin: structure and regulation of the cellular functions]. *Tanpakushitsu kakusan koso Protein, nucleic acid, enzyme* 43:1706-1714.
- Gould E (2007) How widespread is adult neurogenesis in mammals? *Nat Rev Neurosci* 8:481-488.
- Gould E, McEwen BS, Tanapat P, Galea LA, Fuchs E (1997) Neurogenesis in the dentate gyrus of the adult tree shrew is regulated by psychosocial stress and NMDA receptor activation. *The Journal of neuroscience : the official journal of the Society for Neuroscience* 17:2492-2498.
- Gray WP, Sundstrom LE (1998) Kainic acid increases the proliferation of granule cell progenitors in the dentate gyrus of the adult rat. *Brain Res* 790:52-59.
- Hansen DV, Lui JH, Parker PR, Kriegstein AR (2010) Neurogenic radial glia in the outer subventricular zone of human neocortex. *Nature* 464:554-561.
- Haug FM (1974) Light microscopical mapping of the hippocampal region, the pyriform cortex and the corticomedial amygdaloid nuclei of the rat with Timm's sulphide silver method. I. Area dentata, hippocampus and subiculum. *Z Anat Entwicklungsgesch* 145:1-27.
- Hayashi S, Inoue Y, Kiyonari H, Abe T, Misaki K, Moriguchi H, Tanaka Y, Takeichi M (2014) Protocadherin-17 mediates collective axon extension by recruiting actin regulator complexes to interaxonal contacts. *Developmental cell* 30:673-687.
- Heine VM, Maslam S, Zareno J, Joels M, Lucassen PJ (2004) Suppressed proliferation and apoptotic changes in the rat dentate gyrus after acute and chronic stress are reversible. *Eur J Neurosci* 19:131-144.
- Hester MS, Danzer SC (2013) Accumulation of abnormal adult-generated hippocampal granule cells predicts seizure frequency and severity. *The Journal of neuroscience : the official journal of the Society for Neuroscience* 33:8926-8936.

- Higurashi N, Uchida T, Lossin C, Misumi Y, Okada Y, Akamatsu W, Imaizumi Y, Zhang B, Nabeshima K, Mori MX, Katsurabayashi S, Shirasaka Y, Okano H, Hirose S (2013) A human Dravet syndrome model from patient induced pluripotent stem cells. *Molecular brain* 6:19.
- Hockfield S, McKay RD (1985) Identification of major cell classes in the developing mammalian nervous system. *The Journal of neuroscience : the official journal of the Society for Neuroscience* 5:3310-3328.
- Hofmann G, Balgooyen L, Mattis J, Deisseroth K, Buckmaster PS (2016) Hilar somatostatin interneuron loss reduces dentate gyrus inhibition in a mouse model of temporal lobe epilepsy. *Epilepsia* 57:977-983.
- Hosford BE, Liska JP, Danzer SC (2016) Ablation of Newly Generated Hippocampal Granule Cells Has Disease-Modifying Effects in Epilepsy. *The Journal of neuroscience : the official journal of the Society for Neuroscience* 36:11013-11023.
- Hoshina N, Tanimura A, Yamasaki M, Inoue T, Fukabori R, Kuroda T, Yokoyama K, Tezuka T, Sagara H, Hirano S, Kiyonari H, Takada M, Kobayashi K, Watanabe M, Kano M, Nakazawa T, Yamamoto T (2013) Protocadherin 17 regulates presynaptic assembly in topographic corticobasal Ganglia circuits. *Neuron* 78:839-854.
- Houser CR (1990) Granule cell dispersion in the dentate gyrus of humans with temporal lobe epilepsy. *Brain Res* 535:195-204.
- Houser CR, Miyashiro JE, Swartz BE, Walsh GO, Rich JR, Delgado-Escueta AV (1990) Altered patterns of dynorphin immunoreactivity suggest mossy fiber reorganization in human hippocampal epilepsy. *The Journal of neuroscience : the official journal of the Society for Neuroscience* 10:267-282.
- Jakubs K, Nanobashvili A, Bonde S, Ekdahl CT, Kokaia Z, Kokaia M, Lindvall O (2006) Environment matters: synaptic properties of neurons born in the epileptic adult brain develop to reduce excitability. *Neuron* 52:1047-1059.
- Jessberger S, Zhao C, Toni N, Clemenson GD, Jr., Li Y, Gage FH (2007) Seizure-associated, aberrant neurogenesis in adult rats characterized with retrovirus-mediated cell labeling. *The Journal of neuroscience : the official journal of the Society for Neuroscience* 27:9400-9407.
- Jiao J, Yang Y, Shi Y, Chen J, Gao R, Fan Y, Yao H, Liao W, Sun XF, Gao S (2013) Modeling Dravet syndrome using induced pluripotent stem cells (iPSCs) and directly converted neurons. *Human molecular genetics* 22:4241-4252.
- Jin K, Minami M, Lan JQ, Mao XO, Bateur S, Simon RP, Greenberg DA (2001) Neurogenesis in dentate subgranular zone and rostral subventricular zone after focal cerebral ischemia in the rat. *Proceedings of the National Academy of Sciences of the United States of America* 98:4710-4715.

- Johnson WG (1980) Metabolic interference and the + - heterozygote. a hypothetical form of simple inheritance which is neither dominant nor recessive. *American journal of human genetics* 32:374-386.
- Juberg RC, Hellman CD (1971) A new familial form of convulsive disorder and mental retardation limited to females. *J Pediatr* 79:726-732.
- Jung KH, Chu K, Kim M, Jeong SW, Song YM, Lee ST, Kim JY, Lee SK, Roh JK (2004) Continuous cytosine-b-D-arabinofuranoside infusion reduces ectopic granule cells in adult rat hippocampus with attenuation of spontaneous recurrent seizures following pilocarpine-induced status epilepticus. *Eur J Neurosci* 19:3219-3226.
- Juopperi TA, Kim WR, Chiang CH, Yu H, Margolis RL, Ross CA, Ming GL, Song H (2012) Astrocytes generated from patient induced pluripotent stem cells recapitulate features of Huntington's disease patient cells. *Molecular brain* 5:17.
- Kadoshima T, Sakaguchi H, Nakano T, Soen M, Ando S, Eiraku M, Sasai Y (2013) Self-organization of axial polarity, inside-out layer pattern, and species-specific progenitor dynamics in human ES cell-derived neocortex. *Proceedings of the National Academy of Sciences of the United States of America* 110:20284-20289.
- Kempermann G, Kuhn HG, Gage FH (1997) More hippocampal neurons in adult mice living in an enriched environment. *Nature* 386:493-495.
- Kempermann G, Gast D, Gage FH (2002) Neuroplasticity in old age: sustained fivefold induction of hippocampal neurogenesis by long-term environmental enrichment. *Annals of neurology* 52:135-143.
- Kempermann G, Gast D, Kronenberg G, Yamaguchi M, Gage FH (2003) Early determination and long-term persistence of adult-generated new neurons in the hippocampus of mice. *Development* 130:391-399.
- Kim KY, Hysolli E, Park IH (2011a) Neuronal maturation defect in induced pluripotent stem cells from patients with Rett syndrome. *Proceedings of the National Academy of Sciences of the United States of America* 108:14169-14174.
- Kim SY, Yasuda S, Tanaka H, Yamagata K, Kim H (2011b) Non-clustered protocadherin. *Cell Adh Migr* 5:97-105.
- Kim SY, Mo JW, Han S, Choi SY, Han SB, Moon BH, Rhyu IJ, Sun W, Kim H (2010) The expression of non-clustered protocadherins in adult rat hippocampal formation and the connecting brain regions. *Neuroscience* 170:189-199.
- Koo JW, Park CH, Choi SH, Kim NJ, Kim HS, Choe JC, Suh YH (2003) The postnatal environment can counteract prenatal effects on cognitive ability, cell proliferation, and synaptic protein expression. *FASEB J* 17:1556-1558.

- Korn MJ, Mandle QJ, Parent JM (2016) Conditional Disabled-1 Deletion in Mice Alters Hippocampal Neurogenesis and Reduces Seizure Threshold. *Front Neurosci* 10:63.
- Krencik R, Zhang SC (2011) Directed differentiation of functional astroglial subtypes from human pluripotent stem cells. *Nature protocols* 6:1710-1717.
- Krey JF, Pasca SP, Shcheglovitov A, Yazawa M, Schwemberger R, Rasmusson R, Dolmetsch RE (2013) Timothy syndrome is associated with activity-dependent dendritic retraction in rodent and human neurons. *Nature neuroscience* 16:201-209.
- Kron MM, Zhang H, Parent JM (2010) The developmental stage of dentate granule cells dictates their contribution to seizure-induced plasticity. *The Journal of neuroscience : the official journal of the Society for Neuroscience* 30:2051-2059.
- Kronenberg G, Reuter K, Steiner B, Brandt MD, Jessberger S, Yamaguchi M, Kempermann G (2003) Subpopulations of proliferating cells of the adult hippocampus respond differently to physiologic neurogenic stimuli. *J Comp Neurol* 467:455-463.
- Kuhn HG, Dickinson-Anson H, Gage FH (1996) Neurogenesis in the dentate gyrus of the adult rat: age-related decrease of neuronal progenitor proliferation. *The Journal of neuroscience : the official journal of the Society for Neuroscience* 16:2027-2033.
- Lancaster MA, Renner M, Martin CA, Wenzel D, Bicknell LS, Hurles ME, Homfray T, Penninger JM, Jackson AP, Knoblich JA (2013) Cerebral organoids model human brain development and microcephaly. *Nature* 501:373-379.
- Laplagne DA, Esposito MS, Piatti VC, Morgenstern NA, Zhao C, van Praag H, Gage FH, Schinder AF (2006) Functional convergence of neurons generated in the developing and adult hippocampus. *PLoS biology* 4:e409.
- Lefebvre JL, Kostadinov D, Chen WV, Maniatis T, Sanes JR (2012) Protocadherins mediate dendritic self-avoidance in the mammalian nervous system. *Nature* 488:517-521.
- Lemaire V, Koehl M, Le Moal M, Abrous DN (2000) Prenatal stress produces learning deficits associated with an inhibition of neurogenesis in the hippocampus. *Proceedings of the National Academy of Sciences of the United States of America* 97:11032-11037.
- Li XG, Somogyi P, Ylinen A, Buzsaki G (1994) The hippocampal CA3 network: an in vivo intracellular labeling study. *J Comp Neurol* 339:181-208.
- Li Y, Muffat J, Omer A, Bosch I, Lancaster MA, Sur M, Gehrke L, Knoblich JA, Jaenisch R (2016) Induction of Expansion and Folding in Human Cerebral Organoids. *Cell stem cell*.

- Liu J, Koscielska KA, Cao Z, Hulsizer S, Grace N, Mitchell G, Nacey C, Githinji J, McGee J, Garcia-Arocena D, Hagerman RJ, Nolta J, Pessah IN, Hagerman PJ (2012) Signaling defects in iPSC-derived fragile X premutation neurons. *Human molecular genetics* 21:3795-3805.
- Liu Y, Liu H, Sauvey C, Yao L, Zarnowska ED, Zhang SC (2013a) Directed differentiation of forebrain GABA interneurons from human pluripotent stem cells. *Nature protocols* 8:1670-1679.
- Liu Y, Lopez-Santiago LF, Yuan Y, Jones JM, Zhang H, O'Malley HA, Patino GA, O'Brien JE, Rusconi R, Gupta A, Thompson RC, Natowicz MR, Meisler MH, Isom LL, Parent JM (2013b) Dravet syndrome patient-derived neurons suggest a novel epilepsy mechanism. *Annals of neurology* 74:128-139.
- Livide G, Patriarchi T, Amenduni M, Amabile S, Yasui D, Calcagno E, Lo Rizzo C, De Falco G, Ulivieri C, Ariani F, Mari F, Mencarelli MA, Hell JW, Renieri A, Meloni I (2015) GluD1 is a common altered player in neuronal differentiation from both MECP2-mutated and CDKL5-mutated iPS cells. *Eur J Hum Genet* 23:195-201.
- Malberg JE, Duman RS (2003) Cell proliferation in adult hippocampus is decreased by inescapable stress: reversal by fluoxetine treatment. *Neuropsychopharmacology* 28:1562-1571.
- Marchetto MC, Brennand KJ, Boyer LF, Gage FH (2011) Induced pluripotent stem cells (iPSCs) and neurological disease modeling: progress and promises. *Human molecular genetics* 20:R109-115.
- Marchetto MC, Carromeu C, Acab A, Yu D, Yeo GW, Mu Y, Chen G, Gage FH, Muotri AR (2010) A model for neural development and treatment of Rett syndrome using human induced pluripotent stem cells. *Cell* 143:527-539.
- Mariani J, Simonini MV, Palejev D, Tomasini L, Coppola G, Szekely AM, Horvath TL, Vaccarino FM (2012) Modeling human cortical development in vitro using induced pluripotent stem cells. *Proceedings of the National Academy of Sciences of the United States of America* 109:12770-12775.
- Mariani J, Coppola G, Zhang P, Abyzov A, Provini L, Tomasini L, Amenduni M, Szekely A, Palejev D, Wilson M, Gerstein M, Grigorenko EL, Chawarska K, Pelphrey KA, Howe JR, Vaccarino FM (2015) FOXP1-Dependent Dysregulation of GABA/Glutamate Neuron Differentiation in Autism Spectrum Disorders. *Cell* 162:375-390.
- Maroof AM, Keros S, Tyson JA, Ying SW, Ganat YM, Merkle FT, Liu B, Goulburn A, Stanley EG, Elefanty AG, Widmer HR, Eggan K, Goldstein PA, Anderson SA, Studer L (2013) Directed differentiation and functional maturation of cortical interneurons from human embryonic stem cells. *Cell stem cell* 12:559-572.

- Mathern GW, Babb TL, Pretorius JK, Leite JP (1995) Reactive synaptogenesis and neuron densities for neuropeptide Y, somatostatin, and glutamate decarboxylase immunoreactivity in the epileptogenic human fascia dentata. *The Journal of neuroscience : the official journal of the Society for Neuroscience* 15:3990-4004.
- Mekhoubad S, Bock C, de Boer AS, Kiskinis E, Meissner A, Eggan K (2012) Erosion of dosage compensation impacts human iPSC disease modeling. *Cell stem cell* 10:595-609.
- Miller JD, Ganat YM, Kishinevsky S, Bowman RL, Liu B, Tu EY, Mandal PK, Vera E, Shim JW, Kriks S, Taldone T, Fusaki N, Tomishima MJ, Krainc D, Milner TA, Rossi DJ, Studer L (2013) Human iPSC-based modeling of late-onset disease via progerin-induced aging. *Cell stem cell* 13:691-705.
- Mohapel P, Ekdahl CT, Lindvall O (2004) Status epilepticus severity influences the long-term outcome of neurogenesis in the adult dentate gyrus. *Neurobiology of disease* 15:196-205.
- Morgan RJ, Soltesz I (2008) Nonrandom connectivity of the epileptic dentate gyrus predicts a major role for neuronal hubs in seizures. *Proceedings of the National Academy of Sciences of the United States of America* 105:6179-6184.
- Murphy BL, Pun RY, Yin H, Faulkner CR, Loepke AW, Danzer SC (2011) Heterogeneous integration of adult-generated granule cells into the epileptic brain. *The Journal of neuroscience : the official journal of the Society for Neuroscience* 31:105-117.
- Noctor SC, Martinez-Cerdeno V, Ivic L, Kriegstein AR (2004) Cortical neurons arise in symmetric and asymmetric division zones and migrate through specific phases. *Nature neuroscience* 7:136-144.
- Noebels J (2015) Pathway-driven discovery of epilepsy genes. *Nature neuroscience* 18:344-350.
- Overstreet-Wadiche LS, Bromberg DA, Bensen AL, Westbrook GL (2006) Seizures accelerate functional integration of adult-generated granule cells. *The Journal of neuroscience : the official journal of the Society for Neuroscience* 26:4095-4103.
- Parent JM, Anderson SA (2015) Reprogramming patient-derived cells to study the epilepsies. *Nature neuroscience* 18:360-366.
- Parent JM, Tada E, Fike JR, Lowenstein DH (1999) Inhibition of dentate granule cell neurogenesis with brain irradiation does not prevent seizure-induced mossy fiber synaptic reorganization in the rat. *The Journal of neuroscience : the official journal of the Society for Neuroscience* 19:4508-4519.
- Parent JM, Vexler ZS, Gong C, Derugin N, Ferriero DM (2002) Rat forebrain neurogenesis and striatal neuron replacement after focal stroke. *Annals of neurology* 52:802-813.

- Parent JM, Elliott RC, Pleasure SJ, Barbaro NM, Lowenstein DH (2006) Aberrant seizure-induced neurogenesis in experimental temporal lobe epilepsy. *Annals of neurology* 59:81-91.
- Parent JM, Yu TW, Leibowitz RT, Geschwind DH, Sloviter RS, Lowenstein DH (1997) Dentate granule cell neurogenesis is increased by seizures and contributes to aberrant network reorganization in the adult rat hippocampus. *The Journal of neuroscience : the official journal of the Society for Neuroscience* 17:3727-3738.
- Pasca AM, Sloan SA, Clarke LE, Tian Y, Makinson CD, Huber N, Kim CH, Park JY, O'Rourke NA, Nguyen KD, Smith SJ, Huguenard JR, Geschwind DH, Barres BA, Pasca SP (2015) Functional cortical neurons and astrocytes from human pluripotent stem cells in 3D culture. *Nature methods* 12:671-678.
- Pasca SP, Panagiotakos G, Dolmetsch RE (2014) Generating human neurons in vitro and using them to understand neuropsychiatric disease. *Annual review of neuroscience* 37:479-501.
- Pasca SP, Portmann T, Voineagu I, Yazawa M, Shcheglovitov A, Pasca AM, Cord B, Palmer TD, Chikahisa S, Nishino S, Bernstein JA, Hallmayer J, Geschwind DH, Dolmetsch RE (2011) Using iPSC-derived neurons to uncover cellular phenotypes associated with Timothy syndrome. *Nature medicine* 17:1657-1662.
- Pederick DT, Homan CC, Jaehne EJ, Piltz SG, Haines BP, Baune BT, Jolly LA, Hughes JN, Gecz J, Thomas PQ (2016) Pcdh19 Loss-of-Function Increases Neuronal Migration In Vitro but is Dispensable for Brain Development in Mice. *Sci Rep* 6:26765.
- Peng Z, Zhang N, Wei W, Huang CS, Cetina Y, Otis TS, Houser CR (2013) A reorganized GABAergic circuit in a model of epilepsy: evidence from optogenetic labeling and stimulation of somatostatin interneurons. *The Journal of neuroscience : the official journal of the Society for Neuroscience* 33:14392-14405.
- Perez Y, Morin F, Beaulieu C, Lacaille JC (1996) Axonal sprouting of CA1 pyramidal cells in hyperexcitable hippocampal slices of kainate-treated rats. *Eur J Neurosci* 8:736-748.
- Pham K, Nacher J, Hof PR, McEwen BS (2003) Repeated restraint stress suppresses neurogenesis and induces biphasic PSA-NCAM expression in the adult rat dentate gyrus. *Eur J Neurosci* 17:879-886.
- Pierce JP, Melton J, Punsoni M, McCloskey DP, Scharfman HE (2005) Mossy fibers are the primary source of afferent input to ectopic granule cells that are born after pilocarpine-induced seizures. *Exp Neurol* 196:316-331.
- Piper M, Dwivedy A, Leung L, Bradley RS, Holt CE (2008) NF-protocadherin and TAF1 regulate retinal axon initiation and elongation in vivo. *The Journal of neuroscience : the official journal of the Society for Neuroscience* 28:100-105.

- Qian X et al. (2016) Brain-Region-Specific Organoids Using Mini-bioreactors for Modeling ZIKV Exposure. *Cell* 165:1238-1254.
- Ran X, Li J, Shao Q, Chen H, Lin Z, Sun ZS, Wu J (2015) EpilepsyGene: a genetic resource for genes and mutations related to epilepsy. *Nucleic Acids Res* 43:D893-899.
- Reillo I, de Juan Romero C, Garcia-Cabezas MA, Borrell V (2011) A role for intermediate radial glia in the tangential expansion of the mammalian cerebral cortex. *Cereb Cortex* 21:1674-1694.
- Ribak CE, Tran PH, Spigelman I, Okazaki MM, Nadler JV (2000) Status epilepticus-induced hilar basal dendrites on rodent granule cells contribute to recurrent excitatory circuitry. *J Comp Neurol* 428:240-253.
- Ricciardi S, Ungaro F, Hambrock M, Rademacher N, Stefanelli G, Brambilla D, Sessa A, Magagnotti C, Bachi A, Giarda E, Verpelli C, Kilstrup-Nielsen C, Sala C, Kalscheuer VM, Broccoli V (2012) CDKL5 ensures excitatory synapse stability by reinforcing NGL-1-PSD95 interaction in the postsynaptic compartment and is impaired in patient iPSC-derived neurons. *Nat Cell Biol* 14:911-923.
- Ryan SG, Chance PF, Zou CH, Spinner NB, Golden JA, Smietana S (1997) Epilepsy and mental retardation limited to females: an X-linked dominant disorder with male sparing. *Nature genetics* 17:92-95.
- Saavedra D, Richieri-Costa A, Guion-Almeida ML, Cohen MM, Jr. (1996) Craniofrontonasal syndrome: study of 41 patients. *Am J Med Genet* 61:147-151.
- Sanlaville D, Schluth-Bolard C, Turleau C (2009) Distal Xq duplication and functional Xq disomy. *Orphanet J Rare Dis* 4:4.
- Sanlaville D, Prieur M, de Blois MC, Genevieve D, Lapierre JM, Ozilou C, Picq M, Gosset P, Morichon-Delvallez N, Munnich A, Cormier-Daire V, Baujat G, Romana S, Vekemans M, Turleau C (2005) Functional disomy of the Xq28 chromosome region. *Eur J Hum Genet* 13:579-585.
- Scharfman HE, Pierce JP (2012) New insights into the role of hilar ectopic granule cells in the dentate gyrus based on quantitative anatomic analysis and three-dimensional reconstruction. *Epilepsia* 53 Suppl 1:109-115.
- Scharfman HE, Goodman JH, Sollas AL (2000) Granule-like neurons at the hilar/CA3 border after status epilepticus and their synchrony with area CA3 pyramidal cells: functional implications of seizure-induced neurogenesis. *The Journal of neuroscience : the official journal of the Society for Neuroscience* 20:6144-6158.
- Scharfman HE, Sollas AL, Berger RE, Goodman JH (2003) Electrophysiological evidence of monosynaptic excitatory transmission between granule cells after seizure-induced mossy fiber sprouting. *Journal of neurophysiology* 90:2536-2547.

- Scheffer IE et al. (2008) Epilepsy and mental retardation limited to females: an under-recognized disorder. *Brain : a journal of neurology* 131:918-927.
- Schmidt-Hieber C, Jonas P, Bischofberger J (2004) Enhanced synaptic plasticity in newly generated granule cells of the adult hippocampus. *Nature* 429:184-187.
- Seress L, Pokorny J (1981) Structure of the granular layer of the rat dentate gyrus. A light microscopic and Golgi study. *J Anat* 133:181-195.
- Shapiro LA, Ribak CE (2006) Newly born dentate granule neurons after pilocarpine-induced epilepsy have hilar basal dendrites with immature synapses. *Epilepsy Res* 69:53-66.
- Shapiro LA, Figueroa-Aragon S, Ribak CE (2007) Newly generated granule cells show rapid neuroplastic changes in the adult rat dentate gyrus during the first five days following pilocarpine-induced seizures. *Eur J Neurosci* 26:583-592.
- Shcheglovitov A, Shcheglovitova O, Yazawa M, Portmann T, Shu R, Sebastiano V, Krawisz A, Froehlich W, Bernstein JA, Hallmayer JF, Dolmetsch RE (2013) SHANK3 and IGF1 restore synaptic deficits in neurons from 22q13 deletion syndrome patients. *Nature* 503:267-271.
- Sheridan SD, Theriault KM, Reis SA, Zhou F, Madison JM, Daheron L, Loring JF, Haggarty SJ (2011) Epigenetic characterization of the FMR1 gene and aberrant neurodevelopment in human induced pluripotent stem cell models of fragile X syndrome. *PLoS one* 6:e26203.
- Shi Y, Kirwan P, Smith J, Robinson HP, Livesey FJ (2012) Human cerebral cortex development from pluripotent stem cells to functional excitatory synapses. *Nature neuroscience* 15:477-486, S471.
- Shoffner JM, Lott MT, Lezza AM, Seibel P, Ballinger SW, Wallace DC (1990) Myoclonic epilepsy and ragged-red fiber disease (MERRF) is associated with a mitochondrial DNA tRNA(Lys) mutation. *Cell* 61:931-937.
- Smart IH, Dehay C, Giroud P, Berland M, Kennedy H (2002) Unique morphological features of the proliferative zones and postmitotic compartments of the neural epithelium giving rise to striate and extrastriate cortex in the monkey. *Cereb Cortex* 12:37-53.
- Snyder JS, Kee N, Wojtowicz JM (2001) Effects of adult neurogenesis on synaptic plasticity in the rat dentate gyrus. *Journal of neurophysiology* 85:2423-2431.
- Spigelman I, Yan XX, Obenaus A, Lee EY, Wasterlain CG, Ribak CE (1998) Dentate granule cells form novel basal dendrites in a rat model of temporal lobe epilepsy. *Neuroscience* 86:109-120.

- Srikanth P, Young-Pearse TL (2014) Stem cells on the brain: modeling neurodevelopmental and neurodegenerative diseases using human induced pluripotent stem cells. *J Neurogenet* 28:5-29.
- Sutula T, Cascino G, Cavazos J, Parada I, Ramirez L (1989) Mossy fiber synaptic reorganization in the epileptic human temporal lobe. *Annals of neurology* 26:321-330.
- Takahashi K, Yamanaka S (2006) Induction of pluripotent stem cells from mouse embryonic and adult fibroblast cultures by defined factors. *Cell* 126:663-676.
- Takahashi K, Tanabe K, Ohnuki M, Narita M, Ichisaka T, Tomoda K, Yamanaka S (2007) Induction of pluripotent stem cells from adult human fibroblasts by defined factors. *Cell* 131:861-872.
- Tang X, Kim J, Zhou L, Wengert E, Zhang L, Wu Z, Carrromeu C, Muotri AR, Marchetto MC, Gage FH, Chen G (2016) KCC2 rescues functional deficits in human neurons derived from patients with Rett syndrome. *Proceedings of the National Academy of Sciences of the United States of America* 113:751-756.
- Tchieu J, Kuoy E, Chin MH, Trinh H, Patterson M, Sherman SP, Aimiwu O, Lindgren A, Hakimian S, Zack JA, Clark AT, Pyle AD, Lowry WE, Plath K (2010) Female human iPSCs retain an inactive X chromosome. *Cell stem cell* 7:329-342.
- Teixeira CM, Kron MM, Masachs N, Zhang H, Lagace DC, Martinez A, Reillo I, Duan X, Bosch C, Pujadas L, Brunso L, Song H, Eisch AJ, Borrell V, Howell BW, Parent JM, Soriano E (2012) Cell-autonomous inactivation of the reelin pathway impairs adult neurogenesis in the hippocampus. *The Journal of neuroscience : the official journal of the Society for Neuroscience* 32:12051-12065.
- Telias M, Segal M, Ben-Yosef D (2013) Neural differentiation of Fragile X human Embryonic Stem Cells reveals abnormal patterns of development despite successful neurogenesis. *Developmental biology* 374:32-45.
- Terracciano A, Trivisano M, Cusmai R, De Palma L, Fusco L, Compagnucci C, Bertini E, Vigevano F, Specchio N (2016) PCDH19-related epilepsy in two mosaic male patients. *Epilepsia* 57:e51-55.
- Thiffault I, Farrow E, Smith L, Lowry J, Zellmer L, Black B, Abdelmoity A, Miller N, Soden S, Saunders C (2016) PCDH19-related epileptic encephalopathy in a male mosaic for a truncating variant. *Am J Med Genet A* 170:1585-1589.
- Thind KK, Ribak CE, Buckmaster PS (2008) Synaptic input to dentate granule cell basal dendrites in a rat model of temporal lobe epilepsy. *J Comp Neurol* 509:190-202.
- Thind KK, Yamawaki R, Phanwar I, Zhang G, Wen X, Buckmaster PS (2010) Initial loss but later excess of GABAergic synapses with dentate granule cells in a rat model of temporal lobe epilepsy. *J Comp Neurol* 518:647-667.

- Tomoda K, Takahashi K, Leung K, Okada A, Narita M, Yamada NA, Eilertson KE, Tsang P, Baba S, White MP, Sami S, Srivastava D, Conklin BR, Panning B, Yamanaka S (2012) Derivation conditions impact X-inactivation status in female human induced pluripotent stem cells. *Cell stem cell* 11:91-99.
- Tsai NP, Wilkerson JR, Guo W, Maksimova MA, DeMartino GN, Cowan CW, Huber KM (2012) Multiple autism-linked genes mediate synapse elimination via proteasomal degradation of a synaptic scaffold PSD-95. *Cell* 151:1581-1594.
- Turski WA, Cavaleiro EA, Schwarz M, Czuczwar SJ, Kleinrok Z, Turski L (1983) Limbic seizures produced by pilocarpine in rats: behavioural, electroencephalographic and neuropathological study. *Behav Brain Res* 9:315-335.
- Uemura M, Nakao S, Suzuki ST, Takeichi M, Hirano S (2007) OL-Protocadherin is essential for growth of striatal axons and thalamocortical projections. *Nature neuroscience* 10:1151-1159.
- Urbach A, Bar-Nur O, Daley GQ, Benvenisty N (2010) Differential modeling of fragile X syndrome by human embryonic stem cells and induced pluripotent stem cells. *Cell stem cell* 6:407-411.
- van Harssele JJ et al. (2013) Clinical and genetic aspects of PCDH19-related epilepsy syndromes and the possible role of PCDH19 mutations in males with autism spectrum disorders. *Neurogenetics* 14:23-34.
- van Praag H, Kempermann G, Gage FH (1999a) Running increases cell proliferation and neurogenesis in the adult mouse dentate gyrus. *Nature neuroscience* 2:266-270.
- van Praag H, Christie BR, Sejnowski TJ, Gage FH (1999b) Running enhances neurogenesis, learning, and long-term potentiation in mice. *Proceedings of the National Academy of Sciences of the United States of America* 96:13427-13431.
- van Praag H, Schinder AF, Christie BR, Toni N, Palmer TD, Gage FH (2002) Functional neurogenesis in the adult hippocampus. *Nature* 415:1030-1034.
- Vivar C, Peterson BD, van Praag H (2016) Running rewires the neuronal network of adult-born dentate granule cells. *Neuroimage* 131:29-41.
- Vivar C, Potter MC, Choi J, Lee JY, Stringer TP, Callaway EM, Gage FH, Suh H, van Praag H (2012) Monosynaptic inputs to new neurons in the dentate gyrus. *Nature communications* 3:1107.
- Walter C, Murphy BL, Pun RY, Spieles-Engemann AL, Danzer SC (2007) Pilocarpine-induced seizures cause selective time-dependent changes to adult-generated hippocampal dentate granule cells. *The Journal of neuroscience : the official journal of the Society for Neuroscience* 27:7541-7552.

- Wang L, Wang L, Huang W, Su H, Xue Y, Su Z, Liao B, Wang H, Bao X, Qin D, He J, Wu W, So KF, Pan G, Pei D (2013) Generation of integration-free neural progenitor cells from cells in human urine. *Nature methods* 10:84-89.
- Wells MF, Salick MR, Wiskow O, Ho DJ, Worringer KA, Ihry RJ, Kommineni S, Bilican B, Klim JR, Hill EJ, Kane LT, Ye C, Kaykas A, Eggan K (2016) Genetic Ablation of AXL Does Not Protect Human Neural Progenitor Cells and Cerebral Organoids from Zika Virus Infection. *Cell stem cell* 19:703-708.
- Wickersham IR, Lyon DC, Barnard RJ, Mori T, Finke S, Conzelmann KK, Young JA, Callaway EM (2007) Monosynaptic restriction of transsynaptic tracing from single, genetically targeted neurons. *Neuron* 53:639-647.
- Wieland I, Jakubiczka S, Muschke P, Cohen M, Thiele H, Gerlach KL, Adams RH, Wieacker P (2004) Mutations of the ephrin-B1 gene cause craniofrontonasal syndrome. *American journal of human genetics* 74:1209-1215.
- Wolfer DP, Lipp HP (1995) Evidence for physiological growth of hippocampal mossy fiber collaterals in the guinea pig during puberty and adulthood. *Hippocampus* 5:329-340.
- Wolverton T, Lalande M (2001) Identification and characterization of three members of a novel subclass of protocadherins. *Genomics* 76:66-72.
- Yazawa M, Hsueh B, Jia X, Pasca AM, Bernstein JA, Hallmayer J, Dolmetsch RE (2011) Using induced pluripotent stem cells to investigate cardiac phenotypes in Timothy syndrome. *Nature* 471:230-234.
- Yoon KJ et al. (2014) Modeling a genetic risk for schizophrenia in iPSCs and mice reveals neural stem cell deficits associated with adherens junctions and polarity. *Cell stem cell* 15:79-91.
- Yu J, Hu K, Smuga-Otto K, Tian S, Stewart R, Slukvin, II, Thomson JA (2009) Human induced pluripotent stem cells free of vector and transgene sequences. *Science* 324:797-801.
- Yu J, Vodyanik MA, Smuga-Otto K, Antosiewicz-Bourget J, Frane JL, Tian S, Nie J, Jonsdottir GA, Ruotti V, Stewart R, Slukvin, II, Thomson JA (2007) Induced pluripotent stem cell lines derived from human somatic cells. *Science* 318:1917-1920.
- Zecevic N, Chen Y, Filipovic R (2005) Contributions of cortical subventricular zone to the development of the human cerebral cortex. *J Comp Neurol* 491:109-122.
- Zhan RZ, Nadler JV (2009) Enhanced tonic GABA current in normotopic and hilar ectopic dentate granule cells after pilocarpine-induced status epilepticus. *Journal of neurophysiology* 102:670-681.

- Zhan RZ, Timofeeva O, Nadler JV (2010) High ratio of synaptic excitation to synaptic inhibition in hilar ectopic granule cells of pilocarpine-treated rats. *Journal of neurophysiology* 104:3293-3304.
- Zhang W, Huguenard JR, Buckmaster PS (2012) Increased excitatory synaptic input to granule cells from hilar and CA3 regions in a rat model of temporal lobe epilepsy. *The Journal of neuroscience : the official journal of the Society for Neuroscience* 32:1183-1196.
- Zhang W, Yamawaki R, Wen X, Uhl J, Diaz J, Prince DA, Buckmaster PS (2009) Surviving hilar somatostatin interneurons enlarge, sprout axons, and form new synapses with granule cells in a mouse model of temporal lobe epilepsy. *The Journal of neuroscience : the official journal of the Society for Neuroscience* 29:14247-14256.
- Zhou T et al. (2011) Generation of induced pluripotent stem cells from urine. *Journal of the American Society of Nephrology : JASN* 22:1221-1228.

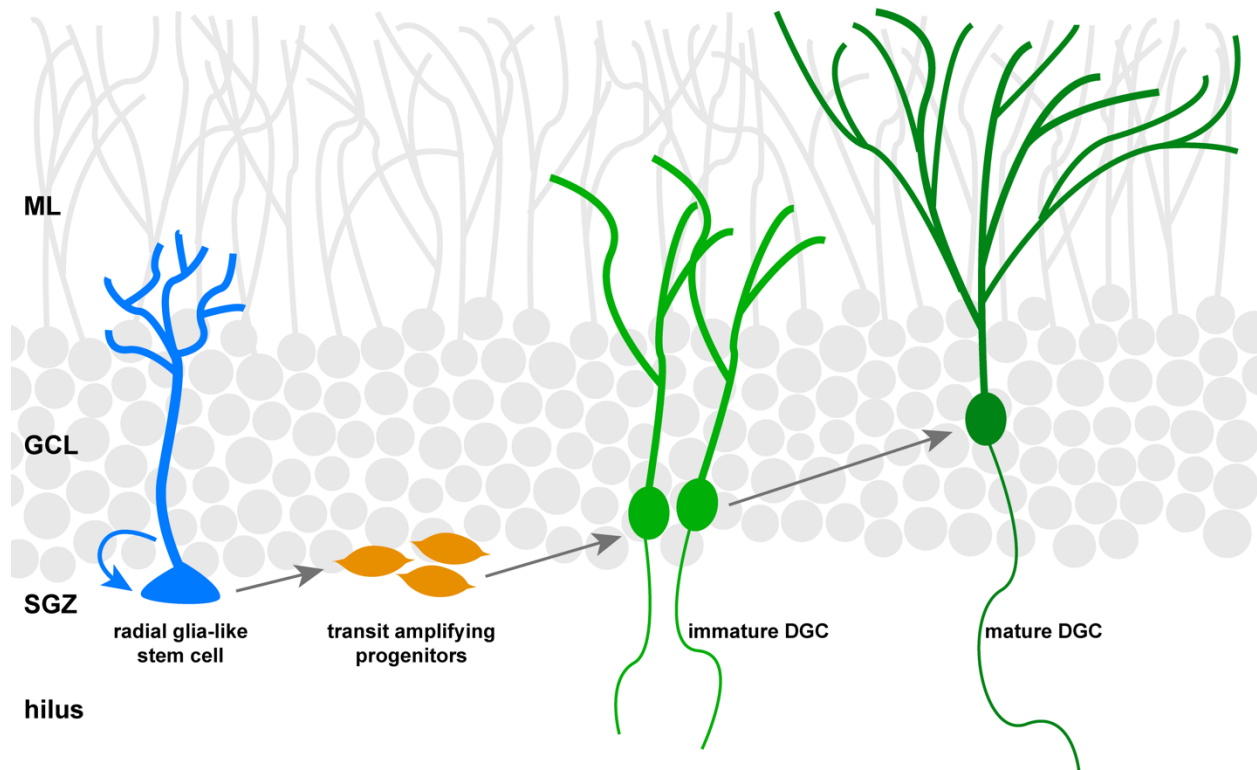


Figure 1.1. Adult neurogenesis in the hippocampal dentate gyrus.

Schematic showing the process of adult neurogenesis in the dentate gyrus. An expansion of stratified layers of the dentate gyrus is depicted organized with the hilus at the bottom followed by the subgranular zone (SGZ), the granule cell layer (GCL) and the molecular layer (ML) at the top. Radial glia-like stem cells, the stem cell population of the dentate gyrus, reside in the SGZ. While they are normally quiescent, this population can become activated to either self-renew or generate transit amplifying progenitors. Transit amplifying progenitors are highly proliferative and eventually terminally differentiate into immature dentate granule cells (DGCs). After a period of 8-10 weeks, a fully mature DGC is formed that extends dendrites into the ML and sends its axon into the hilus and then to stratum lucidum of the hippocampal CA3 subregion (not shown).

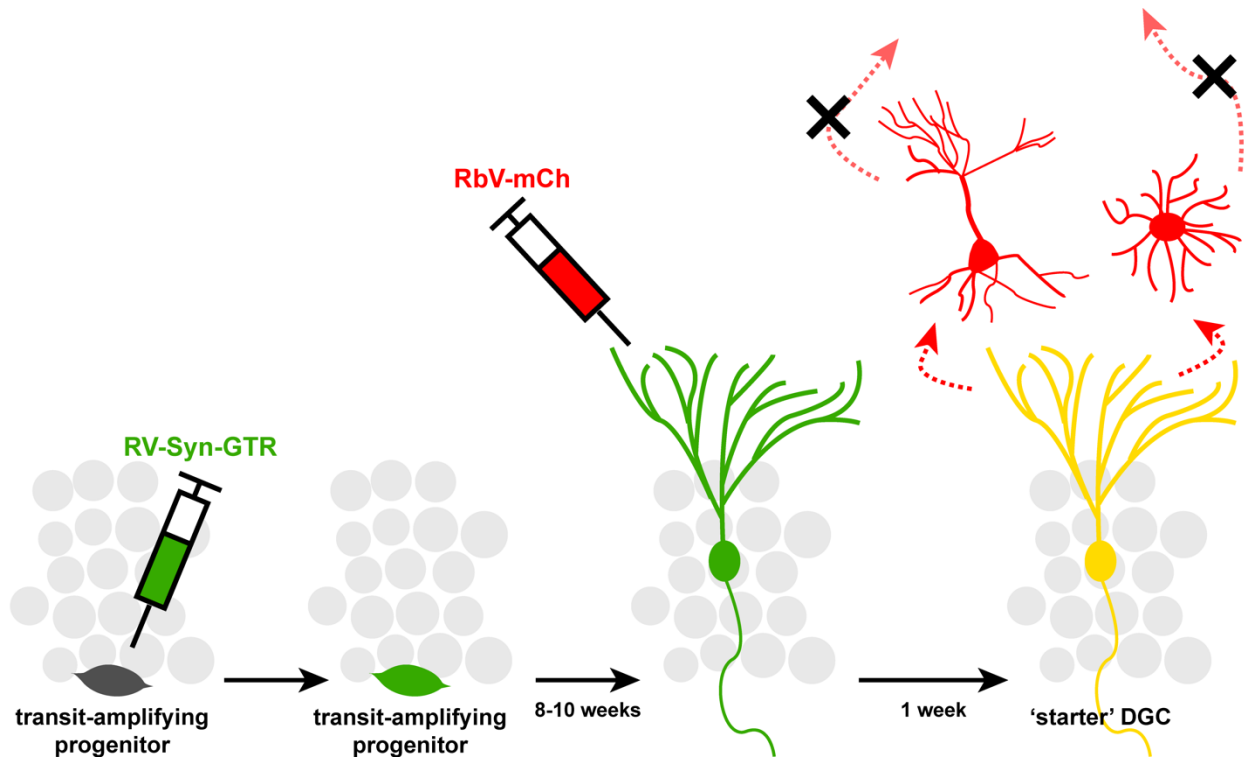


Figure 1.2. Schematic of the dual-viral tracing strategy.

We inject a retrovirus (RV-Syn-GTR) into the dentate gyrus to birthdate DGCs. RV-Syn-GTR expresses GFP, TVA and Rgp driven by a human Synapsin1 promoter. After 8-10 weeks, we inject a rabies virus (RbV-mCh) that is pseudotyped to EnvA thereby restricting its infection to cells that express EnvA's cognate receptor, TVA. This allows for targeting of RbV-mCh infection selectively to cells that have previously received RV-Syn-GTR. RbV-mCh has also been engineered such that the gene that expresses Rgp, necessary for the virus' retrograde spread but not for its replication, has been replaced by mCh. Within the doubly infected GFP+/mCh+ 'starter' cells, RbV-mCh trans-complements with Rgp provided by RV-Syn-GTR and travels retrogradely one synapse. In the mCh+ only first-order presynaptic inputs onto the starter cells, Rgp is no longer present thus RbV-mCh cannot travel any further. This strategy allows us to identify mCh+ monosynaptic inputs onto GFP+/mCh+ birthdated starter DGCs.

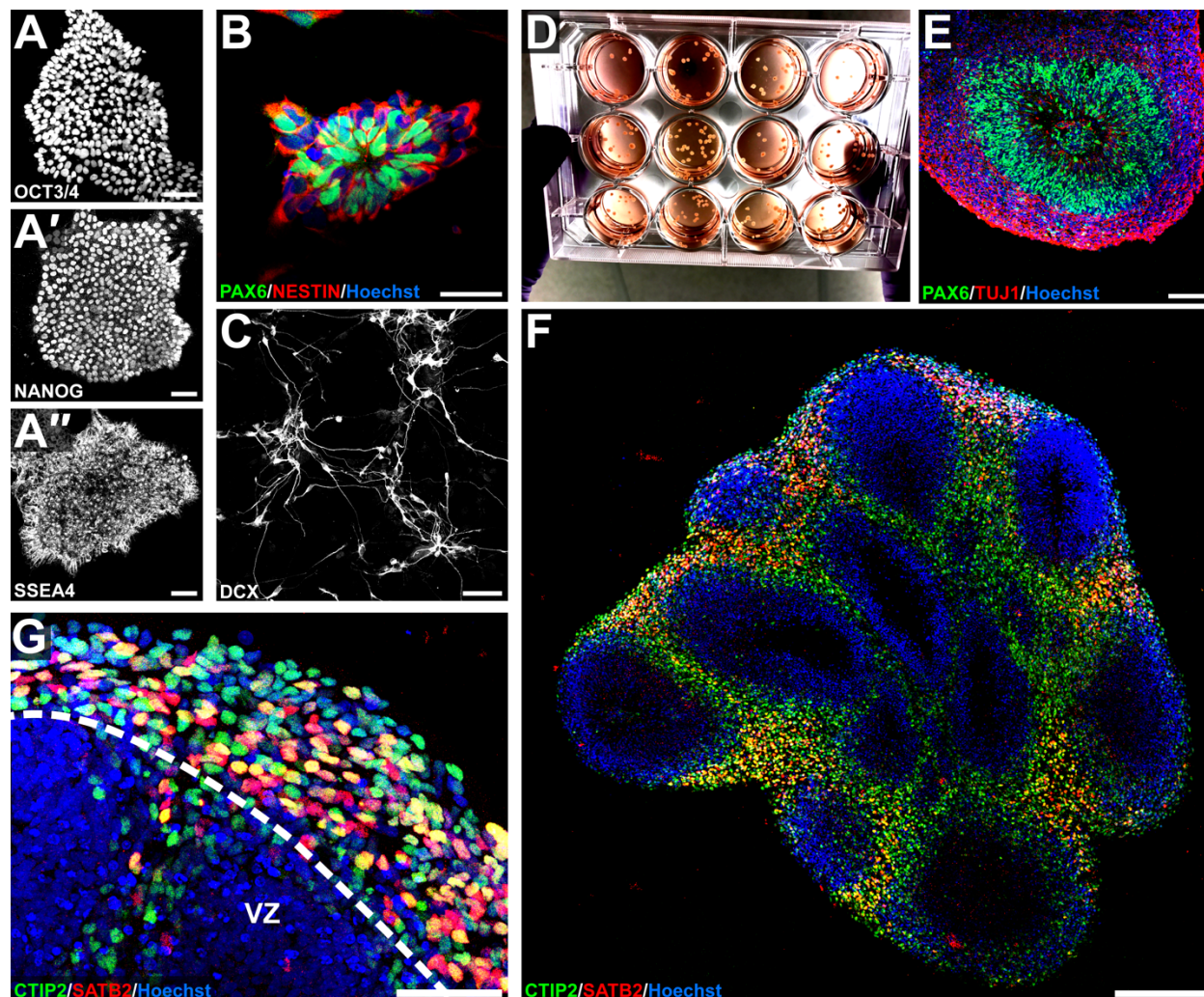


Figure 1.3. The utility of iPSCs for modeling neural development.

(A-A'') iPSC colonies immunostained for pluripotency markers OCT3/4, NANOG and SSEA4. Scale bars represent 100 μm . **(B)** Neural rosettes derived from iPSCs are PAX6+ and NESTIN+. Scale bar represents 50 μm . **(C)** Representative image of doublecortin (DCX)+ cortical-like excitatory neurons derived from iPSCs. Scale bar represents 100 μm . **(D)** Image of a 12-well plate of the Spin Ω system with multiple forebrain organoids in individual wells. **(E)** Example image of a ventricular zone-like area in the forebrain organoid. Neural stem cells are PAX6+ surrounded by TUJ1+ neurons. Scale bar represents 100 μm . **(F)** Representative image of an organoid section stained with cortical deep layer marker CTIP2 and upper layer marker SATB2. Scale bar represents 200 μm . **(G)** Higher magnification of cortical mantle-like region from **F** with demarcation between the ventricular zone-like area (VZ) and the cortical mantle-like region with an abundance of CTIP2+ and SATB2+ neurons. Scale bar represents 50 μm .

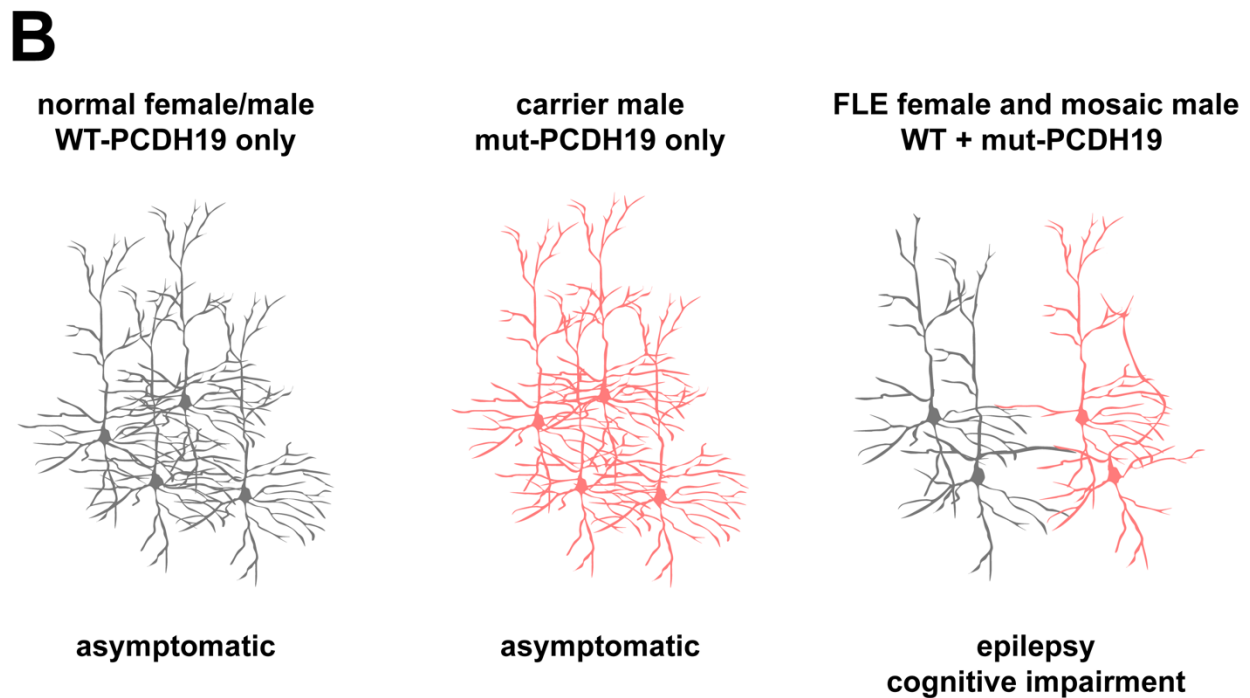
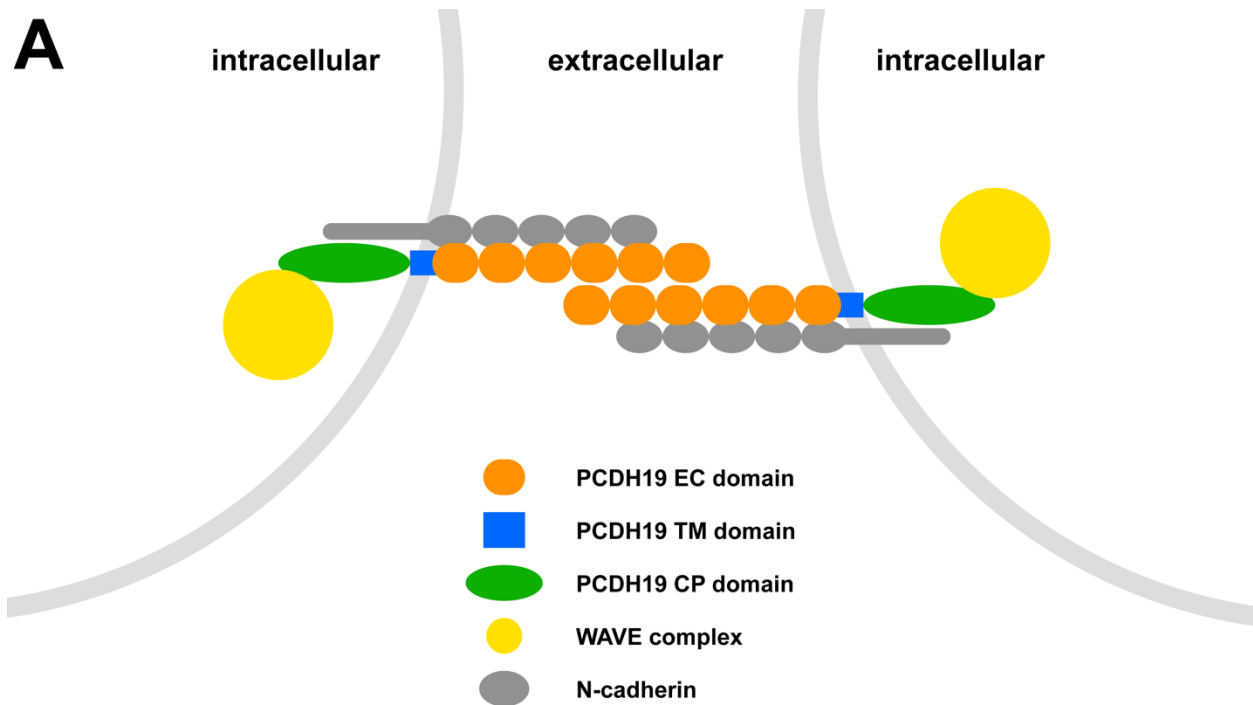


Figure 1.4. Structure of the PCDH19 protein and its postulated role in PCDH19 FLE. (A) Schematic demonstrating the structure of the PCDH19 protein on the cell surface. The protein has six extracellular (EC) domains that are responsible for its adhesive properties, a single transmembrane domain (TM) as well as a cytoplasmic domain (CP) with two conserved motifs. PCDH19 has been shown to interact with N-cadherin and the WAVE complex. (B) Schematic of the cellular interference hypothesis, the postulated

mechanism of pathogenesis of PCDH19 FLE. In normal females and males, all cells homogeneously express wildtype (WT) PCDH19. In carrier males, all cells homogeneously express mutant (mut) PCDH19 with no WT PCDH19 expressed. However, in females with heterozygous *PCDH19* mutations and mosaic males, some cells express WT-PCDH19 while others express mut-PCDH19. These two cell populations interact aberrantly to cause epilepsy and cognitive impairment.

Chapter 2

Monosynaptic Tracing of Hippocampal Circuit Remodeling in Experimental Temporal Lobe Epilepsy

Summary

Many dentate granule cells (DGCs) generated after an epileptogenic insult in experimental temporal lobe epilepsy (TLE) develop aberrantly and are thought to contribute to the development of seizures. Understanding how adult-born DGCs integrate into the epileptic network and whether their integration differs from early-born DGCs that are mature at the time of an epileptogenic insult may provide insights into therapeutic targets. Here we use a dual-viral tracing strategy combining retroviral birthdating with rabies virus-mediated retrograde trans-synaptic tracing to identify and compare presynaptic inputs onto adult- and early-born DGCs in the rat pilocarpine model of TLE. Our results demonstrate that hilar ectopic DGCs preferentially synapse onto adult-born DGCs after status epilepticus (SE) while normotopic DGCs synapse onto both adult- and early-born DGCs. Additionally, as compared with those onto early-born DGCs, adult-born DGCs in the intact brain receive more inputs from other DGCs. We also find that parvalbumin and somatostatin interneuron inputs are greatly diminished onto early-born DGCs after pilocarpine treatment while somatostatin interneuron inputs onto adult-born DGCs are maintained, likely due to preferential

sprouting. Intriguingly, CA3 pyramidal cell backprojections that specifically target adult-born DGCs arise in the epileptic brain, while axons of interneurons and pyramidal cells in CA1 likely sprout across the hippocampal fissure to preferentially synapse onto early-born DGCs. These data support the presence of substantial hippocampal circuit remodeling after an epileptogenic insult that generates prominent excitatory feedback loops involving DGCs. Both adult- and early-born DGCs are targets for novel inputs from other DGCs as well as from CA3 and CA1 pyramidal cells after pilocarpine treatment, changes that likely contribute to epileptogenesis in experimental TLE.

Introduction

TLE is a common epilepsy syndrome estimated to afflict over 25 percent of adults diagnosed with epilepsy (Asadi-Pooya et al., 2016). The pathological hallmarks of human TLE are hippocampal cell loss and gliosis (de Lanerolle et al., 1989; Wolf and Wiestler, 1993), changes that are recapitulated in the rat pilocarpine model of TLE (Cavalheiro et al., 1991; Mello et al., 1993). Although TLE pathogenesis remains poorly understood, accumulating evidence implicates aberrant plasticity within the hippocampal dentate gyrus in this process. In human and experimental TLE, DGCs demonstrate characteristic morphological abnormalities such as mossy fiber sprouting (MFS), persistent hilar basal dendrites (HBDs), granule cell layer dispersion and ectopic soma placement (Tauck and Nadler, 1985; Houser, 1990; Houser et al., 1990; Parent et al., 1997; von Campe et al., 1997; Ribak et al., 2000; Parent et al., 2006; Murphy et al., 2012). DGCs are also the only hippocampal neurons that continue to be generated throughout adulthood (Eriksson et al., 1998). The integration of adult-born DGCs is thought to contribute to learning and memory (reviewed in Deng et al., 2010). Adult DGC neurogenesis is robustly potentiated

by seizures (Parent et al., 1997), but many DGCs born after chemoconvulsant-induced SE integrate aberrantly and are hypothesized to contribute to disease pathogenesis. In fact, dentate gyrus structural changes in experimental TLE are thought to largely arise from the aberrant development of the adult-born DGC population (Jessberger et al., 2007; Walter et al., 2007; Kron et al., 2010; Murphy et al., 2011; Hester and Danzer, 2013), although recent work indicates that pre-existing DGCs also contribute to MFS (Althaus et al., 2016).

Adult-born DGCs are implicated as the major source of hilar ectopic DGCs and normotopic DGCs with HBDs, both of which have been proposed to be 'hub cells' with excitatory hyper-connectivity (Morgan and Soltesz, 2008; Thind et al., 2008; Kron et al., 2010; Murphy et al., 2011). Previous work has largely focused on the postsynaptic targets of DGCs generated after SE (Scharfman et al., 2000; McAuliffe et al., 2011) with less knowledge about how their synaptic inputs change during epileptogenesis. This question is especially crucial in light of the mounting evidence that network remodeling in the epileptic brain is much more extensive and robust than previously believed. Seizure-induced hippocampal synaptic reorganization not only involves excitatory neurons, including DGCs and CA1 pyramidal cells (Tauck and Nadler, 1985; Smith and Dudek, 2001; Buckmaster et al., 2002a; Althaus et al., 2016), but also surviving interneurons (Thind et al., 2008; Zhang et al., 2009; Peng et al., 2013; Yu et al., 2013). Whether excitatory and inhibitory sprouting is preferentially onto the pre-existing (early-born) or newly developed (adult-born) DGC population is unknown, but understanding this process should provide important clues as to how pro-seizure networks develop after an epileptogenic insult.

To determine if pilocarpine-induced SE differentially influences the plasticity of age-defined populations of DGCs, we employed a dual-viral tracing strategy combining retroviral (RV)-mediated birthdating with modified rabies virus (RbV)-mediated retrograde trans-synaptic tracing (Wickersham et al., 2007). This approach was used to study first-order monosynaptic inputs onto adult- and early-born DGCs in the chronically epileptic or intact brain. We found a striking degree of feedback/recurrent excitatory input onto both DGC populations after SE, including direct pyramidal cell to DGC projections from CA3 and CA1, with differential changes in inhibitory inputs onto these two birthdated cohorts. These results suggest that DGCs receive widespread local and long-distance monosynaptic excitation that likely contributes to epileptogenesis in experimental TLE.

Materials and methods

Viral Production

We generated a RV construct (RV-Syn-GTR) that consisted of a Murine Moloney Leukemia virus-based RV vector containing a human Synapsin1 promoter driving GFP, the avian sarcoma leukosis virus receptor (TVA) and the RbV glycoprotein (Rgp). To make the construct pSyn-eGFP-TVA-Rgp-WPRE (pSyn-GTR), the GTR DNA fragment was obtained by polymerase chain reaction (PCR) from the pBOB-Syn-HTB template (a gift from Edward Callaway, Salk Institute, La Jolla, CA) using primers: 5'-atccctgcagatctcgcccttatcgtc-3' and 5'-atgctagactgtcgcacggcctgcgta-3'. Following Sal I and Bgl II restriction enzyme digestion, the obtained GTR fragment was used to replace GFP in pCAG-GFP-WPRE (a gift from Fred Gage, Salk Institute, La Jolla, CA). The Synapsin1 (Syn) promoter fragment was obtained by Acc1 and BamH1 restriction

enzyme digestion of pBob-Syn-HTB and replacing the CAG promoter in pCAG-GTR-WPRE.

To assess for integrity of the RbV, a control RV (con-RV) was generated by deleting Rgp from pSyn-GTR by Hind III and Pme I restriction enzyme digestion. Pseudotyped RV stocks were produced by co-transfection of RV constructs with vesicular stomatitis virus G protein (VSV-G) plasmid into the GP2-293 packaging cell line (Clontech). Harvested supernatant containing RV was filtered through a 0.45 μ M filter (Gelman Sciences) and concentrated by ultracentrifugation. Titers ranged from $2-5 \times 10^8$ cfu/mL.

Avian envelope glycoprotein subgroup A (EnvA)-pseudotyped RbV (RbV-mCh) was produced as described previously (Wickersham et al., 2010) with titers ranging from $1-2 \times 10^8$ cfu/mL.

Lentivirus expressing synaptophysin (Syp)-GFP fusion gene driven by a CAMKII α promoter (CAMKII α -Syp-GFP) was produced by transient transfection of the following plasmids: transIT-LT1 (Mirus Bio, Madison, WI), vector, psPAX2 and pMD2.G. Supernatant was harvested 48 hours later, filtered and concentrated by ultracentrifugation.

Animals and Seizure Induction

All animal procedures were performed following protocols approved by the Institutional Animal Care and Use Committee of the University of Michigan. Animals were purchased from Charles River and maintained between 20-22°C under a constant 12 h light/dark cycle with access to food and water *ad libitum*. A total of 248 animals underwent pilocarpine-induced SE or sham treatment in this study and 36 animals were used for the

final experimental analyses. Approximate numbers of animals excluded during the sequence of procedures includes: 20% loss from pilocarpine treatment; 35% death from one of the two viral injections; 25% from unsuccessful targeting of viral injections; and 5% exclusion due to grossly damaged dentate gyri from injection or SE. Epileptic and sham control rats were generated as previously described (Kron et al., 2010; Althaus et al., 2016). Briefly, adult male Sprague Dawley rats at age postnatal day (P) 56 and ~250 g weight were pretreated with atropine methylbromide (5 mg/kg i.p.; Sigma-Aldrich) and 20 minutes later were administered the chemoconvulsant pilocarpine hydrochloride (340 mg/kg, i.p.; Sigma-Aldrich). Seizures were monitored behaviorally and terminated after 90 minutes of SE with diazepam (10 mg/kg, i.p.; Hospira Inc.). Seizure severity was scored on the standard Racine scale (Racine, 1972) and all SE animals reached a score of 5 (with multiple events of rearing and falling with forelimb clonus). Sham controls received identical treatment except pilocarpine was replaced with an equivalent volume of 0.9% saline.

Intrahippocampal Injections

To birthdate early- or adult-born DGCs and render them RbV-competent, RV-Syn-GTR was injected bilaterally into the dorsal dentate gyrus at either P7 or P60, respectively, as described previously (Kron et al., 2010; Althaus et al., 2016). Briefly, P7 male pups were anesthetized on ice and placed on an ice cold neonatal rat stereotaxic adapter (Stoelting) in a Kopf stereotaxic frame. Bilateral burr holes were drilled into the skull and 1 μ L of RV-Syn-GTR was injected at a rate of 0.1 μ L/min using a 5 μ L Hamilton syringe with the following coordinates (in mm from bregma and mm below the skull): caudal 2.0, lateral 1.5, depth 2.7. P60 adult male rats were anesthetized using a mixture

of Ketamine/Xylazine and placed in a Kopf stereotaxic frame. Bilateral burr holes were drilled into the skull and 2 μ L of RV-Syn-GTR (or con-RV, see **Figure 2.2**) was injected as in the P7 pups except the following coordinates (in mm from bregma and mm below the skull) were used: caudal 3.9, lateral 2.3, depth 4.2.

To trace first-order presynaptic inputs onto RV-Syn-GTR-infected, birthdated DGC populations, RbV-mCh was diluted 500-fold to avoid non-specific labeling and injected bilaterally into the dorsal dentate gyrus at 8-10 weeks after pilocarpine or vehicle injection (P112-126). Animals were anesthetized using a Ketamine/Xylazine mixture and placed in a stereotaxic frame. Bilateral burr holes were drilled and 2 μ L of RbV-mCh was injected at a rate of 0.1 μ L/min at the following coordinates (in mm from bregma and mm below the skull): caudal 4.2, lateral 2.3, depth 4.2.

To label CA1 pyramidal cell axons and synaptic terminals in separate experiments, CAMKII α -Syp-GFP was injected bilaterally into hippocampal area CA1 at 3 weeks after SE or sham treatment (P77). Animals were anesthetized using a Ketamine/Xylazine mixture and 1 μ L of CAMKII α -Syp-GFP was injected at a rate of 0.1 μ L/min using the following coordinates (in mm from bregma and mm below the skull): caudal 3.8, lateral 2.0, depth 2.5.

Immunohistochemistry

At 1 week after injection of RbV-mCh, animals were deeply anesthetized with pentobarbital and transcardially perfused with 0.9% saline followed by 4% paraformaldehyde (PFA). Brains were removed and post-fixed overnight at 4°C in 4% PFA and cryoprotected with 30% sucrose. Frozen coronal sections (40 μ m thickness) were cut using a sliding microtome. Series of 12-16 sections (each 480 μ m apart) were

processed with standard fluorescent immunohistochemical (IHC) techniques (double- and triple-labeling) using the following primary antibodies: chicken anti-GFP (1:1000, Aves), rabbit (Rb) anti-dsRed (1:1000, Clontech), mouse (Ms) anti-mCherry (1:1000, Clontech), Rb anti-Prospero Homeobox 1 (Prox1; 1:1000, a gift from Sam Pleasure, University of California, San Francisco, San Francisco, CA), Ms anti-Parvalbumin (PV; 1:400, Sigma) or Rb anti-SST-14 (1:500, Peninsula Labs). Secondary antibodies (Alexa Fluor, 1:400 dilution, Invitrogen) used were: goat (Gt) anti-chicken 488, Gt anti-rabbit 594 or 647, and Gt anti-mouse 594 or 647. Nuclear counterstain was performed using bisbenzimidazole.

Microscopy

Images were acquired with a Leica TCS SP5X Confocal Microscope. For confirmation of mCh and Prox1 co-localization in DGCs, images were acquired under a 63x objective at 1.0x optical zoom and 1 μm step size through the z-plane with the pinhole set at 1 Airy unit. For analysis of double-labeling for mCh and interneuron markers, as well as quantification of mCh⁺ cells, images were acquired with a 20x objective at 1.0x optical zoom and 2 μm step size through the z-plane with the pinhole set at 1 Airy unit.

Image Analysis and Statistics

Images were imported into Adobe Photoshop CS6 and analyzed for co-localization of immunoreactivity. Quantification was performed blinded to experimental group with coded images on sections spaced 480 μm apart that spanned the rostral-caudal extent of each hippocampus. Animals with a grossly damaged dentate gyrus were excluded from quantification. Within the dentate gyrus, birthdated starter DGCs were counted as cells

that were GFP+/mCh+ and first-order presynaptic inputs were identified as mCh+ only (GFP-negative) cells. Cells in the dentate hilus (including hilar ectopic DGCs) were defined by a location of at least two cell body widths away from the internal border of the granule cell layer. Identification of Prox1+ DGCs as well as PV+ and SST+ interneurons was based on morphology, location and marker labeling. Cells that were both mCh+ and marker+ but GFP-negative were counted. We divided the number of mCh+/marker+ neurons by the number of starter neurons to calculate the average number of marker+ inputs per starter neuron. We also divided the number of mCh+/marker+ neurons by the total number of dentate gyrus mCh+ only neurons to yield the percentage of dentate gyrus inputs arising from a specific marker+ population. In hippocampal CA3 and CA1, identification and distinction of mCh+ only presynaptic interneurons and pyramidal cells were based on soma location and morphology. In the entorhinal cortex and subiculum, all mCh+ only inputs were counted without distinguishing between cell types.

Data for specific regions (i.e. CA3, CA1, entorhinal cortex and subiculum) were pooled between all the sections immunostained per animal (at least 36 sections) and normalized to the total number of GFP+/mCh+ starter DGCs within those sections for that animal. Statistical analyses were performed using GraphPad Prism 7 software. Group means were compared with a one-way ANOVA and post-hoc Tukey's multiple comparisons test with the significance level set at $p < 0.05$. All error bars represent standard error of the mean (SEM).

Results

Validating RV-RbV dual-virus tracing

We combined the RbV-mediated retrograde trans-synaptic tracing technique (Wickersham et al., 2007) with RV reporter birthdating to map monosynaptic connections onto age-defined DGC populations in the intact or epileptic brain. This approach allowed us to identify differences in connections onto adult-born DGCs that were born after SE versus those onto the early-born DGCs that already existed in the network. Furthermore, we could compare how SE changed the integration of these birthdated populations as compared with their age-matched control counterparts. Lastly, we also were interested in identifying the differences in inputs onto adult- and early-born DGCs in the intact brain.

RV-Syn-GTR was delivered to bilateral dentate gyri of rats at either P7 or P60 to birthdate early-born or adult-born DGCs, respectively, and render them RbV infection-competent (**Figure 2.1A, B**). We induced SE at P56 and generated four cohorts of animals for comparison: epileptic animals that received RV at P60 (P60 SE), non-epileptic controls that received RV at P60 (P60 sham), epileptic animals that received RV at P7 (P7 SE), and non-epileptic controls that received RV at P7 (P7 sham). At 8-10 weeks after SE or sham treatment (P112-126) in all cohorts, RbV-mCh was injected into bilateral dentate gyri which, through the recognition of EnvA with its cognate receptor TVA, selectively infects cells that were previously birthdated with RV-Syn-GTR. In these GFP+/mCh+ 'starter cells,' RbV-mCh trans-complements with Rgp thereby allowing it to travel retrogradely to label first-order presynaptic inputs onto starter cells with mCh only. These partner neurons lack Rgp and thus RbV-mCh cannot spread any further (**Figure**

2.1A). This strategy allowed us to restrict trans-synaptic spread to only monosynaptic connections onto starter cells.

To first determine whether the RV-RbV system labels appropriate first-order DGC inputs, we examined monosynaptic connections onto early- and adult-born DGCs in controls. We observed mCh⁺ cells exclusively in areas known to project onto DGCs, including local projections from the dentate hilus and long-distance afferents from the entorhinal cortex (EC), the supramammillary nucleus (SUP) and the septum (**Figure 2.1C, D**, examples of dentate gyrus starter cells are yellow in the insets). Note that more mCh⁺ inputs were labeled for early-born DGCs (**Figure 2.1C**) than for adult-born DGCs (**Figure 2.1D**). This difference that likely reflects the increased number of starter cells in P7 injected animals, consistent with the fact that DGCs are predominantly generated neonatally. Together, these findings support the feasibility of the RV-RbV method for tracing monosynaptic inputs onto birthdated DGCs in the rat.

Differential inputs from Prox1⁺ DGCs after SE

We next assessed the fidelity of RbV trans-synaptic retrograde labeling and examined the local presynaptic inputs of adult-born DGCs in sham versus epileptic rats. After SE, as expected, the number of GFP⁺ adult-born DGCs increased versus controls (**Figure 2.2A, B**) and many GFP⁺ hilar ectopic DGCs appeared, some of which were starter cells. In both cohorts, many mCh⁺/GFP⁻ cells were present throughout the dentate gyrus (**Figure 2.2A'**, arrowheads in inset), representing local monosynaptic inputs onto GFP⁺/mCh⁺ starter DGCs (**Figure 2.2A', B'**, arrows in inset). To eliminate the possibility of RbV spread in the absence of RV-Syn-GTR, we injected P60 SE or sham rats with con-RV that lacked Rgp, the protein necessary for RbV packaging and subsequent

retrograde spread (**Figure 2.2C, D**). One week after RbV infection, we observed many GFP+/mCh+ starter DGCs in sham and pilocarpine-treated animals with no evidence of mCh+ only presynaptic cells (**Figure 2.2C', D'**).

After an epileptogenic insult, DGCs sprout mossy fibers into the inner molecular layer where they form functional synapses onto nearby DGCs (Lynch and Sutula, 2000; Buckmaster et al., 2002b; Scharfman et al., 2003) thereby creating a recurrent excitatory circuit. We recently found that both early- and adult-born DGCs contribute to MFS (Althaus et al., 2016), but it remains unclear whether these populations differ in the extent to which they *receive* recurrent mossy fiber innervation. We used the DGC marker Prox1 to quantify mCh+/Prox1+ (GFP-negative) cells, representing DGCs that monosynaptically innervate birthdated starter neurons. In animals that received RV-Syn-GTR at P60, we found mCh+/Prox1+/GFP- cells in the granule cell layer of both intact (**Figure 2.3A, A'**) and epileptic rats (**Figure 2.3B, B'**). Notably, the mean number of presynaptic DGC inputs in the granule cell layer onto adult-born starter cells did not differ significantly between SE and sham groups (**Figure 2.3E**, GCL, P60 sham vs. P60 SE). When we examined presynaptic DGC inputs onto early-born DGCs in controls, we found significantly fewer DGCs that innervated early-born DGCs than adult-born DGCs under basal conditions (**Figure 2.3C, C'** and **E**, left side, P60 sham vs. P7 sham). Our analysis also demonstrated that early-born DGCs received Prox1+ DGC presynaptic inputs after SE (**Figure 2.3D, D'**), and the amount per starter cell was not significantly different than the other three groups (**Figure 2.3E**). Intriguingly, despite the relatively low ratio of hilar ectopic DGCs to normotopic DGCs after SE, we observed significantly more mCh+/Prox1+/GFP- cells in the hilus of P60-injected animals after SE than in the other three groups, which

represented hilar ectopic DGC inputs specifically onto adult-born DGCs (**Figure 2.3B'**, arrow and **E**, right side). Hilar ectopic DGC inputs onto P7 injected early-born DGCs were rare after SE (**Figure 2.3D**, **D'** and **E**, right side).

We also analyzed the mCh+/Prox1+/GFP- proportion of all mCh+ non-starter cells in the dentate gyrus, which represented the proportion of all mCh+ only inputs that arose from presynaptic DGCs. We found that ~29% (25% from normotopic and 4% from hilar ectopic) of all dentate gyrus presynaptic inputs onto adult-born DGCs arose from other DGCs after SE versus only ~5% in the intact brain (**Figure 2.3F**). Additionally, early-born DGCs after SE received ~31% of their presynaptic inputs from other normotopic DGCs and less than 1% from hilar ectopic DGCs, while early-born DGCs in the intact brain received only ~7% of inputs from other DGCs (**Figure 2.3F**). These results suggest that a greater proportion of dentate gyrus presynaptic inputs onto both DGC populations in the epileptic brain were from other DGCs. Moreover, some DGC-to-DGC connections arising after SE involved hilar ectopic DGC selectively synapsing onto adult-born DGCs. Because hilar ectopic DGCs arise only from the adult-generated DGCs (Kron et al., 2010), these data indicate that seizure-induced neurogenesis results in a specific recurrent excitatory network involving connections between ectopic and normotopic (or ectopic and ectopic) adult-generated neurons.

Dentate gyrus inhibitory inputs change after SE

The SST-positive hilar perforant path-associated interneurons primarily target DGC dendrites and are highly susceptible to SE-induced death. Despite their massive loss, there is also evidence to suggest that surviving SST interneurons sprout axon collaterals in the chronically epileptic brain (Zhang et al., 2009; Peng et al., 2013). To

assess SST interneuron inputs onto birthdated DGCs, we triple labeled for GFP, mCh and SST in all cohorts (**Figure 2.4A-D'**). We found that both adult- and early-born DGCs in epileptic animals received fewer inhibitory inputs from hilar SST interneurons as compared with adult-born DGCs in the control brain, but not versus early-born DGCs in controls (**Figure 2.4E**). In addition, more SST interneurons provided inputs onto adult-born DGCs as compared with early-born DGCs in the intact brain (**Figure 2.4E**). When we calculated the percentage of all dentate gyrus mCh+/GFP- presynaptic inputs that arose from SST interneurons, we found that a smaller fraction of inputs onto early-born DGCs after SE arose from SST interneurons as compared with early-born DGCs in controls or with adult-born DGCs in epileptic rats (**Figure 2.4F**). Together, these findings suggest that early-born DGCs in the epileptic brain are excessively disinhibited, and probably also reflect preferential sprouting of hilar SST interneurons onto adult-born neurons after SE to prevent loss of inhibition.

Despite an overall loss, certain populations of interneurons are less affected by SE-induced death, including the PV-expressing basket cells (Sun et al., 2007). PV interneurons are a major GABAergic subtype in the dentate gyrus that primarily target the perisomatic regions and axon initial segments of DGCs. To explore changes in PV+ inputs, we triple labeled animals for GFP, mCh and PV (**Figure 2.5A-D'**) and examined mCh+/PV+ (GFP-negative) interneurons. We calculated the mean number of mCh+/PV+ interneurons per starter DGC and found more mCh+/PV+ interneurons projecting monosynaptically onto adult-born DGCs in the intact brain as compared with the other three groups (**Figure 2.5E**). No significant differences were observed in the ratio of mCh+/PV+ cells to all dentate gyrus mCh+ presynaptic input between any of the cohorts

(**Figure 2.5F**). Taken together, these findings suggest that early-born DGCs in the epileptic brain are excessively disinhibited, while hilar SST interneurons likely sprout preferentially onto adult-born neurons after SE. Moreover, adult-born DGCs in controls receive more inhibitory inputs than their early-born counterparts.

Inputs from other regions of the hippocampus

We next focused on potential innervation from hippocampal CA regions onto birthdated DGCs. Prior work supports the presence of intra-hippocampal projections into the dentate gyrus, particularly from CA3 pyramidal cells, under basal and pathological conditions (Li et al., 1994; Scharfman et al., 2000; Zhang et al., 2012). Remarkably, we found evidence of robust projections directly onto DGCs, particularly after SE, with the presence of mCh⁺ cells in CA3 and CA1 (**Figure 2.6A-L**). We also found sparse mCh-labeled cells in area CA2 in all groups (data not shown). Presynaptic cells expressing mCh were present in all CA subregions in controls, and nearly all exhibited an interneuron morphology (**Figure 2.6A, C**). Although we found no significant differences in the mean number of CA3 mCh⁺ cells per starter cell between the four cohorts (**Figure 2.6E**), a much larger proportion of CA3 mCh⁺ inputs onto adult-born DGCs after SE arose from cells with pyramidal cell location and morphology (**Figure 2.6B, D, F**). Examination of CA1 showed significantly more mCh⁺ cells per starter cell in epileptic animals (**Figure 2.6G-K**), particularly for early-born DGCs (**Figure 2.6K**), and more of these cells in both SE groups displayed a pyramidal neuron morphology and location than in controls (**Figure 2.6L**).

Evidence in the literature suggests that CA1 pyramidal cells innervate the dentate gyrus in epilepsy models (Bausch and McNamara, 2000; Smith and Dudek, 2001; Vivar

et al., 2016), and recent work indicates that SST-expressing interneurons in CA1 sprout axon collaterals across the hippocampal fissure into the dentate gyrus after SE (Peng et al., 2013). RbV tracing showed significant numbers of mCh⁺ processes that appear to cross the hippocampal fissure in SE animals (**Figure 2.6H, J**, arrows). To further examine these projections, we injected a lentivirus carrying a CAMKII α promoter driving a synaptophysin-GFP (CAMKII α -Syp-GFP) fusion gene into CA1 of rats 3 weeks after SE or sham treatment to specifically label the axonal projections of pyramidal neurons (**Figure 2.6M**). In controls, labeled CA1 pyramidal cell processes appeared in strata radiatum and lacunosum moleculare, but largely respected the border of the hippocampal fissure and only rarely appeared to cross into the dentate gyrus (**Figure 2.6N**). In contrast, many more Syp-GFP-labeled processes in pilocarpine-treated rats appeared to cross the hippocampal fissure from CA1 into the dentate gyrus (**Figure 2.6O, O'**), supporting the potential of CA1 pyramidal neurons to innervate DGC dendrites after SE. Together, these findings suggest that substantial numbers of new excitatory feedback projections from CA3 and CA1 onto adult- and early-born DGCs arise in experimental TLE.

Inputs from extra-hippocampal regions

To assess the major long-distance afferent pathway onto DGCs, the perforant path, we explored whether SE alters RbV labeling in the entorhinal cortex. We identified mCh⁺ presynaptic neurons in the entorhinal cortex (**Figure 2.7A-D**) and quantified the average number of presynaptic inputs per starter cell. We found no statistically significant differences in the number of labeled entorhinal cortex neurons amongst the four groups (**Figure 2.7E**). We also found sparse inputs from the subiculum onto DGCs in all cohorts (**Figure 2.7F-I**) consistent with recent work describing these connections (Bergami et al.,

2015). No statistically significant differences in the number of labeled subicular neurons were present between groups (**Figure 2.7J**).

Discussion

Here we combine RV birthdating with RbV retrograde trans-synaptic tracing to identify changes in monosynaptic inputs onto age-defined DGC populations in the intact and epileptic brain. Our results suggest that adult- and early-born DGCs show some similarities as well as distinct differences in seizure-induced plasticity in the epileptic hippocampus. We find that adult-born DGCs receive significant excitatory backprojections from CA3 pyramidal cells and substantial recurrent excitatory inputs from other DGCs. In particular, adult-born DGCs are selectively targeted by hilar ectopic DGCs, representing a novel DGC-to-DGC recurrent excitatory pathway exclusively involving DGCs generated after SE. Interestingly, a significant proportion of presynaptic inputs onto early-born DGCs also arise from other DGCs after SE, albeit not as high as for adult-born DGCs. Early-born DGCs are preferential targets of CA1 pyramidal cell sprouting that likely involves pyramidal cell axons crossing the hippocampal fissure. In addition, early-born DGCs after SE display the least hilar PV and SST inhibitory inputs, while hilar SST interneurons likely sprout selectively onto adult-born DGCs.

Recurrent DGC-to-DGC connections after SE

We describe for the first time the finding that adult-born DGCs receive more recurrent excitatory inputs from hilar ectopic DGCs than do early-born DGCs that were mature at the time of SE. These changes may relate to the presence and positioning of

persistent HBDs on DGCs after SE (Spigelman et al., 1998; Buckmaster and Dudek, 1999), a seizure-induced pathology that is unique to adult-born DGCs (Jessberger et al., 2007; Walter et al., 2007; Kron et al., 2010). Indeed, hilar basal dendrites are known to receive excessive excitatory synapses (Ribak et al., 2000; Thind et al., 2008). Moreover, as adult-born-DGCs are undergoing developmental synaptogenesis, they demonstrate enhanced plasticity (Schmidt-Hieber et al., 2004; Ge et al., 2007) that likely heightens their potential for receiving new connections. While early-born DGCs in the epileptic brain appear to receive a similar proportion of all their presynaptic inputs from other DGCs as adult-born DGCs, the overall network-wide decrease in the number of inputs to early-born DGCs after SE makes DGC-to-DGC connections a more prominent proportion of their presynaptic inputs.

We also show that adult-born DGCs in the intact brain receive inputs from other DGCs to a much greater extent than early-born DGCs, suggesting that intrinsic differences exist between these two populations. This idea is contrary to the long-held belief that fully mature adult-born DGCs are functionally indistinguishable from their early-born counterpart and accumulating evidence suggests that adult-born DGCs contribute in a specific manner to learning and memory (McHugh et al., 2007; Aimone et al., 2009; Deng et al., 2010). In intact rodents, Timm staining to identify mossy fibers typically is the most pronounced in the dentate hilus but there exists faint staining in the granule cell layer suggesting minor DGC-to-DGC connections (Haug, 1974). While our work suggests that these connections exist, it is important to emphasize that they are relatively rare given the small number of adult-born neurons in intact animals compared to the total DGC population that receives DGC-to-DGC inputs after SE. Additionally, work using similar

RbV retrograde trans-synaptic tracing in mice suggests that DGCs synapse onto neighboring adult-born DGCs under normal, non-epileptic conditions (Vivar et al., 2016). Combined with our interneuron tracing findings, these results support the notion that the innervation of adult-born DGCs differs from that of their early-born counterparts. In the future, modeling studies that take into account these differential connections may inform mechanisms by which adult-born DGCs contribute to pattern separation and pattern completion functions of the hippocampus.

Importantly, we did not observe differences in the number of presynaptic DGC inputs onto adult-born DGCs in epileptic versus intact rats. At first, this finding may seem counterintuitive to the notion that DGC-to-DGC connections increase onto adult-born DGCs after SE. However, based upon our data showing that DGC presynaptic inputs constitute a much smaller proportion of all inputs onto adult-born DGCs in controls, along with their lack of hilar ectopic DGC inputs, we reason that adult-born DGCs in the intact brain receive a significant amount of input from other cell types, most likely inhibitory interneurons, which counterbalances the increased DGC inputs.

Inputs from SST and PV interneurons have different behaviors

The extensive inhibitory interneuron network in the dentate gyrus consists of a diverse population of cell types including two important subtypes: the SST-positive and PV-positive interneurons. It has been estimated that up to 83 percent of the inhibitory interneurons lost in the dentate gyrus after SE are SST-positive (Buckmaster and Jongen-Relo, 1999). However, surviving SST interneurons hypertrophy and undergo axonal sprouting (Mathern et al., 1995; Zhang et al., 2009). Our data suggest a loss of SST+ inputs onto early-born DGCs after SE, most likely due to the SE-induced death. On the

other hand, the adult-born DGC population shows greater proportions of mCh⁺ inputs that are SST⁺ than do the early-born DGC cohort after SE, suggesting that surviving SST interneurons preferentially sprout onto adult-born DGCs. Interestingly, the mean number of inputs from SST interneurons onto labeled DGCs is highest for adult-born neurons in controls. A potential reason for increased numbers of SST⁺ inputs onto adult- versus early-born DGCs in the intact brain is that they may help counterbalance increases in DGC inputs onto adult-born DGCs. An important caveat is that we cannot determine with these techniques whether a single SST interneuron is connected to one or multiple postsynaptic starter DGCs. Thus, it is possible that adult-born DGCs after SE receive similar numbers or even increased SST⁺ synapses compared to controls, but they simply arise from fewer SST⁺ cells. In contrast to the SST population, the PV interneurons are relatively resistant to SE-induced death (Sun et al., 2007) and we found similar numbers of PV⁺ inputs onto early-born DGCs in SE and control animals. Furthermore, we found more PV⁺ inputs onto adult-born than early-born DGCs in controls, similar to what was seen for SST⁺ inputs.

Extensive feedback connections from the hippocampus proper after SE

Hippocampal CA3 pyramidal cells are the main targets of DGC mossy fiber axons as part of the classic trisynaptic circuit. Previous work indicates low levels of CA3 backprojections onto DGCs, particularly at the CA3/hilar border, with most of the backprojecting cells identified as inhibitory interneurons (Li et al., 1994; Bergami et al., 2015; Vivar et al., 2016). We found evidence of mostly CA3 inhibitory synapses onto DGCs under basal conditions. In the chronically epileptic brain, tracing studies suggest that CA3 pyramidal cells project axon collaterals into the dentate gyrus (Siddiqui and

Joseph, 2005) and electrophysiological recordings reveal functional evidence of CA3 pyramidal cell to DGC connections (Scharfman et al., 2000; Zhang et al., 2012). Our data support and extend this work with the finding of extensive CA3 pyramidal cell backprojections onto adult-born DGCs, and to a lesser extent onto early-born DGCs, in the epileptic brain. The preferential targeting of CA3 pyramidal cell axons onto adult-born DGCs after SE may reflect the proximity of hilar ectopic DGCs or persistent HBDs to backprojecting pyramidal cell axons.

Surprisingly, we found RbV-traced CA1 pyramidal cells, suggesting that they sprout axon collaterals across the hippocampal fissure to directly innervate DGCs. Although the finding was unexpected, rare monosynaptic connections from CA1 onto adult-born DGCs in intact mice have been reported in RbV tracing studies (Vivar et al., 2016), and CA1 pyramidal cells exhibit axonal sprouting in various epilepsy models (Perez et al., 1996; Esclapez et al., 1999; Bausch and McNamara, 2000, 2004). Recent work also indicates that SST interneurons in CA1 project axon collaterals across the hippocampal fissure to form functional synapses onto DGCs in the mouse pilocarpine TLE model (Peng et al., 2013). Our tracing studies are consistent with and augment their results as we also see increased numbers of mCh/SST, as well as mCh/PV, co-labeled interneurons in CA1 after SE. These connections also were traced in control brains, albeit at much lower levels. We observed CA1 inputs preferentially onto early-born DGCs in the epileptic rats. This selectivity may relate to the fact that, unlike DGCs generated after SE, dendrites of the mature pre-existing DGCs already extend into the middle and outer molecular layers in the first few weeks after SE when much of the axonal reorganization is occurring.

The dentate 'gate' hypothesis proposes that the dentate gyrus acts as a gate that tempers hippocampal excitability through the relatively high threshold for activation of DGCs (Lothman et al., 1992). Previous work suggests that recurrent seizures in experimental TLE may reflect a breakdown of the dentate gate (Heinemann et al., 1992; Krook-Magnuson et al., 2015). We found increased recurrent excitatory DGC-to-DGC inputs, increased recurrent backprojections from CA3 pyramidal cells onto adult-born DGCs, and increased CA1 pyramidal cell sprouting onto early- and adult-born DGCs after SE (**Figure 2.8**). These changes support a case for a breakdown of the dentate gate where excessive, aberrant excitatory connections lead to the development of seizures.

Some limitations of the present work warrant discussion. First, we were unable to identify RbV-labeled inputs from hilar mossy cells in either epileptic or control brains. This result is likely because hilar mossy cells are an extremely vulnerable population such that the RbV may have induced death of traced mossy cells rapidly after retrograde spread. While other groups have shown mossy cell labeling in mouse RbV tracing studies (Vivar et al., 2012; Deshpande et al., 2013), species differences between rat and mouse (e.g., mossy cells express calretinin in mouse but not rat) may account for the discrepancy. Second, we cannot distinguish specific patterns of inputs onto normotopic versus starter cells with aberrant morphology after SE. Targeting specific starter DGCs at a single cell level to trace inputs onto individual DGCs with differing seizure-induced morphology is a challenge for future work. Exploring other interneuron subtypes not examined in this study, both within the dentate gyrus and the hippocampus proper, is also an important future direction. Regarding the specificity of RbV retrograde trans-synaptic tracing, evidence suggests that RbV travels across chemical synapses (Ugolini, 1995; Tang et

al., 1999; Morcuende et al., 2002). However, its mechanism of retrograde transport is still not fully understood and it remains possible that RbV can spread in other ways. Additionally, we most likely identified only a fraction of all the existing presynaptic inputs onto starter cells in our studies as we are limited by factors such as the amount of time before RbV begins to elicit cell death as well as less well-understood issues such as how retrograde spread is affected by neuronal subtype, synaptic density, strength and activity (Callaway and Luo, 2015). There is recent evidence that an improved glycoprotein may facilitate more robust retrograde spread of RbV (Kim et al., 2016) which may aid in identifying other inputs, particularly long-distance projections that were not characterized in detail in these studies.

In summary, our dual-viral tracing strategy provides unique insight into inherent differences in first-order presynaptic inputs onto adult- and early-born DGCs under both control and epileptic conditions. We identify novel connectivity as well as differences in existing inputs, and found that adult-born and early-born DGCs have unique properties and afferent connections that may contribute to aspects of epileptogenesis. An important focus for future studies is the functional consequences of these different inputs and how they alter network physiology. Such work should inform future efforts for developing therapeutics that strategically target aberrant populations of DGCs for the treatment or prevention of TLE.

Notes to Chapter 2

A modified version of this chapter was accepted for publication as:

Du X, Zhang H, Parent JM (2017) Rabies Tracing of Birthdated Dentate Granule Cells in Rat Temporal Lobe Epilepsy. *Annals of Neurology*, in press.

Helen Zhang generated the RV and RbV constructs. Andrew Tidball generated the lentivirus.

We thank Ed Callaway and Fred Gage for providing the viral constructs; Sam Pleasure for providing the Prox1 antibody; Ali Althaus for her contributions to this work.

References

- Aimone JB, Wiles J, Gage FH (2009) Computational influence of adult neurogenesis on memory encoding. *Neuron* 61:187-202.
- Althaus AL, Zhang H, Parent JM (2016) Axonal plasticity of age-defined dentate granule cells in a rat model of mesial temporal lobe epilepsy. *Neurobiology of disease* 86:187-196.
- Asadi-Pooya AA, Stewart GR, Abrams DJ, Sharan A (2016) Prevalence and incidence of drug-resistant mesial temporal lobe epilepsy in the United States. *World Neurosurg.*
- Bausch SB, McNamara JO (2000) Synaptic connections from multiple subfields contribute to granule cell hyperexcitability in hippocampal slice cultures. *Journal of neurophysiology* 84:2918-2932.
- Bausch SB, McNamara JO (2004) Contributions of mossy fiber and CA1 pyramidal cell sprouting to dentate granule cell hyperexcitability in kainic acid-treated hippocampal slice cultures. *Journal of neurophysiology* 92:3582-3595.
- Bergami M, Masserdotti G, Temprana SG, Motori E, Eriksson TM, Gobel J, Yang SM, Conzelmann KK, Schinder AF, Gotz M, Berninger B (2015) A critical period for experience-dependent remodeling of adult-born neuron connectivity. *Neuron* 85:710-717.
- Buckmaster PS, Dudek FE (1999) In vivo intracellular analysis of granule cell axon reorganization in epileptic rats. *Journal of neurophysiology* 81:712-721.
- Buckmaster PS, Jongen-Relo AL (1999) Highly specific neuron loss preserves lateral inhibitory circuits in the dentate gyrus of kainate-induced epileptic rats. *The Journal of neuroscience : the official journal of the Society for Neuroscience* 19:9519-9529.
- Buckmaster PS, Zhang GF, Yamawaki R (2002a) Axon sprouting in a model of temporal lobe epilepsy creates a predominantly excitatory feedback circuit. *The Journal of neuroscience : the official journal of the Society for Neuroscience* 22:6650-6658.
- Buckmaster PS, Yamawaki R, Zhang GF (2002b) Axon arbors and synaptic connections of a vulnerable population of interneurons in the dentate gyrus in vivo. *J Comp Neurol* 445:360-373.
- Callaway EM, Luo L (2015) Monosynaptic Circuit Tracing with Glycoprotein-Deleted Rabies Viruses. *The Journal of neuroscience : the official journal of the Society for Neuroscience* 35:8979-8985.
- Cavalheiro EA, Leite JP, Bortolotto ZA, Turski WA, Ikonomidou C, Turski L (1991) Long-term effects of pilocarpine in rats: structural damage of the brain triggers kindling and spontaneous recurrent seizures. *Epilepsia* 32:778-782.

- de Lanerolle NC, Kim JH, Robbins RJ, Spencer DD (1989) Hippocampal interneuron loss and plasticity in human temporal lobe epilepsy. *Brain Res* 495:387-395.
- Deng W, Aimone JB, Gage FH (2010) New neurons and new memories: how does adult hippocampal neurogenesis affect learning and memory? *Nat Rev Neurosci* 11:339-350.
- Deshpande A, Bergami M, Ghanem A, Conzelmann KK, Lepier A, Gotz M, Berninger B (2013) Retrograde monosynaptic tracing reveals the temporal evolution of inputs onto new neurons in the adult dentate gyrus and olfactory bulb. *Proceedings of the National Academy of Sciences of the United States of America* 110:E1152-1161.
- Eriksson PS, Perfilieva E, Bjork-Eriksson T, Alborn AM, Nordborg C, Peterson DA, Gage FH (1998) Neurogenesis in the adult human hippocampus. *Nature medicine* 4:1313-1317.
- Esclapez M, Hirsch JC, Ben-Ari Y, Bernard C (1999) Newly formed excitatory pathways provide a substrate for hyperexcitability in experimental temporal lobe epilepsy. *J Comp Neurol* 408:449-460.
- Ge S, Yang CH, Hsu KS, Ming GL, Song H (2007) A critical period for enhanced synaptic plasticity in newly generated neurons of the adult brain. *Neuron* 54:559-566.
- Haug FM (1974) Light microscopical mapping of the hippocampal region, the pyriform cortex and the corticomedial amygdaloid nuclei of the rat with Timm's sulphide silver method. I. Area dentata, hippocampus and subiculum. *Z Anat Entwicklungsgesch* 145:1-27.
- Heinemann U, Beck H, Dreier JP, Ficker E, Stabel J, Zhang CL (1992) The dentate gyrus as a regulated gate for the propagation of epileptiform activity. *Epilepsy Res Suppl* 7:273-280.
- Hester MS, Danzer SC (2013) Accumulation of abnormal adult-generated hippocampal granule cells predicts seizure frequency and severity. *The Journal of neuroscience : the official journal of the Society for Neuroscience* 33:8926-8936.
- Houser CR (1990) Granule cell dispersion in the dentate gyrus of humans with temporal lobe epilepsy. *Brain Res* 535:195-204.
- Houser CR, Miyashiro JE, Swartz BE, Walsh GO, Rich JR, Delgado-Escueta AV (1990) Altered patterns of dynorphin immunoreactivity suggest mossy fiber reorganization in human hippocampal epilepsy. *The Journal of neuroscience : the official journal of the Society for Neuroscience* 10:267-282.
- Jessberger S, Zhao C, Toni N, Clemenson GD, Jr., Li Y, Gage FH (2007) Seizure-associated, aberrant neurogenesis in adult rats characterized with retrovirus-mediated cell labeling. *The Journal of neuroscience : the official journal of the Society for Neuroscience* 27:9400-9407.

- Kim EJ, Jacobs MW, Ito-Cole T, Callaway EM (2016) Improved Monosynaptic Neural Circuit Tracing Using Engineered Rabies Virus Glycoproteins. *Cell reports* 15:692-699.
- Kron MM, Zhang H, Parent JM (2010) The developmental stage of dentate granule cells dictates their contribution to seizure-induced plasticity. *The Journal of neuroscience : the official journal of the Society for Neuroscience* 30:2051-2059.
- Krook-Magnuson E, Armstrong C, Bui A, Lew S, Oijala M, Soltesz I (2015) In vivo evaluation of the dentate gate theory in epilepsy. *J Physiol* 593:2379-2388.
- Li XG, Somogyi P, Ylinen A, Buzsaki G (1994) The hippocampal CA3 network: an in vivo intracellular labeling study. *J Comp Neurol* 339:181-208.
- Lothman EW, Stringer JL, Bertram EH (1992) The dentate gyrus as a control point for seizures in the hippocampus and beyond. *Epilepsy Res Suppl* 7:301-313.
- Lynch M, Sutula T (2000) Recurrent excitatory connectivity in the dentate gyrus of kindled and kainic acid-treated rats. *Journal of neurophysiology* 83:693-704.
- Mathern GW, Babb TL, Pretorius JK, Leite JP (1995) Reactive synaptogenesis and neuron densities for neuropeptide Y, somatostatin, and glutamate decarboxylase immunoreactivity in the epileptogenic human fascia dentata. *The Journal of neuroscience : the official journal of the Society for Neuroscience* 15:3990-4004.
- McAuliffe JJ, Bronson SL, Hester MS, Murphy BL, Dahlquist-Topala R, Richards DA, Danzer SC (2011) Altered patterning of dentate granule cell mossy fiber inputs onto CA3 pyramidal cells in limbic epilepsy. *Hippocampus* 21:93-107.
- McHugh TJ, Jones MW, Quinn JJ, Balthasar N, Coppari R, Elmquist JK, Lowell BB, Faselow MS, Wilson MA, Tonegawa S (2007) Dentate gyrus NMDA receptors mediate rapid pattern separation in the hippocampal network. *Science* 317:94-99.
- Mello LE, Cavalheiro EA, Tan AM, Kupfer WR, Pretorius JK, Babb TL, Finch DM (1993) Circuit mechanisms of seizures in the pilocarpine model of chronic epilepsy: cell loss and mossy fiber sprouting. *Epilepsia* 34:985-995.
- Morcuende S, Delgado-Garcia JM, Ugolini G (2002) Neuronal premotor networks involved in eyelid responses: retrograde transneuronal tracing with rabies virus from the orbicularis oculi muscle in the rat. *The Journal of neuroscience : the official journal of the Society for Neuroscience* 22:8808-8818.
- Morgan RJ, Soltesz I (2008) Nonrandom connectivity of the epileptic dentate gyrus predicts a major role for neuronal hubs in seizures. *Proceedings of the National Academy of Sciences of the United States of America* 105:6179-6184.
- Murphy BL, Hofacer RD, Faulkner CN, Loepke AW, Danzer SC (2012) Abnormalities of granule cell dendritic structure are a prominent feature of the intrahippocampal

- kainic acid model of epilepsy despite reduced postinjury neurogenesis. *Epilepsia* 53:908-921.
- Murphy BL, Pun RY, Yin H, Faulkner CR, Loepke AW, Danzer SC (2011) Heterogeneous integration of adult-generated granule cells into the epileptic brain. *The Journal of neuroscience : the official journal of the Society for Neuroscience* 31:105-117.
- Parent JM, Elliott RC, Pleasure SJ, Barbaro NM, Lowenstein DH (2006) Aberrant seizure-induced neurogenesis in experimental temporal lobe epilepsy. *Annals of neurology* 59:81-91.
- Parent JM, Yu TW, Leibowitz RT, Geschwind DH, Sloviter RS, Lowenstein DH (1997) Dentate granule cell neurogenesis is increased by seizures and contributes to aberrant network reorganization in the adult rat hippocampus. *The Journal of neuroscience : the official journal of the Society for Neuroscience* 17:3727-3738.
- Peng Z, Zhang N, Wei W, Huang CS, Cetina Y, Otis TS, Houser CR (2013) A reorganized GABAergic circuit in a model of epilepsy: evidence from optogenetic labeling and stimulation of somatostatin interneurons. *The Journal of neuroscience : the official journal of the Society for Neuroscience* 33:14392-14405.
- Perez Y, Morin F, Beaulieu C, Lacaille JC (1996) Axonal sprouting of CA1 pyramidal cells in hyperexcitable hippocampal slices of kainate-treated rats. *Eur J Neurosci* 8:736-748.
- Racine RJ (1972) Modification of seizure activity by electrical stimulation. II. Motor seizure. *Electroencephalogr Clin Neurophysiol* 32:281-294.
- Ribak CE, Tran PH, Spigelman I, Okazaki MM, Nadler JV (2000) Status epilepticus-induced hilar basal dendrites on rodent granule cells contribute to recurrent excitatory circuitry. *J Comp Neurol* 428:240-253.
- Scharfman HE, Goodman JH, Sollas AL (2000) Granule-like neurons at the hilar/CA3 border after status epilepticus and their synchrony with area CA3 pyramidal cells: functional implications of seizure-induced neurogenesis. *The Journal of neuroscience : the official journal of the Society for Neuroscience* 20:6144-6158.
- Scharfman HE, Sollas AL, Berger RE, Goodman JH (2003) Electrophysiological evidence of monosynaptic excitatory transmission between granule cells after seizure-induced mossy fiber sprouting. *Journal of neurophysiology* 90:2536-2547.
- Schmidt-Hieber C, Jonas P, Bischofberger J (2004) Enhanced synaptic plasticity in newly generated granule cells of the adult hippocampus. *Nature* 429:184-187.
- Siddiqui AH, Joseph SA (2005) CA3 axonal sprouting in kainate-induced chronic epilepsy. *Brain Res* 1066:129-146.

- Smith BN, Dudek FE (2001) Short- and long-term changes in CA1 network excitability after kainate treatment in rats. *Journal of neurophysiology* 85:1-9.
- Spigelman I, Yan XX, Obenaus A, Lee EY, Wasterlain CG, Ribak CE (1998) Dentate granule cells form novel basal dendrites in a rat model of temporal lobe epilepsy. *Neuroscience* 86:109-120.
- Sun C, Mchedlishvili Z, Bertram EH, Erisir A, Kapur J (2007) Selective loss of dentate hilar interneurons contributes to reduced synaptic inhibition of granule cells in an electrical stimulation-based animal model of temporal lobe epilepsy. *J Comp Neurol* 500:876-893.
- Tang Y, Rampin O, Giuliano F, Ugolini G (1999) Spinal and brain circuits to motoneurons of the bulbospongiosus muscle: retrograde transneuronal tracing with rabies virus. *J Comp Neurol* 414:167-192.
- Tauk DL, Nadler JV (1985) Evidence of functional mossy fiber sprouting in hippocampal formation of kainic acid-treated rats. *The Journal of neuroscience : the official journal of the Society for Neuroscience* 5:1016-1022.
- Thind KK, Ribak CE, Buckmaster PS (2008) Synaptic input to dentate granule cell basal dendrites in a rat model of temporal lobe epilepsy. *J Comp Neurol* 509:190-202.
- Ugolini G (1995) Specificity of rabies virus as a transneuronal tracer of motor networks: transfer from hypoglossal motoneurons to connected second-order and higher order central nervous system cell groups. *J Comp Neurol* 356:457-480.
- Vivar C, Peterson BD, van Praag H (2016) Running rewires the neuronal network of adult-born dentate granule cells. *Neuroimage* 131:29-41.
- Vivar C, Potter MC, Choi J, Lee JY, Stringer TP, Callaway EM, Gage FH, Suh H, van Praag H (2012) Monosynaptic inputs to new neurons in the dentate gyrus. *Nature communications* 3:1107.
- von Campe G, Spencer DD, de Lanerolle NC (1997) Morphology of dentate granule cells in the human epileptogenic hippocampus. *Hippocampus* 7:472-488.
- Walter C, Murphy BL, Pun RY, Spieles-Engemann AL, Danzer SC (2007) Pilocarpine-induced seizures cause selective time-dependent changes to adult-generated hippocampal dentate granule cells. *The Journal of neuroscience : the official journal of the Society for Neuroscience* 27:7541-7552.
- Wickersham IR, Sullivan HA, Seung HS (2010) Production of glycoprotein-deleted rabies viruses for monosynaptic tracing and high-level gene expression in neurons. *Nature protocols* 5:595-606.

- Wickersham IR, Lyon DC, Barnard RJ, Mori T, Finke S, Conzelmann KK, Young JA, Callaway EM (2007) Monosynaptic restriction of transsynaptic tracing from single, genetically targeted neurons. *Neuron* 53:639-647.
- Wolf HK, Wiestler OD (1993) Surgical pathology of chronic epileptic seizure disorders. *Brain pathology* 3:371-380.
- Yu J, Proddatur A, Elgammal FS, Ito T, Santhakumar V (2013) Status epilepticus enhances tonic GABA currents and depolarizes GABA reversal potential in dentate fast-spiking basket cells. *Journal of neurophysiology* 109:1746-1763.
- Zhang W, Huguenard JR, Buckmaster PS (2012) Increased excitatory synaptic input to granule cells from hilar and CA3 regions in a rat model of temporal lobe epilepsy. *The Journal of neuroscience : the official journal of the Society for Neuroscience* 32:1183-1196.
- Zhang W, Yamawaki R, Wen X, Uhl J, Diaz J, Prince DA, Buckmaster PS (2009) Surviving hilar somatostatin interneurons enlarge, sprout axons, and form new synapses with granule cells in a mouse model of temporal lobe epilepsy. *The Journal of neuroscience : the official journal of the Society for Neuroscience* 29:14247-14256.

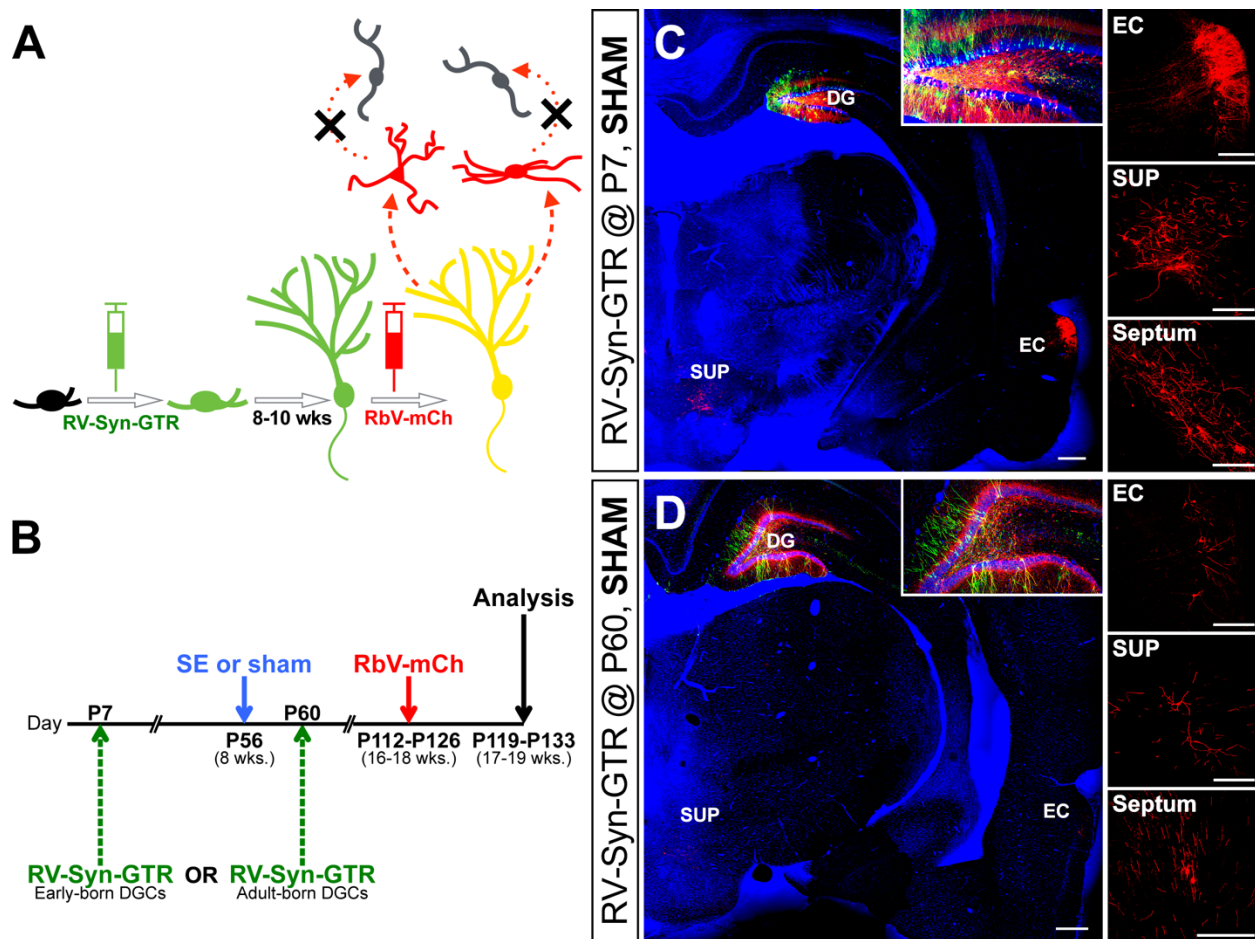


Figure 2.1. RV-RbV dual-viral tracing of presynaptic inputs onto early- and adult-born DGCs.

(A) RV-Syn-GTR injection into the dentate gyrus birthdates dividing DGC progenitors with GFP and renders them competent for RbV-mCh infection 8-10 weeks later. The expression of Rgp by RV-Syn-GTR restricts RbV-mCh spread to only one synapse, thereby selectively labeling first-order presynaptic inputs with mCh. **(B)** Experimental paradigm: RV-Syn-GTR is injected into bilateral dentate gyri at either P7 or P60 to birthdate early- or adult-born DGCs. Rats are treated with pilocarpine (SE) or vehicle (sham) at P56 and RbV-mCh is injected 8-10 weeks later. Animals are euthanized 1 week after RbV-mCh injection. **(C, D)** Confocal images of brain slices showing dual-viral tracing of early- (**C**) and adult-born (**D**) DGCs in controls. There are presynaptic inputs from known areas that target DGCs such as the dentate hilus (insets), entorhinal cortex (EC), supramammillary nucleus (SUP), and septum (right panels). Note that GFP+/mCh+ (yellow) cells are starter DGCs and their presynaptic inputs are mCh+ only. Bisbenzimidazole nuclear stain is shown in blue. Scale bars represent 100 μm (40 μm for insets).

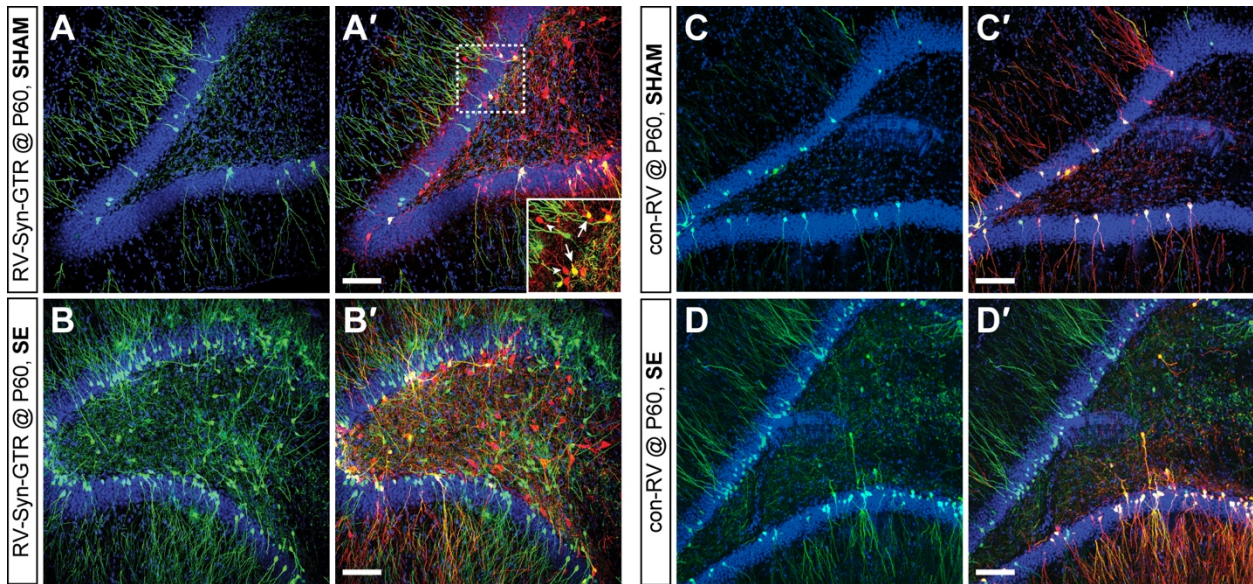


Figure 2.2. RbV-mCh retrograde spread in epileptic and control rats is dependent on the presence of Rgp.

(A) Confocal image of GFP labeling in the dentate gyrus of a control animal injected with RV-Syn-GTR at P60 to label adult-born DGCs. **(A')** GFP/mCh double labeling (same image as in **A**) showing that GFP+/mCh+ starter cells (arrows in inset) appear after RbV-mCh injection 8-10 weeks later, as well as traced mCh+ only presynaptic inputs (arrowheads in inset). **(B)** Confocal image from a pilocarpine-treated rat injected with RV-Syn-GTR at P60 showing increased GFP labeling, including the appearance of GFP+ hilar ectopic adult-born DGCs. **(B')** RbV-mCh tracing (same image as in **B** shows robust mCh+ only labeling in the hilus in addition to the presence of starter hilar ectopic GFP+/mCh+ DGCs. **(C, D)** Confocal image of GFP labeling in the dentate gyrus after control RV (con-RV) was injected into sham or epileptic rats at P60. **(C', D')** Without Rgp, RbV-mCh enters GFP+ cells to generate starter cells (yellow), but it cannot travel retrogradely as demonstrated by the lack of mCh+ only cells. Bisbenzimidazole nuclear stain shown in blue. Scale bars represent 100 μm (50 μm for inset).

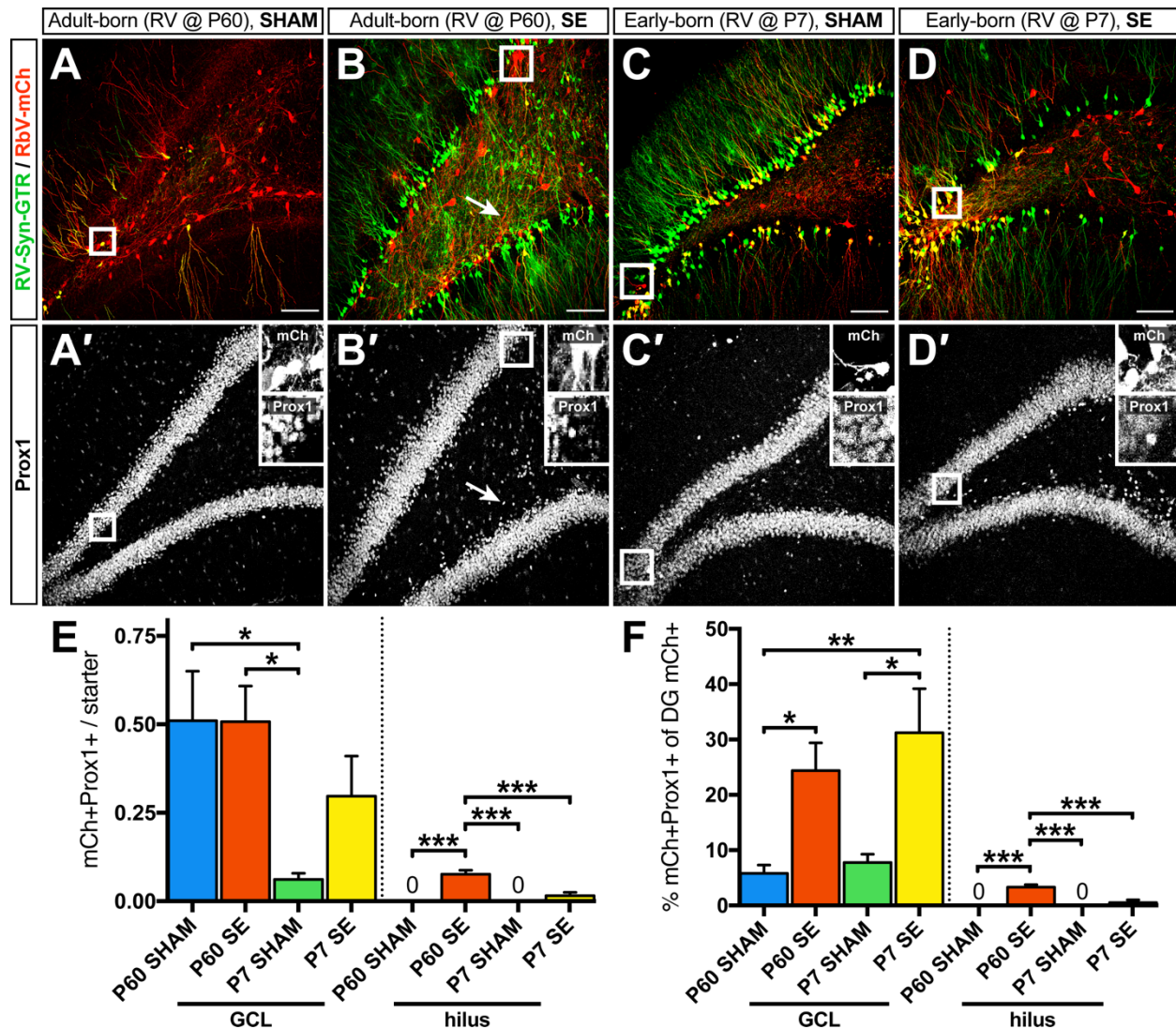


Figure 2.3. Prox1+ DGC inputs onto early- and adult-born DGCs differ in the sham versus epileptic brain.

(A-D) Four cohorts of animals were used for the experimental paradigm. Representative confocal images of GFP/mCh double labeling in sham (**A, C**) and epileptic (**B, D**) dentate gyri that were injected with RV-Syn-GTR at P60 to label adult-born DGCs (**A, B**) or at P7 to label early-born DGCs (**C, D**). **(A'-D')** The same sections as in **A-D** labeled for Prox1 to identify DGCs (GFP and mCh were removed for clarity). Insets are high magnification images of mCh+ only cells that are also Prox1+ corresponding to the outlined areas in **A-D**. Arrows in **B** and **B'** show a traced mCh+ only/Prox1+ presynaptic hilar ectopic DGC.

(E) Quantification of average number of mCh+/Prox1+ (GFP-) presynaptic DGCs in the granule cell layer (GCL, left) and the hilus (right) per starter DGC. **(F)** Quantification of the percentage of all dentate gyrus mCh+ only inputs that were also Prox1+ in the granule cell layer (left) and the hilus (right). Scale bars represent 100 μ m (50 μ m for insets). (n = 5-6 animals per group, *p<0.05, **p<0.01, ***p<0.001).

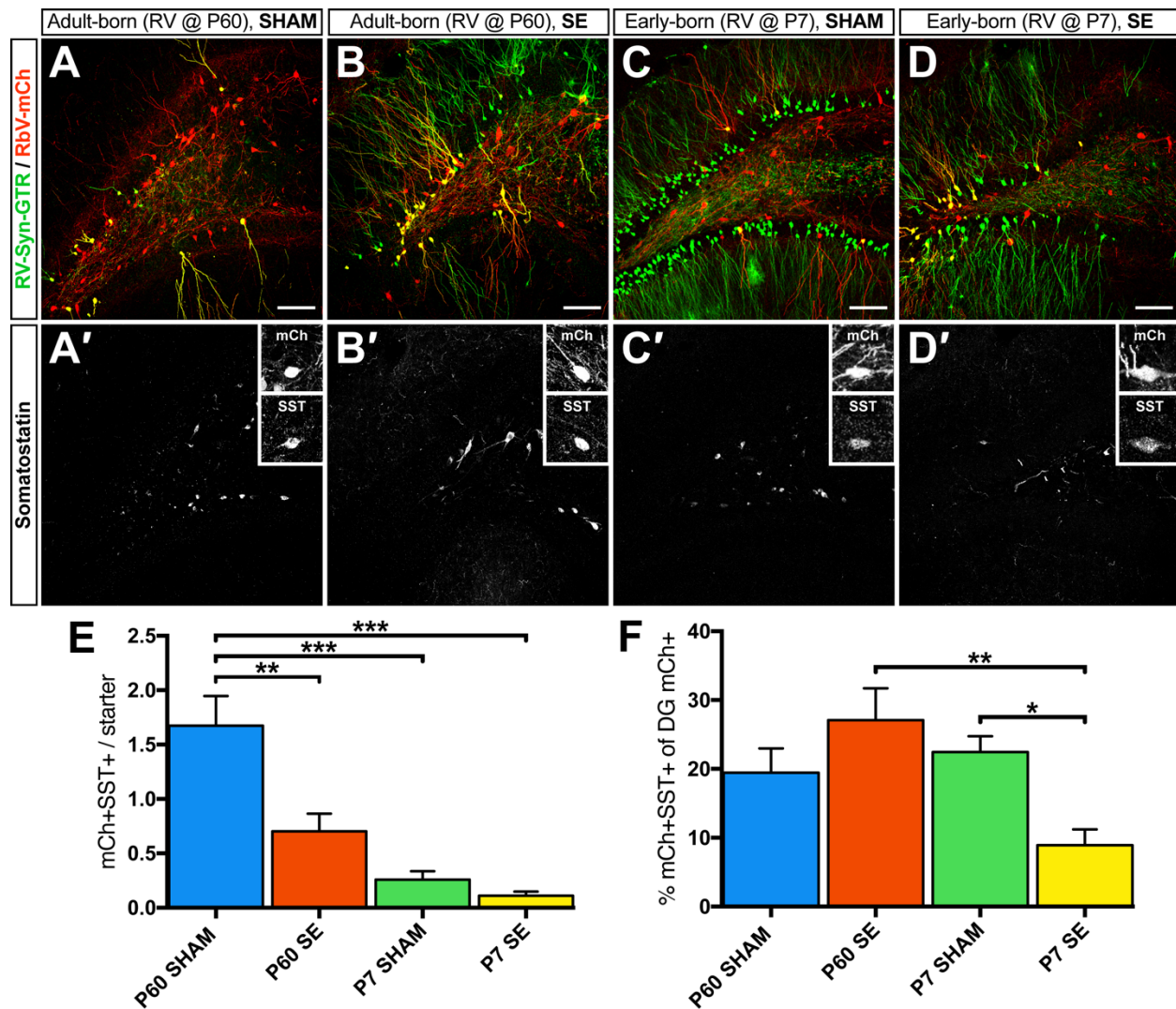
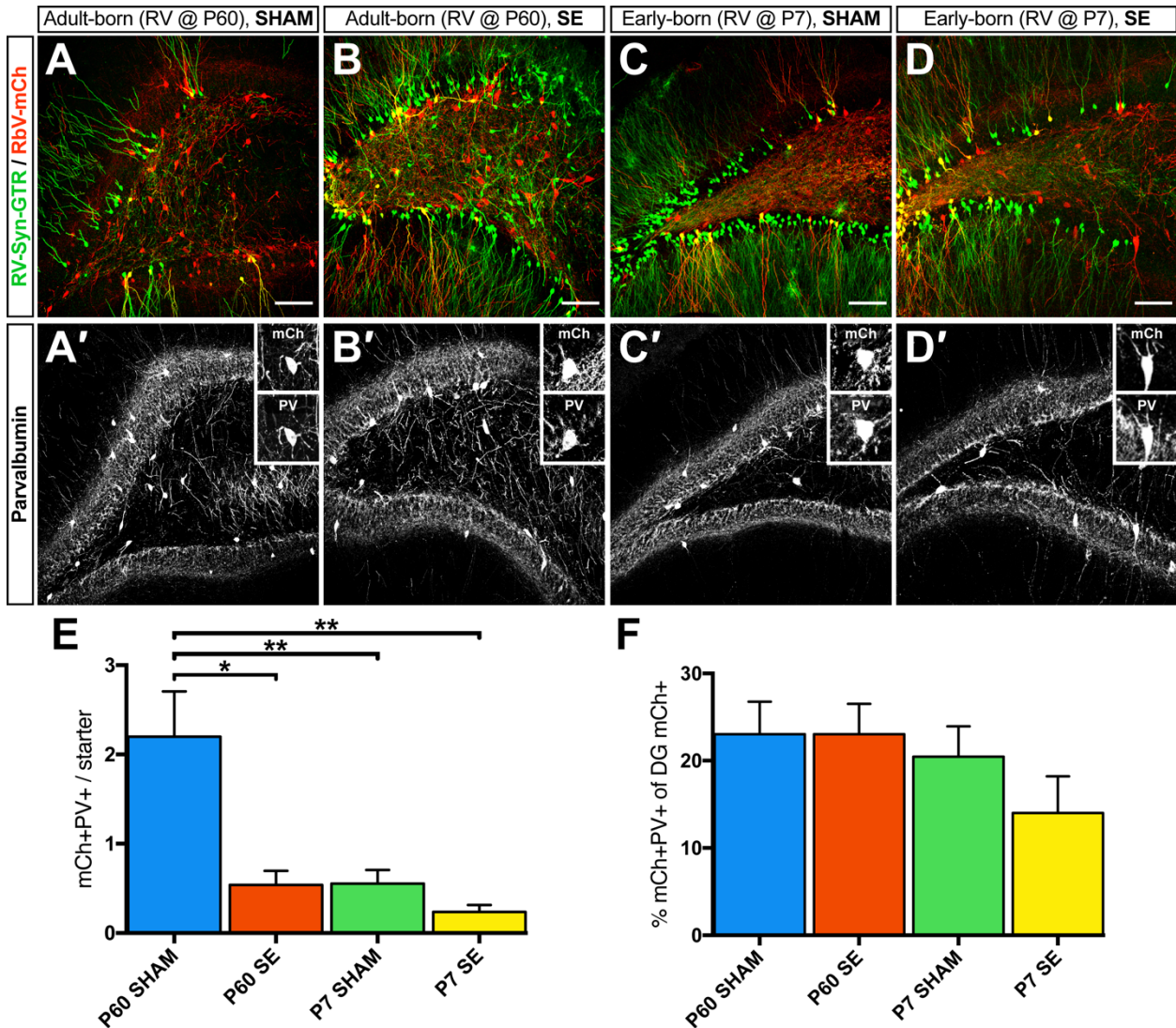


Figure 2.4. RbV tracing of hilar somatostatin-expressing interneuron inputs onto birthdated DGCs.

(A-D) Representative confocal images of the dentate gyrus from each of the four groups of animals immunolabeled for GFP and mCh. (A'-D') Triple labeling with SST in the same sections in A-D (GFP and mCh were removed for clarity). Insets show examples of mCh+ only traced inputs that were also SST+. Note that after SE, fewer SST+ cells are present but the surviving cells hypertrophy (B' and D'). (E) Quantification of the mean number of mCh+ only presynaptic inputs that are also SST+ normalized to the number of starter cells. (F) Quantification of the proportion of total dentate gyrus mCh+ only presynaptic inputs that are also SST+. Scale bars represent 100 μ m (50 μ m for insets). (n = 5-6 animals per group, *p<0.05, **p<0.01, ***p<0.001).



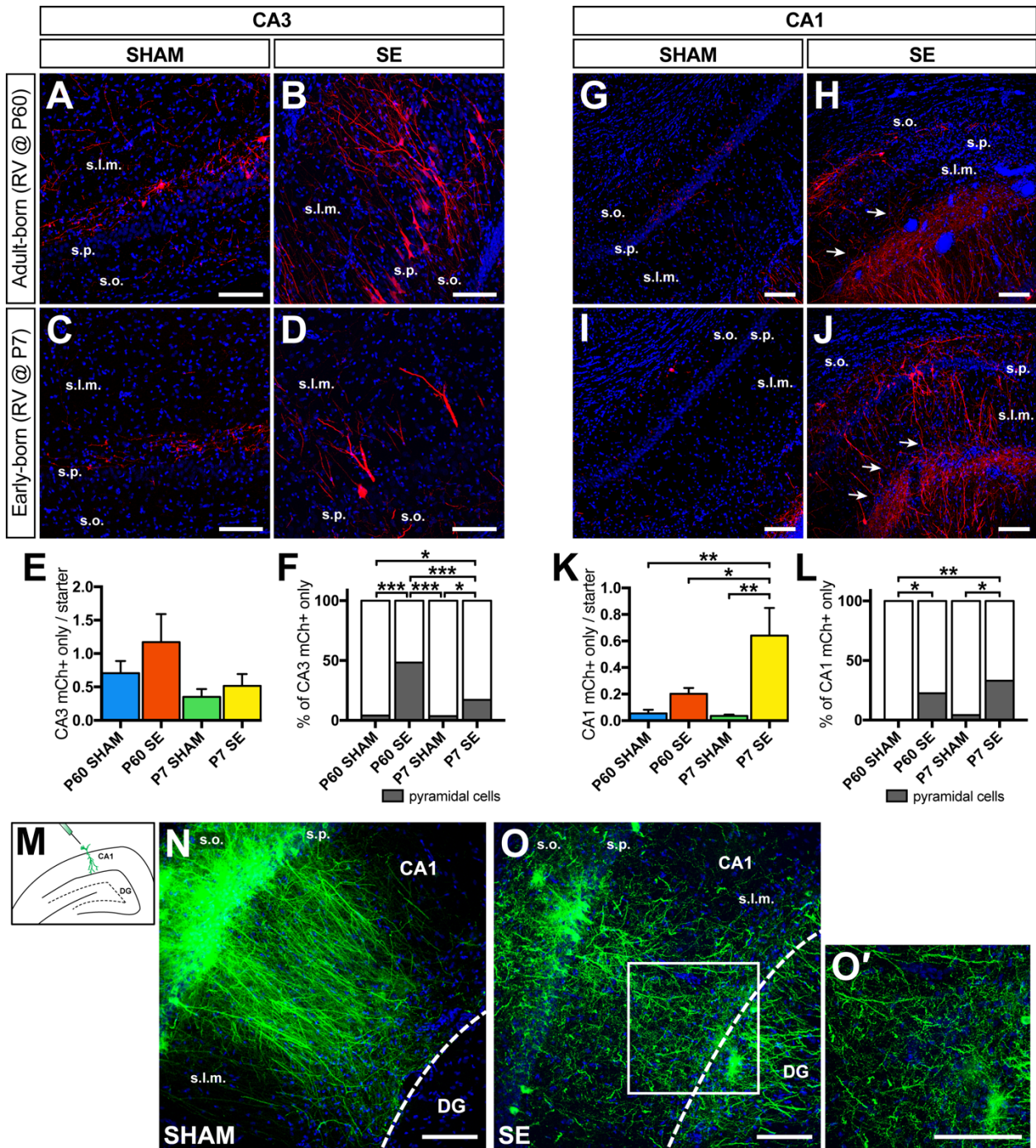


Figure 2.6. Hippocampal CA3 and CA1 pyramidal cells innervate DGCs in the epileptic brain.

(A-D) Representative confocal images of mCh immunolabeling of the hippocampal CA3 region for the four groups of animals. Note the increase in mCh+ cells with pyramidal neuron morphology within stratum pyramidale (s.p.) in the SE groups (B, D). (E) Quantification of the ratio of total mCh+ only cells in CA3 to total starter DGCs amongst the four cohorts. (F) Quantification of the percentage of all traced mCh+ only CA3 pyramidal vs. non-pyramidal cells. Dark gray represents pyramidal cells while white

represents putative interneurons. **(G-J)** Representative confocal images of mCh immunolabeling in the CA1 region for the four groups. Note mCh⁺ fibers extending towards the dentate gyrus in epileptic rats (arrows in **H, J**). The dentate gyrus is at the lower right in **G-J**. **(K)** Quantification of the ratio of mCh⁺ cells in CA1 to total starter DGCs in each group. **(L)** Quantification of the percentage of all CA1 mCh⁺ only cells stratified into pyramidal vs. non-pyramidal cells. Dark gray represents the proportion of pyramidal cells while white represents putative inhibitory neurons. **(M)** Schematic showing the location of the injection of CAMKII α -Syp-GFP lentivirus. **(N)** Representative confocal image of Syp-GFP labeled CA1 pyramidal cells from a sham animal. The dashed line represents the hippocampal fissure separating CA1 from the dentate gyrus (DG). Note that nearly all GFP⁺ processes terminate at the hippocampal fissure. **(O)** Representative confocal image of Syp-GFP labeled CA1 pyramidal cells from an epileptic animal. Note the abundant processes from CA1 that appear to cross the hippocampal fissure (white dashed line) into the dentate gyrus. **(O')** Magnification of the region demarcated by the white solid box in **O**. Bisbenzimidazole nuclear stain in blue for all photomicrographs. Scale bars represent 100 μ m. s.o., stratum oriens; s.p., stratum pyramidale; s.l.m., stratum lacunosum-moleculare. (n = 5-6 animals per group, *p<0.05, **p<0.01, ***p<0.001).

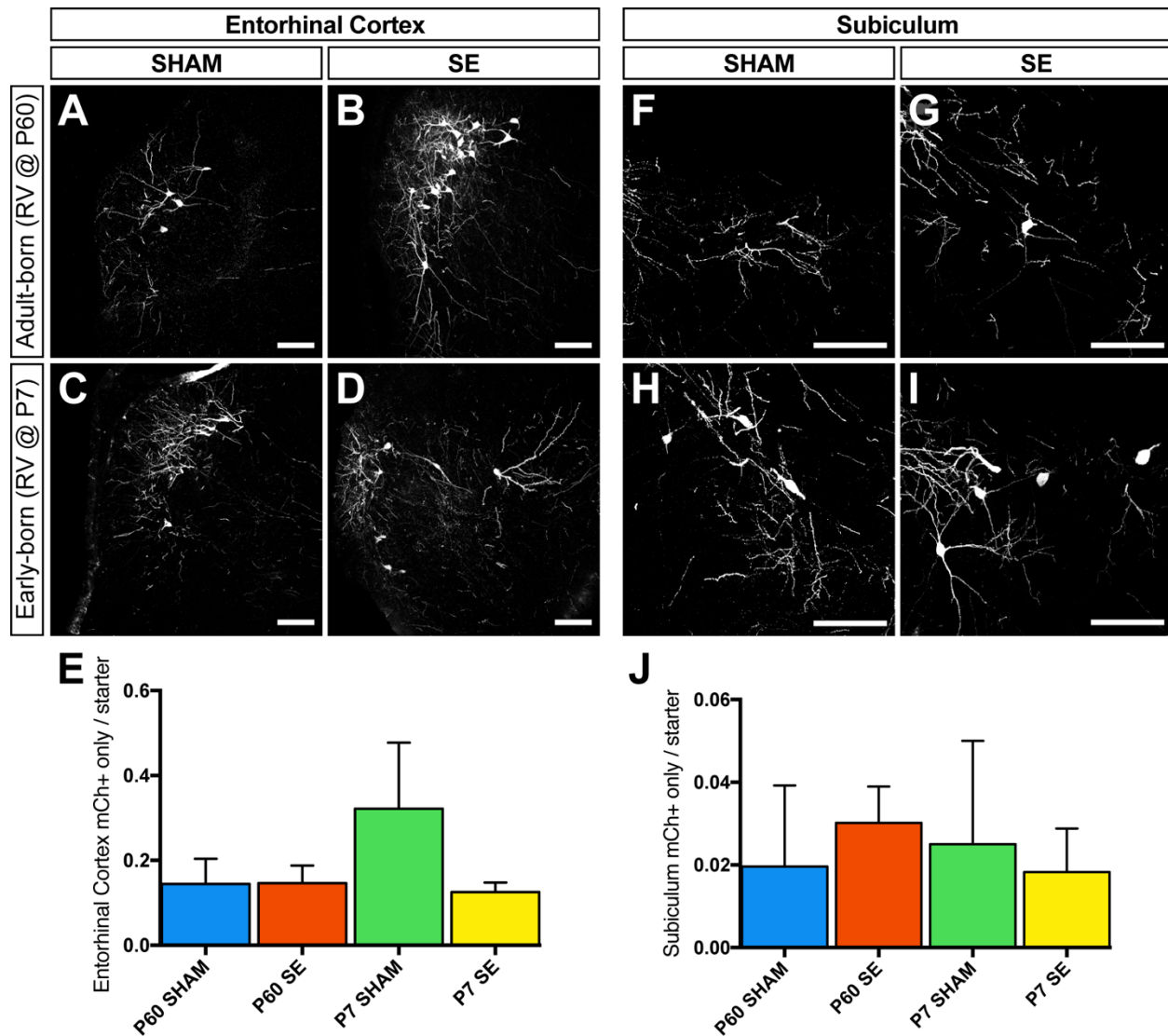


Figure 2.7. Quantification of entorhinal cortex and subicular inputs.

(A-D) Example images of inputs from the entorhinal cortex of all four groups. **(E)** Quantification of mCh⁺ only inputs from the entorhinal cortex to the ratio of starter cells. **(F-I)** Representative images of inputs from the subiculum of all four groups. **(J)** Analysis of the ratio of mCh⁺ only subicular cells to the number of starter cells. Bisbenzimidazole nuclear stain shown in blue. Scale bars represent 100 μ m. (n = 5-6 animals per group).

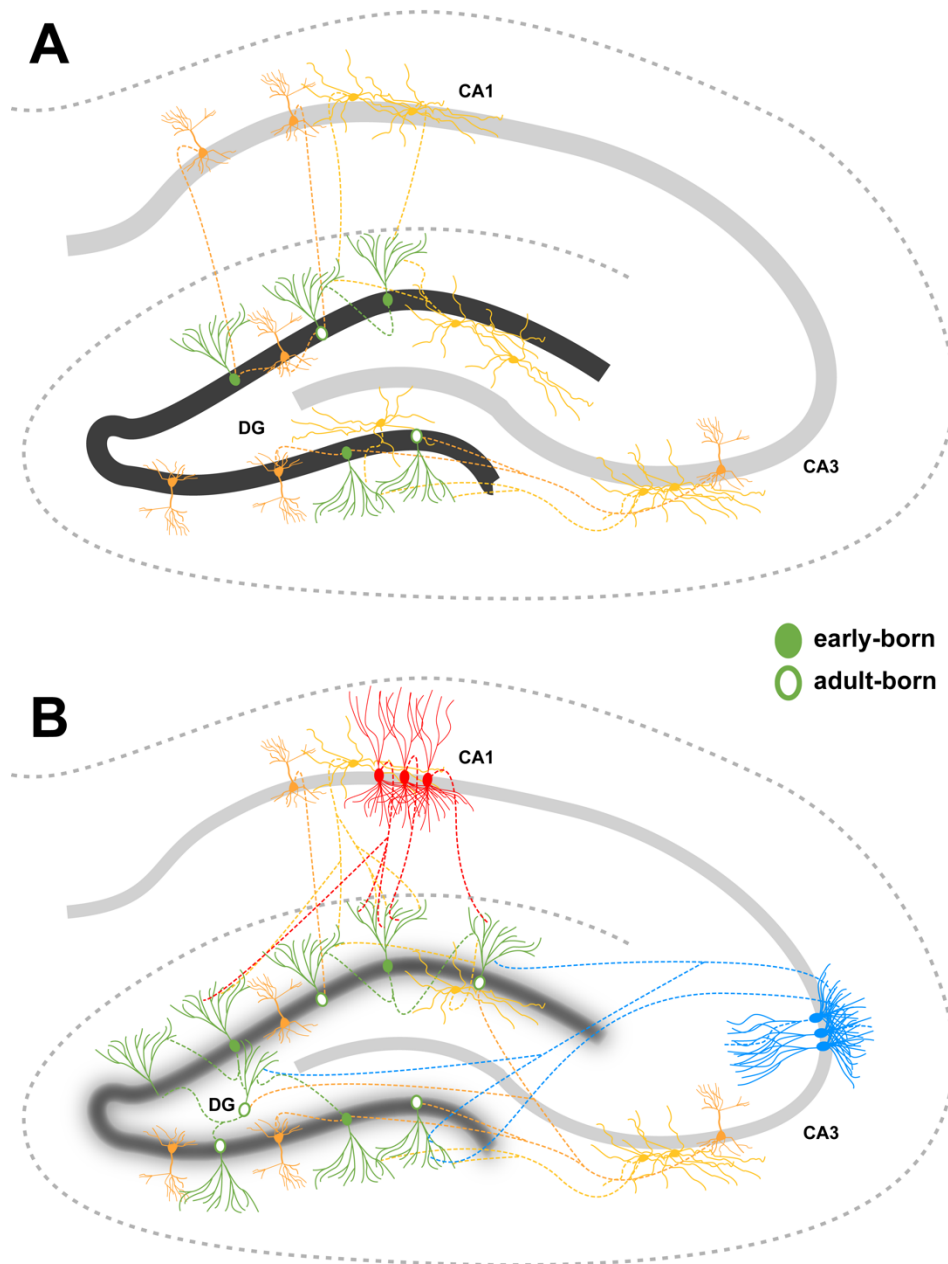


Figure 2.8. Hippocampal circuitry remodeling in the epileptic brain.

(A) Schematic of the control hippocampus displaying inhibitory inputs (yellow and orange) from the dentate hilus, CA3, and CA1 onto early- (filled green cell bodies) and adult-born (open green cell bodies) DGCs. Sparse DGC-DGC connections are also shown. **(B)** Schematic of the epileptic brain demonstrating increased recurrent DGC-DGC connections onto both early- and adult-born DGCs after SE. Preferential inputs from hilar ectopic DGCs to adult-born DGCs also arise. CA3 pyramidal cells sprout axonal backprojections preferentially onto adult-born DGCs and CA1 pyramidal neurons project axons across the hippocampal fissure onto early-born, and to a lesser extent, adult-born DGCs. ML, molecular layer; GCL, granule cell layer.

Chapter 3

Potential Mechanisms of Protocadherin-19 in Early Infantile Epileptic Encephalopathy type 9

Summary

Protocadherin-19 (PCDH19) Female Limited Epilepsy (FLE), also known as Early Infantile Epileptic Encephalopathy type 9 (EIEE9), is a pediatric epilepsy that is caused by mutations in the *PCDH19* gene on the X-chromosome. PCDH19 is a member of the cadherin superfamily of cell-cell adhesion molecules that has been shown to participate in homophilic binding. While the normal function of PCDH19 remains unknown, other members of the protocadherin family have been shown to be critical for neural development. Perhaps the most interesting feature of PCDH19 FLE is its inheritance pattern: females who carry heterozygous *PCDH19* mutations are affected with seizures and cognitive impairment while mutation-carrying males are asymptomatic. This atypical genotype-phenotype correlation is perhaps best explained by the cellular interference hypothesis. The hypothesis postulates that random X-inactivation in females with heterozygous *PCDH19* mutations leads to two different cell populations, one expressing wild type (WT) *PCDH19* and the other expressing mutant *PCDH19*, and that these two cell populations interact aberrantly to cause the disorder. The hypothesis is consistent with the fact that cells of unaffected carrier males with germline mutations only express

mutant PCDH19 and thus do not develop the disorder, while mosaic males exhibit typical EIEE9 phenotypes. To further test this hypothesis and explore EIEE9 mechanisms in human neurons, we generated induced pluripotent stem cells (iPSCs) from two female patients with clinical PCDH19 FLE and associated pathogenic mutations in *PCDH19*. We found that cortical-like excitatory neurons differentiated from FLE patients have atypical outgrowth of processes and accelerated maturation, as well as increased excitability on multielectrode array (MEA) recordings. We also found that inhibitory interneurons derived from FLE patient iPSCs have atypical morphology and increased MEA activity. Additionally, we used CRISPR/Cas9 technology to generate a *PCDH19*-null male iPSC line. We mixed this line with WT *PCDH19*-expressing isogenic controls to recapitulate the mosaic male phenotype *in vitro*. When we differentiated mixed WT/*PCDH19*-null male iPSCs into cortical-like excitatory neurons, we found atypical segregation of the two cell populations accompanied by decreased activity. Lastly, we differentiated mixed cultures into inhibitory interneurons and found increased neuronal firing activity, similar to the female FLE lines. Our results support the cellular interference hypothesis and suggest that aberrant cell-cell interactions of cortical neurons alter brain development and contribute to epileptogenesis.

Introduction

PCDH19 FLE, also known as EIEE9 and formerly called Epilepsy in Females with Mental Retardation (EFMR), is a form of pediatric epilepsy that presents with early-onset seizures, cognitive impairment and behavioral problems (Juberg and Hellman, 1971; Scheffer et al., 2008). The intellectual disability ranges from none to severely impaired while MRIs from patients reveal no structural brain abnormalities (Scheffer et al., 2008).

It is now known that PCDH19 FLE is caused by *de novo* or inherited (from an affected female or unaffected carrier male) loss-of-function mutations in the *PCDH19* gene on the X-chromosome (Dibbens et al., 2008). *PCDH19* encodes for a calcium-dependent cell-cell adhesion protein in the cadherin superfamily that has been shown to be widely expressed in the central nervous system (CNS) of mammals, including humans, at different developmental stages (Gaitan and Bouchard, 2006; Kim et al., 2010; Uhlen et al., 2015). As a member of the $\delta 2$ protocadherin subfamily, PCDH19 demonstrates weak homophilic binding properties (Hirano et al., 1999; Tai et al., 2010). Almost all of the pathogenic mutations reported to date are found in exon 1 of the *PCDH19* gene (Dibbens et al., 2008; Depienne et al., 2009), which encodes for the extracellular domain responsible for the cellular adhesion properties of the protein (**Figure 3.1A**) and is highly conserved across species (Depienne et al., 2011). Truncation mutations or deletions of the gene also cause FLE, however, consistent with loss-of-function. Additionally, PCDH19 has been shown to interact with N-cadherin and this interaction is important for cell migration during early zebrafish brain development (Biswas et al., 2010; Emond et al., 2011).

While the specific biological role of PCDH19 remains unclear, several other protocadherins are thought to influence various aspects of neural development, including cell migration, dendritic patterning, synaptic pruning, and axonal outgrowth (Uemura et al., 2007; Amar and Dawid, 2008; Piper et al., 2008; Tsai et al., 2012; Hoshina et al., 2013; Biswas et al., 2014; Hayashi et al., 2014). Lefebvre et al. found that knocking out the 22 genes of the protocadherin γ -subcluster (*Pcdhg*) in mice disrupts neuronal dendritic tiling and self-avoidance. Furthermore, restoring a single isoform of the *Pcdhg*

cluster rescued the dendritic phenotype, indicating that high levels of redundancies of protocadherins exist in mice (Lefebvre et al., 2012). Other groups have demonstrated that γ -protocadherins participate in homophilic cell-cell binding to regulate dendritic arborization and spine formation (Garrett et al., 2012; Molumby et al., 2017). Molumby et al. recently suggested that protocadherins regulate the dendritic complexity of developing cortical neurons depending on whether an individual cell and its neighboring neurons express the same or different isoforms of protocadherins (Molumby et al., 2016). These studies suggest that protocadherins mediate critical aspects of interneuronal communication via homophilic interactions.

PCDH19 FLE has a highly unusual mode of inheritance: only females with heterozygous mutations of *PCDH19* develop the disorder while mutation-carrying males are unaffected (Ryan et al., 1997). This is atypical for X-linked disorders in which males are usually more severely affected than females. This unique inheritance pattern is thought to arise from developmental defects related to abnormal cell-cell interactions between mixed WT and mutant populations, a concept known as cellular interference (Johnson, 1980; Wieland et al., 2004). Because of random X-inactivation in females, both WT and mutant *PCDH19*-expressing cells arise during development. These cells, including neurons, are postulated to interact aberrantly thereby leading to the neurological changes. Supporting this theory, several cases of EIEE9 have been described in males who have somatic mosaicism for pathogenic mutations of *PCDH19* (Depienne et al., 2009; Terracciano et al., 2016; Thiffault et al., 2016). Furthermore, another disorder, craniofrontonasal syndrome (CFNS), shares a similar X-linked dominant with male sparing inheritance pattern (Saavedra et al., 1996). CFNS manifests with skeletal

abnormalities and has been linked to mutations in the *EFNB1* gene which encodes for the Ephrin-B1 protein (Wieland et al., 2004). In *Efnb1*^{+/-} transgenic mice, as a result of random X-inactivation, *Efnb1*-positive and *Efnb1*-negative cells self-segregate into separate compartments, evidence for the cellular interference hypothesis in this disease. This segregation of cells leads to various skeletal abnormalities and defects such as polydactyly (Compagni et al., 2003). Despite the distinct phenotypes in the *Efnb1*^{+/-} mouse, *Pcdh19*^{+/-} β -*Geo* heterozygous knockout mice demonstrate no overt anatomical or functional phenotypes (Pederick et al., 2016). This finding may partially be explained by the reported high levels of redundancies in mouse protocadherins (Lefebvre et al., 2012).

To understand how mutations in *PCDH19* impact neural development, we use iPSC methods for disease modeling in patient-derived neurons (Takahashi et al., 2007; Yu et al., 2007). The difficulty in establishing a phenotype in the heterozygous mouse model highlights the potential drawbacks of animal studies and the importance of using human-based systems. In addition to being able to model diseases in human cells, iPSCs have the added advantage of being a renewable source of cellular material for us to generate multiple cellular lineages of interest. Lastly, key differences exist between primate and rodent neural development, one of which is the presence versus relative absence of an outer SVZ (oSVZ) (Smart et al., 2002; Zecevic et al., 2005). The oSVZ is a neurogenic region that is largely absent in rodents but has been shown to contribute significantly to primate, including human, cortical expansion (Fietz et al., 2010; Hansen et al., 2010). Previous studies show that outer radial glia cells (oRGs), the progenitor population in the oSVZ, are recapitulated in human iPSC-derived neuronal cultures (Shi et al., 2012b; Lancaster et al., 2013; Qian et al., 2016).

We reprogrammed somatic cells, specifically dermal fibroblasts, and established iPSC lines from two female *PCDH19* FLE patients who have confirmed pathogenic mutations of *PCDH19*, one asymptomatic mutation-carrying father of one of the patients, as well as an unaffected female control. Additionally, we took advantage of the CRISPR/Cas9 genome editing technology to delete *PCDH19* in a control male iPSC line to generate a “virtual” unaffected mutation-carrying male. We differentiated cortical-like excitatory neurons as well as cortical-like medial ganglion eminence (MGE)-derived inhibitory interneurons and found that patient cells have abnormal rosette formation, processes outgrowth, cell-cell segregation and hyperactivity.

Materials and methods

Guide RNA design and px330 annealing

A single-guide RNA (sgRNA) for CRISPR/Cas9 targeting of exon 1 of the *PCDH19* gene was designed using the MIT CRISPR design tool with sequence as follows: 5' ggagtggacaccacgcxgaa 3'. The sgRNA sequence was designed to generate insertions/deletions (indels) leading to a frameshift mutation that would result in a complete loss-of-function of the *PCDH19* gene. Forward and reverse oligonucleotides with the appropriate 5' overhang were obtained (Invitrogen). The px330 (WT Cas9) plasmid was digested with Bbs1 (New England Biolabs) and the pair of annealed oligos were then ligated with the T4 ligase into the vector.

Reprogramming of iPSCs

Skin biopsy-derived fibroblasts were obtained from the University of Michigan Institute for Clinical and Health Research as well as Stanford University (a gift from

Ricardo Dolmetsch, Stanford University, Palo Alto, CA) under a protocol approved by the University of Michigan Institutional Review Board. Fibroblasts were maintained in fibroblast medium containing: DMEM, 10% fetal bovine serum (FBS), 1× GlutaMAX and 50 U/mL of Penicillin/Streptomycin (P/S). Fibroblasts were reprogrammed using 1 µg of episomal expression plasmids (pCXLE-hOCT3/4-p53 shRNA, pCXLE-hUL and pCXLE-hSK) electroporated into 1×10^5 fibroblasts using the Neon Electroporation System (Invitrogen) with a 100 µL kit as described previously (Okita et al., 2011). Conditions for electroporation were 1650 volts, 10 ms pulse width and 3 pulses. For simultaneous reprogramming with CRISPR/Cas9 to generate *PCDH19*-null male lines, 1 µg of CRISPR/Cas9 plasmid (px330; Addgene) was also added during reprogramming. Fibroblasts were then plated in a Matrigel-coated 6-well plate in fibroblast medium for 3 days with daily media changes before the medium was replaced with TeSR-E7 (STEMCELL Technologies).

iPSC colony isolation and maintenance

TeSR-E7 was changed daily until the appearance of iPSC colonies approximately 14-21 days later. iPSCs were then manually isolated and cultured in Matrigel-coated plates under feeder-free conditions on Matrigel in TeSR-E8 medium (STEMCELL Technologies) supplemented with 10 µM ROCK inhibitor (Y27632; Tocris Bioscience) Media was changed the next day without Y27632 and replaced daily thereafter. iPSCs were manually passaged when the cultures reached ~75% confluency and 10 µM of Y27632 was added the day of passaging.

For simultaneously reprogramming with CRISPR/Cas9 editing, iPSC colonies emerged approximately 14-21 days after electroporation. To eliminate the possibility of

multiple genotypes, small, individual colonies with no evidence of multiple merged clones were isolated and transferred into a Matrigel coated 96-well plate containing mTeSR1 (STEMCELL Technologies) supplemented with 10 μ M Y27632. Colonies were maintained in mTESR1 with daily media changes.

Selection of CRISPR clones

Genomic DNA was isolated from the 96-well plate using the ZR-96 Quick-gDNA Kit (Zymo Research) following the manufacturer recommended protocol. For Sanger sequencing, PCR primers were designed to amplify a 200-250 bp product evenly flanking the CRISPR/Cas9 cut site with sequences shown in **Table 1**. The PCR product was purified using the ZR-96 DNA Clean-up Kit (Zymo Research) and samples were submitted to the University of Michigan Sequencing Core for Sanger sequencing. Two clones that had a 2 bp and a 5 bp deletion, respectively, were selected as the deletion was predicted to result in a loss-of-function frameshift mutation.

Characterization of patient iPSC cells

For sequencing and quantitative real-time PCR (qRT-PCR) experiments, RNA was extracted from iPSCs using the RNeasy Mini Kit (Qiagen) according to manufacturer's recommended protocol. 1 μ g of RNA template was used to synthesize cDNA using the SuperScript III First-Strand Synthesis Kit (Invitrogen) according to manufacturer's recommended protocol. To confirm the expression of WT and mutant *PCDH19* in the *PCDH19* FLE patient with a heterozygous c.602 A>C missense mutation in exon 1 of the *PCDH19* gene (FLE1) by Sanger sequencing, PCR primers were designed that flanked the site with sequences shown in **Table 1**. Samples were submitted to the University of

Michigan Sequencing Core for Sanger sequencing. qRT-PCR was performed using 5 ng of cDNA template with SYBR Green detection (Applied Biosystems) using the QuantStudio 3 Real-Time PCR System (Applied Biosystems). Primers used are shown in **Table 2**. Karyotyping analysis by standard G-banding technique was performed and interpreted by Cell Line Genetics.

RNA fluorescence *in situ* hybridization (RNA FISH) was performed using probes for human *XIST* (A gift from Sundeep Kalantry, University of Michigan, Ann Arbor, MI). Cells mounted on coverslips were dehydrated through a series of 70%, 85%, 95% and 100% ethanol solutions and then air-dried. The cells were subsequently hybridized with *XIST* probe overnight in a humid chamber at 37°C. The next day, cells were washed at 39°C through a series of 1X saline-sodium citrate (SSC)/50% formamide, 2X SSC and 1X SSC solutions. Cell nuclei were counterstained using DAPI.

Differentiation of iPSCs into forebrain specific progenitors and cortical-like neurons

Cortical-like excitatory neurons were generated using dual SMAD inhibition following an established protocol (Shi et al., 2012a; Shi et al., 2012b). iPSCs were dissociated using Accutase (Innovative Cell Technologies) and 1×10^6 cells were plated on Matrigel-coated dishes in TeSR-E8 supplemented with Y27632. The next day, media was changed to neural induction media which contained neural maintenance media (3N) supplemented with 1 μ M Dorsomorphin (Tocris Biosciences) and 10 μ M SB431542 (Tocris Biosciences). 3N media contains a 1:1 mixture of DMEM/F12 and Neurobasal media with 1 \times N2, 1 \times B27, 1 \times MEM non-essential amino acids (NEAA), 1 \times GlutaMAX, 50 U/mL P/S, 5 μ g/mL insulin and 1 \times β -mercaptoethanol (BME). Cells were maintained in neural induction media with daily media changes for 10-12 days at which point the

primitive neuroepithelium was dissociated using Dispase (Gibco) and re-plated on Matrigel-coated 6-well plates in 3N medium. When the neural epithelium formed rosettes, media was supplemented with 20 ng/mL fibroblast growth factor-2 (FGF2; Peprotech) for 4 days for the expansion of neural stem cells. Rosettes were dissociated with Dispase and re-plated on Matrigel-coated 6-well plates and maintained in 3N media. At this point, rosettes were either fixed for analysis or passaged using Accutase for maturation of cortical-like excitatory neurons. Final plating of neurons for histology was performed on poly-L-ornithine (PLO)/laminin coated coverslips in 3N media. Media was replaced every other day and was supplemented with 200 nM γ -Secretase Inhibitor XXI (Compound E; EMD Millipore) for the first 7 days to inhibit cell division and promote maturation.

Differentiation of iPSCs into MGE-derived inhibitory interneurons

GABAergic interneurons were differentiated from iPSCs following an established protocol (Liu et al., 2013a; Liu et al., 2013b) using the sonic hedgehog agonist, purmorphamine, for patterning. iPSC colonies were lifted using Dispase and re-suspended as embryoid bodies (EBs) in ultra-low attachment flasks in human pluripotent stem cell medium (hPSCM) containing: DMEM/F12, 20% knockout serum replacement, 1 \times GlutaMAX, 1 \times MEM NEAA and 1 \times BME supplemented with 4 ng/mL of FGF2 and 10 μ M of Y27632. hPSCM was replaced the next day but without Y27632. On day 4, medium was changed to neural induction medium (NIM) which contained DMEM/F12, 1 \times MEM NEAA, 1 \times N2 and 2 μ g/mL heparin. Medium was changed every other day until day 7 when EBs were plated on Matrigel-coated 6-well plates. EBs were allowed to attach and medium was changed every other day until day 10 when neural rosettes appeared. At this point, media was supplemented with 1.5 μ M purmorphamine (StemGent) with media

changes every other day. At day 16, neural rosettes with columnar appearances were manually isolated and re-suspended as neurospheres in ultra-low attachment flasks in NIM supplemented with 1× B27 and 1.5 μM purmorphamine. Media was changed every other day until day 26 when neurospheres were dissociated with glass pipettes for final plating. Single cells were plated on PLO/laminin-coated coverslips in neural differentiation medium containing Neurobasal, 1× NEAA, 1× N2 and 2 μg/mL heparin supplemented with 1 μM dibutyryl cyclic-AMP (dbcAMP; Sigma), 10 ng/mL brain-derived neurotrophic factor (BDNF; Peprotech), 10 ng/mL glial cell-line derived neurotrophic factor (GDNF; Peprotech) and 10 ng/mL insulin-like growth factor-1 (IGF-1; Peprotech). Media was also supplemented with 200 nM Compound E for the first 7 days.

MEA recordings

A multi-well MEA system (Axion Biosystems) was used for recording the functional activity of neurons. MEA plates were composed of 96 wells with each well containing an array of eight electrodes for recording. Wells were coated with a polyethylenimine (PEI)/laminin solution prior to culturing of neurons. Both excitatory and inhibitory interneurons were plated at a density of 150,000 cells/well in Brainphys (STEMCELL Technologies) supplemented with 20 ng/mL BDNF, 20 ng/mL GDNF and 200 μM dbcAMP; for inhibitory interneurons, 10 ng/mL IGF-1 was also included in the media. Media was changed every other day with compound E supplemented for the first 7 days.

Spontaneous activity recordings were performed for 5 minutes at 37°C once per week starting at approximately 3 days after plating and continuing until day 35. All channels on the MEA were sampled simultaneously at a sampling rate of 12.5 kHz/channel with a bandpass Butterworth filter (200 Hz – 3 kHz). A spike detector with

adaptive threshold crossings set at 6x standard deviations with a burst detector set at 100 ms inter-spike interval threshold were also applied.

Immunocytochemistry

Cells were fixed with 4% PFA at room temperature for 20 minutes and processed with standard fluorescent immunocytochemistry (ICC) techniques. Cells were blocked with blocking buffer comprised of 1x phosphate buffered saline (PBS), 10% normal goat or horse serum, 2% bovine serum albumin (BSA) and 0.05% Triton-X. The following primary antibodies were used: chicken anti-GFP (1:1000, Aves), rabbit (Rb) anti-dsRed (1:1000, Clontech), mouse (Ms) anti-mCherry (1:1000, Clontech), Ms anti-SSEA4 (1:200, DSHB), Rb anti-Nanog (1:500, Abcam), Goat (Gt) anti-Oct3/4 (1:100, Santa Cruz), Rb anti-Sox2 (1:5000, Chemicon), Ms anti-Nestin (1:300, Millipore), Rb anti-Pax6 (1:300, Covance), Rb anti-PKC γ (1:500, BD Transduction Laboratories), N-cadherin (1:500, Life Technologies), Rb anti-Doublecortin (DCX; 1:500, Abcam), Ms anti-MAP2ab (1:500, Sigma), Rb anti-H3K27me3 (1:500, Millipore), Rb anti-Tbr1 (1:300, Millipore), Rt anti-Ctip2 (1:300, Abcam), Ms anti-Satb2 (1:100, Abcam), Ms anti-Tuj1 (1:2000, Covance), Rb anti-Somatostatin (1:500, Peninsula Labs) and Rb anti-GABA (1:2000, Sigma). Secondary antibodies (Alexa Fluor, 1:400 dilution, Invitrogen) used were: Gt anti-chicken 488, Gt anti-rat 488, Donkey anti-Gt 488, Gt anti-rabbit 488, 594 or 647, Gt anti-mouse 488, 594 or 647. Nuclei were counterstained with bisbenzimidazole.

Microscopy

Images were acquired with a Leica TCS SP5X Confocal Microscope. For neural rosette analysis, images were acquired under a 63x objective at 2.5x optical zoom and 1

μm step size through the z-plane with the pinhole set at 1 Airy unit. For all other analyses, images were acquired with a 20x objective at 1.0x optical zoom and 2 μm step size through the z-plane with the pinhole set at 1 Airy unit.

Statistics

Statistics were performed using GraphPad Prism 7 software. Comparison between patient FLE1 and female CON neuronal excitability parameters were made with a student's t-test with the significance level set at $p < 0.05$. Comparisons between neuronal excitability parameters of mixed male neuronal cultures were made with a one-way ANOVA and post-hoc Tukey's multiple comparisons test with the significance level set at $p < 0.05$. All error bars represent standard error of the mean (SEM).

Results

Generation of PCDH19 FLE patient iPSCs

We reprogrammed skin biopsy-derived dermal fibroblasts from two female patients with clinically diagnosed and genetically confirmed PCDH19 FLE. Patient #1 (FLE1) is a girl (12-years-old at the time of skin biopsy) with a *de novo* heterozygous c.602 A>C missense mutation in exon 1 of the *PCDH19* gene resulting in a substitution of proline for glutamine (p.Gln201Pro). Patient #2 (FLE2) is a girl (3-years-old at the time of skin biopsy) with an inherited frameshift mutation c.1683_1696del14 in exon 1 of the *PCDH19* gene leading to a premature stop codon (p.Val562ThrfsX4) (**Figure 3.1A**). We also reprogrammed an unaffected healthy female control fibroblast line (CON). Lastly, we reprogrammed fibroblasts from the father of FLE2 (cFLE), an asymptomatic mutation-carrier male from whom patient #2 inherited the mutation. We transduced fibroblasts with

non-integrating episomal vectors (Okita et al., 2011) and after approximately 3 weeks, colonies were manually isolated and maintained under feeder-free conditions. To assess for successful reprogramming, we performed ICC and showed expression of the pluripotency markers NANOG, OCT3/4, SOX2 and SSEA4 (**Figure 3.1B**). We also performed karyotype analysis and confirmed that the iPSCs maintained a normal karyotype and did not undergo chromosomal aberration through the reprogramming process (**Figure 3.1C**).

Some evidence suggests that female iPSCs maintain an inactivated X-chromosome (Xi) (Tchieu et al., 2010) while others demonstrate that culture conditions can influence the X-inactivation status of iPSCs and lead to the reactivation of Xi (Mekhoubad et al., 2012; Tomoda et al., 2012). As PCDH19 FLE is an X-linked disorder, the X-inactivation status is particularly important in establishing the validity of iPSC lines. We performed RNA FISH for *XIST* and established that some iPSCs maintained a single *XIST* cloud (**Figure 3.1D**) indicating maintenance of X-inactivation while other iPSCs did not have *XIST* (**Fig 3.1D'**) suggesting that X-chromosome reactivation occurs in some iPSC lines. Analysis for X-inactivation was also performed on neurons (described below) to ensure that differentiated cell types only had a single active X-chromosome. Quantitative RT-PCR analysis confirmed that iPSC lines derived from FLE patients had lower mRNA levels of *PCDH19* as compared with H9 human embryonic stem cells (hESCs) (**Figure 3.1E**).

Generation of PCDH19-null male iPSCs

There are several male patients with EIEE9 as a result of somatic mosaicism for *PCDH19*. To assess whether we could reproduce a neurodevelopmental phenotype of

the male patients *in vitro*, we sought to conduct mixing experiments using control male and null/mutant *PCDH19*-expressing male cells. In addition to the iPSCs from the asymptomatic carrier father (cFLE), we wanted to create “virtual” *PCDH19*-knockout male cell lines so that we could mix isogenic control and *PCDH19*-null male cells, a paradigm that more closely mimics what occurs in affected mosaic male patients. To this end, we performed simultaneous reprogramming and genome editing utilizing the CRISPR/Cas9 system to introduce indels into exon 1 of the *PCDH19* gene in control male fibroblasts to generate a frameshift mutation, thereby generating a knockout of the gene in male cells (**Figure 3.2A**). At 3 weeks after reprogramming, we established two gene edited iPSC lines (mFLE1 and mFLE2) with 2 bp and 5 bp deletions, respectively, in exon 1 of *PCDH19* (**Figure 3.2B**). We also reprogrammed control male iPSC lines (mCON) that were, aside from *PCDH19*, otherwise isogenic to mFLE1 and mFLE2. We validated a loss of *PCDH19* mRNA by quantitative RT-PCR (**Figure 3.2C**) as shown by the lower expression of *PCDH19* in mFLE iPSCs as compared with mCON and female CON iPSCs. An interesting finding is that mCON iPSCs had lower expression of *PCDH19* as compared with female CON iPSCs. We believe this may be a result of X-reactivation in female CON iPSCs, leading to the expression of two X-chromosomes. This is supported by the finding of increased expression of *HPRT1*, another X-linked gene, by female control iPSCs (CON in **Figure 3.2C**) as compared with male control (mCON) and mFLE iPSCs (**Figure 3.2C**).

PCDH19 FLE neural rosettes show defects in apical polarity and adherens junctions

In the human CNS, expression of *PCDH19* is particularly enriched in areas such as the cerebral cortex and hippocampus (Uhlen et al., 2015). To understand how mutations in *PCDH19* affect patient iPSC-derived neurons, we generated forebrain

cortical-like excitatory neurons from patient and control iPSCs. We used dual SMAD signaling inhibition (Chambers et al., 2009; Shi et al., 2012b) to generate neural ectoderm from adherent iPSC cultures. After 10-12 days of neural induction, the primitive neural ectoderm was manually dissociated and cultured until the appearance of neural rosettes, polarized structures with a distinctive morphology of radially-organized neural progenitor cells (NPCs). These rosettes express the NPC markers PAX6 and NESTIN (**Figure 3.3A**). There is evidence that PCDH19 interacts with members of the WAVE complex (Tai et al., 2010) as well as N-cadherin (Biswas et al., 2010; Emond et al., 2011) to regulate actin cytoskeletal dynamics. Neural rosettes derived from female CON iPSCs at day 27 (**Figure 3.3C**) showed immunoreactivity for PKC λ , an apical polarity marker, in a ring-like pattern at the luminal surface of the rosette (**Figure 3.3C'**). This appearance reflects the typical apical-basal polarity established by NPCs *in vitro*. Rosettes also demonstrated N-cadherin staining at the luminal surface (**Figure 3.3C''**) indicative of an organized structure of adherens junctions. In contrast, day 27 rosettes from FLE1 patient-derived iPSCs (**Figure 3.3D**) demonstrated defects in PKC λ and N-cadherin staining (**Figure 3.3D', D''**) suggesting that PCDH19 plays an important role in regulating the polarity and the structure of adherens junctions of NPCs.

To understand how neural development is altered by mosaic expression of *PCDH19* in affected males, we mixed *PCDH19*-null (mFLE) and control (mCON) male iPSCs and differentiated them into neural rosettes (**Figure 3.3B**). Notably, mCON is the isogenic control of mFLE1, making the mixing experiments representative of human mosaic male disease. We mixed the two cell populations at the iPSC stage in a 50:50 ratio and differentiated them into neural rosettes via dual SMAD inhibition (**Figure 3.3E**).

At day 25, Mixed male (control and *PCDH19*-null) rosettes had normal expression of PKC λ (**Figure 3.3E'**) in a tight ring-like structure at the luminal surface that resembled those seen in female control rosettes. However, we saw abnormal, dispersed expression of N-cadherin in the mixed male rosettes (**Figure 3.3E''**) that was reminiscent of FLE rosettes. Unmixed *PCDH19*-null male neural rosettes (**Figure 3.3F**) displayed normal expression of PKC λ and N-cadherin, reminiscent of controls (**Figure 3.3F', F''**). These results suggest that a mosaic culture of WT and *PCDH19*-null expressing male NPCs can partially, but not fully capture the phenotype seen in female cells.

PCDH19 FLE cortical-like excitatory neurons have morphological defects

We initiated neural differentiation by dissociating CON and FLE1 neural rosettes and re-plating the NPCs. We maintained the NPCs in adherent monolayer cultures for 5-7 weeks. As some of our iPSCs reactivated Xi manifested by the lack of *XIST* expression (**Figure 3.1D'**), we first wanted to ensure that our differentiated neurons underwent random X-inactivation. We performed RNA FISH for *XIST* on both CON and FLE1 neurons and detected a single *XIST* cloud indicating the presence of an inactive X-chromosome (**Figure 3.4A, C**). We further validated these results by immunostaining for H3 lysine 27 trimethylation (H3K27me3), another marker of Xi, and found a single foci within each nuclei (**Figure 3.4B, D**) in both CON and FLE1 neurons. We also wanted to ensure that differentiated FLE1 neurons expressed both the mutant and wildtype *PCDH19* allele. Therefore, we performed Sanger sequencing on synthesized cDNA from collected mRNA from FLE1 neurons and found that, at the site of the mutation, we saw two peaks indicating the expression of both WT and mutant *PCDH19* alleles (**Figure**

3.4E). These results show that, despite reactivation of Xi in iPSCs, differentiated neurons undergo random X-inactivation and only express one X-chromosome.

Other members of the protocadherin family have been implicated in various aspects of dendritic tiling and self-avoidance (Lefebvre et al., 2012). We immunostained female control (CON) iPSC-derived cortical-like excitatory neurons with DCX and MAP2ab to label immature and mature neurons, respectively, and found neurons that were dispersed throughout the culture with regularly spaced processes and minimal redundancies and overlap (**Figure 3.4F, G**). However, neurons derived from FLE1 patient iPSCs show a markedly different organization with clumping of their processes and somas, likely reflecting altered migration, and a high frequency of self-crossing of the processes (**Figure 3.4H, I**). High magnification images of control neurons show that individual somas have a limited number of outgrowing processes that are very long, relatively linear and organized spatially to reduce redundancies in dendritic coverage with neighboring cells (**Figure 3.4G'**). However, FLE1 neurons have excessive numbers of processes per soma that are short and blunted with high levels of disorganization (**Figure 3.4I'**). These data suggest that excitatory neurons derived from FLE patients that express both WT and mutant *PCDH19* have defects in cell migration, processes outgrowth and dendritic tiling suggesting that homophilic interactions between PCDH19 proteins may mediate these processes.

In addition to the migration and morphology of developing neurons, we wanted to determine whether PCDH19 mediated other aspects of cortical development such as the expression of layer-specific markers. To this end, we immunostained neuronal cultures for the deep layer marker TBR1 and found that control cortical-like neurons had a high

level of expression of TBR1 (**Figure 3.4J**) while FLE1 neurons had much fewer numbers of TBR1+ cells (**Figure 3.4L**). We also analyzed the two groups for expression for CTIP2 and SATB2, markers of layers V and II/III cortical neurons, respectively. We found that control cultures had some CTIP2+ neurons with very few SATB2+ neurons (**Figure 3.4K**) indicating the culture was composed of mainly deep layer neurons. Meanwhile FLE1 neurons expressed high levels of both CTIP2 and SATB2 (**Figure 3.4M**), indicating that the culture contained both deep layer and upper layer neurons. These results suggest that FLE1 neurons may have accelerated maturation as compared with control neurons.

Abnormal segregation in mixed WT and mutant PCDH19-expressing male neuronal cultures

We next wanted to assess whether we could recapitulate the female FLE patient iPSC-derived neuronal findings in mixed male cultures (**Figure 3.3B, E-E''**) to mimic the disease findings in mosaic males. In order to distinguish the two populations, we infected male control iPSCs (mCON) with a retrovirus expressing GFP driven by a CAG promoter (CAG-GFP) and *PCDH19*-null male iPSCs (mFLE) with a retrovirus expressing mCh also driven by a CAG promoter (CAG-mCh). We dissociated and re-plated mixed NPCs (**Figure 3.5A**), maintained them for 5-7 weeks and confirmed their neuronal identity with TUJ1 immunostaining (**Figure 3.5C**). We found that mixing the two populations of neurons led to cell segregation marked by dense regions of mCh+ cells with very few GFP+ cells intermingled (**Figure 3.5A**) and vice versa. We also saw neurons with atypical morphologies marked by disorganized processes (**Figure 3.5A'**) that were reminiscent of the morphologies that we found in FLE1 neurons (**Figure 3.4I'**). To ensure that the process of mixing and labeling iPSCs was not a confounding factor that led to the

abnormalities, we also infected two populations of the same mCON iPSCs with either CAG-GFP or CAG-mCh and mixed them together at a 50:50 ratio. After differentiation and re-plating, we found that mixed cultures of mCON with mCON neurons, confirmed with TUJ1 immunolabeling (**Figure 3.5D**), did not demonstrate the cellular segregation that we found in *WT/PCDH19*-null mixed cultures (**Figure 3.5B**). In addition, individual neurons had relatively linear, organized processes (**Figure 3.5B'**).

We also repeated these mixing experiments with control male iPSCs and asymptomatic mutant-*PCDH19* carrier male iPSCs, cFLE. We infected mCON iPSCs with CAG-GFP and cFLE iPSCs with CAG-mCh, mixed the iPSCs together at a 50:50 ratio and differentiated them into neurons, confirmed with MAP2ab immunostaining (**Figure 3.5H**). We found a similar phenotype as mCON/mFLE mosaic cultures (**Figure 3.5A**) where GFP+ and mCh+ cells segregated into different regions with little overlap (**Figure 3.5E**). In order to eliminate any confounding variable from mixing and labeling, we also performed two additional experiments where we mixed GFP+ mCON iPSCs with mCh+ mCON iPSCs as well as GFP+ cFLE iPSCs with mCh+ cFLE iPSCs and differentiated the cultures into neurons. We confirmed the neuronal identities using MAP2ab (**Figure 3.5I, J**). We found that both mCON + mCON (**Figure 3.5F**) and cFLE + cFLE (**Figure 3.5G**) neurons did not segregate into isolated cellular regions but rather the GFP+ and mCh+ cells intermingled in a relatively homogeneous manner. These results suggest that altered cell-cell interactions between *WT* and mutant *PCDH19*-expressing neurons induced aberrant neuronal segregation and morphology.

Functional analysis of FLE cortical-like excitatory neurons

In order to understand how heterozygous mutations in *PCDH19* affect the functional properties of excitatory neurons, we analyzed their electrical properties on a MEA system integrated on a 96-well plate. Each plate contains 768 electrodes across 96-wells, effectively recording from eight electrodes per well. We plated female CON or FLE2 patient-iPSC derived cortical-like excitatory neurons on 96-well MEA plates in Brainphys media (Bardy et al., 2015) and recorded their activity for 5 minute epochs at 37°C beginning 3 days after plating and repeating approximately once per week thereafter for 5 weeks (**Figure 3.6A**). Our results demonstrate that FLE patient neurons (red) had significantly increased excitability as compared with female CON neurons (blue) as measured by increased mean firing rate (**Figure 3.6B**), increased number of action potential bursts (**Figure 3.6C**) and increased burst frequency (**Figure 3.6D**). We did not find differences in the burst duration or the number of spikes per burst (**Figure 3.6E, F**). Additionally, we found that FLE neurons had significantly increased network burst frequency (defined as synchronous bursts seen in at least 25% of electrodes in a well) at day 12, 19 and 26 of recording (**Figure 3.6G**) as compared with control neurons. We did not find differences in the network burst duration or the number of spikes per network burst between FLE and CON neurons except at day 33 of recording (**Figure 3.6H, I**). These results suggest that FLE cortical-like excitatory neurons have increased excitability on MEA recordings as compared with their female control counterparts.

Functional analysis of male mixed cultures

We next analyzed our mixed male control and *PCDH19*-null neurons (mCON + mFLE) on the MEA system to assess for functional changes in the neuronal network in

cultures modeling the mosaic male state. To eliminate any confounding variables from the mixing process, we also plated mixed cultures of mCON + mCON as well as mFLE + mFLE neurons. We found that, contrary to FLE female patient iPSC-derived neurons, mCON + mFLE mixed neurons (red) as well as mFLE + mFLE mixed neurons (gray) both showed a significant decrease in mean firing rate and number of bursts as compared with mCON + mCON neurons (blue) (**Figure 3.7A, B**, asterisks). MEA activity of mCON + mFLE neurons did not significantly differ from mFLE + mFLE neurons. At a few timepoints, only mCON + mFLE neuronal activity was significantly different from mCON + mCON neuronal activity (**Figure 3.7A, B**, daggers). When we analyzed the specific bursting behaviors of the three different conditions, we did not find differences between burst frequency, burst duration, or the number of spikes per burst amongst the groups (**Figure 3.7 C, D, E**). These results suggest that male mixed cultures of control and null *PCDH19*-expressing neurons as well as neurons that had no expression of *PCDH19* have decreased excitability as compared with control neurons.

GABAergic interneurons from FLE patient and mixed cultures

Another integral cell type of the cerebral cortex is the GABAergic interneurons that serve to modulate the excitability of cortical excitatory neurons. To understand whether heterozygous mutations in *PCDH19* could impact the development and function of GABAergic cells, we differentiated FLE2 patient iPSCs into MGE-derived inhibitory interneurons using purmorphamine, an activator of the sonic hedgehog (SHH) pathway, based on an established protocol (Liu et al., 2013b). We cultured iPSCs as EBs and differentiated them into neuroepithelium. After plating the primitive neuroepithelium, we patterned them into MGE progenitors using purmorphamine before differentiating them

into GABAergic interneurons. After 8 weeks of terminal differentiation, we confirmed the interneuron identity using GABA and MAP2ab immunolabeling (**Figure 3.8A**) and also found that many of the cells were SST-positive interneurons (**Figure 3.8A**, inset). We observed that female control (CON) interneurons had GABA+ processes that were interspersed homogeneously (**Figure 3.8A**, top) throughout the cultures while the GABA+ processes of FLE neurons tended to fasciculate and create bundles (**Figure 3.8A**, bottom).

We next plated FLE2 inhibitory interneurons on 96-well MEA plates in Brainphys medium to assess for functional changes. We began recording around day 3-7 and recorded approximately once per week for 5 minute epochs. We did not have female control GABAergic interneurons available for MEA recording, so we plotted female FLE patient GABAergic recordings against male control GABAergic neuron recordings made at a different time (and used in the experiments shown in **Figure 3.9**). While this control is not ideal and a female control would be most suitable, it did give us a general sense of how female patient-iPSC derived GABAergic interneurons behaved (although the experimental design precluded statistical comparisons). Upon inspection, FLE interneurons (red) may possibly have a higher mean firing rate, increased number of bursts and increased burst frequency as compared with male control interneurons (blue) (**Figure 3.8B-D**) with no detectable differences in the burst duration or number of spikes per burst (**Figure 3.8E, F**). When we assessed for changes in the network behavior of FLE and control interneurons, we also visually detected an increase in the network burst duration and frequency of network bursts in FLE interneurons as compared with controls (**Figure 3.8G, H**) with no overt differences in the number of spikes per network burst

(**Figure 3.8I**). Our results indicate that FLE interneurons may have increased activity as compared with male control interneurons; however, more rigorous studies with the appropriate controls and statistical analyses are necessary for the proper interpretation of these results.

Finally, we differentiated mixed male cultures into GABAergic interneurons for morphological and electrophysiological studies. We analyzed mixed cultures of mCON + mFLE, mCON + mCON as well as mFLE + mFLE interneurons at 8 weeks after terminal differentiation. We immunostained the cultures for GABA and MAP2ab and did not find any morphological differences between the three groups (**Figure 3.9A**). We also performed MEA recordings on the cultures in Brainphys medium starting at day 7 after plating and thereafter approximately once per week for 5 minute epochs. When we analyzed the mean firing rate between the three cultures, we found that mCON + mFLE mixed interneurons (red) had significantly increased firing rate as compared with mCON + mCON interneurons (blue) and mFLE + mFLE interneurons (gray) (**Figure 3.9B**, asterisks) at days 7, 10, 14 and 21. We did not find differences in activity between mCON + mCON and mFLE + mFLE cultures. We also assessed for the number of bursts and found that mCON + mFLE interneurons had significantly increased numbers of bursts at days 10 and 14 as compared with mCON + mCON and mFLE + mFLE neurons with no differences between the latter (**Figure 3.9C**). We did not find any differences in burst duration, number of spikes per burst or burst frequency between the three groups (**Figure 3.9D-F**). Lastly, we also analyzed for various network properties such as network burst frequency, network burst duration and number of spikes per network burst (**Figure 3.9G-I**). We found that mCON + mFLE interneurons had significantly increased network burst

frequency at day 14 as compared with mCON + mCON and mFLE + mFLE interneurons (**Figure 3.9G**, asterisk). Meanwhile at day 10, both mCON + mFLE interneurons and mFLE + mFLE interneurons had significantly increased network burst frequency as compared with mCON + mCON interneurons (**Figure 3.9G**, dagger). We did not detect statistically significant differences in the network burst duration or the number of spikes per network burst between the three groups. These results suggest that GABAergic interneurons derived from mixed cultures of male control and *PCDH19*-null iPSCs show increased activity on MEAs that may reflect the results seen in *PCDH19* FLE patient GABAergic neurons.

Discussion

We utilized iPSCs to understand how heterozygous mutations in the *PCDH19* gene lead to alterations in neural development of cortical-like excitatory neurons and MGE-derived inhibitory interneurons. Using iPSCs derived from two female FLE patients with two different mutations and a female control, we uncovered cellular phenotypes in neural progenitors as well as neurons. As there have been several reports of EIEE9 in males who were mosaic for the gene (Depienne et al., 2009; Terracciano et al., 2016; Thiffault et al., 2016), we also mixed WT and mutant *PCDH19*-expressing male cells in an effort to recapitulate the male disease *in vitro*. To this end, we took advantage of simultaneous reprogramming with CRISPR/Cas9 gene-editing to introduce indels into the *PCDH19* gene in control male fibroblasts to generate *PCDH19*-null male iPSCs. We mixed these *PCDH19*-null iPSCs with isogenic control male iPSCs and differentiated them into both cortical-like excitatory neurons and MGE-derived inhibitory interneurons. We found these mixed cultures displayed several *in vitro* abnormalities similar to those

found FLE female patient neurons, further lending support to the cellular interference hypothesis.

Our studies provide insight into how homophilic PCDH19 cell-cell interactions regulate early mammalian neural development. Previous studies in the zebrafish show that *Pcdh19* regulates early steps in neural tube formation (Emond et al., 2009) through interactions with N-cadherin (Biswas et al., 2010). N-cadherin is critical for maintaining adherens junctions in the neuroepithelium (Hatta and Takeichi, 1986; Ganzler-Odenthal and Redies, 1998) and has been also been shown to complex with PCDH19 to mediate robust adhesive properties (Emond et al., 2011). In addition to N-cadherin, PCDH19 interacts with members of the WAVE complex (Tai et al., 2010), a critical regulator of actin cytoskeletal dynamics implicated in modulating neural stem cell development (Yoon et al., 2014). The actin cytoskeleton provides the cytoplasmic anchor for cadherin proteins, such as N-cadherin, and destabilizations in the WAVE complex may alter the organization of adherens junctions. Indeed, our study unveiled defects in apical polarity and adherens junctions in FLE patient iPSC-derived neural rosettes. Furthermore, these adherens junction defects were also seen in the mixed control and *PCDH19*-null expressing male neural rosettes. Our results suggest that PCDH19-mediated cell-cell interactions are critical for proper maintenance of neural progenitor cells, perhaps through a complex with N-cadherin to regulate the WAVE complex. Abnormal organization of NPCs during development may result in abnormal neuronal migration and integration to ultimately cause seizures or intellectual disability. The morphological findings in FLE patient neural rosettes would suggest severe structural defects in the patient brains, yet MRIs of FLE patients do not reveal gross structural abnormalities. This may reflect the inherent

reductionist nature of *in vitro* modeling where cells are plated on an artificial substrate in a 2D environment without many of the other supporting cells that exist *in vivo*. Similar rosette polarity findings have been seen in other iPSC models of human disease without gross abnormalities such as the 15q11.2 copy number variants, a risk for schizophrenia, epilepsy and ASD (Yoon et al., 2014).

Members of the protocadherin family have been shown to be important in regulating dendritic architecture and synaptic structure (Tsai et al., 2012; Molumby et al., 2016; Molumby et al., 2017). In particular, protocadherins play a critical role in mediating dendritic self-avoidance (Lefebvre et al., 2012; Kostadinov and Sanes, 2015), a process that aids in establishing full coverage of a dendritic territory as well as minimizing gaps and overlaps (Kramer and Stent, 1985; Grueber and Sagasti, 2010). We found that FLE patient cortical-like excitatory neurons had abnormal outgrowth of processes accompanied by frequent clumping, suggesting abnormal migration and impaired self-avoidance. We also found that FLE neurons demonstrated accelerated maturation with increased excitability on MEA recordings. Our mixed male cultures contained neurons with atypical morphology and demonstrated abnormal segregation of control and *PCDH19*-null cortical-like excitatory neurons, consistent with the cellular interference hypothesis. However, mixed cultures of control and *PCDH19*-null male neurons had decreased excitability on MEAs as compared with controls. This discrepancy in functional changes between FLE female excitatory neurons and mixed male excitatory neurons may be a result of timing of X-inactivation. In female iPSCs, both X-chromosomes are active therefore all cells are expressing both mutant and WT *PCDH19*. In contrast, the iPSCs in male mixed cultures only express one X-chromosome, either WT or mutant. It is possible

that the male cells segregate prior to rosette formation, thus forming rosettes of either all WT or all mutant *PCDH19*-expressing cells, while female cells undergo X-inactivation during rosette formation, therefore leading to rosettes comprised of mosaic cells. It seems plausible that the timing and mechanism of X-inactivation is important for the development of *PCDH19* FLE as the heterozygous mouse model of the disorder has no overt phenotype (Pederick et al., 2016), perhaps because X-inactivation in mice is very different from that in humans. Additionally, patient rosettes were only analyzed for FLE1, a line that contains a missense mutation for *PCDH19* that may encode for a functional protein. It is conceivable that cell-cell interactions between cells that express WT and mutant *PCDH19* proteins are very different than those between cells that express WT and *no* *PCDH19* protein.

There is some evidence that *PCDH19* expression increases during regional differentiation of ventral forebrain areas, particularly the MGE (Maroof et al., 2013). The MGE is responsible for generating a large proportion of GABAergic precursors that migrate into the neocortex to form as many as 50 percent of the GABAergic population in the cortex (Lavdas et al., 1999; Sussel et al., 1999). Most of the precursors from the MGE eventually become SST and PV interneurons that most often synapse onto cortical excitatory neurons (Xu et al., 2004; Butt et al., 2005). When we differentiated FLE patient iPSCs into MGE-derived GABAergic interneurons, we found that their processes showed greater fasciculation as compared with female control interneurons, suggesting abnormal self-avoidance. On crude MEA analysis, we visually noticed a possible increase in activity of female FLE interneurons as compared with control male interneurons. Similarly, control and *PCDH19*-null mixed male GABAergic interneurons also demonstrated increased

activity on MEA recordings as compared with control male neurons alone and *PCDH19*-null male neurons alone. At first glance, increased inhibition does not fit with the classic increased excitation-decreased inhibition theory of epileptogenesis. However, our results indicate increased excitation during the early stages of development of inhibitory interneurons. It is plausible that this hyperactivity may affect proper migration of precursors to the cortex thereby ultimately leading to decreased inhibition. A second possibility is that at early stages of brain development, because intracellular Cl⁻ concentrations are higher than extracellular concentrations, GABA produces a depolarizing current in immature neurons. In the developing hippocampus, GABAergic transmission can initiate ictal activity (Dzhala and Staley, 2003) and lead to epileptogenesis (Khalilov et al., 2005). Perhaps GABAergic hyperactivity in developing FLE interneurons ultimately leads to the development of seizures through their excitatory effects. Finally, our cultures contain a pure population of inhibitory interneurons with very few, if any, excitatory neurons. These pure populations may behave in a way that does not reflect what occurs in the human brain. Future studies aim to mix excitatory neurons and inhibitory interneurons in a more physiologically relevant manner.

Human iPSCs provide a unique and powerful platform for modeling diseases and probing their molecular and cellular mechanisms. In combination with the CRISPR/Cas9 gene editing technique, we generated strategies to model various aspects of an epilepsy disorder, *EIEE9*, *in vitro*. We uncovered morphological and functional changes that were previously not identified in mouse models of the disorder. However, much of the morphological data shown in these results are descriptive. Careful morphometric analysis using techniques such as the Sholl method are necessary to quantify and further establish

these findings. Furthermore, a limitation of these studies as well as other iPSC-based models of neurological disorders is that we are unable to generate fully mature neurons. Thus, certain aspects of the disorder, especially during the postnatal stage, still elude investigation with this platform. In addition, our data suggests that specific cortical layer markers may be aberrantly expressed by FLE patient neurons yet we are unable to model cortical lamination in monolayer cultures. One approach to overcome this hurdle is using organoid technology, a strategy that is described in Appendix B of this dissertation. Despite the limitations, this study is an important first step in understanding how aberrant cell-cell interactions during neural development may lead to hyperexcitability and seizures. Using human iPSCs as a discovery tool will inform future efforts to identify pharmacological agents that may aid in treating and preventing monogenic epilepsies.

Notes to Chapter 3

Wei Niu performed the qRT-PCR analysis on female FLE patient iPSCs and gave technical guidance with performing the qRT-PCR on male iPSCs. Andrew Tidball and Trevor Glenn conducted the simultaneous reprogramming with CRISPR/Cas9 gene editing protocol to generate the *PCDH19*-null male iPSC lines. Helen Zhang generated the CAG-GFP and CAG-mCh RV constructs.

We thank Ricardo Dolmetsch for providing FLE1 fibroblasts; Sundeep Kalantry and Michael Hinton for providing the human *XIST* probe and assisting with the RNA FISH experiments.

References

- Aamar E, Dawid IB (2008) Protocadherin-18a has a role in cell adhesion, behavior and migration in zebrafish development. *Developmental biology* 318:335-346.
- Bardy C, van den Hurk M, Eames T, Marchand C, Hernandez RV, Kellogg M, Gorris M, Galet B, Palomares V, Brown J, Bang AG, Mertens J, Bohnke L, Boyer L, Simon S, Gage FH (2015) Neuronal medium that supports basic synaptic functions and activity of human neurons in vitro. *Proceedings of the National Academy of Sciences of the United States of America*.
- Biswas S, Emond MR, Jontes JD (2010) Protocadherin-19 and N-cadherin interact to control cell movements during anterior neurulation. *The Journal of cell biology* 191:1029-1041.
- Biswas S, Emond MR, Duy PQ, Hao le T, Beattie CE, Jontes JD (2014) Protocadherin-18b interacts with Nap1 to control motor axon growth and arborization in zebrafish. *Mol Biol Cell* 25:633-642.
- Butt SJ, Fuccillo M, Nery S, Noctor S, Kriegstein A, Corbin JG, Fishell G (2005) The temporal and spatial origins of cortical interneurons predict their physiological subtype. *Neuron* 48:591-604.
- Chambers SM, Fasano CA, Papapetrou EP, Tomishima M, Sadelain M, Studer L (2009) Highly efficient neural conversion of human ES and iPS cells by dual inhibition of SMAD signaling. *Nature biotechnology* 27:275-280.
- Compagni A, Logan M, Klein R, Adams RH (2003) Control of skeletal patterning by ephrinB1-EphB interactions. *Developmental cell* 5:217-230.
- Depienne C et al. (2009) Sporadic infantile epileptic encephalopathy caused by mutations in PCDH19 resembles Dravet syndrome but mainly affects females. *PLoS genetics* 5:e1000381.
- Depienne C et al. (2011) Mutations and deletions in PCDH19 account for various familial or isolated epilepsies in females. *Human mutation* 32:E1959-1975.
- Dibbens LM et al. (2008) X-linked protocadherin 19 mutations cause female-limited epilepsy and cognitive impairment. *Nature genetics* 40:776-781.
- Dzhala VI, Staley KJ (2003) Excitatory actions of endogenously released GABA contribute to initiation of ictal epileptiform activity in the developing hippocampus. *The Journal of neuroscience : the official journal of the Society for Neuroscience* 23:1840-1846.
- Emond MR, Biswas S, Jontes JD (2009) Protocadherin-19 is essential for early steps in brain morphogenesis. *Developmental biology* 334:72-83.

- Emond MR, Biswas S, Blevins CJ, Jontes JD (2011) A complex of Protocadherin-19 and N-cadherin mediates a novel mechanism of cell adhesion. *The Journal of cell biology* 195:1115-1121.
- Fietz SA, Kelava I, Vogt J, Wilsch-Brauninger M, Stenzel D, Fish JL, Corbeil D, Riehn A, Distler W, Nitsch R, Huttner WB (2010) OSVZ progenitors of human and ferret neocortex are epithelial-like and expand by integrin signaling. *Nature neuroscience* 13:690-699.
- Gaitan Y, Bouchard M (2006) Expression of the delta-protocadherin gene Pcdh19 in the developing mouse embryo. *Gene expression patterns : GEP* 6:893-899.
- Ganzler-Odenthal SI, Redies C (1998) Blocking N-cadherin function disrupts the epithelial structure of differentiating neural tissue in the embryonic chicken brain. *The Journal of neuroscience : the official journal of the Society for Neuroscience* 18:5415-5425.
- Garrett AM, Schreiner D, Lobas MA, Weiner JA (2012) gamma-protocadherins control cortical dendrite arborization by regulating the activity of a FAK/PKC/MARCKS signaling pathway. *Neuron* 74:269-276.
- Grueber WB, Sagasti A (2010) Self-avoidance and tiling: Mechanisms of dendrite and axon spacing. *Cold Spring Harb Perspect Biol* 2:a001750.
- Hansen DV, Lui JH, Parker PR, Kriegstein AR (2010) Neurogenic radial glia in the outer subventricular zone of human neocortex. *Nature* 464:554-561.
- Hatta K, Takeichi M (1986) Expression of N-cadherin adhesion molecules associated with early morphogenetic events in chick development. *Nature* 320:447-449.
- Hayashi S, Inoue Y, Kiyonari H, Abe T, Misaki K, Moriguchi H, Tanaka Y, Takeichi M (2014) Protocadherin-17 mediates collective axon extension by recruiting actin regulator complexes to interaxonal contacts. *Developmental cell* 30:673-687.
- Hirano S, Yan Q, Suzuki ST (1999) Expression of a novel protocadherin, OL-protocadherin, in a subset of functional systems of the developing mouse brain. *The Journal of neuroscience : the official journal of the Society for Neuroscience* 19:995-1005.
- Hoshina N, Tanimura A, Yamasaki M, Inoue T, Fukabori R, Kuroda T, Yokoyama K, Tezuka T, Sagara H, Hirano S, Kiyonari H, Takada M, Kobayashi K, Watanabe M, Kano M, Nakazawa T, Yamamoto T (2013) Protocadherin 17 regulates presynaptic assembly in topographic corticobasal Ganglia circuits. *Neuron* 78:839-854.
- Johnson WG (1980) Metabolic interference and the + - heterozygote. a hypothetical form of simple inheritance which is neither dominant nor recessive. *American journal of human genetics* 32:374-386.

- Juberg RC, Hellman CD (1971) A new familial form of convulsive disorder and mental retardation limited to females. *J Pediatr* 79:726-732.
- Khalilov I, Le Van Quyen M, Gozlan H, Ben-Ari Y (2005) Epileptogenic actions of GABA and fast oscillations in the developing hippocampus. *Neuron* 48:787-796.
- Kim SY, Mo JW, Han S, Choi SY, Han SB, Moon BH, Rhyu IJ, Sun W, Kim H (2010) The expression of non-clustered protocadherins in adult rat hippocampal formation and the connecting brain regions. *Neuroscience* 170:189-199.
- Kostadinov D, Sanes JR (2015) Protocadherin-dependent dendritic self-avoidance regulates neural connectivity and circuit function. *eLife* 4.
- Kramer AP, Stent GS (1985) Developmental arborization of sensory neurons in the leech *Haementeria ghilianii*. II. Experimentally induced variations in the branching pattern. *The Journal of neuroscience : the official journal of the Society for Neuroscience* 5:768-775.
- Lancaster MA, Renner M, Martin CA, Wenzel D, Bicknell LS, Hurles ME, Homfray T, Penninger JM, Jackson AP, Knoblich JA (2013) Cerebral organoids model human brain development and microcephaly. *Nature* 501:373-379.
- Lavdas AA, Grigoriou M, Pachnis V, Parnavelas JG (1999) The medial ganglionic eminence gives rise to a population of early neurons in the developing cerebral cortex. *The Journal of neuroscience : the official journal of the Society for Neuroscience* 19:7881-7888.
- Lefebvre JL, Kostadinov D, Chen WV, Maniatis T, Sanes JR (2012) Protocadherins mediate dendritic self-avoidance in the mammalian nervous system. *Nature* 488:517-521.
- Liu Y, Liu H, Sauvey C, Yao L, Zarnowska ED, Zhang SC (2013a) Directed differentiation of forebrain GABA interneurons from human pluripotent stem cells. *Nature protocols* 8:1670-1679.
- Liu Y, Weick JP, Liu H, Krencik R, Zhang X, Ma L, Zhou GM, Ayala M, Zhang SC (2013b) Medial ganglionic eminence-like cells derived from human embryonic stem cells correct learning and memory deficits. *Nature biotechnology* 31:440-447.
- Maroof AM, Keros S, Tyson JA, Ying SW, Ganat YM, Merkle FT, Liu B, Goulburn A, Stanley EG, Elefanty AG, Widmer HR, Eggan K, Goldstein PA, Anderson SA, Studer L (2013) Directed differentiation and functional maturation of cortical interneurons from human embryonic stem cells. *Cell stem cell* 12:559-572.
- Mekhoubad S, Bock C, de Boer AS, Kiskinis E, Meissner A, Eggan K (2012) Erosion of dosage compensation impacts human iPSC disease modeling. *Cell stem cell* 10:595-609.

- Molumby MJ, Keeler AB, Weiner JA (2016) Homophilic Protocadherin Cell-Cell Interactions Promote Dendrite Complexity. *Cell reports* 15:1037-1050.
- Molumby MJ, Anderson RM, Newbold DJ, Koblesky NK, Garrett AM, Schreiner D, Radley JJ, Weiner JA (2017) gamma-Protocadherins Interact with Neuroligin-1 and Negatively Regulate Dendritic Spine Morphogenesis. *Cell reports* 18:2702-2714.
- Okita K, Matsumura Y, Sato Y, Okada A, Morizane A, Okamoto S, Hong H, Nakagawa M, Tanabe K, Tezuka K, Shibata T, Kunisada T, Takahashi M, Takahashi J, Saji H, Yamanaka S (2011) A more efficient method to generate integration-free human iPS cells. *Nature methods* 8:409-412.
- Pederick DT, Homan CC, Jaehne EJ, Piltz SG, Haines BP, Baune BT, Jolly LA, Hughes JN, Gecz J, Thomas PQ (2016) Pcdh19 Loss-of-Function Increases Neuronal Migration In Vitro but is Dispensable for Brain Development in Mice. *Sci Rep* 6:26765.
- Piper M, Dwivedy A, Leung L, Bradley RS, Holt CE (2008) NF-protocadherin and TAF1 regulate retinal axon initiation and elongation in vivo. *The Journal of neuroscience : the official journal of the Society for Neuroscience* 28:100-105.
- Qian X et al. (2016) Brain-Region-Specific Organoids Using Mini-bioreactors for Modeling ZIKV Exposure. *Cell* 165:1238-1254.
- Ryan SG, Chance PF, Zou CH, Spinner NB, Golden JA, Smietana S (1997) Epilepsy and mental retardation limited to females: an X-linked dominant disorder with male sparing. *Nature genetics* 17:92-95.
- Saavedra D, Richieri-Costa A, Guion-Almeida ML, Cohen MM, Jr. (1996) Craniofrontonasal syndrome: study of 41 patients. *Am J Med Genet* 61:147-151.
- Scheffer IE et al. (2008) Epilepsy and mental retardation limited to females: an under-recognized disorder. *Brain : a journal of neurology* 131:918-927.
- Shi Y, Kirwan P, Livesey FJ (2012a) Directed differentiation of human pluripotent stem cells to cerebral cortex neurons and neural networks. *Nature protocols* 7:1836-1846.
- Shi Y, Kirwan P, Smith J, Robinson HP, Livesey FJ (2012b) Human cerebral cortex development from pluripotent stem cells to functional excitatory synapses. *Nature neuroscience* 15:477-486, S471.
- Smart IH, Dehay C, Giroud P, Berland M, Kennedy H (2002) Unique morphological features of the proliferative zones and postmitotic compartments of the neural epithelium giving rise to striate and extrastriate cortex in the monkey. *Cereb Cortex* 12:37-53.

- Sussel L, Marin O, Kimura S, Rubenstein JL (1999) Loss of Nkx2.1 homeobox gene function results in a ventral to dorsal molecular respecification within the basal telencephalon: evidence for a transformation of the pallidum into the striatum. *Development* 126:3359-3370.
- Tai K, Kubota M, Shiono K, Tokutsu H, Suzuki ST (2010) Adhesion properties and retinofugal expression of chicken protocadherin-19. *Brain Res* 1344:13-24.
- Takahashi K, Tanabe K, Ohnuki M, Narita M, Ichisaka T, Tomoda K, Yamanaka S (2007) Induction of pluripotent stem cells from adult human fibroblasts by defined factors. *Cell* 131:861-872.
- Tchieu J, Kuoy E, Chin MH, Trinh H, Patterson M, Sherman SP, Aimiwu O, Lindgren A, Hakimian S, Zack JA, Clark AT, Pyle AD, Lowry WE, Plath K (2010) Female human iPSCs retain an inactive X chromosome. *Cell stem cell* 7:329-342.
- Terracciano A, Trivisano M, Cusmai R, De Palma L, Fusco L, Compagnucci C, Bertini E, Vigeveno F, Specchio N (2016) PCDH19-related epilepsy in two mosaic male patients. *Epilepsia* 57:e51-55.
- Thiffault I, Farrow E, Smith L, Lowry J, Zellmer L, Black B, Abdelmoity A, Miller N, Soden S, Saunders C (2016) PCDH19-related epileptic encephalopathy in a male mosaic for a truncating variant. *Am J Med Genet A* 170:1585-1589.
- Tomoda K, Takahashi K, Leung K, Okada A, Narita M, Yamada NA, Eilertson KE, Tsang P, Baba S, White MP, Sami S, Srivastava D, Conklin BR, Panning B, Yamanaka S (2012) Derivation conditions impact X-inactivation status in female human induced pluripotent stem cells. *Cell stem cell* 11:91-99.
- Tsai NP, Wilkerson JR, Guo W, Maksimova MA, DeMartino GN, Cowan CW, Huber KM (2012) Multiple autism-linked genes mediate synapse elimination via proteasomal degradation of a synaptic scaffold PSD-95. *Cell* 151:1581-1594.
- Uemura M, Nakao S, Suzuki ST, Takeichi M, Hirano S (2007) OL-Protocadherin is essential for growth of striatal axons and thalamocortical projections. *Nature neuroscience* 10:1151-1159.
- Uhlen M et al. (2015) Proteomics. Tissue-based map of the human proteome. *Science* 347:1260419.
- Wieland I, Jakubiczka S, Muschke P, Cohen M, Thiele H, Gerlach KL, Adams RH, Wieacker P (2004) Mutations of the ephrin-B1 gene cause craniofrontonasal syndrome. *American journal of human genetics* 74:1209-1215.
- Xu Q, Cobos I, De La Cruz E, Rubenstein JL, Anderson SA (2004) Origins of cortical interneuron subtypes. *The Journal of neuroscience : the official journal of the Society for Neuroscience* 24:2612-2622.

- Yoon KJ et al. (2014) Modeling a genetic risk for schizophrenia in iPSCs and mice reveals neural stem cell deficits associated with adherens junctions and polarity. *Cell stem cell* 15:79-91.
- Yu J, Vodyanik MA, Smuga-Otto K, Antosiewicz-Bourget J, Frane JL, Tian S, Nie J, Jonsdottir GA, Ruotti V, Stewart R, Slukvin, II, Thomson JA (2007) Induced pluripotent stem cell lines derived from human somatic cells. *Science* 318:1917-1920.
- Zecevic N, Chen Y, Filipovic R (2005) Contributions of cortical subventricular zone to the development of the human cerebral cortex. *J Comp Neurol* 491:109-122.

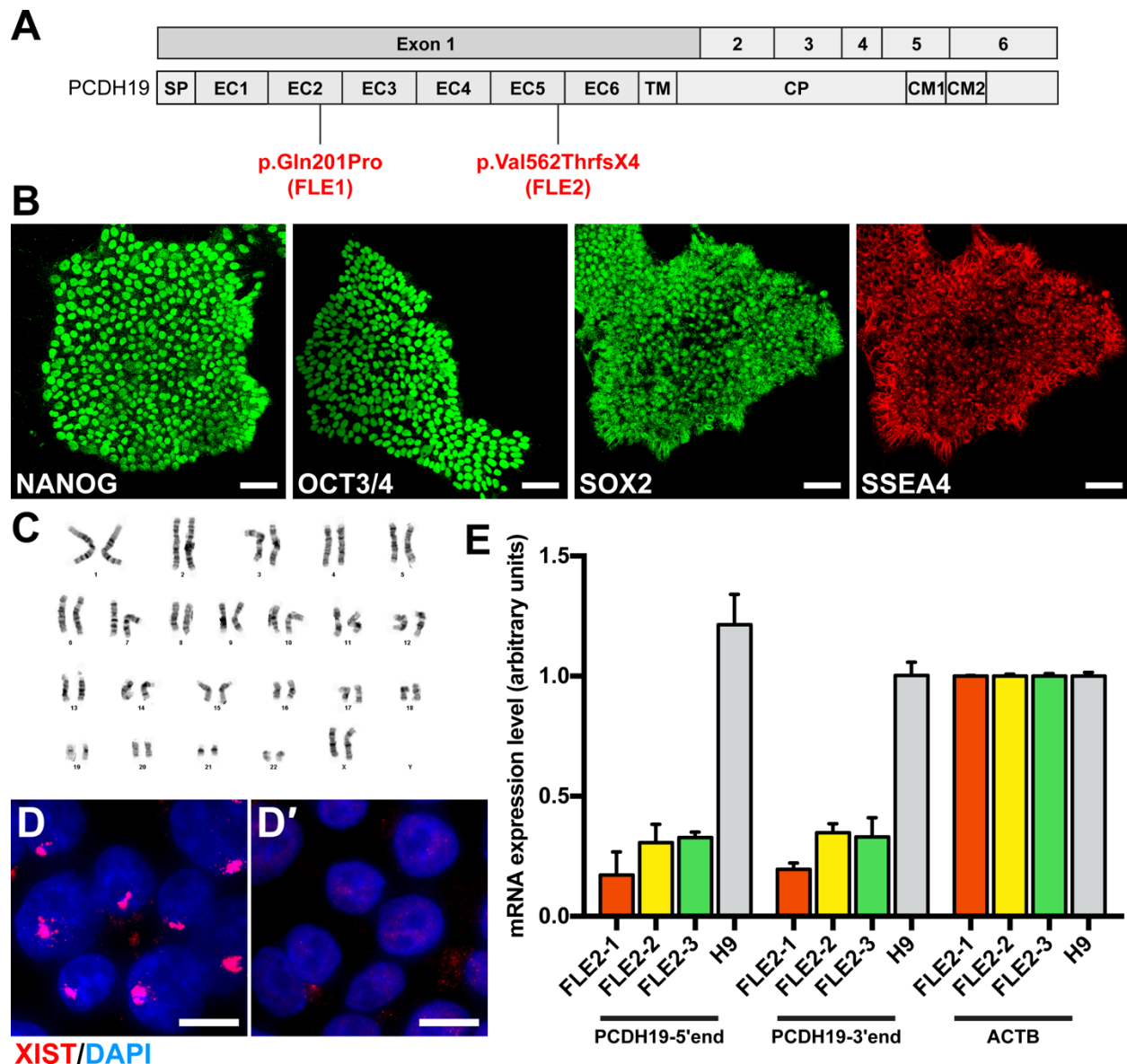


Figure 3.1. Generation and validation of PCDH19 FLE patient iPSC lines.

(A) Schematic of the *PCDH19* gene and protein showing the signal peptide (SP), six extracellular cadherin domains (EC), a transmembrane domain (TM), a cytoplasmic domain (CP) and two cytoplasmic motifs (CM). The location of the two *PCDH19* mutations of patients FLE1 and FLE2 are demarcated. (B) ICC in FLE iPSC cell lines demonstrate that iPSCs express pluripotency markers NANOG, OCT3/4, SOX2 and SSEA4. Scale bars represent 100 μ m. (C) Karyotype analysis of a representative iPSC line shows a normal karyotype. (D, D') RNA FISH in two different female iPSC lines demonstrate that one iPSC line has the presence of a single *XIST* cloud (D) indicating maintenance X-inactivation while another iPSCs line has no *XIST* (D') indicating reactivation of the previously inactive X-chromosome. Scale bars represent 20 μ m. (E) qRT-PCR analysis for *PCDH19* expression indicates that several clones of female FLE2 patient-derived iPSCs have decreased expression of *PCDH19* as compared with female H9 hESCs, versus no difference in expression of housekeeping gene β -actin (ACTB).

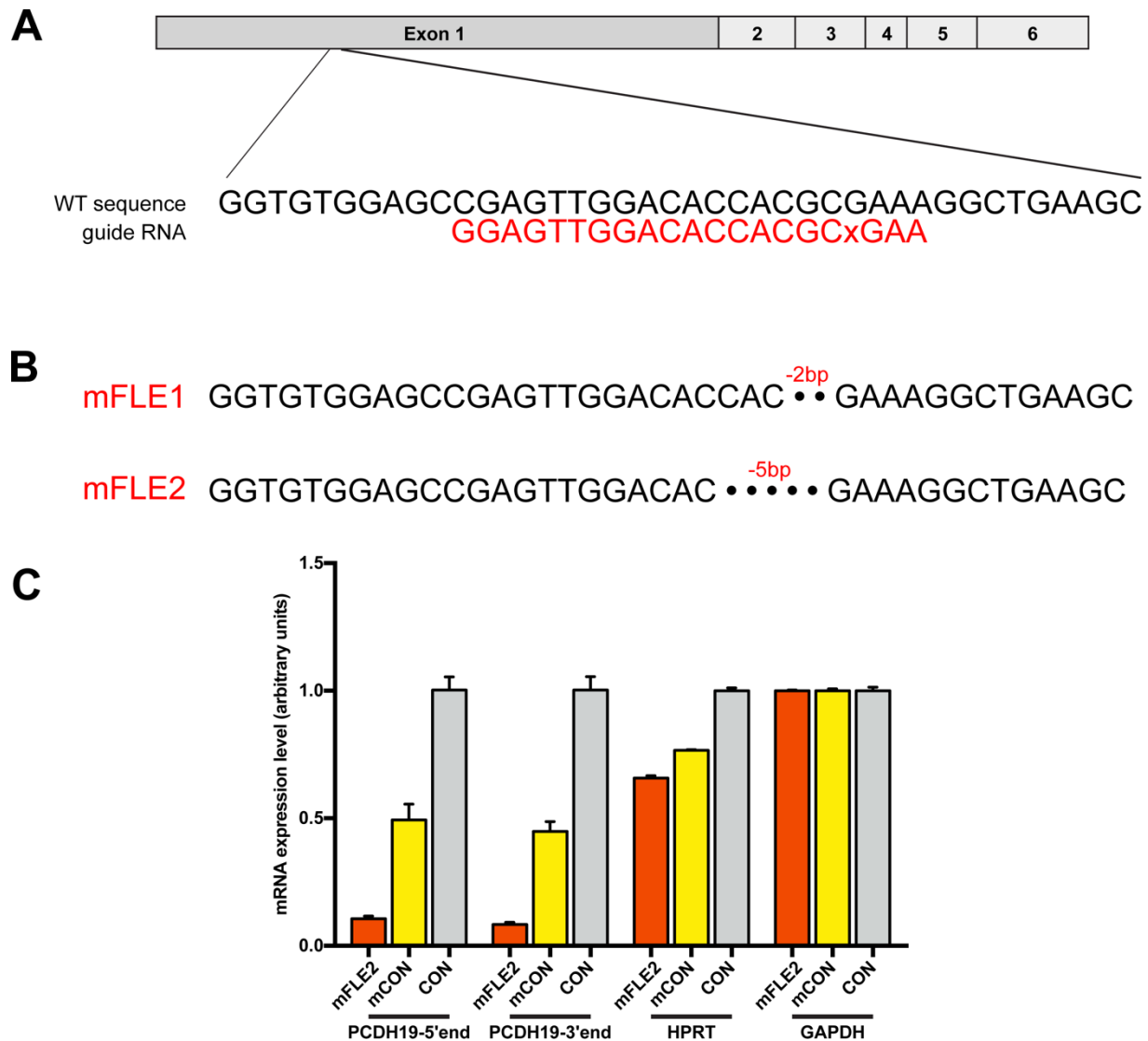


Figure 3.2. Generation of *PCDH19*-null male lines using CRISPR/Cas9.

(A) Schematic showing the design of the guide RNA targeting exon 1 of *PCDH19* for CRISPR/Cas9 mediated knockout of the gene in male control cells. **(B)** Two different *PCDH19*-null male iPSC lines were generated. mFLE1 had a 2bp deletion and mFLE2 had a 5bp deletion, each of which causes a frameshift mutation thereby creating a premature stop codon in the gene. **(C)** qRT-PCR confirming the loss of *PCDH19* mRNA in mFLE iPSCs as compared with male control iPSCs (mCON) and female control iPSCs (CON), versus no difference in expression of the housekeeping gene GAPDH. Note that the expression of the X-linked gene, *HPRT*, is higher in female iPSCs (CON) than male iPSCs (mFLE and mCON), representing the reactivation of Xi and expression of two X-chromosomes.

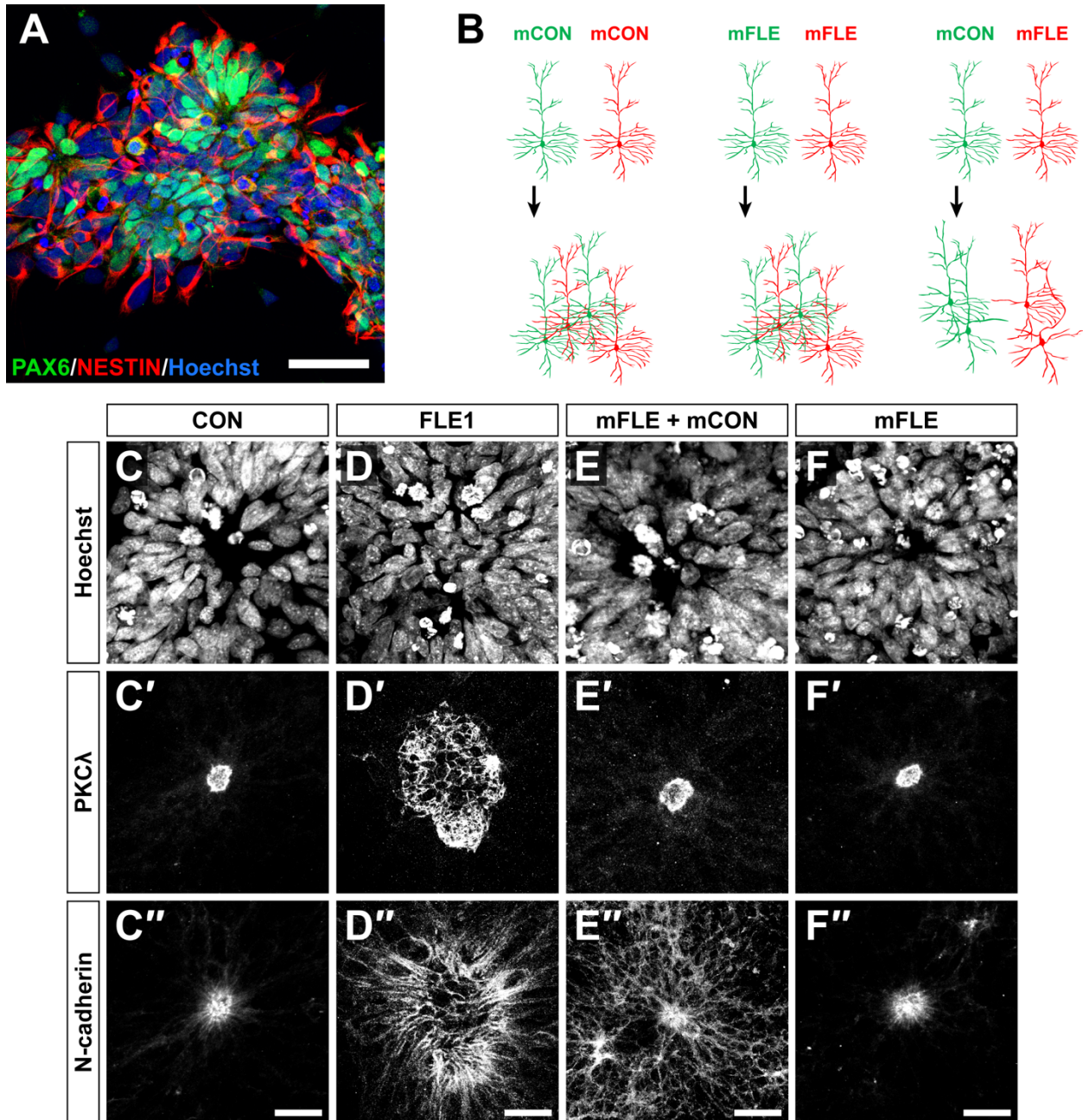


Figure 3.3. Neural rosettes derived from PCDH19 FLE patient iPSCs have defects in apical polarity and adherens junctions.

(A) Representative confocal image of neural rosettes in culture expressing PAX6 (green) and NESTIN (red). Scale bar represents 50 μ m. **(B)** Schematic of the mixing experimental paradigm. We rationalize that mixing control with other control male cells (mCON) or mixing *PCDH19*-mutant male cells with other *PCDH19*-mutant cells (mFLE) would demonstrate no morphological abnormalities, reminiscent of normal controls and asymptomatic *PCDH19*-mutation carrying males, respectively. However, mixing control with *PCDH19*-mutant male cells would lead to cellular interference with abnormal segregation of the two populations, representing the phenotype seen in affected mosaic

males and female patients. **(C-C')** Female control (CON) neural rosettes stain for PKC λ and N-cadherin in a typical ring-like pattern at the luminal surface. **(D-D')** FLE1 neural rosettes demonstrate defects in PKC λ and N-cadherin expression suggesting that PCDH19 is important for maintenance of apical polarity and adherens junctions. **(E-E')** Neural rosettes differentiated from 50:50 mixed male cultures of *PCDH19*-null iPSCs (mFLE) with isogenic controls (mCON) demonstrate normal PKC λ expression but a disruption of N-cadherin. **(F-F')** Neural rosettes derived from *PCDH19*-null male iPSCs (mFLE) alone demonstrate no defects in PKC λ or N-cadherin, reminiscent of control iPSCs. Scale bars in **C-F'** represent 20 μ m.

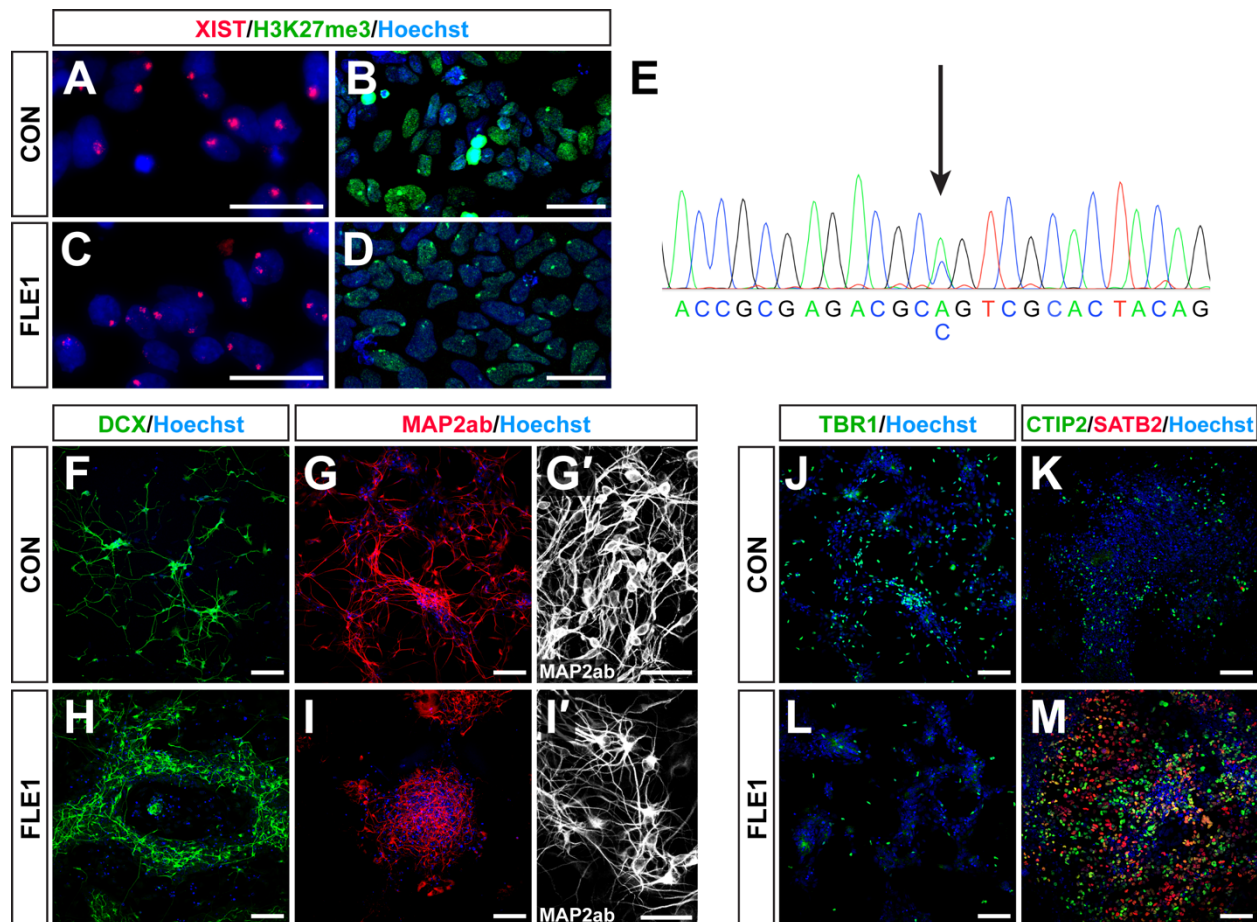


Figure 3.4. Cortical-like excitatory neurons differentiated from PCDH19 FLE patient iPSCs demonstrate abnormal migration and morphology.

(A) Female control (CON) iPSC-derived neurons express a single *XIST* cloud and (B) a single H3K27me3 foci within individual nuclei demonstrating random X-inactivation upon differentiation. (C) FLE1 iPSC-derived neurons also undergo random X-inactivation with the presence of single *XIST* and (D) H3K27me3 foci within each nucleus. Scale bars in A-D represent 50 μ m. (E) Sanger sequencing reveals FLE1 neurons inactivate the X-chromosome randomly and express both the mutant and WT alleles of *PCDH19* as shown by the two peaks (arrow) on the chromatogram. (F) Female control iPSC-derived neurons immunostained for DCX and (G) MAP2ab show processes that grow out to cover the extent of the territory of the cell with minimal overlap. (G') High magnification image of MAP2ab staining of female control neurons showing that cells have relatively straight processes with few outgrowths per soma. (H) DCX and (I) MAP2ab staining of FLE1 iPSC-derived neurons show that processes tend to clump together with minimal outgrowth and an abundance of self-crossings. (I') High magnification of MAP2ab immunostaining of FLE1 neurons show abundant processes are disorganized. (J) TBR1 staining of control neurons reveals many TBR1+ deep layer neurons with (K) some CTIP2+ deep layer neurons and minimal SATB2+ upper layer neurons. (L) FLE1 neurons have fewer TBR1+ neurons as compared with controls but contain many neurons that express (M) CTIP2 and SATB2, suggesting accelerated maturation. Scale bars in F-M represent 100 μ m except in G' and I' where they represent 50 μ m.

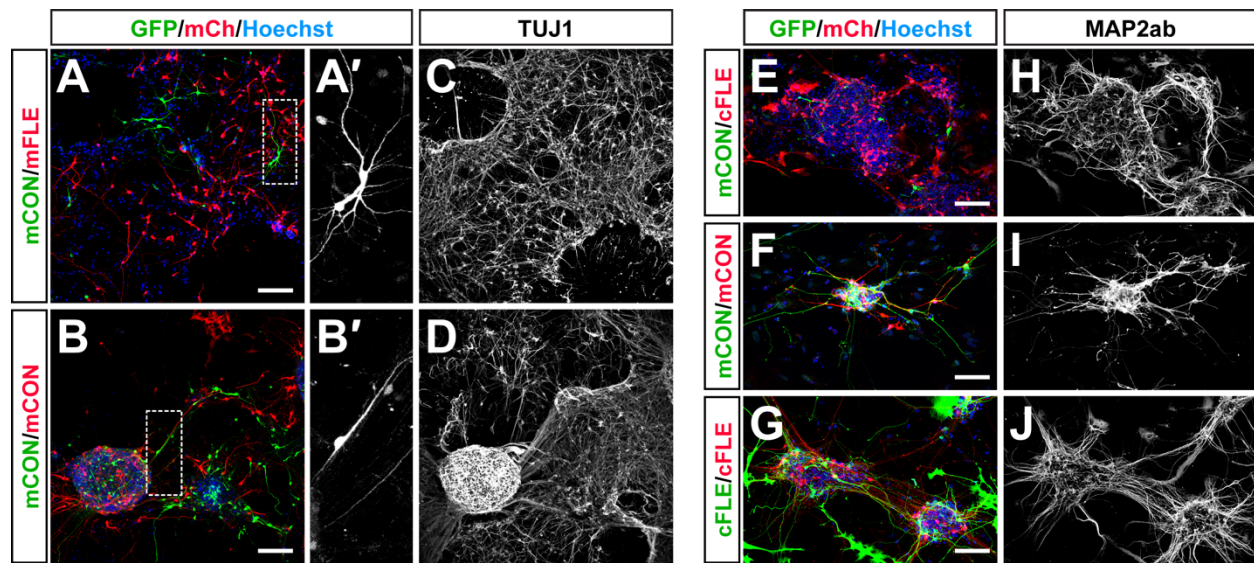


Figure 3.5. Mixed cultures of male control and *PCDH19*-mutant neurons demonstrate morphologic defects and abnormal segregation of cell populations. (A) Mixed cultures of GFP+ male isogenic control neurons (mCON) with mCh+ *PCDH19*-null neurons (mFLE) demonstrate segregation of the two populations marked by mCh+ dense regions with few GFP+ cells. (A') High magnification of the outlined area in A showing a GFP+ neuron with abnormal morphology marked by abundant, disorganized processes. (B) Mixed cultures of GFP+ control neurons with mCh+ control neurons demonstrate that the two neuronal populations intermingle without segregation, as expected. (B') High magnification of the outlined area in B showing a single GFP+ neuron with normal bipolar morphology. (C-D) TUJ1 immunostaining of the cultures shown in A and B confirming their neuronal identities. (E) Mixing GFP+ male control neurons (mCON) with mCh+ asymptomatic *PCDH19*-mutation carrier male neurons (cFLE) also results in abnormal segregation with regions of mCh+ cells with very few intermixed GFP+ cells. (F) Mixing GFP+ mCON neurons with mCh+ mCON neurons shows a homogeneous distribution of cells without any segregation of the two cell populations. (G) GFP+ cFLE neurons mixed with mCh+ cFLE neurons also do not demonstrate any abnormal segregation. (H-J) MAP2ab immunostaining of the cultures showing in E-G confirming their neuronal identities. Scale bars represent 100 μ m.

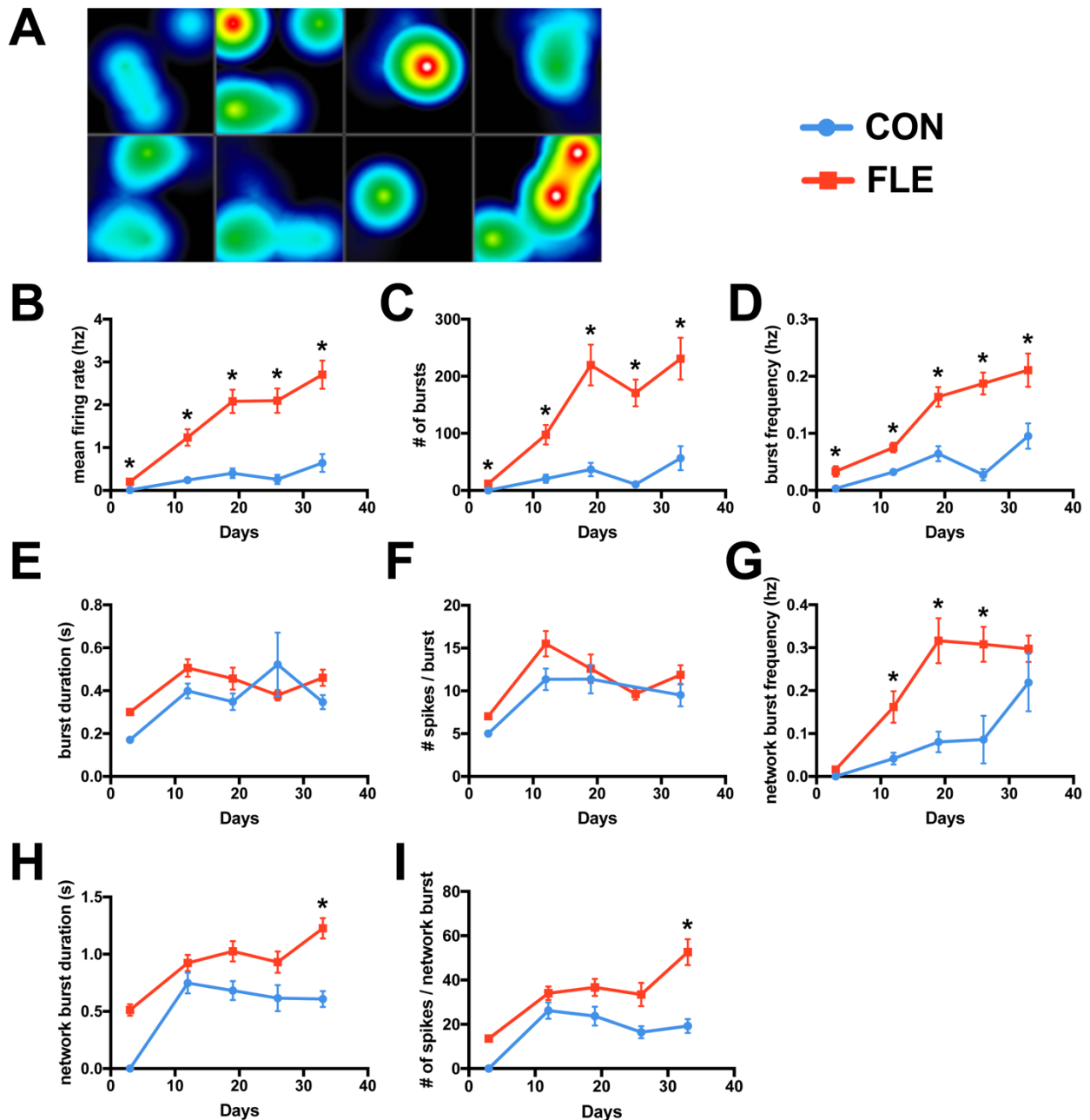


Figure 3.6. MEA recordings suggest that PCDH19 FLE cortical-like excitatory neurons have increased excitability as compared with female control neurons.

(A) Example illustrating the activity heat map on the MEA system across eight different wells with eight recording electrodes per well. (B) Mean firing rate, (C) number of bursts and (D) burst frequency of FLE cortical-like excitatory neurons (red) over 35 days are significantly increased at every timepoint as compared with female control (CON) neurons (blue). (E) The burst duration and (F) number of spikes per burst did not differ between FLE and CON neurons. (G) The network burst frequency was significantly increased in FLE neurons at days 12, 19 and 26 as compared with control neurons but the (H) network burst duration and (I) number of spikes per network burst did not differ between the two conditions except at day 35. (n = 3 plates; *p<0.05, Student's t-test).

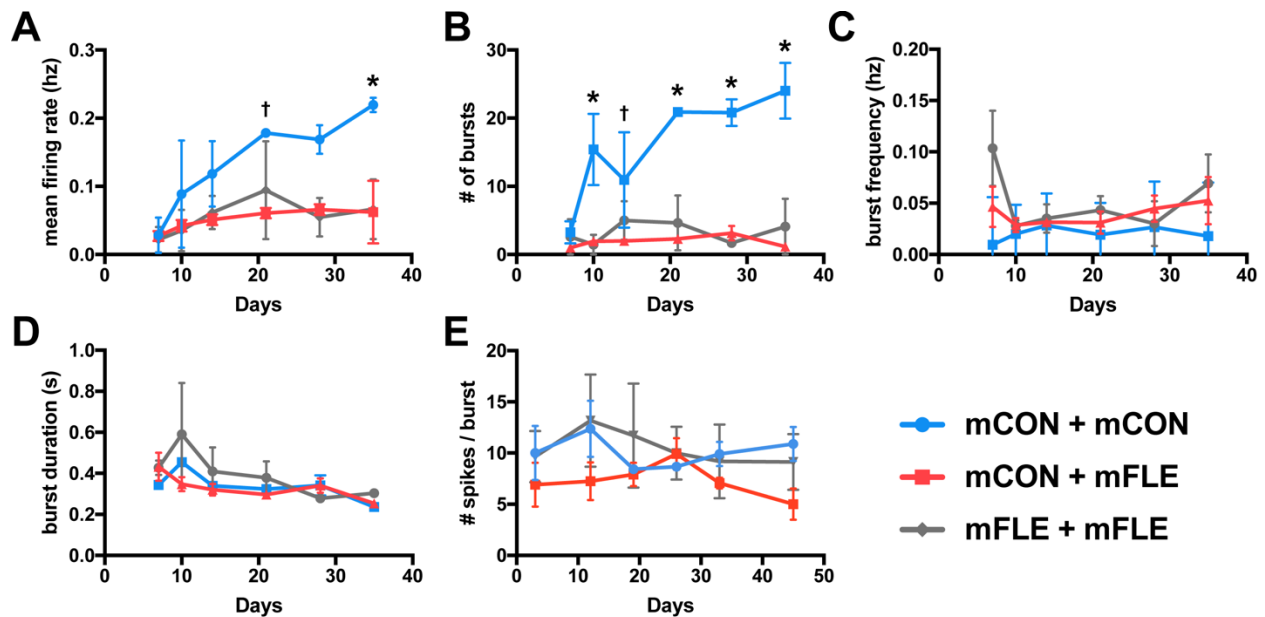


Figure 3.7. MEA analysis of male mixed cultures of control and *PCDH19*-null cortical-like excitatory neurons.

(A) Mixed mosaic male neurons (mCON + mFLE; red) and mixed male *PCDH19*-null neurons (mFLE + mFLE; gray) both show a significantly decreased mean firing rate at day 33, statistically represented as *, when compared with mixed male control neurons (mCON + mCON; blue). At day 20, only mCON + mFLE neurons have a significantly decreased mean firing rate, statistically represented as †, as compared with mCON + mCON neurons. mCON + mFLE neurons and mFLE + mFLE do not differ in their mean firing rate. (B) mCON + mFLE neurons and mFLE + mFLE neurons have significantly fewer number of bursts at days 10, 21, 28 and 35 as compared with mCON + mCON neurons. At day 14, only mCON + mFLE neurons have fewer bursts than mCON + mCON neurons. We did not detect statistically significant differences in the number of bursts between mCON + mFLE and mFLE + mFLE neurons. (C) The burst frequency, (D) burst duration and (E) the number of spikes per burst did not differ between the three groups. (n = 5 plates; *p<0.05, †p<0.05, one-way ANOVA with Tukey's post-hoc test).

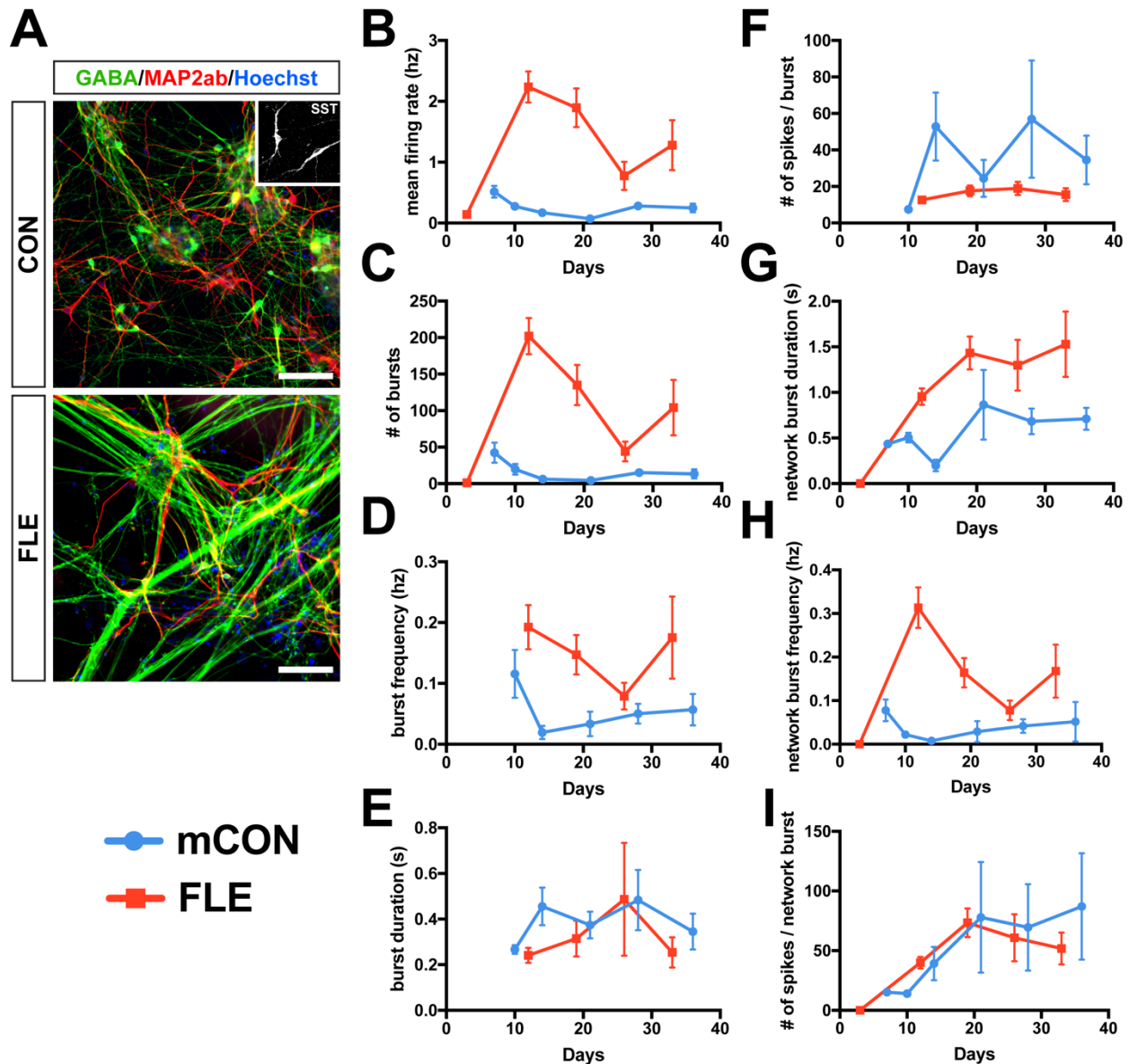


Figure 3.8. PCDH19 FLE GABAergic interneurons show morphological abnormalities and possible increased MEA activity as compared with controls.

(A) GABA and MAP2ab staining of control and FLE interneurons confirm their identity. Inset shows SST⁺ staining which comprise of most the GABAergic population in our cultures. Note that FLE interneurons have axonal fasciculation as compared with CON interneurons. Scale bars represent 100 μ m. (B) MEA analysis demonstrate that FLE interneurons may possibly have a higher mean firing rate, (C) number of bursts and (D) burst frequency as compared with male control interneurons. We did not visually detect a change in (E) burst duration or (F) number of spikes per burst between FLE and control interneurons. (G) FLE interneurons may also have increased network burst duration and (H) network burst frequency as compared with male controls interneurons with no overt differences in the (I) number of spikes per network burst between the two groups. (n = 3 plates for FLE interneurons).

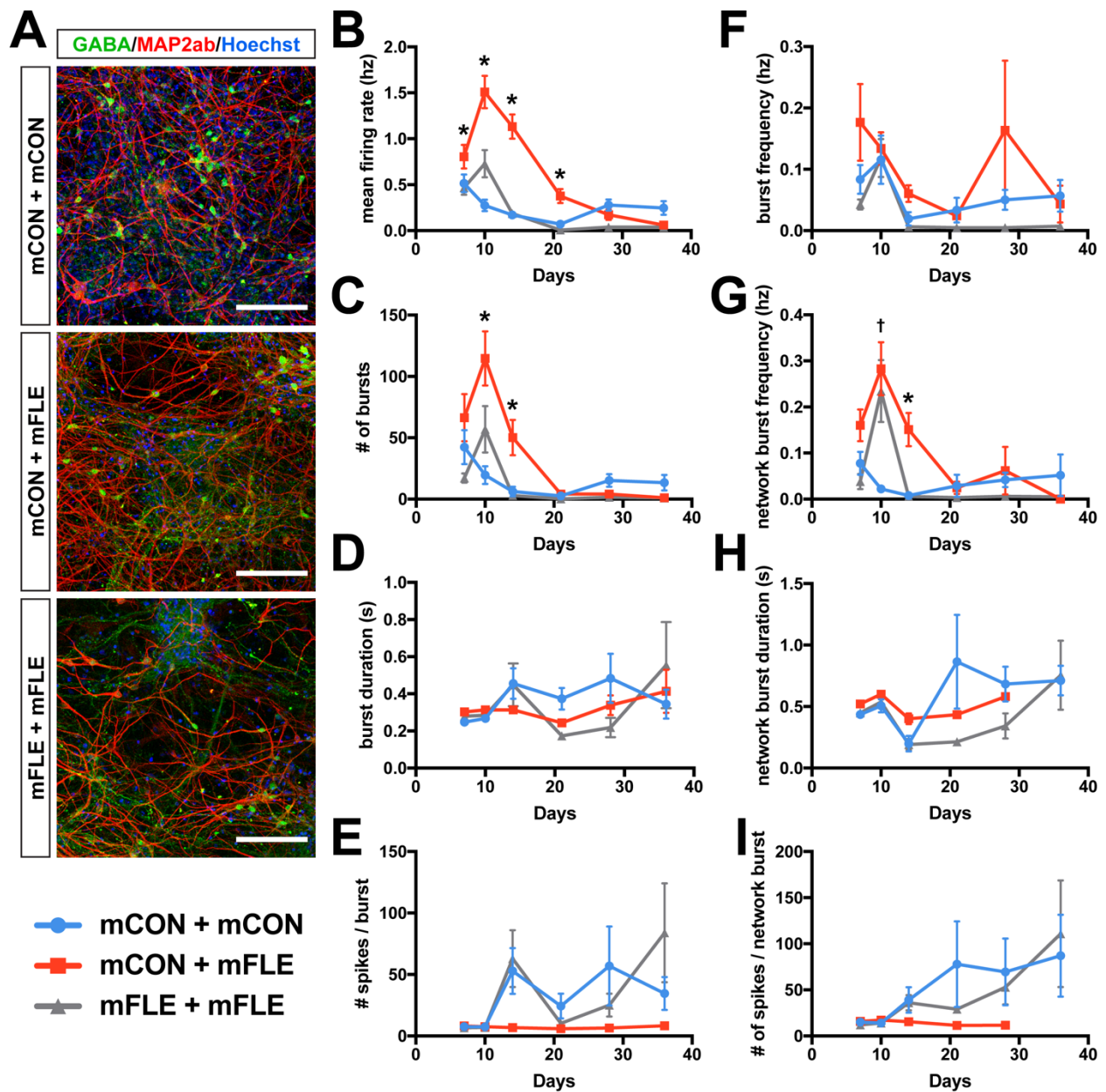


Figure 3.9. Mixed control and *PCDH19*-null GABAergic interneurons have normal morphology but demonstrate increased excitability on MEA recordings.

(A) GABA and MAP2ab staining of mCON + mCON, mCON + mFLE and mFLE + mFLE GABAergic interneurons confirming their identity. Scale bars represent 100 μ m. (B) MEA recordings of mixed cultures show that mCON + mFLE interneurons have significantly increased mean firing rate and (C) number of bursts as compared with mCON + mCON and mFLE + mFLE interneurons. We did not detect statistically significant differences in mean firing rate or number of bursts between mCON + mCON and mFLE + mFLE interneurons. (D-F) We did not detect statistically significant differences in the burst duration, the number of spikes per burst or the burst frequency between the three groups. (G) Network analysis show that mCON + mFLE interneurons have significantly increased network burst frequency at day 14, statistically represented as *, as compared with mCON

+ mCON and mFLE + mFLE interneurons. At day 10, both mCON + mFLE and mFLE + mFLE have higher network burst frequencies, statistically represented as †, when compared with mCON + mCON interneurons. **(H, I)** We did not find differences in the network burst duration or the number of spikes per network burst between the three groups. (n = 2 plates; *p<0.05, †p<0.05, one-way ANOVA with Tukey's post-hoc test).

Sequencing primer	Sequence
PCDH19 CRISPR/Cas9 (f)	tgagctcgtaagtctgcacg
PCDH19 CRISPR/Cas9 (r)	gctgccgccctcattaatct.
FLE1 sequencing (f)	ttgactgacagcaggtgatga
FLE1 sequencing (r)	ggagatcaaggacctgaacga

Table 1. Primer sequences for Sanger sequencing.

qRT-PCR primer	Sequence
pcdh19-5' end (f)	cgagagcaggggacaagtag
pcdh19-5' end (r)	aatggcgaagtcagaaccac
pcdh19-3' end (f)	ctcacatgctcaggggactt
pcdh19-3' end (r)	tgtgctgaacaccagtgtga
hprt1 (f)	gcagactttgctttccttg
hprt1 (r)	tcaagggcatatcctacaaca
actb (f)	acatctgctggaaggtggac
actb (r)	cccagcacaatgaagatcaa
gapdh (f)	atgttcgtcatgggtgtgaa
gapdh (r)	gggtctaagcagttggtggt

Table 2. Primer sequences for qRT-PCR.

Chapter 4

Dissertation Summary and Future Directions

Summary of results

Epileptogenesis is the process by which a genetic or acquired brain abnormality leads to the development of spontaneous recurrent seizures. However, it remains unclear how neural network alterations in various epileptic syndromes lead to changes in excitability. The long-term goal of the experiments described in this dissertation is to elucidate how perturbations of neural development and neurogenesis, during both the embryonic period and adulthood, contribute to the development of seizures. We approach this question in two separate systems: an animal model of TLE and an iPSC model of PCDH19 FLE. Our data indicate that the dentate gyrus reorganizes with the entire hippocampus to establish aberrant circuitry in experimental TLE. Both the adult-born and the early-born DGCs serve as targets for recurrent, feedback connections that may contribute to overall increases in network excitability. In addition to changes in adult neurogenesis, we also provide evidence that changes in early developmental neurogenesis have an impact on network excitability. We show that intercellular mismatches in a cell-cell adhesive protein, PCDH19, can result in aberrant neuronal morphologies and functional changes that may contribute to the development of seizures.

Adult-born and early-born DGCs are hyperconnected in the hippocampal circuitry in experimental TLE

After epileptic seizures, the dentate gyrus exhibits characteristic morphological abnormalities that include MFS, HBDs, hilar ectopic DGCs and granule cell layer dispersion. These changes are believed to arise from the adult-born population of DGCs and are thought to contribute to epileptogenesis. Indeed, hyperactivation of the mammalian target of rapamycin pathway (mTOR) in adult-born DGCs in an otherwise naïve animal can reproduce the changes seen in experimental TLE and induce spontaneous seizures (Pun et al., 2012). Studies eliminating adult-born DGCs immediately before SE using a nestin-tk transgenic mouse (Cho et al., 2015) or by expressing a diphtheria toxin (Hosford et al., 2016) have shown that these manipulations reduce seizure frequency but do not impede the development of epilepsy, suggesting that there are other mechanisms at play. While these studies implicate the postnatally generated DGCs as major contributors to disease pathogenesis, it is largely unclear how aberrantly integrated DGCs promote epileptogenesis.

Previous studies report that DGCs born after SE receive increased excitatory inputs (Thind et al., 2008; Zhan et al., 2010; Cameron et al., 2011) but do not identify these presynaptic sources. Other work suggests that there is compensatory inhibitory sprouting onto DGCs to decrease excitability after SE (Thind et al., 2010; Peng et al., 2013) but do not identify the age of the targeted DGCs. These mixed findings indicate that there may be heterogeneous groups of cells differentially involved to orchestrate hyperexcitability. Our use of a dual-viral tracing strategy gave us the opportunity to identify specific inputs onto birthdated populations of DGCs. The data reported in Chapter 2 of this dissertation show that both adult-born and early-born DGCs receive significant

recurrent excitatory inputs from other DGCs (**Figure 2.3**) suggesting that both populations are involved in post-SE excitatory remodeling. It was a long-held belief that early-born DGCs that were mature at the time of SE do not contribute to dentate gyrus abnormalities, but recent data from our laboratory indicate that both age groups are involved (Althaus et al., 2016), consistent with our current findings. Interestingly, hilar ectopic DGCs preferentially target adult-born DGCs, suggesting that they are hyperconnected with each other and onto nearby HBDs. These cells may serve as the ‘hub cells’ described by Morgan and Soltesz: a small subset of highly interconnected groups of cells that are more effective at promoting seizure activity than net increases in excitability in the entire dentate gyrus (Morgan and Soltesz, 2008). Our results also indicate that after SE, CA3 pyramidal cells preferentially backproject onto adult-born DGCs while CA1 pyramidal cells sprout axons across the hippocampal fissure to synapse onto early-born DGCs (**Figure 2.7**). These data suggest that the epileptic hippocampus is capable of much more extensive remodeling than previously believed and that considerations need to be made to target several populations or individual networks when developing therapeutic strategies.

The data presented in Chapter 2 of this dissertation give important insights into hippocampal circuit remodeling after seizures but also raise important questions about heterogeneity within the dentate gyrus neural stem cell population. What causes some DGCs to develop aberrantly while others display normal morphologies? What are the substrates that guide aberrant migration? How does the integration of hilar ectopic DGCs and DGCs with HBDs differ from normotopic DGCs in the epileptic brain and intact brain?

Why do some DGCs develop aberrantly after SE?

Lineage tracing studies demonstrate that hilar ectopic DGCs in the epileptic rodent brain arise from clonal populations within which the majority of cells migrate ectopically (Singh et al., 2015). If hilar ectopic DGCs are the hypothesized hub cell population (Morgan and Soltesz, 2008; Cameron et al., 2011), then understanding their development is a crucial first step in targeting them for therapeutics. While loss of reelin signaling has been implicated in this process (Gong et al., 2007), additional molecular cues are most likely involved. Do hilar ectopic DGCs possess intrinsic features that cause them to migrate aberrantly? Recent advances in single cell RNA-sequencing (scRNA-seq) technology have allowed for identification of molecular signatures of individual cells in the hippocampus that were previously not accessible in population studies (Shin et al., 2015; Zeisel et al., 2015; Lacar et al., 2016). scRNA-seq is well suited for exploring transcriptional profiles of individual birthdated DGCs because it is sensitive enough to detect small, stochastic changes that may contribute to global patterns of gene expression. To this end, a potential strategy would be to retrovirally birthdate adult-born DGCs in SE and sham animals and dissect them from the dentate gyrus at specific cell ages after labeling (e.g., 1 day, 3 days, 1 week, 2 weeks, 4 weeks and 8 weeks). One would then sort the labeled cells using fluorescence-activated cell sorting (FACS) and subsequently submit the samples for scRNA-seq. Using this approach, one could establish a profile of the temporal evolution of individual transcriptomes of adult-born DGCs in the epileptic and sham brain.

Once we have knowledge of transcriptional dynamics of the maturation process of adult-born DGCs in the epileptic versus intact brain, then we could use clustering analysis to delineate specific mRNA-level differences at selected timepoints between normotopic

sham versus normotopic SE versus ectopic SE groups. While the ectopic DGCs could be difficult to separate from the normotopic DGCs, particularly at the early ages, one way to overcome this is to carefully dissect out the granule cell layer and the hilus separately. If we can precisely identify the molecular signatures that are unique to hilar ectopic DGCs, then we can use targeted genetic manipulation strategies such as *in vivo* CRISPR/Cas9 editing (Swiech et al., 2015) as a research tool to knock out those genes at selected timepoints and potentially prevent aberrant migration. Current strategies that target hilar ectopic DGCs are unfavorable because they either eliminate or silence *all* of the adult-born DGCs after SE (Cho et al., 2015; Hosford et al., 2016), rather than only the abnormal subset. This strategy is not ideal because there is evidence that normotopic adult-born DGCs may mitigate increased excitation (Jakubs et al., 2006) and their complete deletion could have other consequences such as detrimental effects on learning and memory. By using *in vivo* gene editing to knockout candidate genes, we may be able to better retain DGCs in the granule cell layer after SE without inhibiting their function. We would subsequently determine whether “forcing” would-be hilar ectopic DGCs to remain in the granule cell layer has any effects on seizures.

If, in fact, hilar ectopic DGCs are hub cells, then the question to ask is whether they are intrinsically hyperexcitable or if their location near hilar mossy fibers that likely innervate them causes their hyperexcitability. That is to say, do they become hub cells because of their positioning in the dentate hilus or are they hub cells because of intrinsic factors regardless of spatial location? The answer is probably a combination of both. Regardless, if it is the former, then we would expect a decrease in seizures with normotopic position. If it is the latter, then we would not expect any changes in the

behavioral seizures of the animal. Such a finding, however, would also suggest that other mechanisms of epileptogenesis are at play. Finally, *in vivo* gene editing requires delivery of Cas9 protein sgRNAs to the brain, oftentimes with adeno-associated viruses (AAVs). An added advantage of AAVs is that they have recently been approved for human use, making this approach particularly promising for future clinical applications. One would, of course, have to make sure that AAVs are able to infect DGC progenitors for this approach to work.

What are the substrates that guide ectopic migration?

Neuronal precursors in the dentate gyrus are closely associated with the vasculature (Palmer et al., 2000) and a recent study from Sun et al. suggests that neuroblasts initially migrate tangentially along dense SGZ blood vessels before migrating radially (Sun et al., 2015). In the rodent dentate gyrus, many processes promote angiogenesis including exercise (Pereira et al., 2007; Ekstrand et al., 2008) as well as seizures (Rigau et al., 2007). Hilar ectopic DGCs arise as a result of chain migration of progenitors (Gong et al., 2007), a pattern that is reminiscent of SVZ neuroblast migration through the rostral migratory stream (RMS; Wichterle et al., 1997). Within the RMS, chain migration is guided by glial tubes as well as blood vessels (Whitman et al., 2009). However, whether newly developed blood vessels in the dentate gyrus after SE have an impact on DGC migration has not been fully characterized. It is plausible that if a newly developing vessel was directly apposed to a dividing RGL after SE, then most progenitors within that clone would track along the vasculature. This could explain why hilar ectopic DGCs often arise from clonal populations (Singh et al., 2015). Does new vasculature serve as a scaffold by which adult-born DGCs in the epileptic brain migrate into the hilus?

If so, would reducing angiogenesis reduce ectopic movement of neuroblasts? To study this question, one would perform lineage tracing studies using a tamoxifen-inducible *Nestin^{CreERT2}* mouse line. By sparsely labeling RGLs in the dentate gyrus using low-dose tamoxifen immediately after SE, one would sacrifice animals at age-defined timepoints after SE to track both the dynamics of CD31+ vessels as well as the movement of neuronal precursors along them. If, in fact, neuroblasts migrate along newly developed vessels towards the hilus, then these experiments could be repeated after giving animals an angiogenesis inhibitor to determine whether reducing the number of vessels could reduce the means by which neuroblasts can track, thereby preventing their ectopic movement. Further analyses should also focus on mechanisms of this angiogenesis and how it relates to blood-brain barrier (BBB) integrity after seizures. In fact, there is interest in using angiogenesis inhibitors to ameliorate BBB dysfunction for the treatment of human TLE (Rigau et al., 2007; Morin-Brureau et al., 2012). These studies should better inform the complexities of vascular dynamics in the development of seizures.

How does the integration of hilar ectopic DGCs and DGCs with HBDs compare with that of normotopic DGCs?

While the dual-virus tracing strategy gives insights into how adult-born and early-born DGCs as populations are integrated in the epileptic brain, a limitation of the study was the inability to distinguish inputs based on the morphology of the starter cell. In other words, we were unable to identify the input onto *only* hilar ectopic DGCs or cells with HBDs. An intriguing solution to overcoming this obstacle is to use *in vivo* single cell genetic manipulation techniques to deliver vectors to individual cells. Rancz et al. found that neurons remained intact after whole-cell recording and developed a method for

delivering plasmid DNA to the recorded cell through the patch pipette. In the same study, they recorded from pyramidal cells in the visual cortex and simultaneously delivered the plasmids necessary for subsequent rabies transfection. After introducing RbV two days later, they were able to show robust tracing of presynaptic inputs onto individual pyramidal cells (Rancz et al., 2011). This system could be utilized to trace presynaptic inputs onto single hilar ectopic DGCs or DGCs with HBDs. One would birthdate adult-born DGCs after SE and then perform patch clamp recording from selected GFP+ cells with aberrant features and then introduce TVA and Rgp plasmids through the patch pipette. After RbV-mCh injection, one would be able to identify monosynaptic inputs onto the previously recorded cell and compare the integration patterns of SE hilar ectopic DGCs versus SE DGCs with HBDs versus SE normotopic DGCs versus sham normotopic DGCs. A particularly attractive feature of this strategy is that it offers the opportunity to establish a complete physiological profile of a single, targeted cell. By elucidating the presynaptic inputs onto aberrant cells and the resulting electrophysiological consequences, we can begin to understand network-wide circuit dynamics that underlie the pathogenesis of TLE.

Disruptions in PCDH19 alter cell-cell homophilic interactions and contribute to altered excitability

The protocadherins are a large family of cell-cell adhesion proteins that have been shown to play important roles in neural development. Previous studies suggest mixed roles of protocadherins with evidence that homophilic recognition between cells promotes self-avoidance (Lefebvre et al., 2012) while others have shown that recognition actually facilitates outgrowth and dendritic complexity (Garrett et al., 2012; Molumby et al., 2016). *PCDH19* is expressed on the X-chromosome and heterozygous mutations cause the

epileptic disorder PCDH19 FLE (Dibbens et al., 2008). To date, no iPSC models of PCDH19 FLE exists in the literature. The *Pcdh19*^{+/β-Geo} heterozygous knockout mice do not appear to have overt morphologically abnormalities and do not exhibit seizures (Pederick et al., 2016).

The preliminary data presented in Chapter 3 of this dissertation suggest that cortical-like excitatory neural progenitors and neurons derived from PCDH19 FLE patient iPSCs have atypical morphology, clumping of processes as well as increased activity on MEA recordings (**Figure 3.4** and **3.6**). These morphological changes can be partially recapitulated in mixed mosaic cultures of WT/*PCDH19*-null expressing male neurons but the functional data are opposite with mixed cultures having *decreased* excitability. We also find that FLE patient iPSC-derived inhibitory interneurons have atypical development of processes that are accompanied by increased activity on the MEA system (**Figure 3.8**). Mixed male mosaic cultures of GABAergic interneurons also demonstrate increased activity but do not have morphological changes (**Figure 3.9**).

A key feature missing in these studies is the ability to directly visualize the PCDH19 protein in female FLE patient-derived cells. As some of our female iPSC lines reactivate the inactive X-chromosome and then undergo random X-inactivation upon differentiation, it is necessary for us to establish which cells express WT *PCDH19* versus mutant *PCDH19*. As commercially-available antibodies are unreliable, our current strategy is to use CRISPR/Cas9 to introduce a FLAG-HA-tag at the C-terminus of the PCDH19 protein in control, FLE1 and FLE2 iPSCs. In collaboration with Wei Niu, we aim to only tag a single allele, WT *PCDH19*, and then visualize the tag by ICC for either HA or FLAG. Cells that are HA⁺ or FLAG⁺ are expressing WT protein while cells that are HA⁻ or FLAG⁻ are

expressing mutant or no (null mutations) *PCDH19*. The ability to distinguish the two cell populations should help us identify X-inactivation skewing, aberrant cell-cell interactions and correlate cellular genotype with phenotype.

How do causative FLE mutations affect the adhesive properties of PCDH19?

Our results suggest that *PCDH19* is important for facilitating self-avoidance as well as dendritic tiling and its disruption may lead to abnormal propagation of electrical signals leading to hyperexcitability. However, they also indicate that it may be reductionist in nature to mix WT and *PCDH19*-null male cells in an effort to mimic the female FLE phenotype. Much of the FLE morphological data shown in Chapter 3 is derived from FLE1 who possesses a missense mutation of *PCDH19*. It is possible that a functional, albeit abnormal, *PCDH19* protein is transcribed from the gene and traffics to the cell surface to participate in intercellular interactions. These interactions between wildtype and mutant *PCDH19* proteins may be very different than those found in male mosaic cultures where wildtype *PCDH19* on control cells has *no* *PCDH19* with which to interact on mutant cells.

There are various cell aggregation assays that are used to establish interactions between adhesive proteins. Schreiner et al. established a technique for assessing intercellular adhesion using the human leukemia cell line K562 (Schreiner and Weiner, 2010). As K562 cells do not express endogenous cadherins or protocadherins, they are an appropriate cell type for these studies. One would transfect a “bait” cell group with constructs encoding extracellular, N-terminal HA-tagged forms of either WT *PCDH19*, mutant *PCDH19* carrying the c.602 A>C mutation from FLE1 (FLE1 *PCDH19*) or mutant *PCDH19* carrying the c.1683_1696del14 mutation from FLE2 (FLE2 *PCDH19*). A second “reporter” cell group would then be co-transfected with two plasmids, one encoding β -gal

and another encoding WT, FLE1 or FLE2 *PCDH19*. One would allow these two groups of cells to aggregate before using anti-HA antibody bound magnetic beads to isolate bait cells attached to any reporter cells. By lysing the attached cells and quantifying the level of β -gal activity, one could determine the size of the aggregates thus the *trans* interaction between cells. One would assess whether mutant and WT *PCDH19* show stronger or weaker adherence than WT *PCDH19* with WT *PCDH19* or mutant *PCDH19* with mutant *PCDH19*. Additionally, as *PCDH19* has been shown to interact with N-cadherin (Biswas et al., 2010; Emond et al., 2011), these aggregation experiments could be repeated but with an additional construct for N-cadherin co-transfected into the bait cells along either WT, FLE1 or FLE2 *PCDH19*. N-cadherin would also be co-transfected into the reporter cells along with β -gal and WT, FLE1, or FLE2 *PCDH19*. A second group of reporter cells that would only express constructs for N-cadherin or β -gal to mimic a *PCDH19*-null scenario would also be included. One would then mix the bait group with either reporter group and assess for β -gal activity. Data from these studies would aid in determining whether N-cadherin affects the adhesive properties of WT and mutant *PCDH19* and also how this interaction compares with those between cells that express WT *PCDH19* and no *PCDH19*. These results may provide critical information about how specific mutations in *PCDH19* affect cell-cell interactions during neural development and also give some insight into why female FLE neurons behave differently from mosaic mixed male neurons *in vitro*.

Do astrocytes have a role in the pathogenesis of PCDH19 FLE?

Astrocytes are important mediators in many aspects of brain development and function. Not only do they secrete proteins that are critical for excitatory (Pfrieger and

Barres, 1997; Christopherson et al., 2005; Allen et al., 2012) and inhibitory synaptogenesis (Elmariah et al., 2005; Hughes et al., 2010), but their direct contacts with neurons are also essential for proper synapse formation (Hama et al., 2004; Barker et al., 2008) and dendritic spine maturation (Ventura and Harris, 1999; Haber et al., 2006). Astrocytic defects have been shown to play a role in various neurodevelopmental disorders. In Rett syndrome caused by mutations in MeCP2, astrocytic deficiencies have non-cell-autonomous effects on neurons in both mouse (Ballas et al., 2009; Liroy et al., 2011; Nguyen et al., 2012) and iPSC models. Williams et al. showed that astrocytes derived from Rett syndrome patient iPSCs have detrimental effects on the morphology of wild-type neurons in co-cultures *in vitro* (Williams et al., 2014). Interestingly, astrocytes express protocadherins at their perisynaptic processes and mediate neuronal synaptogenesis through the matching of protocadherin isoforms (Garrett and Weiner, 2009; Molumby et al., 2016). Generally, protocols to differentiate neurons from iPSCs do not generate many astrocytes in the process thus making it difficult to study their role in disease pathogenesis *in vitro*. Fortunately, several established methods exist for generating astrocytes from iPSCs (Krencik et al., 2011; Emdad et al., 2012; Shaltouki et al., 2013) making it an interesting future consideration to add astrocytes to neuronal cultures. We would differentiate FLE patient iPSCs separately into cortical-like excitatory neurons and astrocytes and then co-culture the two populations together. One would have to determine the exact X-inactivation status of each cell type so that we could co-culture WT neurons with WT astrocytes, WT neurons with mutant astrocytes, mutant neurons with mutant astrocytes and mutant neurons with WT astrocytes. One could assess for morphological changes as the cultures develop and also conduct functional

analyses using both whole-cell electrophysiological recordings and MEA recordings. These same experiments could also be repeated but with MGE-derived, cortical-like GABAergic interneurons to determine the effects of astrocytes on the development of interneurons.

How do heterozygous mutations in PCDH19 affect the development of forebrain organoids?

Our data indicate that FLE patient iPSC-derived neurons may have accelerated maturation as demonstrated by early expression of cortical layer markers. However, it is difficult to tease out what this accelerated maturation means in the greater context of cortical development using monolayer cultures. Fortunately, 3D culturing techniques are becoming increasingly utilized as a strategy for iPSC disease modeling as they promote spatial organization in a more anatomically relevant manner. Organoids recapitulate important aspects of human brain development such as the radially organized progenitors and cortical cells around ventricular-like structures as found in the embryonic neural tube (Lancaster et al., 2013; Pasca et al., 2015; Qian et al., 2016). We have adopted a recently developed technology from Hongjun Song's lab, SpinΩ, for generating much more spatially organized forebrain organoids with six cortical layers (described in Appendix B). This model is particularly promising for understanding developmental disorders with pathologies thought to arise from cell-cell interactions because the 3D architecture fosters communication between cells in a way that may be much more relevant than those found in 2D systems. In particular, for FLE modeling, we can extend our findings in monolayer cultures and compare various aspects of organoid development between FLE and control

organoids such as the cortical mantle thickness, cell types and lamination as well as neural progenitor changes such as cell cycle properties, migration and cell division.

While forebrain organoids contain multiple cell types including astrocytes and GABAergic interneurons, these populations are sparse when compared with those in the human brain. As GABAergic signaling is a critical component of neocortical development (LoTurco et al., 1995; Heck et al., 2007; Wang and Kriegstein, 2008), the importance of their presence during organoid development cannot be understated. One way to introduce them in higher quantities is to grow forebrain organoids and MGE spheroids separately before combining them in a co-culture system (Liu et al., 2013). It is our experience that, if organoids are cultured together in close proximity, they tend to fuse together. As interneurons in the MGE migrate long distances to travel to cortex, it is likely that progenitors in the MGE spheroids would migrate into the forebrain organoids where they could integrate and possibly promote further maturation. Using this strategy, we could devise a system where we test multiple conditions: WT forebrain organoid with FLE MGE spheroid, FLE MGE forebrain organoid with WT spheroid, WT with WT and FLE with FLE. We would perform histological analyses and compare features such as migration, processes outgrowth and cellular morphology in the heterogeneous (WT with FLE) co-cultures compared with the homogeneous cultures.

Lastly, the ability to generate organoids in large quantities makes them an attractive tool for drug screening. One could use MEA technology as well as all-optical electrophysiology (Optopatch) (Hochbaum et al., 2014) for high-throughput measurements and candidate drug selection. Optopatch is particularly suited for organoid physiology because of its ability to make measurements from many cells relatively quickly

and with robust statistics. Because of the heterogeneity that arises with organoids or any iPSC system, for that matter, it is necessary to perform analyses across a large population of cells. One would infect organoids with a lentivirus driven by a Synapsin promoter expressing QuasArs2, a highly-sensitive genetically-encoded voltage indicator and CheRiff, a blue-light activated channelrhodopsin with fast kinetics and minimal optical crosstalk with QuasArs2. By making slices from organoids and then using Optopatch to stimulate and record from targeted cells, one could measure network properties such as synaptic transmission and action potential propagation in large numbers of cells. The ultimate goal of these studies is to screen for potential drug therapies. One could add different AEDs to individual organoids before measuring changes in function with either MEA recordings or Optopatch. As PCDH19 FLE patients often encompass a broad spectrum of clinical manifestations, it suggests that the disorder is heterogeneous and that not every drug will work for every patient. If we are able to develop next-generation therapeutics targeted for *individual* patients with specific mutations, then it is a first step towards personalized medicine and translating our research findings into a real-world clinical setting.

A look ahead

The work presented in this dissertation gives new insights into how the adult neural circuitry remodels after epileptic seizures as well as how deviations in embryonic development can mediate hyperexcitability. However, these two processes are not mutually exclusive and understanding both should better inform our knowledge of the mechanisms of epileptogenesis. There are aspects of both systems that remain less well characterized but could offer critical insights into neurogenesis that impact our ability to

derive curative treatments for epilepsy. For one, are fully mature adult-born DGCs different from neonatally-born DGCs? The general consensus is that immature adult-born DGCs have unique properties that are thought to contribute to learning and memory (Deng et al., 2009; Sahay et al., 2011; Gu et al., 2012) but these features disappear as the DGCs reach maturity (Esposito et al., 2005; Laplagne et al., 2006). However, our data in Chapter 2 suggest that even at 8 weeks after their birth, adult-born DGCs may have differential inputs from the hippocampal circuit. Dissecting out the molecular pathways that specifically regulate adult neurogenesis could allow for more precision when devising targets for treating TLE. Secondly, the oRG has been proposed to be a major contributor to upper-layer neurogenesis (Smart et al., 2002; Lukaszewicz et al., 2005; Hansen et al., 2010). What regulates oRG development and can these changes be disrupted to lead to seizures? This question is difficult to answer in both iPSC monolayer cultures and rodent models because oRGs are sparse in both systems. However, oRGs can be reliably generated in organoid systems (Lancaster et al., 2013; Qian et al., 2016). Probing their functional and regulatory cues may uncover answers about human neurodevelopment and shed light on the mysteries that remain in understanding developmental epilepsies.

In studying these changes, careful selection of a model system is critical as each one can only faithfully recapitulate certain, but not all features, of a disease. While the data presented in this dissertation use two different approaches to model two different epileptic disorders, human iPSC studies and animal models should be utilized as complementary systems because each has unique features that the other lacks. That is to say, a readily observable phenotype in iPSC-derived neurons may be subtler in an animal model, yet these subtleties should not be overlooked because they may lead to

other, more salient changes that are not observable in the iPSC system. For instance, a recent study modeling 15q11.2 copy number variations, a risk factor for schizophrenia, epilepsy and autism, showed that patient iPSC-derived neural rosettes had apical polarity defects but the differentiated neurons were normal. The authors were able to recapitulate this same progenitor defect in the SVZ of a mouse model and also extend these findings to show that cortical neurons migrated aberrantly, a feature that would not have been readily demonstrable in iPSC studies (Yoon et al., 2014).

Cell-based therapies are becoming increasingly considered for the treatment of neurological disorders, particularly now that iPSCs are readily available and are essentially an unlimited, renewable source of cellular material. Transplantation strategies can be useful for both structural repair as well as anticonvulsant or disease modifying properties. An elegant study by Hunt et al. demonstrated that transplanting embryonic MGE precursors into the hippocampus of epileptic mice could ameliorate the frequency of seizures and attenuate other behavioral changes (Hunt et al., 2013). However, for the purposes of treating human disease, transplanting fetal-derived tissue is not a viable option. But the accessibility of patient-derived iPSCs holds great promise for deriving specific neuronal cell populations for autologous grafting purposes. Another study recently differentiated human iPSC-derived GABAergic progenitors and transplanted these cells into the epileptic mouse brain. The progenitors integrated over time into the neural network to suppress seizures and correct behavioral abnormalities (Cunningham et al., 2014). These results demonstrate the therapeutic potential of human iPSC-derived materials but the dosing strategy, efficacy and long-term safety and survival remain to be evaluated.

Despite the successes that we have achieved in understanding mechanisms of epileptogenesis in experimental models, a major consideration in all these studies is their translational relevance. Our knowledge of human TLE remains limited with most studies conducted in postmortem tissues or tissues from resected hippocampi of patients who have had chronic disease for a long period of time. While informative, these studies offer limited information on the acute stages of disease pathogenesis. In fact, it remains unknown whether seizure-induced neurogenesis is potentiated in human disease in a similar manner as in rodents. Despite these hurdles, investigators are beginning to acquire valuable tools to study physiological mechanisms in the human brain in an unprecedented manner. For instance, we have recently garnered a much clearer picture of the dynamics of adult human hippocampus neurogenesis using nuclear-bomb-test-derived ^{14}C dating (Spalding et al., 2013). Others have utilized human tissue to study dynamics of embryonic neurodevelopment that greatly informed our understanding of how the cortex forms (Hansen et al., 2010). We are also developing next-generation *in vitro* models with 3D organoids that more and more closely resemble the human brain *in vivo*. I am optimistic that if we, as a scientific community, openly share ideas and continue to conduct research in a rigorous and ethical manner, that this is merely just the beginning of a new era of scientific exploration.

Conclusions

Our understanding of neurogenesis and its impact on epileptogenesis has greatly increased in the last two decades. We now have powerful techniques and model systems that are capable of driving the scientific process at speeds and precision that were previously unachievable. In parallel with our scientific achievements, the questions that

we ask as a community are also becoming more and more complex. Thus, it is important that we turn to multiple model systems for answering multidimensional scientific questions, particularly when they address intricate processes such as development of the CNS, and not overlook the drawbacks that exist within each system. In this way, we can ask rigorous questions and make experimental advances that are ultimately translatable into a clinical setting.

References

- Allen NJ, Bennett ML, Foo LC, Wang GX, Chakraborty C, Smith SJ, Barres BA (2012) Astrocyte glypicans 4 and 6 promote formation of excitatory synapses via GluA1 AMPA receptors. *Nature* 486:410-414.
- Althaus AL, Zhang H, Parent JM (2016) Axonal plasticity of age-defined dentate granule cells in a rat model of mesial temporal lobe epilepsy. *Neurobiology of disease* 86:187-196.
- Ballas N, Liou DT, Grunseich C, Mandel G (2009) Non-cell autonomous influence of MeCP2-deficient glia on neuronal dendritic morphology. *Nature neuroscience* 12:311-317.
- Barker AJ, Koch SM, Reed J, Barres BA, Ullian EM (2008) Developmental control of synaptic receptivity. *The Journal of neuroscience : the official journal of the Society for Neuroscience* 28:8150-8160.
- Biswas S, Emond MR, Jontes JD (2010) Protocadherin-19 and N-cadherin interact to control cell movements during anterior neurulation. *The Journal of cell biology* 191:1029-1041.
- Cameron MC, Zhan RZ, Nadler JV (2011) Morphologic integration of hilar ectopic granule cells into dentate gyrus circuitry in the pilocarpine model of temporal lobe epilepsy. *J Comp Neurol* 519:2175-2192.
- Cho KO, Lybrand ZR, Ito N, Brulet R, Tafacory F, Zhang L, Good L, Ure K, Kernie SG, Birnbaum SG, Scharfman HE, Eisch AJ, Hsieh J (2015) Aberrant hippocampal neurogenesis contributes to epilepsy and associated cognitive decline. *Nature communications* 6:6606.
- Christopherson KS, Ullian EM, Stokes CC, Mallowney CE, Hell JW, Agah A, Lawler J, Moshier DF, Bornstein P, Barres BA (2005) Thrombospondins are astrocyte-secreted proteins that promote CNS synaptogenesis. *Cell* 120:421-433.
- Cunningham M, Cho JH, Leung A, Savvidis G, Ahn S, Moon M, Lee PK, Han JJ, Azimi N, Kim KS, Bolshakov VY, Chung S (2014) hPSC-derived maturing GABAergic interneurons ameliorate seizures and abnormal behavior in epileptic mice. *Cell stem cell* 15:559-573.

- Deng W, Saxe MD, Gallina IS, Gage FH (2009) Adult-born hippocampal dentate granule cells undergoing maturation modulate learning and memory in the brain. *The Journal of neuroscience : the official journal of the Society for Neuroscience* 29:13532-13542.
- Dibbens LM et al. (2008) X-linked protocadherin 19 mutations cause female-limited epilepsy and cognitive impairment. *Nature genetics* 40:776-781.
- Ekstrand J, Hellsten J, Tingstrom A (2008) Environmental enrichment, exercise and corticosterone affect endothelial cell proliferation in adult rat hippocampus and prefrontal cortex. *Neurosci Lett* 442:203-207.
- Elmariah SB, Oh EJ, Hughes EG, Balice-Gordon RJ (2005) Astrocytes regulate inhibitory synapse formation via Trk-mediated modulation of postsynaptic GABAA receptors. *The Journal of neuroscience : the official journal of the Society for Neuroscience* 25:3638-3650.
- Emdad L, D'Souza SL, Kothari HP, Qadeer ZA, Germano IM (2012) Efficient differentiation of human embryonic and induced pluripotent stem cells into functional astrocytes. *Stem Cells Dev* 21:404-410.
- Emond MR, Biswas S, Blevins CJ, Jontes JD (2011) A complex of Protocadherin-19 and N-cadherin mediates a novel mechanism of cell adhesion. *The Journal of cell biology* 195:1115-1121.
- Esposito MS, Piatti VC, Laplagne DA, Morgenstern NA, Ferrari CC, Pitossi FJ, Schinder AF (2005) Neuronal differentiation in the adult hippocampus recapitulates embryonic development. *The Journal of neuroscience : the official journal of the Society for Neuroscience* 25:10074-10086.
- Garrett AM, Weiner JA (2009) Control of CNS synapse development by {gamma}-protocadherin-mediated astrocyte-neuron contact. *The Journal of neuroscience : the official journal of the Society for Neuroscience* 29:11723-11731.
- Garrett AM, Schreiner D, Lobas MA, Weiner JA (2012) gamma-protocadherins control cortical dendrite arborization by regulating the activity of a FAK/PKC/MARCKS signaling pathway. *Neuron* 74:269-276.

- Gong C, Wang TW, Huang HS, Parent JM (2007) Reelin regulates neuronal progenitor migration in intact and epileptic hippocampus. *The Journal of neuroscience : the official journal of the Society for Neuroscience* 27:1803-1811.
- Gu Y, Arruda-Carvalho M, Wang J, Janoschka SR, Josselyn SA, Frankland PW, Ge S (2012) Optical controlling reveals time-dependent roles for adult-born dentate granule cells. *Nature neuroscience* 15:1700-1706.
- Haber M, Zhou L, Murai KK (2006) Cooperative astrocyte and dendritic spine dynamics at hippocampal excitatory synapses. *The Journal of neuroscience : the official journal of the Society for Neuroscience* 26:8881-8891.
- Hama H, Hara C, Yamaguchi K, Miyawaki A (2004) PKC signaling mediates global enhancement of excitatory synaptogenesis in neurons triggered by local contact with astrocytes. *Neuron* 41:405-415.
- Hansen DV, Lui JH, Parker PR, Kriegstein AR (2010) Neurogenic radial glia in the outer subventricular zone of human neocortex. *Nature* 464:554-561.
- Heck N, Kilb W, Reiprich P, Kubota H, Furukawa T, Fukuda A, Luhmann HJ (2007) GABA-A receptors regulate neocortical neuronal migration in vitro and in vivo. *Cereb Cortex* 17:138-148.
- Hochbaum DR et al. (2014) All-optical electrophysiology in mammalian neurons using engineered microbial rhodopsins. *Nature methods* 11:825-833.
- Hosford BE, Liska JP, Danzer SC (2016) Ablation of Newly Generated Hippocampal Granule Cells Has Disease-Modifying Effects in Epilepsy. *The Journal of neuroscience : the official journal of the Society for Neuroscience* 36:11013-11023.
- Hughes EG, Elmariah SB, Balice-Gordon RJ (2010) Astrocyte secreted proteins selectively increase hippocampal GABAergic axon length, branching, and synaptogenesis. *Mol Cell Neurosci* 43:136-145.
- Hunt RF, Girskis KM, Rubenstein JL, Alvarez-Buylla A, Baraban SC (2013) GABA progenitors grafted into the adult epileptic brain control seizures and abnormal behavior. *Nature neuroscience* 16:692-697.

- Jakubs K, Nanobashvili A, Bonde S, Ekdahl CT, Kokaia Z, Kokaia M, Lindvall O (2006) Environment matters: synaptic properties of neurons born in the epileptic adult brain develop to reduce excitability. *Neuron* 52:1047-1059.
- Krencik R, Weick JP, Liu Y, Zhang ZJ, Zhang SC (2011) Specification of transplantable astroglial subtypes from human pluripotent stem cells. *Nature biotechnology* 29:528-534.
- Lacar B, Linker SB, Jaeger BN, Krishnaswami S, Barron J, Kelder M, Parylak S, Paquola A, Venepally P, Novotny M, O'Connor C, Fitzpatrick C, Erwin J, Hsu JY, Husband D, McConnell MJ, Lasken R, Gage FH (2016) Nuclear RNA-seq of single neurons reveals molecular signatures of activation. *Nature communications* 7:11022.
- Lancaster MA, Renner M, Martin CA, Wenzel D, Bicknell LS, Hurles ME, Homfray T, Penninger JM, Jackson AP, Knoblich JA (2013) Cerebral organoids model human brain development and microcephaly. *Nature* 501:373-379.
- Laplagne DA, Esposito MS, Piatti VC, Morgenstern NA, Zhao C, van Praag H, Gage FH, Schinder AF (2006) Functional convergence of neurons generated in the developing and adult hippocampus. *PLoS biology* 4:e409.
- Lefebvre JL, Kostadinov D, Chen WV, Maniatis T, Sanes JR (2012) Protocadherins mediate dendritic self-avoidance in the mammalian nervous system. *Nature* 488:517-521.
- Lioy DT, Garg SK, Monaghan CE, Raber J, Foust KD, Kaspar BK, Hirrlinger PG, Kirchhoff F, Bissonnette JM, Ballas N, Mandel G (2011) A role for glia in the progression of Rett's syndrome. *Nature* 475:497-500.
- Liu Y, Liu H, Sauvey C, Yao L, Zarnowska ED, Zhang SC (2013) Directed differentiation of forebrain GABA interneurons from human pluripotent stem cells. *Nature protocols* 8:1670-1679.
- LoTurco JJ, Owens DF, Heath MJ, Davis MB, Kriegstein AR (1995) GABA and glutamate depolarize cortical progenitor cells and inhibit DNA synthesis. *Neuron* 15:1287-1298.
- Lukaszewicz A, Savatier P, Cortay V, Giroud P, Huissoud C, Berland M, Kennedy H, Dehay C (2005) G1 phase regulation, area-specific cell cycle control, and cytoarchitectonics in the primate cortex. *Neuron* 47:353-364.

- Molumby MJ, Keeler AB, Weiner JA (2016) Homophilic Protocadherin Cell-Cell Interactions Promote Dendrite Complexity. *Cell reports* 15:1037-1050.
- Morgan RJ, Soltesz I (2008) Nonrandom connectivity of the epileptic dentate gyrus predicts a major role for neuronal hubs in seizures. *Proceedings of the National Academy of Sciences of the United States of America* 105:6179-6184.
- Morin-Brureau M, Rigau V, Lerner-Natoli M (2012) Why and how to target angiogenesis in focal epilepsies. *Epilepsia* 53 Suppl 6:64-68.
- Nguyen MV, Du F, Felice CA, Shan X, Nigam A, Mandel G, Robinson JK, Ballas N (2012) MeCP2 is critical for maintaining mature neuronal networks and global brain anatomy during late stages of postnatal brain development and in the mature adult brain. *The Journal of neuroscience : the official journal of the Society for Neuroscience* 32:10021-10034.
- Palmer TD, Willhoite AR, Gage FH (2000) Vascular niche for adult hippocampal neurogenesis. *J Comp Neurol* 425:479-494.
- Pasca AM, Sloan SA, Clarke LE, Tian Y, Makinson CD, Huber N, Kim CH, Park JY, O'Rourke NA, Nguyen KD, Smith SJ, Huguenard JR, Geschwind DH, Barres BA, Pasca SP (2015) Functional cortical neurons and astrocytes from human pluripotent stem cells in 3D culture. *Nature methods* 12:671-678.
- Pederick DT, Homan CC, Jaehne EJ, Piltz SG, Haines BP, Baune BT, Jolly LA, Hughes JN, Gecz J, Thomas PQ (2016) Pcdh19 Loss-of-Function Increases Neuronal Migration In Vitro but is Dispensable for Brain Development in Mice. *Sci Rep* 6:26765.
- Peng Z, Zhang N, Wei W, Huang CS, Cetina Y, Otis TS, Houser CR (2013) A reorganized GABAergic circuit in a model of epilepsy: evidence from optogenetic labeling and stimulation of somatostatin interneurons. *The Journal of neuroscience : the official journal of the Society for Neuroscience* 33:14392-14405.
- Pereira AC, Huddlestone DE, Brickman AM, Sosunov AA, Hen R, McKhann GM, Sloan R, Gage FH, Brown TR, Small SA (2007) An in vivo correlate of exercise-induced neurogenesis in the adult dentate gyrus. *Proceedings of the National Academy of Sciences of the United States of America* 104:5638-5643.

- Pfrieger FW, Barres BA (1997) Synaptic efficacy enhanced by glial cells in vitro. *Science* 277:1684-1687.
- Pun RY, Rolle IJ, Lasarge CL, Hosford BE, Rosen JM, Uhl JD, Schmeltzer SN, Faulkner C, Bronson SL, Murphy BL, Richards DA, Holland KD, Danzer SC (2012) Excessive activation of mTOR in postnatally generated granule cells is sufficient to cause epilepsy. *Neuron* 75:1022-1034.
- Qian X et al. (2016) Brain-Region-Specific Organoids Using Mini-bioreactors for Modeling ZIKV Exposure. *Cell*.
- Rancz EA, Franks KM, Schwarz MK, Pichler B, Schaefer AT, Margrie TW (2011) Transfection via whole-cell recording in vivo: bridging single-cell physiology, genetics and connectomics. *Nature neuroscience* 14:527-532.
- Rigau V, Morin M, Rousset MC, de Bock F, Lebrun A, Coubes P, Picot MC, Baldy-Moulinier M, Bockaert J, Crespel A, Lerner-Natoli M (2007) Angiogenesis is associated with blood-brain barrier permeability in temporal lobe epilepsy. *Brain : a journal of neurology* 130:1942-1956.
- Sahay A, Scobie KN, Hill AS, O'Carroll CM, Kheirbek MA, Burghardt NS, Fenton AA, Dranovsky A, Hen R (2011) Increasing adult hippocampal neurogenesis is sufficient to improve pattern separation. *Nature* 472:466-470.
- Schreiner D, Weiner JA (2010) Combinatorial homophilic interaction between gamma-protocadherin multimers greatly expands the molecular diversity of cell adhesion. *Proceedings of the National Academy of Sciences of the United States of America* 107:14893-14898.
- Shaltouki A, Peng J, Liu Q, Rao MS, Zeng X (2013) Efficient generation of astrocytes from human pluripotent stem cells in defined conditions. *Stem cells* 31:941-952.
- Shin J, Berg DA, Zhu Y, Shin JY, Song J, Bonaguidi MA, Enikolopov G, Nauen DW, Christian KM, Ming GL, Song H (2015) Single-Cell RNA-Seq with Waterfall Reveals Molecular Cascades underlying Adult Neurogenesis. *Cell stem cell* 17:360-372.
- Singh SP, LaSarge CL, An A, McAuliffe JJ, Danzer SC (2015) Clonal Analysis of Newborn Hippocampal Dentate Granule Cell Proliferation and Development in Temporal Lobe Epilepsy. *eNeuro* 2.

- Smart IH, Dehay C, Giroud P, Berland M, Kennedy H (2002) Unique morphological features of the proliferative zones and postmitotic compartments of the neural epithelium giving rise to striate and extrastriate cortex in the monkey. *Cereb Cortex* 12:37-53.
- Spalding KL, Bergmann O, Alkass K, Bernard S, Salehpour M, Huttner HB, Bostrom E, Westerlund I, Vial C, Buchholz BA, Possnert G, Mash DC, Druid H, Frisen J (2013) Dynamics of hippocampal neurogenesis in adult humans. *Cell* 153:1219-1227.
- Sun GJ, Zhou Y, Stadel RP, Moss J, Yong JH, Ito S, Kawasaki NK, Phan AT, Oh JH, Modak N, Reed RR, Toni N, Song H, Ming GL (2015) Tangential migration of neuronal precursors of glutamatergic neurons in the adult mammalian brain. *Proceedings of the National Academy of Sciences of the United States of America* 112:9484-9489.
- Swiech L, Heidenreich M, Banerjee A, Habib N, Li Y, Trombetta J, Sur M, Zhang F (2015) In vivo interrogation of gene function in the mammalian brain using CRISPR-Cas9. *Nature biotechnology* 33:102-106.
- Thind KK, Ribak CE, Buckmaster PS (2008) Synaptic input to dentate granule cell basal dendrites in a rat model of temporal lobe epilepsy. *J Comp Neurol* 509:190-202.
- Thind KK, Yamawaki R, Phanwar I, Zhang G, Wen X, Buckmaster PS (2010) Initial loss but later excess of GABAergic synapses with dentate granule cells in a rat model of temporal lobe epilepsy. *J Comp Neurol* 518:647-667.
- Ventura R, Harris KM (1999) Three-dimensional relationships between hippocampal synapses and astrocytes. *The Journal of neuroscience : the official journal of the Society for Neuroscience* 19:6897-6906.
- Wang DD, Kriegstein AR (2008) GABA regulates excitatory synapse formation in the neocortex via NMDA receptor activation. *The Journal of neuroscience : the official journal of the Society for Neuroscience* 28:5547-5558.
- Whitman MC, Fan W, Relu L, Rodriguez-Gil DJ, Greer CA (2009) Blood vessels form a migratory scaffold in the rostral migratory stream. *J Comp Neurol* 516:94-104.
- Wichterle H, Garcia-Verdugo JM, Alvarez-Buylla A (1997) Direct evidence for homotypic, glia-independent neuronal migration. *Neuron* 18:779-791.

- Williams EC, Zhong X, Mohamed A, Li R, Liu Y, Dong Q, Ananiev GE, Mok JC, Lin BR, Lu J, Chiao C, Cherney R, Li H, Zhang SC, Chang Q (2014) Mutant astrocytes differentiated from Rett syndrome patients-specific iPSCs have adverse effects on wild-type neurons. *Human molecular genetics* 23:2968-2980.
- Yoon KJ et al. (2014) Modeling a genetic risk for schizophrenia in iPSCs and mice reveals neural stem cell deficits associated with adherens junctions and polarity. *Cell stem cell* 15:79-91.
- Zeisel A, Munoz-Manchado AB, Codeluppi S, Lonnerberg P, La Manno G, Jureus A, Marques S, Munguba H, He L, Betsholtz C, Rolny C, Castelo-Branco G, Hjerling-Leffler J, Linnarsson S (2015) Brain structure. Cell types in the mouse cortex and hippocampus revealed by single-cell RNA-seq. *Science* 347:1138-1142.
- Zhan RZ, Timofeeva O, Nadler JV (2010) High ratio of synaptic excitation to synaptic inhibition in hilar ectopic granule cells of pilocarpine-treated rats. *Journal of neurophysiology* 104:3293-3304.

Appendix A

Inhibitory Inputs to the Dentate Gyrus from Extra-dentate Hippocampal Regions

Summary

The hippocampus has an extensive inhibitory interneuron network that includes PV and SST interneurons that innervate the perisomatic and dendritic regions of DGCs, respectively. After pilocarpine-induced SE, there is compensatory network sprouting of interneurons that involves the dentate gyrus, CA3 and CA1. We use RV birthdating in conjunction with RbV-mediated retrograde trans-synaptic tracing to delineate how the presynaptic inputs onto adult-born and early-born DGCs differ in the intact and epileptic brain. We found that, after SE, adult-born DGCs are the targets of CA3 PV interneuron sprouting while early-born DGCs are preferentially targeted by CA1 SST interneurons. We also found that, in the intact brain, both interneuron populations in CA3 send backprojections onto adult-born and early-born DGCs, while interneurons in CA1 only synapse onto early-born DGCs. These findings suggest that inhibition of DGCs extends from multiple regions of the hippocampus and that these connections increase after SE, perhaps as a mechanism to compensate for network hyperexcitability.

Introduction

The dentate gyrus is hypothesized to be the 'gate' of the hippocampus by modulating the inputs from the entorhinal cortex in the classic trisynaptic pathway. DGCs are intrinsically difficult to excite due to hyperpolarized membrane potentials and high thresholds for firing (Lothman et al., 1992; Mody et al., 1992) in addition to being the subjects of extensive feedback and feedforward inhibition (Acsady et al., 1998). Most of the inhibition onto DGCs is thought to arise from local inputs in the dentate hilus. Multiple classes of hilar interneurons exist but the most well characterized are the fast-spiking basket cells that express PV as well as the hilar perforant path-associated cells that express SST (Bakst et al., 1986; Sik et al., 1997). Both populations primarily inhibit DGCs with PV interneurons selectively targeting perisomatic regions and the axon initial segments, while SST interneurons synapse primarily onto dendrites. Aside from these local inhibitory inputs, some evidence suggests that interneurons from other regions including CA3 and CA1 also synapse onto DGCs, albeit sparsely (Hajos and Mody, 1997; Szabadics et al., 2010; Lasztocki et al., 2011).

Both human and experimental models of TLE exhibit massive cell death of hilar interneurons (de Lanerolle et al., 1989; Mathern et al., 1995; Houser and Esclapez, 1996). The SST-expressing interneuron population is the most vulnerable (Buckmaster and Jongen-Relo, 1999) while the PV interneurons remains relatively resistant to SE-induced death. Despite this loss, several studies have indicated that, at later time points, the remaining hilar SST interneurons actually sprout axon collaterals that may serve to mitigate excitability in the dentate gyrus (Mathern et al., 1995; Zhang et al., 2009; Thind et al., 2010). Interestingly, Peng et al. showed that SST interneurons in CA1 sprout across

the hippocampal fissure after SE to form functional synapses onto DGCs (Peng et al., 2013).

We utilize the dual-virus tracing strategy relying on RV-birthdating in tandem with RbV mediated retrograde trans-synaptic tracing to identify first-order presynaptic inputs onto DGCs from PV and SST interneurons in the dentate gyrus, CA3 and CA1. We aimed to identify the composition of PV+ and SST+ inputs onto adult- and early-born DGCs and how these inputs changed after SE.

Materials and methods

Viral Production

We generated a RV construct (RV-Syn-GTR) using a vesicular stomatitis virus G-protein (VSV-G) pseudotyped Murine Moloney Leukemia virus-based vector containing a human Synapsin1 promoter driving GFP, TVA and Rgp. Titers ranged from $2-5 \times 10^8$ cfu/mL. EnvA-pseudotyped RbV (RbV-mCh) was produced as described previously (Wickersham et al., 2010; Du et al., 2017) with titers of $2-4 \times 10^5$ cfu/mL used.

Animals and seizure induction

Animal procedures were performed following protocols approved by the Institutional Animal Care and Use Committee of the University of Michigan. Animals were purchased from Charles River and maintained between 20-22°C under a constant 12 h light/dark cycle with access to food and water *ad libitum*. To generate epileptic rats, adult male Sprague Dawley rats at P56 were pretreated with atropine methylbromide (5 mg/kg i.p.; Sigma-Aldrich). After 20 minutes, animals were administered the chemoconvulsant pilocarpine hydrochloride (340 mg/kg, i.p.; Sigma-Aldrich). Seizures were monitored

behaviorally and terminated after 90 minutes of SE with diazepam (10 mg/kg, i.p.; Hospira Inc.). Sham controls received identical treatment except pilocarpine was replaced with an equivalent volume of 0.9% saline.

Intrahippocampal Injections

We injected RV-Syn-GTR bilaterally into the dorsal dentate gyrus at P7 or P60 as previously described (Kron et al., 2010; Althaus et al., 2016) to birthdate early-born or adult-born DGCs, respectively, and render them RbV-competent. Briefly, P7 male Sprague Dawley pups were anesthetized on ice and placed on an ice-cold neonatal rat stereotaxic adapter (Stoelting) in a Kopf stereotaxic frame. Bilateral burr holes were drilled into the skull and 1 μ L of RV-Syn-GTR was injected at a rate of 0.1 μ L/min using a 5 μ L Hamilton syringe with the following coordinates (in mm from bregma and mm below the skull): caudal 2.0, lateral 1.5, depth 2.7. For injections at P60, rats were anesthetized using a Ketamine/Xylazine mixture and placed into a Kopf stereotaxic frame. Bilateral burr holes were drilled into the skull and 2 μ L of RV-Syn-GTR was injected with the following coordinates (in mm from bregma and mm below the skull): caudal 3.9, lateral 2.3, depth 4.2.

At P112-126, RbV-mCh was injected bilaterally into the dorsal dentate gyrus to trace monosynaptic inputs onto RV-Syn-GTR infected DGCs. Animals were anesthetized using a Ketamine/Xylazine mixture. RbV-mCh (2 μ L) was injected at a rate of 0.1 μ L/min at the following coordinates (in mm from bregma and mm below the skull): caudal 4.2, lateral 2.3, depth 4.2.

Immunohistochemistry

On day 7 after RbV-mCh injection, animals were deeply anesthetized with pentobarbital and transcardially perfused with 0.9% saline and 4% paraformaldehyde (PFA). Brains were removed and post-fixed overnight in 4% PFA and cryoprotected with 30% sucrose. Frozen coronal sections (40 μm thickness) were cut in the coronal plane using a sliding microtome. Series' of 12-16 sections (each 480 μm apart) in the rostro-caudal axis of the brain were processed with standard fluorescent immunohistochemical techniques (double- and triple-labeling) using the following primary antibodies: chicken anti-GFP (1:1000, Aves), rabbit (Rb) anti-dsRed (1:1000, Clontech), mouse (Ms) anti-mCherry (1:1000, Clontech), Ms anti-Parvalbumin (PV; 1:400, Sigma), or Rb anti-Somatostatin (SST; 1:500, Peninsula Labs). Secondary antibodies (Alexa Fluor, 1:400 dilution, Invitrogen) used were: goat (Gt) anti-chicken 488, Gt anti-rabbit 594 or 647, and Gt anti-mouse 594 or 647. Nuclear counterstain was performed using bisbenzimidazole.

Microscopy and Image Analysis

Images were acquired using a Leica TCS SP5X upright confocal microscope. For analysis of double-labeling for mCh and PV or SST, images were acquired with a 20x objective at 1.0x optical zoom and 2 μm step size through the z-plane with the pinhole set at 1 Airy unit. Images were imported into Adobe Photoshop CS6 and analyzed for co-localization of immunoreactivity. Quantification was performed on sections spaced 480 μm apart that spanned the rostral-caudal extent of each hippocampus. Within the dentate gyrus, CA3 and CA1, identification of PV and SST interneurons was based on morphology, location and marker labeling. Cells that were both mCh⁺ and marker⁺ but GFP-negative were counted. The data for each region were

then divided by the total number of mCh+/marker+ cells summed from all three regions. Statistical analyses were performed using GraphPad Prism 7 software. Group means were compared with a one-way ANOVA and post-hoc Tukey's multiple comparisons test with the significance level set at $p < 0.05$.

Results

Hippocampal PV-expressing interneurons sprout preferentially onto adult-born DGCs after SE

We traced monosynaptic inputs onto adult-born (P60 injected) and early-born (P7 injected) DGCs in both the intact and epileptic rat brain. We found that local dentate gyrus PV interneuron inputs comprised ~95% and ~79% of the total PV+ inputs onto adult-born and early-born DGCs, respectively, in the intact brains. In the hippocampus proper, there was a trend towards more PV interneuron inputs from CA3 and CA1 onto early-born DGCs than adult-born DGCs (**Figure A.1A, C, E**). While these results did not reach statistical significance, we found adult-born DGCs received <1% of inputs from CA1 PV interneurons compared with ~8% in early-born DGCs. Furthermore, adult-born DGCs receive ~5% of PV interneuron inputs from CA3 versus ~13% for early-born DGCs. After SE, however, we found that extra-dentate PV interneurons sprout preferentially onto adult-born DGCs as manifested by an increase in composition from ~5% to ~20% from CA3 PV interneurons and <1% to ~14% from CA1 PV interneurons (**Figure A.1A, B, E**). No changes appeared in hippocampal PV+ inputs onto early-born DGCs after SE (**Figure A.1C, D, E**).

Hippocampal SST-expressing interneurons target early-born DGCs after SE

We next explored monosynaptic connections from SST interneurons onto birthdated DGCs in the intact and epileptic brain. In controls, we found that local dentate gyrus SST+ inputs constituted similar amounts of total SST+ inputs onto adult-born DGCs (~90%) and early-born DGCs (~84%). Furthermore, similar amounts of axonal backprojections from CA3 SST interneurons onto both populations were seen (**Figure A.2A, C, E**). Additionally, early-born DGCs received a small amount of SST+ inputs (~5%) from CA1 SST interneurons (**Figure A.2C**). After SE, there was significant sprouting from CA1 SST interneurons preferentially onto early-born DGCs as compared with all cohorts with a compositional increase from ~5% to ~31% of all SST+ inputs (**Figure A.2B, D, E**) onto this age-defined cohort. In contrast, CA1 SST interneurons that synapsed onto adult-born DGCs after SE were sparser and not statistically significant (**Figure A.2B**), making up approximately 7% of the total SST inputs. No apparent differences in CA3 SST+ inputs onto either population were observed after SE.

Discussion

We combined RV-birthdating with RbV-mediated retrograde trans-synaptic tracing to assess the hippocampal inhibitory network innervating age-defined cohorts of DGCs and how it changes after SE. In the intact brain, we found that PV interneurons from the dentate gyrus and CA3 constitute ~95% and 5%, respectively, of all the PV+ inputs onto adult-born DGCs. Meanwhile, early-born DGCs receive ~79%, 13% and 8% of their PV+ inputs from dentate hilus, CA3 and CA1, respectively. Additionally, SST interneurons in the dentate hilus and CA3 contribute 90% and 10% of the total SST+ inputs to adult-born DGCs. Early-born DGCs receive ~84%, 11% and 5% of their total SST+ inputs from

dentate hilus, CA3 and CA1, respectively. Our findings suggest that interneurons from extra-dentate regions play a greater role in inhibiting DGCs under basal conditions than previously appreciated. Our results demonstrate that an epileptogenic insult significantly alters some of these inhibitory inputs, and that the changes differentially affect early-versus adult-born DGCs. After SE, PV interneurons from CA3 preferentially backproject onto adult-born DGCs while CA1 SST interneurons target early-born DGCs. While it is well-accepted that the inhibitory interneurons in the dentate hilus are capable of significant remodeling, this study suggests that other hippocampal regions are also extensively involved.

The PV-expressing cells are a major class of hippocampal interneurons and represent up to 30 percent of the GABAergic population in stratum oriens of CA3 and CA1 and up to 20 percent of the dentate hilar interneuron population (Freund and Buzsaki, 1996). This population is relatively resistant to seizure-induced death (Sloviter, 1987, 1989) in contrast to the SST population. We describe an increase in sprouting from CA3 and CA1 PV interneurons onto adult-born DGCs after SE. It is possible these changes represent a compensatory mechanism to replace the loss of dentate gyrus PV+ inputs onto adult-born DGCs after SE, which we describe in Chapter 2 of this dissertation (Du et al., in press).

Several reports suggest that, despite their initial loss, SST interneurons in the hippocampus hypertrophy and sprout after SE (Zhang et al., 2009; Thind et al., 2010; Peng et al., 2013). We show that SST interneurons in CA1 preferentially target early-born DGCs after SE with some minor synapses onto adult-born DGCs as well. One potential explanation for why these changes arise is that they serve as a means of homeostatic

network compensation, with targeting of early-born DGCs from CA1 as a way to balance the major loss of dentate hilar SST+ inputs onto early-born DGCs (as described in Chapter 2 of this dissertation). Because adult-born DGCs after SE actually have increased inputs from SST interneurons in the dentate hilus, they are not targeted for this inhibitory synaptic reorganization. The other form of SE-induced remodeling that may stimulate CA1 SST interneuron sprouting onto early-born DGCs is CA1 pyramidal cell sprouting onto this population (See Chapter 2 and Du et al., in press). Taken together, these results and the PV findings suggest that the epileptic hippocampus attempts to re-balance the loss of inhibition/increased excitation onto specific cell populations by increasing inhibitory sprouting from different regions. Nonetheless, there appear to be limits in the total inhibition that a cell can receive as demonstrated by differential sprouting from different regions onto birthdated populations. This notion is supported by evidence from interneuron transplantation studies where, once a threshold number of transplanted cells is reached, inhibition plateaus and becomes insensitive to increasing numbers of cells (Southwell et al., 2010).

The finding of substantial feedback inhibition of DGCs from the hippocampus proper has implications for understanding information processing in the hippocampal formation and mechanisms of learning and memory. Further studies should be aimed at delineating the behavior of additional inhibitory interneuron subtypes in the hippocampus and how they differentially respond to SE-induced plasticity. Future work will also need to address the functional status of novel inhibitory synapses generated after SE. Understanding the hippocampal inhibitory network is critical for elucidating mechanisms underlying the development of TLE. Strategies to fine tune the nature and timing of

interneuron axonal sprouting may lead to therapies that control or even prevent the onset of seizures.

References

- Acsady L, Kamondi A, Sik A, Freund T, Buzsaki G (1998) GABAergic cells are the major postsynaptic targets of mossy fibers in the rat hippocampus. *The Journal of neuroscience : the official journal of the Society for Neuroscience* 18:3386-3403.
- Althaus AL, Zhang H, Parent JM (2016) Axonal plasticity of age-defined dentate granule cells in a rat model of mesial temporal lobe epilepsy. *Neurobiology of disease* 86:187-196.
- Bakst I, Avendano C, Morrison JH, Amaral DG (1986) An experimental analysis of the origins of somatostatin-like immunoreactivity in the dentate gyrus of the rat. *The Journal of neuroscience : the official journal of the Society for Neuroscience* 6:1452-1462.
- Buckmaster PS, Jongen-Relo AL (1999) Highly specific neuron loss preserves lateral inhibitory circuits in the dentate gyrus of kainate-induced epileptic rats. *The Journal of neuroscience : the official journal of the Society for Neuroscience* 19:9519-9529.
- de Lanerolle NC, Kim JH, Robbins RJ, Spencer DD (1989) Hippocampal interneuron loss and plasticity in human temporal lobe epilepsy. *Brain Res* 495:387-395.
- Freund TF, Buzsaki G (1996) Interneurons of the hippocampus. *Hippocampus* 6:347-470.
- Hajos N, Mody I (1997) Synaptic communication among hippocampal interneurons: properties of spontaneous IPSCs in morphologically identified cells. *The Journal of neuroscience : the official journal of the Society for Neuroscience* 17:8427-8442.
- Houser CR, Esclapez M (1996) Vulnerability and plasticity of the GABA system in the pilocarpine model of spontaneous recurrent seizures. *Epilepsy Res* 26:207-218.
- Kron MM, Zhang H, Parent JM (2010) The developmental stage of dentate granule cells dictates their contribution to seizure-induced plasticity. *The Journal of neuroscience : the official journal of the Society for Neuroscience* 30:2051-2059.
- Lasztocki B, Tukker JJ, Somogyi P, Klausberger T (2011) Terminal field and firing selectivity of cholecystokinin-expressing interneurons in the hippocampal CA3 area. *The Journal of neuroscience : the official journal of the Society for Neuroscience* 31:18073-18093.
- Lothman EW, Stringer JL, Bertram EH (1992) The dentate gyrus as a control point for seizures in the hippocampus and beyond. *Epilepsy Res Suppl* 7:301-313.
- Mathern GW, Babb TL, Pretorius JK, Leite JP (1995) Reactive synaptogenesis and neuron densities for neuropeptide Y, somatostatin, and glutamate decarboxylase immunoreactivity in the epileptogenic human fascia dentata. *The Journal of neuroscience : the official journal of the Society for Neuroscience* 15:3990-4004.

- Mody I, Kohr G, Otis TS, Staley KJ (1992) The electrophysiology of dentate gyrus granule cells in whole-cell recordings. *Epilepsy Res Suppl* 7:159-168.
- Peng Z, Zhang N, Wei W, Huang CS, Cetina Y, Otis TS, Houser CR (2013) A reorganized GABAergic circuit in a model of epilepsy: evidence from optogenetic labeling and stimulation of somatostatin interneurons. *The Journal of neuroscience : the official journal of the Society for Neuroscience* 33:14392-14405.
- Sik A, Penttonen M, Buzsaki G (1997) Interneurons in the hippocampal dentate gyrus: an in vivo intracellular study. *Eur J Neurosci* 9:573-588.
- Sloviter RS (1987) Decreased hippocampal inhibition and a selective loss of interneurons in experimental epilepsy. *Science* 235:73-76.
- Sloviter RS (1989) Calcium-binding protein (calbindin-D28k) and parvalbumin immunocytochemistry: localization in the rat hippocampus with specific reference to the selective vulnerability of hippocampal neurons to seizure activity. *J Comp Neurol* 280:183-196.
- Southwell DG, Froemke RC, Alvarez-Buylla A, Stryker MP, Gandhi SP (2010) Cortical plasticity induced by inhibitory neuron transplantation. *Science* 327:1145-1148.
- Szabadics J, Varga C, Brunner J, Chen K, Soltesz I (2010) Granule cells in the CA3 area. *The Journal of neuroscience : the official journal of the Society for Neuroscience* 30:8296-8307.
- Thind KK, Yamawaki R, Phanwar I, Zhang G, Wen X, Buckmaster PS (2010) Initial loss but later excess of GABAergic synapses with dentate granule cells in a rat model of temporal lobe epilepsy. *J Comp Neurol* 518:647-667.
- Wickersham IR, Sullivan HA, Seung HS (2010) Production of glycoprotein-deleted rabies viruses for monosynaptic tracing and high-level gene expression in neurons. *Nature protocols* 5:595-606.
- Zhang W, Yamawaki R, Wen X, Uhl J, Diaz J, Prince DA, Buckmaster PS (2009) Surviving hilar somatostatin interneurons enlarge, sprout axons, and form new synapses with granule cells in a mouse model of temporal lobe epilepsy. *The Journal of neuroscience : the official journal of the Society for Neuroscience* 29:14247-14256.

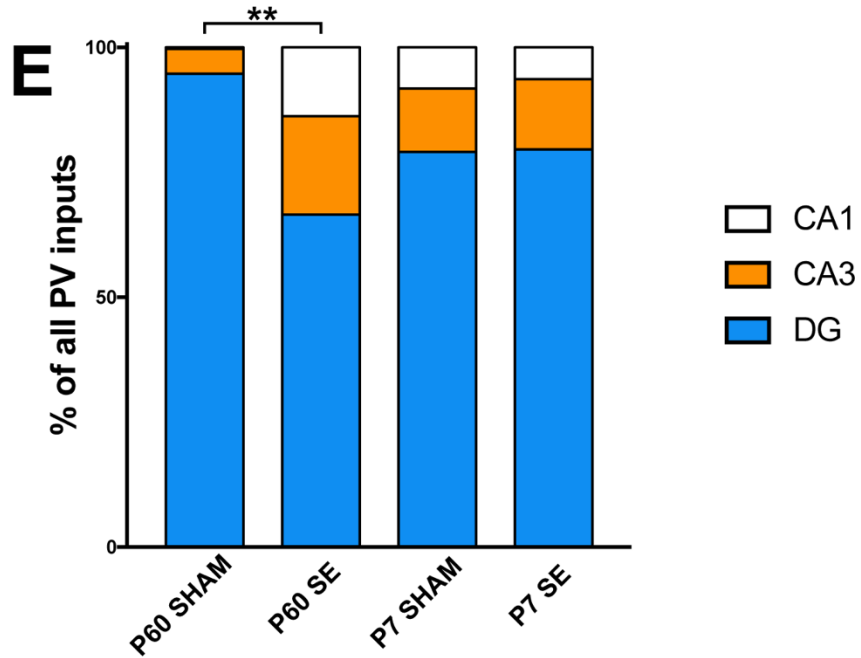
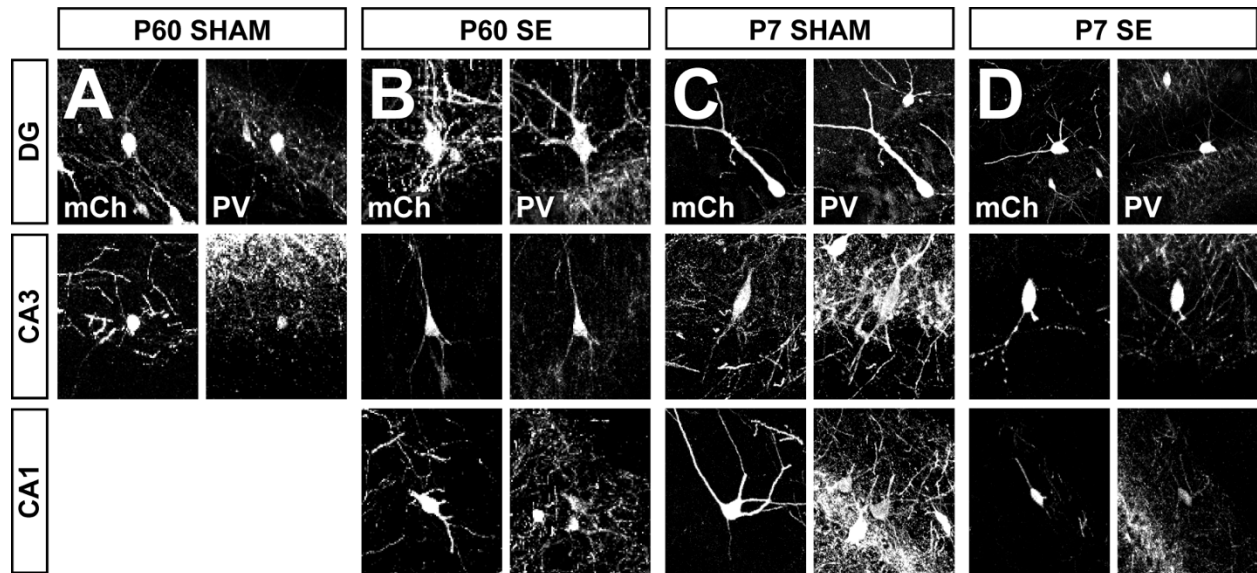


Figure A.1. Hippocampal PV-expressing interneuron inputs onto birthdated DGCs in the intact and epileptic brain.

(A-D) Representative images from the dentate gyrus (DG), CA3 and CA1 in all four cohorts showing mCh⁺ presynaptic inputs that are also PV⁺. (E) Quantification of the percentage composition of PV interneurons that arise from CA1, CA3 or DG and are monosynaptically connected onto starter cells in each of the 4 cohorts (n = 5-6 animals per group; **p<0.01, one-way ANOVA with Tukey's post-hoc test).

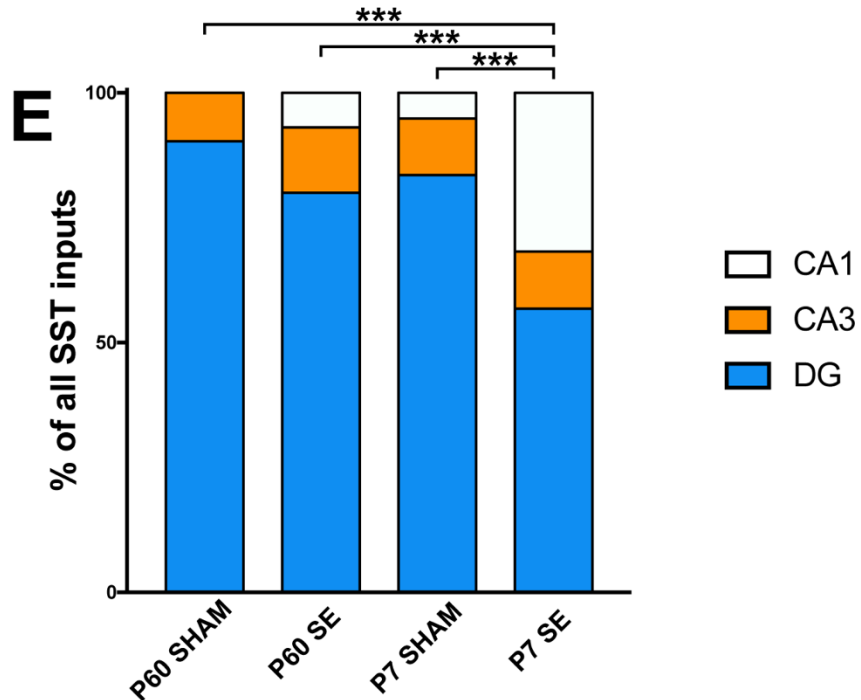
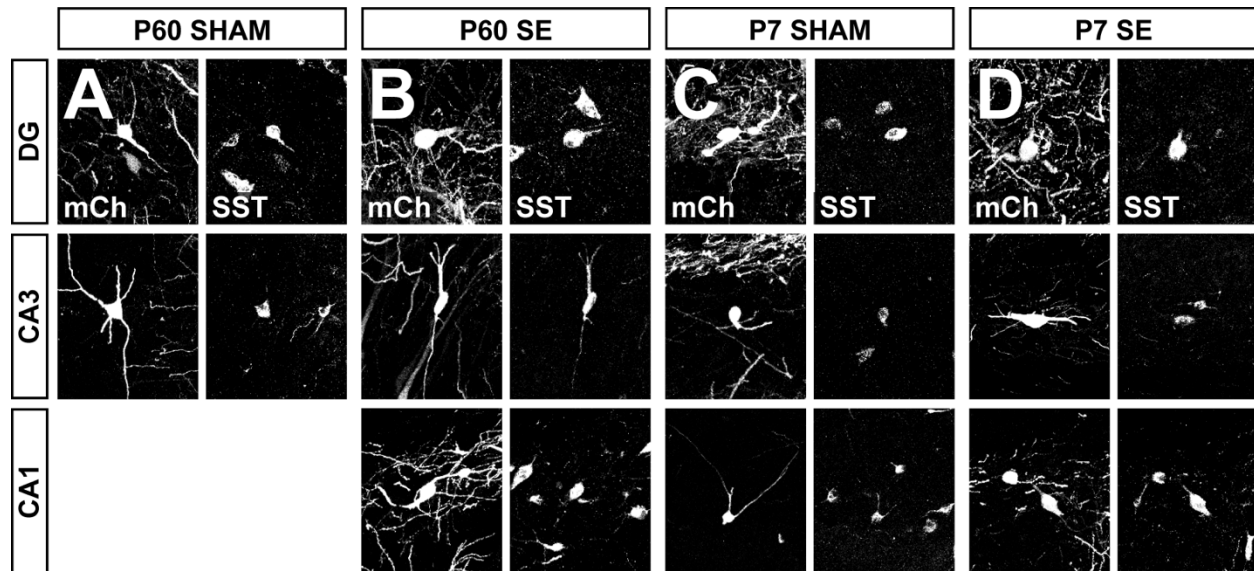


Figure A.2. Hippocampal SST-expressing interneuron inputs onto age-defined populations of DGCs in the intact and epileptic brain.

(A-D) Representative confocal images of mCh+/SST+ cells in the dentate gyrus (DG), CA3 and CA1 that synapse onto age-defined populations of DGCs in the epileptic and intact brains. (E) Quantitative analysis of the percentage of SST interneurons from CA1, CA3 and DG that make up the entire composition of SST+ inputs onto adult-born or early-born DGCs in epileptic or control brains. (n = 5-6 animals per group; ***p<0.001, one-way ANOVA with Tukey's post-hoc test).

Appendix B

Forebrain Organoids as a Model for Neural Development

Summary

Human brain development exhibits many unique features such as an expanded oSVZ as well as inside-out development that are difficult to model in monolayer cultures. The use of 3D cerebral organoids provides a powerful platform for understanding disorders that may affect cortical development, such as the genetic epilepsies. We compare two different strategies for generating cerebral or forebrain organoids. One strategy, termed the intrinsic protocol, does not utilize external morphogenic cues and favors self-patterning to develop multiple regions of the brain. The second strategy introduces patterning factors to direct the organoids towards a forebrain fate that generates dorsal and some ventral cell types. Our results demonstrate that the forebrain organoids are much more organized and have laminated cortical regions with the presence of oRGs. These results suggest that forebrain organoids may be more suited for studying disorders that affect cortical development and may have broad utility for understanding disease mechanisms and testing potential precision therapies.

Introduction

Recent advances in 3D culture technology hold great promise for understanding neural development in an anatomically relevant manner that more closely resembles tissue organization found *in vivo*. Organoids take advantage of the intrinsic property of pluripotent stem cells to self-organize into 3D aggregates when allowed to grow in suspension (Eiraku et al., 2008; Eiraku et al., 2011). Recently, Lancaster et al. pioneered the cerebral organoid, the first 3D structure derived from human iPSCs that resembled parts of the developing brain (Lancaster et al., 2013). The technique takes advantage of a spinning bioreactor that promotes expansion of the tissue in a manner that was previously unachievable. Since then, the field began to establish more region-specific 3D neural cultures to model human brain development and disorders (Mariani et al., 2012; Kadoshima et al., 2013; Mariani et al., 2015; Pasca et al., 2015; Qian et al., 2016). In an effort to improve upon the original cerebral organoid strategy both in scalability and the ability to form more organized structures, Qian et al. used 3D printing technology to design SpinΩ, a 12-well spinning culture that allowed for more organoid growths conditions to be tested in parallel. In addition, the group developed a new protocol that generated forebrain-specific organoid structures that expressed markers for all six cortical layers and showed gene expression patterns resembling that of late second trimester to early third trimester human fetal tissue for certain cortical regions (Qian et al., 2016).

Several studies have already emerged employing organoids to model various diseases of human neural development such as microcephaly (Lancaster et al., 2013), lissencephaly (Bershteyn et al., 2017), mTORopathy (Li et al., 2016), ASD (Mariani et al., 2015) and Zika virus infection (Cugola et al., 2016; Garcez et al., 2016; Wells et al., 2016;

Gabriel et al., 2017). To study genetic epilepsies, organoids hold great promise for expanding our current knowledge of neural development beyond what we have garnered from 2D cultures. For greater understanding of endogenous features of the human brain such as cortical lamination, more complex cellular diversity and cell-cell interactions in 3D spatial orientation, studies using organoids are critical. To this end, we compared the organization and structural integrity of the intrinsic protocol (Lancaster et al., 2013) and the forebrain organoid protocol (Qian et al., 2016). We found that the intrinsic protocol generated cell types of the entire brain but in a disorganized, heterogeneous manner. In contrast, the forebrain organoids were much more consistent and organized with laminated structures resembling human cortical development.

Materials and methods

Reprogramming and culturing iPSCs

Fibroblasts from PCDH19 FLE patients and a control female were reprogrammed as described in Chapter 3 of this dissertation. Briefly, fibroblasts were electroporated with 1 µg of episomal expression plasmids (pCXLE-hOCT3/4-p53 shRNA, pCXLE-hUL and pCXLE-hSK) and maintained in TeSR-E7 reprogramming media. iPSC colonies were manually isolated 3 weeks later and maintained in TeSR-E8 on feeder-free Matrigel-coated plates.

Generation of cerebral organoids using the intrinsic protocol

Cerebral organoids were generated according to a previously described protocol (Lancaster and Knoblich, 2014). We formed embryoid bodies (EBs) in pluripotent stem cell medium (PSCM) containing DMEM/F12, 20% Knockout serum replacement (KOSR),

1× MEM NEAA, 1× GlutaMAX, 1× BME and 4 ng/mL FGF2 until they reach 500-600 µm in diameter, typically 5-6 days. The EBs were then transferred into an N2 organoid neural induction medium containing DMEM/F12, 1× N2, 1× MEM NEAA, 1× GlutaMAX and 1 µg/mL heparin until their edges show radial organization indicating neuroectodermal differentiation, typically 4-5 days. We then embedded these neuroepithelial aggregates into 3D Matrigel droplets and cultured them in cerebral organoid differentiation medium (CODM) containing a 1:1 mixture of DMEM/F12 and Neurobasal media with 1× N2, 1× GlutaMAX, 50 U/mL P/S, 5 µg/mL insulin, 1× BME and 1× B27 without vitamin A. Within approximately 24 hours, the neuroepithelial tissue began budding within the Matrigel structure and contained fluid-filled cavities. After 4 days of growth in static culture with media changes every 48 hours, the embedded primitive organoids were transferred into CODM with vitamin A in a 125-mL spinning flask. The flask was spun at 85 rpm in a 37°C incubator with media changes once per week.

Generation of forebrain organoids using SpinΩ

Forebrain organoids were generated according to the Song lab protocol (Qian et al., 2016). EBs were formed in Aggrewell 800 plates (STEMCELL Technologies) in PSCM. On the following day, EBs were transferred into ultra-low attachment flasks in Dorsomorphin/A83 media containing DMEM/F12, 20% KOSR, 1× GlutaMAX, 1× MEM NEAA, 1× BME, 2 µM Dorsomorphin and 2 µM A-83 (Tocris Biosciences). Media was changed every other day and after 4 days, media was gradually replaced with CHIR99021/SB431542 (CS) induction media containing DMEM/F12, 1× N2, 1× GlutaMAX, 1× NEAA, 50 U/mL P/S, 10 µg/mL heparin, 1 µM CHIR99021 (Tocris Biosciences) and 1 µM SB431542. On day 7, EBs were embedded in Matrigel and

maintained in CS induction media for another 7 days with media changes every other day. On day 14, organoids were lightly triturated to dissociate them from the Matrigel and then transferred into SpinΩ in differentiation media (DM) containing DMEM/F12, 1× N2, 1× MEM NEAA, 1× GlutaMAX, 50 U/mL P/S, 1× BME, 2.5 µg/mL insulin and 1× B27 without vitamin A. Media was changed every other day. On day 28, vitamin A was added to the media. On day 71, organoid media was changed to maturation media which contained Neurobasal, 1× B27, 1× GlutaMAX, 50 U/mL P/S, 20 ng/mL BDNF, 20 ng/mL GDNF, 1 ng/mL transforming growth factor-β (TGF-β; Peprotech), 0.2 mM ascorbic acid (Sigma) and 0.5 mL dbcAMP.

Organoid processing and immunocytochemistry

Whole organoids were washed once with PBS and fixed in 4% PFA for 30 minutes at room temperature. Organoids were then washed 3 times with PBS and incubated in 30% sucrose at 4°C overnight. The next day, organoids were washed twice in PBS and then embedded in Tissue-Tek optimum cutting temperature (O.C.T.) (Sakura Finetek) and sectioned at 20 µM thickness in a freezing cryostat. Organoid sections were immunostained with standard fluorescent ICC techniques as described in Chapter 3. The following primary antibodies were used: rabbit (Rb) anti-Pax6 (1:300, Covance), rat anti-CTIP2 (1:300, Abcam), mouse (Ms) anti-SATB2 (1:100, Abcam), Ms anti-TUJ1 (1:2000, Covance), Rb anti-GABA (1:2000, Sigma),), Ms anti-MAP2ab (1:500, Sigma) and Rb anti-HOPX (1:500, Sigma). Secondary antibodies (Alexa Fluor, 1:400 dilution, Invitrogen) used were: Gt anti-rat 488, Donkey anti-goat 488, Gt anti-rabbit 488, 594 or 647, Gt anti-mouse 488, 594 or 647. Nuclear counterstain was performed using bisbenzimidazole.

Preparation of acute organoid slices for whole-cell sodium and potassium current recordings

Fresh organoid slices were prepared as modified from (Brackenbury et al., 2013). Organoids at 90 days old were immersed in oxygenated “slicing” solution saturated with 95% O₂/5% CO₂. The slicing solution contained the following (in mM): 110 sucrose; 62.5 NaCl; 2.5 KCl; 4 MgCl₂; 1.25 KH₂PO₄; 26 NaHCO₃; 0.5 CaCl₂ and 20 D-glucose (pH 7.35–7.4 when saturated with 95% O₂/5% CO₂ at 4°C). Organoids were then embedded in 4% Type-1B low melt agarose prepared with slice solution and 200 µm thick slices were cut on a VF-300 Compressstome. Slices were collected and incubated in a custom chamber filled with 95% O₂/5% CO₂ saturated slice solution for 30 minutes at room temperature (22–25°C). Slices were then transferred to artificial cerebrospinal fluid (ACSF) consisting of the following (in mM): 125 NaCl; 2.5 KCl; 1 MgCl₂; 1.25 KH₂PO₄; 26 NaHCO₃; 2 CaCl₂, and 25 D-glucose (pH 7.35–7.4), aerated continuously with 95% O₂/5% CO₂ at room temperature for at least 30 minutes before recording.

Whole-cell patch-clamp recording of sodium and potassium currents

Individual organoid slices were transferred to a submersion recording chamber and mechanically fixed using a U-shaped anchor made of a platinum wire frame with nylon mesh. Slices were superfused (2–4 mL/min) continuously with oxygenated ACSF. Cells were visualized with a Nikon A1R confocal microscope equipped with infrared differential interference contrast optics using a 40× water immersion objective. Recording electrodes had a resistance of 3–6 MΩ when filled with pipette solution containing (in mM): 140 K-gluconate; 4 NaCl; 0.5 CaCl₂; 10 Hepes; 5 EGTA; 2 Mg-ATP; and 0.4 GTP (pH 7.3 adjusted with KOH). Signals were filtered at 10 kHz and digitized at 20 kHz for offline

analysis using pClamp10 software. Inward and outward currents were elicited with voltage steps from a -120 mV holding potential to test pulses in 5-10 step increments to a maximum of +40 mV.

Preparation of acute organoid sections for action potential recordings

All recordings were performed with 300 μm thick slices taken from 80 day old organoids. Individual organoids were mounted on an agar block, immersed in the ice-cold Hibernate-A media (BrainBits, LLC) and sliced on a VT-1200S vibratome (Leica). 1-3 slices per organoid were taken, depending on the organoid size. Slices were then stored in the refrigerator at 4°C in fresh Hibernate-A for up to 8 hours.

Whole-cell and cell-attached action potential recordings

Slices were transferred to the recording chamber containing Hibernate-A at room temperature and mounted on an upright microscope. Slices were visualized using a differential contrast light microscopy. Targeted whole-cell and cell-attached recordings were performed using appropriate internal solutions and 3-5 M Ω or 1-2 M Ω glass pipettes, respectively. Whole-cell recording of passive properties including input resistance, series resistance and cell capacitance, were measured under voltage-clamp mode. Single action potentials were then evoked in current-clamp mode by a brief depolarizing current injection. Cell-attached mode was used to monitor spontaneous action potential firing. Data were acquired at 20 kHz using Clampex software (Molecular Devices, LLC) and a Multiclamp 700B amplifier (Molecular Devices, LLC), digitized with Digidata 1440A (Molecular Devices, LLC) and filtered at 5 kHz.

Results

We first generated cerebral organoids using the intrinsic protocol (Lancaster et al., 2013; Lancaster and Knoblich, 2014) in a large spinning bioreactor flask. We found that 2-month-old organoids were able to reach sizes as large as 4 mm in diameter (**Figure B.1A**) and we could identify scattered areas of PAX6⁺ neural progenitors surrounding a ventricular-like lumen (VL) with numerous TUJ1⁺ immature neurons in a cortical mantle-like structure (**Figure B.1C**). Organoids at 4 months age were disorganized with various PAX6⁺ progenitor regions and TUJ1⁺ neurons scattered throughout (**Figure B.1B**). There were also several areas of unidentifiable cell types. Additionally, we found various regions of mature neurons as shown by MAP2ab⁺ immunostaining (**Figure B.1D**) as well as some areas with CTIP2⁺ and SATB2⁺ putative deep and superficial laminar cortical regions, respectively (**Figure B.1E-E''**). We also performed whole-cell patch clamp recordings to assess whether neurons in the organoids were functionally active. We found that neurons near the “cortical surface” of the organoids displayed sodium and potassium currents (**Figure B.1F**) and fired action potentials (albeit of an immature quality) in both whole-cell (**Figure B.1G**) and cell-attached (**Figure B.1H**) configurations. The formation of neural progenitor zones, cells expressing markers of deep and superficial cortical projection neurons, and presence of functionally active neurons were positive aspects of this organoid method. However, the overall disorganization (**Figure B.1B**) and lack of batch-to-batch consistency (data not shown) led us to seek a better approach.

We next tested a different 3D culture technique by building our own SpinΩ system and employing it to generate forebrain organoids (Qian et al., 2016). At approximately 8 weeks, SpinΩ forebrain organoids were much more organized structurally with PAX6⁺ ventricular zone-like regions on the inside of the organoid that were surrounded by TUJ1⁺

immature neurons resembling the developing human cortex (**Figure B.2C**). We found that the vast majority of the mature neurons in the forebrain organoids were cortical as manifested by CTIP2+ and SATB2+ immunostaining (**Figure B.2A**). Upon closer examination of the cortical-like regions, we observed that they included CTIP2+ deep layer neurons with SATB2+ upper layer neurons (**Figure B.2B**) surrounding the ventricular zone-like areas. We also found that forebrain organoids included some ventral cell types such as GABAergic cells (**Figure B.2D**). Additionally, immunolabeling for HOPX, a marker of oRGs, demonstrated that organoids had regions of HOPX+ cells on the outside of the ventricular-like regions that resembled the oSVZ in human development (**Figure B.2E, F**). Overall, the Spin Ω method more consistently generated well-organized progenitor zones and cortical-like regions than the intrinsic protocol.

Discussion

We used two different, well-established protocols to generate cerebral organoids and forebrain organoids. The intrinsic protocol does not rely on patterning factors which theoretically allows for generation of multiple brain regions and diverse cell populations. In contrast, the Spin Ω organoid protocol utilizes dual SMAD inhibition in combination with a Wnt agonist to induce early forebrain patterning events. We found that the intrinsic protocol generated organoids that were somewhat more disorganized with erratic locations of ventricular zones and neurons and areas of unidentifiable cell types. Furthermore, these organoids had cortical-like regions that contained neurons that expressed cortical markers but their appearance was sporadic and often did not appear next to any ventricular-like areas. In contrast, forebrain organoids generated using Spin Ω created structures with organized ventricular zones that included a HOPX+ oSVZ.

Surrounding these ventricular-like zones were CTIP2+ and SATB2+ deep layer and upper layer neurons, respectively. We also found GABA+ neurons scattered throughout the organoids suggesting that these organoids included components of both the dorsal and ventral forebrain. Longer culture duration than we used are necessary to develop the full complement of cortical laminae and this is one of the next steps necessary to confirm the utility of the Spin Ω approach.

Forebrain organoids appear to be more broadly applicable for studying genetic epilepsies such as PCDH19 FLE where there is evidence from patient studies that the cerebral cortex is involved. Using this approach, we would compare patient organoids with control organoids to assess for morphological changes to the cortical mantle region such as differences in the thickness of the cortical neuronal layer and the types of cortical layers that are formed. While the organoids shown here had not been cultured for a long enough period of time to have upper layer neurons that express markers such as cut-like homeobox 1 (CUX1) and brain-specific homeobox protein 2 (BRN2), we would expect them to appear around 84 days. We would also assess the ventricular region to determine if there are changes in the composition and cellular dynamics of the neural progenitors both in the VZ as well as the inner SVZ (iSVZ) and oSVZ.

It remains unclear how the circuitry and connectivity within the forebrain organoids develop and whether they can recapitulate the physiological features of the human brain. One critical challenge is to generate mature organoids as all the current protocols lack the ability to overcome the hypoxia and nutrient depletion that occurs in the center of the structures as their sizes increase. Another reason for their immaturity is the lack of important cell types such as vascular cells, oligodendrocytes and microglia that are critical

for the normal development of the human brain. Future directions should include generating chimeric structures where multiple organoids are patterned towards different cell fates and then fused together to promote migration and integration of different cell types.

It is already possible to generate large quantities of forebrain organoids using SpinΩ for higher throughput applications. When used in combination with sophisticated technologies such as MEA recordings and all-optical electrophysiology (Hochbaum et al., 2014), it is possible to generate an enormous wealth of data to develop targeted next-generation therapeutics.

Notes to Appendix B

Jacob M. Hull and Lori Isom performed the whole-cell sodium and potassium current recordings. Kasia Glanowska performed the whole-cell and cell-attached action potential recordings. Louis Dang provided technical assistance with assembling and troubleshooting the Spin Ω platform.

References

- Bershteyn M, Nowakowski TJ, Pollen AA, Di Lullo E, Nene A, Wynshaw-Boris A, Kriegstein AR (2017) Human iPSC-Derived Cerebral Organoids Model Cellular Features of Lissencephaly and Reveal Prolonged Mitosis of Outer Radial Glia. *Cell stem cell*.
- Brackenbury WJ, Yuan Y, O'Malley HA, Parent JM, Isom LL (2013) Abnormal neuronal patterning occurs during early postnatal brain development of *Scn1b*-null mice and precedes hyperexcitability. *Proceedings of the National Academy of Sciences of the United States of America* 110:1089-1094.
- Cugola FR et al. (2016) The Brazilian Zika virus strain causes birth defects in experimental models. *Nature* 534:267-271.
- Eiraku M, Takata N, Ishibashi H, Kawada M, Sakakura E, Okuda S, Sekiguchi K, Adachi T, Sasai Y (2011) Self-organizing optic-cup morphogenesis in three-dimensional culture. *Nature* 472:51-56.
- Eiraku M, Watanabe K, Matsuo-Takasaki M, Kawada M, Yonemura S, Matsumura M, Wataya T, Nishiyama A, Muguruma K, Sasai Y (2008) Self-organized formation of polarized cortical tissues from ESCs and its active manipulation by extrinsic signals. *Cell stem cell* 3:519-532.
- Gabriel E et al. (2017) Recent Zika Virus Isolates Induce Premature Differentiation of Neural Progenitors in Human Brain Organoids. *Cell stem cell*.
- Garcez PP, Loiola EC, Madeiro da Costa R, Higa LM, Trindade P, Delvecchio R, Nascimento JM, Brindeiro R, Tanuri A, Rehen SK (2016) Zika virus impairs growth in human neurospheres and brain organoids. *Science* 352:816-818.
- Hochbaum DR et al. (2014) All-optical electrophysiology in mammalian neurons using engineered microbial rhodopsins. *Nature methods* 11:825-833.
- Kadoshima T, Sakaguchi H, Nakano T, Soen M, Ando S, Eiraku M, Sasai Y (2013) Self-organization of axial polarity, inside-out layer pattern, and species-specific progenitor dynamics in human ES cell-derived neocortex. *Proceedings of the National Academy of Sciences of the United States of America* 110:20284-20289.
- Lancaster MA, Knoblich JA (2014) Generation of cerebral organoids from human pluripotent stem cells. *Nature protocols* 9:2329-2340.
- Lancaster MA, Renner M, Martin CA, Wenzel D, Bicknell LS, Hurles ME, Homfray T, Penninger JM, Jackson AP, Knoblich JA (2013) Cerebral organoids model human brain development and microcephaly. *Nature* 501:373-379.

- Li Y, Muffat J, Omer A, Bosch I, Lancaster MA, Sur M, Gehrke L, Knoblich JA, Jaenisch R (2016) Induction of Expansion and Folding in Human Cerebral Organoids. *Cell stem cell*.
- Mariani J, Simonini MV, Palejev D, Tomasini L, Coppola G, Szekely AM, Horvath TL, Vaccarino FM (2012) Modeling human cortical development in vitro using induced pluripotent stem cells. *Proceedings of the National Academy of Sciences of the United States of America* 109:12770-12775.
- Mariani J, Coppola G, Zhang P, Abyzov A, Provini L, Tomasini L, Amenduni M, Szekely A, Palejev D, Wilson M, Gerstein M, Grigorenko EL, Chawarska K, Pelphrey KA, Howe JR, Vaccarino FM (2015) FOXP1-Dependent Dysregulation of GABA/Glutamate Neuron Differentiation in Autism Spectrum Disorders. *Cell* 162:375-390.
- Pasca AM, Sloan SA, Clarke LE, Tian Y, Makinson CD, Huber N, Kim CH, Park JY, O'Rourke NA, Nguyen KD, Smith SJ, Huguenard JR, Geschwind DH, Barres BA, Pasca SP (2015) Functional cortical neurons and astrocytes from human pluripotent stem cells in 3D culture. *Nature methods* 12:671-678.
- Qian X et al. (2016) Brain-Region-Specific Organoids Using Mini-bioreactors for Modeling ZIKV Exposure. *Cell* 165:1238-1254.
- Wells MF, Salick MR, Wiskow O, Ho DJ, Worringer KA, Ihry RJ, Kommineni S, Bilican B, Klim JR, Hill EJ, Kane LT, Ye C, Kaykas A, Eggan K (2016) Genetic Ablation of AXL Does Not Protect Human Neural Progenitor Cells and Cerebral Organoids from Zika Virus Infection. *Cell stem cell* 19:703-708.

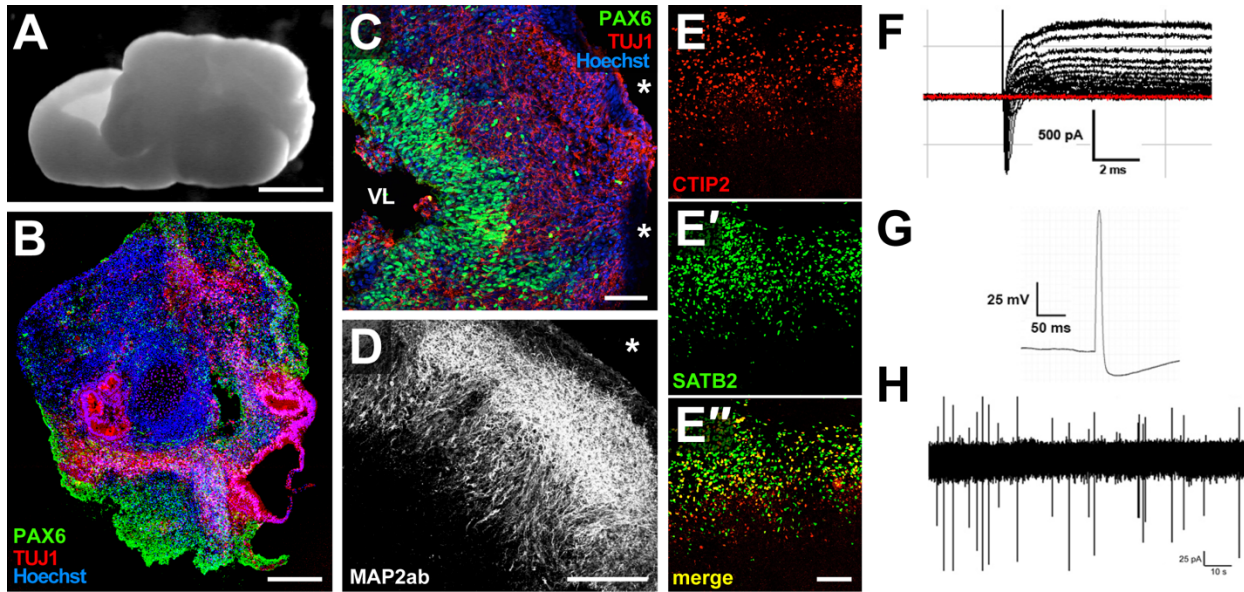


Figure B.1. Cerebral organoids generated with the intrinsic protocol have sparse cortical-like regions and are electrophysiologically active.

(A) Gross morphology of cerebral organoid after 2 month culture growth in the spinning bioreactor. Scale bar represents 1 mm. (B) ICC shows that a 4-month-old organoid has various regions of PAX6+ progenitors with scattered TUJ1+ neurons throughout. Scale bar represents 200 μ m. (C) 2-month-old organoid shows PAX6+ neural progenitors surrounding a ventricular-like lumen (VL) with TUJ1+ immature neurons in a more external cortical mantle-like structure. Asterisks represent outer surface of organoid. Scale bar represents 100 μ m. (D) 4-month-old organoid shows MAP2ab+ mature neurons in a structured cortical-like region. Asterisk represents outer surface of organoid. Scale bar represents 200 μ m. (E-E'') Organoids have some cortical-like regions demonstrating CTIP2+ deep layer neurons and SATB2+ upper layer neurons. Scale bar represents 100 μ m. (F) Patch clamp recordings show that neurons in cerebral organoids have sodium and potassium currents and fire action potentials as seen with (G) whole-cell and (H) cell-attached configurations.

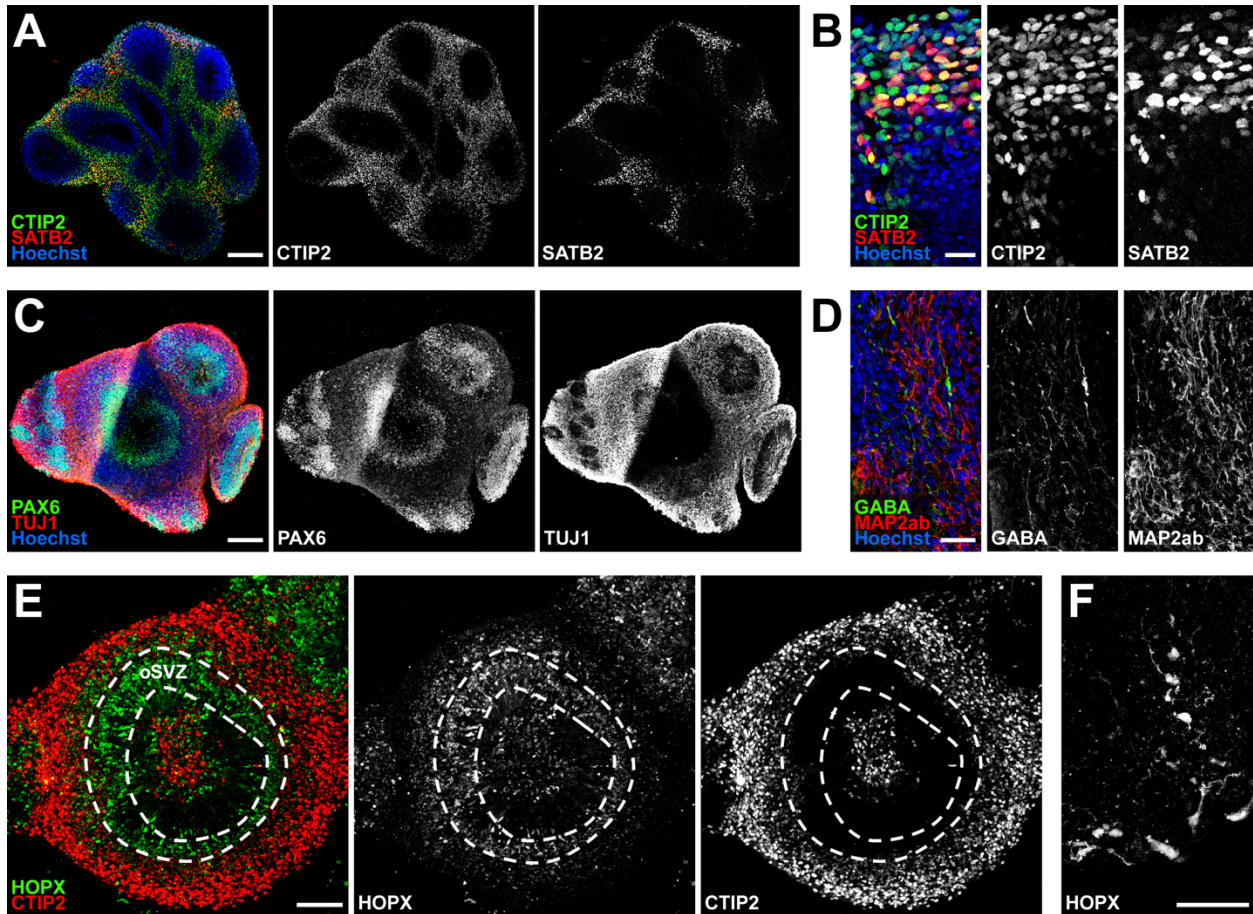


Figure B.2. Forebrain organoids generated with Spin Ω mimic the developing human cortex with ventricular zone-like areas surrounded by cortical-like neurons. (A-B) Representative image of 8-week-old forebrain organoid immunostained for CTIP2+ and SATB2+ showing cortical-like regions. Scale bar represents 200 μm in **A** and 20 μm in **B**. (C) Organoids have PAX6+ ventricular zone-like regions on the inside that are surrounded by TUJ1+ immature neurons. Scale bar represents 100 μm . (D) Organoids also display small numbers of GABAergic interneurons. Scale bar represents 50 μm . (E) Immunostaining for HOPX shows that the progenitor zones have an oSVZ area that includes HOPX+ oRGs. Scale bar represents 100 μm . (F) High magnification image of HOPX+ oRGs demonstrating their characteristic morphology. Scale bar represents 50 μm .